

**DEVELOPING A CONCEPT THAT CAN BE USED TO  
QUANTIFY THE MOTION OF FLYROCK, WITH THE  
INTENTION OF EVENTUALLY PRODUCING A MEASURING  
TOOL FOR FUTURE FLYROCK RESEARCH.**

**JENNIFER VAN DER WALT**

Presented as partial fulfilment for the degree

**M.Eng (Mining Engineering)**

**IN THE FACULTY OF ENGINEERING, BUILT ENVIRONMENT AND  
INFORMATION TECHNOLOGY  
DEPARTMENT OF MINING ENGINEERING  
UNIVERSITY OF PRETORIA**



**02 DECEMBER 2019**

I hereby declare that this dissertation is my own unaided work. It is being submitted for the degree M.Eng. (Mining Engineering) at the University of Pretoria, Pretoria. It has not been submitted before for any degree or examination in any other University. This document represents my own opinion and interpretation of information received from the mine or people on the mine.



---

Jennifer van der Walt

Dated: **02 DECEMBER 2019**

UNIVERSITY OF PRETORIA  
FACULTY OF ENGINEERING, BUILT ENVIRONMENT AND INFORMATION TECHNOLOGY  
DEPARTMENT OF MINING ENGINEERING

*The Department of Mining Engineering places great emphasis on integrity and ethical conduct in the preparation of all written work submitted for academic evaluation. While academic staff teaches you about systems of referring and how to avoid plagiarism, you too have a responsibility in this regard. If you are at any stage uncertain as to what is required, you should speak to your lecturer before any written work is submitted.*

*You are guilty of plagiarism if you copy something from a book, article or website without acknowledging the source and pass it off as your own. In effect, you are stealing something that belongs to someone else. This is not only the case when you copy work word-by-word (verbatim), but also when you submit someone else's work in a slightly altered form (paraphrase) or use a line of argument without acknowledging it. You are not allowed to use another student's past written work. You are also not allowed to let anybody copy your work with the intention of passing it off as his/her work.*

*Students who commit plagiarism will lose all credits obtained in the plagiarised work. The matter may also be referred to the Disciplinary Committee (Students) for a ruling. Plagiarism is regarded as a serious contravention of the University's rules and can lead to expulsion from the University. The declaration which follows must be appended to all written work submitted while you are a student of the Department of Mining Engineering. No written work will be accepted unless the declaration has been completed and attached.*

*I (full names): Jennifer van der Walt*

*Student number: 106 880 73*

*Topic of work: Developing a concept that can be used to quantify the motion of flyrock, with the intention of eventually producing a measuring tool for future flyrock research.*

**Declaration**

- 1. I understand what plagiarism is and am aware of the University's policy in this regard.*
- 2. I declare that this dissertation is my own original work. Where other people's work has been used (either from a printed source, internet or any other source), this has been properly acknowledged and referenced in accordance with departmental requirements.*
- 3. I have not used another student's past written work to hand in as my own.*
- 4. I have not allowed, and will not allow, anyone, to copy my work with the intention of passing it off as his or her own work.*

Signature  \_\_\_\_\_

## LANGUAGE EDIT

I, Jennifer van der Walt, hereby declare that I performed an English language edit on the final version of this project report.

  
\_\_\_\_\_  
Signature

3 February 2020  
Date



## ABSTRACT

# DEVELOPING A CONCEPT THAT CAN BE USED TO QUANTIFY THE MOTION OF FLYROCK, WITH THE INTENTION OF EVENTUALLY PRODUCING A MEASURING TOOL FOR FUTURE FLYROCK RESEARCH.

**JENNIFER VAN DER WALT**

**Supervisor:** Professor William Spiteri

**Department:** Mining Engineering

**University:** University of Pretoria

**Degree:** M.Eng. (Mining Engineering)

Flyrock remains a significant risk to the health and safety of the mine's employees and infrastructure as well as the safety of the neighbouring communities and their property. Losses and damages can result in significant financial and reputation consequences. The lack of fundamental research in recent years and quantifiable data relating to the relationship between blast design parameters and the risk of flyrock motivated this project. A number of authors concluded that major gaps in knowledge relative to flyrock caused by its random nature still remain a weakness in the field.

Recent papers published (since 2010) proposed a wide range of potential approaches and techniques to predict or investigate flyrock. However, the majority of these papers concluded that the proposed results were site-specific and could not be applied to other environments.

The focus of this project was to develop a concept that is able to quantify the flight path of the flyrock resulting from a blast. The motivation behind the development of this concept was to enable future researchers to quantify the impact of the different blast design parameters on the measured flyrock.

Various technologies were considered and investigated during this project. After a comparative analysis of these technologies, it was decided to use photogrammetry as the foundation of the proposed concept tool. The proposed concept consists of three main

phases, namely (1) data acquisition, (2) image processing and data analysis and (3) data interpretation.

To date, progress has been achieved with phase one and phase two. In phase one, all objectives have been met. However, there are still areas which need refinement, specifically regarding the placement of the cameras in the field. In phase two, success was achieved with the proof of concept exercise in a controlled environment using a clay pigeon as the projectile. The process of calibrating the lenses has been established, however, further optimization is possible. Point-cloud data was successfully generated in the concept test, but converting the image data from subsequent quarry test blasts proved more challenging and is still a work in progress. Once phase two has been satisfactorily resolved, attention will focus on phase three.

Results to date have given a positive indication that the concept is viable and that additional work will prove the technology functional. Ultimately, it is envisioned that this tool can be used for one of three purposes, namely:

- Mines can generate a database with accurate historical flyrock of their blasting operations.
- Research teams can implement this tool to conduct quantitative research and investigations into flyrock and the impact of different blast design parameters on the risk of flyrock.
- Point-cloud data combined with ballistics calculations can be used to visualise blasts and flyrock in Virtual Reality for training and education.

## ACKNOWLEDGEMENTS

I wish to express my appreciation to the following organisations and persons who made this project report possible:

- 1 AEL Intelligent Blasting for their financial support through their research chair at the Department of Mining Engineering at the University of Pretoria and their assistance with industry participation.
- 2 The following persons are gratefully acknowledged for their assistance during the course of the study:
  - a. Mr Robin Kock and Mr Gordon McGill (Premier Mapping)
  - b. Mr Hans Grobler (University of Pretoria, EECE)
  - c. Professor Walter Meyer (University of Pretoria, Physics)
  - d. Mr Wolter de Graaf
- 3 Professor William Spiteri, my supervisor, for his guidance and support throughout this project.
- 4 Mr Alix van der Walt (my husband) and my parents for their continued support and guidance throughout this project.

# TABLE OF CONTENTS

<b>1. INTRODUCTION</b> .....	<b>2</b>
1.1. GENERAL INTRODUCTION AND PROJECT BACKGROUND.....	2
1.2. RESEARCH PROBLEM STATEMENT AND RESEARCH OBJECTIVES.....	8
1.2.1. <i>Problem Statement</i> .....	8
1.2.2. <i>Research Objectives</i> .....	8
1.2.3. <i>Research Questions</i> .....	8
1.2.4. <i>Limitations and Assumptions of the Study</i> .....	9
1.2.5. <i>Research Methodology</i> .....	9
1.3. PROJECT MOTIVATION SUMMARY.....	13
1.4. REFERENCES .....	14
<b>2. LITERATURE SURVEY</b> .....	<b>16</b>
2.1. INITIAL RESEARCH AND MOTIVATION TO THIS PROJECT .....	16
2.1.1. <i>Sources of flyrock</i> .....	16
2.1.2. <i>Root causes of flyrock</i> .....	17
2.1.3. <i>Drilling and blasting factors that can contribute to flyrock</i> .....	18
2.1.4. <i>Flyrock predictive models</i> .....	20
2.2. TECHNIQUES OR CONCEPTS THAT HAVE PREVIOUSLY BEEN USED TO MEASURE, ESTIMATE OR MODEL (PREDICT) FLYROCK.....	26
2.2.1. <i>Artificial intelligence (AI)</i> .....	26
2.2.2. <i>Rock engineering systems-based model</i> .....	32
2.2.3. <i>Empirical- and statistical analysis</i> .....	34
2.2.4. <i>A forensic approach based on ballistics principles</i> .....	40
2.3. EXISTING TECHNOLOGIES THAT CAN BE CONSIDERED DURING THE DEVELOPMENT OF THE CONCEPT OR TECHNIQUE .....	46
2.3.1. <i>Sensor technology</i> .....	46
2.3.2. <i>Measuring and monitoring techniques and technologies</i> .....	50
2.4. REFERENCES .....	106
<b>3. RESULTS AND ANALYSIS</b> .....	<b>117</b>
3.1. RECENT WORK (SINCE 2010) CONDUCTED IN THE FIELD OF FLYROCK PREDICTION.....	117
3.2. EXISTING TECHNIQUES AND TECHNOLOGIES .....	130
3.2.1. <i>Sensors</i> .....	130

3.2.2.	<i>Available techniques and technologies</i> .....	132
3.3.	DEVELOPMENT OF A NEW PHOTOGRAMMETRIC CONCEPT THAT CAN BE USED TO QUANTIFY THE MOTION OF RANDOM FLYROCK RESULTING FROM A BLAST.....	144
3.3.1.	<i>Phase 1</i> .....	145
3.3.2.	<i>Phase 2</i> .....	153
3.3.3.	<i>Phase 3</i> .....	156
3.4.	INITIAL PROOF OF CONCEPT TESTS.....	159
3.4.1.	<i>Proof of concept test results</i> .....	162
<b>4.</b>	<b>CONCLUSIONS</b> .....	<b>173</b>
<b>5.</b>	<b>RECOMMENDATIONS</b> .....	<b>176</b>
<b>6.</b>	<b>SUGGESTIONS FOR FURTHER WORK</b> .....	<b>178</b>
<b>APPENDIX A</b>	.....	<b>180</b>
<b>7.</b>	<b>ADDITIONAL RESEARCH AND RELEVANT LITERATURE</b> .....	<b>180</b>
7.1.	BLAST DESIGN PARAMETERS AND OTHER FACTORS THAT INFLUENCE THE RISK OF FLYROCK.....	180
7.2.	ARTIFICIAL INTELLIGENCE (AI) PRINCIPLES.....	185
7.3.	ALGORITHMS RELATED TO DEGHANI & SHAFAGHI'S (2017) DIFFERENTIAL EVOLUTION ALGORITHM APPROACH TO PREDICT FLYROCK.....	194
7.3.1.	<i>Dimensional Analysis Algorithm</i> .....	194
7.3.2.	<i>Differential Evaluation Algorithm</i> .....	195
7.3.3.	<i>Regression tree analysis presented by Hasanipanah, et al. (2017)</i> .....	196
7.4.	SENSOR TECHNOLOGY.....	197
7.4.1.	<i>Temperature sensors</i> .....	197
7.4.2.	<i>Infrared (IR) sensors</i> .....	198
7.4.3.	<i>Ultra-violet (UV) sensors</i> .....	199
7.4.4.	<i>Ultrasonic sensors</i> .....	200
7.4.5.	<i>Touch sensors</i> .....	202
7.4.6.	<i>Pressure Sensors</i> .....	206
7.4.7.	<i>Proximity sensors</i> .....	209
7.5.	HISTORY OF HIGH-SPEED PHOTOGRAPHY.....	210

<b>APPENDIX B .....</b>	<b>212</b>
<b>8. SUPPORTIVE RESULTS.....</b>	<b>212</b>
8.1. ANGLES OF VIEW OF SIGMA LENSES.....	212
8.2. SYNCHRONIZATION TEST RESULTS TO IDENTIFY POTENTIAL DELAYS IN AN IMAGE CAPTURING BETWEEN CAMERAS .....	214
8.3. EXPORTED DATA OR RESULTS FROM USMART MAPPING SOFTWARE .....	216

## LIST OF TABLES

Table 1.1: Accident Statistics of Reported Flyrock cited by Different Authors (Raina, et al., 2015).....	2
Table 1.2: Summary of the available Flyrock Predictive Models and Equations.....	4
Table 1.3: Research Objectives and related Methodology.....	10
Table 2.1: Blast outcomes, nature and objectives (Raina, et al., 2015).....	20
Table 2.2: Comparison between causative factors and their use in flyrock distance prediction (Raina, et al., 2015).....	25
Table 2.3: Model input parameters and their ranges (Monjezi, et al., 2010).....	27
Table 2.4: Input and output parameters of the proposed system (Monjezi, et al., 2012) .....	28
Table 2.5: Detectable physical phenomena with sensor systems (Committee on New Sensor Technologies, 1995), (Sobhan, 2005).....	47
Table 2.6: Key differences between active and passive sensors (Pramoda, 2017).....	49
Table 2.7: High-speed photography definition classification (Fuller, 2007).....	52
Table 2.8: Exposure recommendations for different photographic genres (Cox, 2017) .....	58
Table 2.9: History of photogrammetry (Premier Mapping, n.d.).....	61
Table 2.10: Categories of photogrammetry (Luhmann, et al., 2006) .....	64
Table 2.11: Differences between LiDAR and RADAR.....	86
Table 2.12: Hawk-eye timeline (Hawk-Eye Innovations Ltd., 2018) .....	96
Table 3.1: Summary of work conducted relative to flyrock and flyrock prediction since 2010 .....	118
Table 3.2: Summary of various sensors .....	131
Table 3.3: Summary of the existing techniques and technologies that can support this project's objective.....	134
Table 3.4: Weighting matrix used to evaluate the comparative criteria .....	141
Table 3.5: Comparative analysis between the existing techniques and technologies.....	142
Table 3.6: Summary of essential considerations relating to the placement of the cameras in the field .....	146
Table 3.7: Camera timing or synchronisation tests' results .....	152
Table 3.8: Initial concept tests' focus elements and desired outcomes .....	159
Table 3.9: Visually detecting and "tracking" a moving object through multiple cameras.....	166
Table 3.10: Results for three successive positions of the clay pigeon.....	170
Table 7.1: Types of ANN (Mehta, 2019) .....	189
Table 7.2: Advantages and disadvantages for capacitive touch sensors (TCI.de, 2019).....	204
Table 7.3: Advantages and disadvantages for resistive touch sensors (TCI.de, 2019) .....	205
Table 8.1: Synchronization tests results .....	214

Table 8.2: An example of the .csv file exported from the uSMART Softcopy stereo mapping software .....216



# LIST OF FIGURES

Figure 1.1: The influence of stemming height on the maximum projection range (or minimum clearance distance) .....	5
Figure 1.2: Flow Diagram indicating the inter-dependency of the Blast Design Parameters (based on the industry rules-of-thumb published in various field guides) .....	6
Figure 1.3: Causative Parameters vs. Predictive Parameters .....	7
Figure 1.4: Proposed Research Approach and Project Flow .....	9
Figure 2.1: Three key mechanisms of flyrock (Richards & Moore, 2005) .....	16
Figure 2.2: Surface blast design parameters (de Graaf, 2016) .....	19
Figure 2.3: Illustration of Equation 2.3 (Chiappetta, 2014) .....	23
Figure 2.4: Scaled Depth of Burial (Chiappetta & Treleven, 1997) .....	24
Figure 2.5: The relative importance and sensitivity of the variables for throw and flyrock (Raina & Murthy, 2016) .....	32
Figure 2.6: Basic forces that act on flyrock fragments during its flight (Stojadinović, et al., 2011) .....	41
Figure 2.7: Classification of sensors (Bouzgou, 2006) .....	48
Figure 2.8: Non-contact measuring techniques (Luhmann, et al., 2006) .....	51
Figure 2.9: The working of a camera, illustrating the three pillars of exposure (Dunlop, 2011) .....	53
Figure 2.10: Aperture scale including depth of field (Dunlop, 2011) .....	54
Figure 2.11: Exposure triangle .....	57
Figure 2.12: Photogrammetry portrayed as a system (Schenk, 2005) .....	66
Figure 2.13: Photogrammetry from an object (or surface) to a three-dimensional digital model (Luhmann, et al., 2006) .....	67
Figure 2.14: Pipeline for digital image capturing process (Sužiedelytė-Visockienė, et al., 2015) .....	68
Figure 2.15: Overlap of photogrammetry images including ideal GCP placement (Colorado Department of Transportation, 2015) .....	70
Figure 2.16: Common photogrammetric products resulting from the processing and analysis of images (Luhmann, et al., 2006) .....	73
Figure 2.17: Photogrammetry accuracy factors (PhotoModeler Technologies, n.d.) .....	75
Figure 2.18: Basic working of a radar system (Wolff, 2019) .....	81
Figure 2.19: Classification of radar sets (Wolff, 2019) .....	82
Figure 2.20: Schematic of a LiDAR system (Elprocus, 2019) .....	88

Figure 2.21: Hawk-eye technology camera layout in a stadium (the focus of the system is the target area) (Bandaru, 2016) .....	97
Figure 2.22: Workflow of the Hawk-eye ball tracking system (Vijayakumar & Anand, 2016 )	98
Figure 2.23: Hawk-eye in sports, (a) Tennis, (b) Soccer or Football, (c) Cricket (Hawk-Eye Innovations Ltd., 2018).....	98
Figure 2.24: Basic steps for detecting and tracking an object (Trambadiya & Varnagar, 2015) .....	99
Figure 2.25: Layout and components of the active infrared system (Stančić, et al., 2017) ..	103
Figure 2.26: Concept test setup of the active infrared system for detecting and tracking a projectile (Stančić, et al., 2017) .....	104
Figure 3.1: Approaches or Techniques used in the recent flyrock prediction studies .....	126
Figure 3.2: Frequency of input parameters used in the proposed flyrock (or flyrock-related) prediction models discussed in the aforementioned publications .....	127
Figure 3.3: Most influential input parameters (frequency) based on the proposed models in the aforementioned publications .....	128
Figure 3.4: Model of the developed tool concept .....	145
Figure 3.5: An example of the GCPs (ground control points) used in the field .....	147
Figure 3.6: PocketWizard PlusX trigger (PocketWizard, 2019) .....	149
Figure 3.7: Long-range trigger system designed for this project. ....	149
Figure 3.8: Basic communication diagram between the remote control and the transceiver, and between the transceiver and the receiving triggers connected to each camera. ....	150
Figure 3.9: Layout of timing or synchronisation tests .....	151
Figure 3.10: Timing results from one test illustrating the fluctuation in the timings and that the error is not cumulative. ....	153
Figure 3.11: Marked GCPs on a calibration image using Pix4D.....	154
Figure 3.12: Some of the tie-points shown in one image .....	155
Figure 3.13: All of the tie-points shown in one image.....	155
Figure 3.14: Full process flow of the proposed flyrock measuring tool.....	158
Figure 3.15: Concept tests setup .....	160
Figure 3.16: Proof of concept tests' methodology .....	161
Figure 3.17: Camera placement for the proof of concept tests.....	161
Figure 3.18: GCP placement in the FoV of the cameras, within the target area .....	162
Figure 3.19: Calibration image data and the path followed (green dots) .....	163
Figure 3.20: Point-cloud of the test environment (without GCPs).....	164
Figure 3.21: Point-cloud of the test environment including the aligned GCPs (blue and green markers).....	164
Figure 3.22: High-quality image of a moving object while travelling through the air .....	165

Figure 3.23: Quarry test blasts image data, showing the same projectiles at different time intervals.....	171
Figure 7.1: Artificial Intelligence developmental timeline (SAS Institute Inc., 2019).....	185
Figure 7.2: The six main sub-fields or categories of AI (Intelliplate.com, 2019).....	187
Figure 7.3: Neural network architecture (Kukreja, et al., 2016) .....	189
Figure 7.4: Feed-forward ANN (Mehta, 2019).....	189
Figure 7.5: Radial Basis Function ANN (Mehta, 2019).....	190
Figure 7.6: Multilayer Perception ANN (Mehta, 2019).....	190
Figure 7.7: Convolutional ANN (Mehta, 2019) .....	191
Figure 7.8: Recurrent Neural Network (Mehta, 2019) .....	191
Figure 7.9: Modular ANN (Mehta, 2019).....	191
Figure 7.10: Fuzzy inference system (Jang, 1993) .....	193
Figure 7.11: Dimensional analysis algorithm (Dehghani & Shafaghi, 2017) .....	194
Figure 7.12: Differential evaluation algorithm (Dehghani & Shafaghi, 2017) .....	195
Figure 7.13: Simple decision tree structure (Hasanipanah, et al., 2017).....	196
Figure 7.14: Structure of the developed regression tree model (Hasanipanah, et al., 2017) .....	196
Figure 7.15: Thermocouple working principle (Sterling Sensors, 2018) .....	198
Figure 7.16: Construction of ultrasonic sensors (Coulton.com, 2019).....	200
Figure 7.17: Working principle of an ultrasonic sensor (Beg, 2017).....	201
Figure 7.18: Disadvantages or weaknesses relating to ultrasonic sensors (GeeksTips.com, 2019).....	202
Figure 7.19: Touch screen based on the capacitive sensor principle (TCI.de, 2019) .....	204
Figure 7.20: Touch screen based on the resistive sensor principle (Gudino, 2018) .....	205
Figure 7.21: Piezo-resistive pressure sensor (Avnet Inc., 2019).....	206
Figure 7.22: Capacitive pressure sensor (Avnet Inc., 2019) .....	207
Figure 7.23: A circuit diagram of a strain-gauge pressure sensor, containing a Wheatstone bridge layout (Avnet Inc., 2019).....	207
Figure 7.24: Piezoelectric pressure sensor (Avnet Inc., 2019).....	208
Figure 7.25: A simplified optical pressure sensor (Avnet Inc., 2019).....	209
Figure 7.26: Types of photoelectric proximity sensors (Fargo Controls Inc., 2018).....	210
Figure 7.27: The first high-speed images captured by Eadweard Muybridge in 1879 (Yigiter, 2018).....	211
Figure 8.1: FoV schematic for a Sigma 35mm lens .....	212
Figure 8.2: FoV schematic for a Sigma 50mm lens .....	213
Figure 8.3: FoV schematic for a Sigma 85mm lens .....	214

## LIST OF EQUATIONS

Equation 1.1: SveDeFo Equation for Maximum Flyrock Projection Range.....	4
Equation 1.2: Scaled Depth of Burial Equation .....	4
Equation 1.3: Minimum Clearance Distance using SDoB .....	4
Equation 1.4: Maximum Throw Equation from AEL .....	4
Equation 1.5: Maximum Throw Equation from Sasol .....	4
Equation 2.1: SveDeFo Equation for predicting maximum projection range of flyrock (ISEE, 2011).....	21
Equation 2.2: Scaled Depth of Burial Equation (ISEE, 2011).....	22
Equation 2.3: Simplified Scaled Depth of Burial (Chiappetta, 2014) .....	22
Equation 2.4: Maximum projection range including Scaled Depth of Burial (McKenzie, 2009) .....	24
Equation 2.5: Empirical equation for predicting flyrock proposed by Ghasemi, et al. (2012) .	35
Equation 2.6: Empirical flyrock equation presented by Armaghani, et al. (2016) using MRA	36
Equation 2.7: Empirical equations developed using DA (Dehghani & Shafaghi, 2017) .....	37
Equation 2.8: Empirical equations developed using DE (Dehghani & Shafaghi, 2017) .....	38
Equation 2.9: Equation created during MLR model development (Hasanipanah, et al., 2017) .....	39
Equation 2.10: Differential equation for motion in the x-direction (Stojadinović, et al., 2011)	41
Equation 2.11: Differential equation for motion in the y-direction (Stojadinović, et al., 2011)	41
Equation 3.1: Differential equation for motion in the x-direction (Stojadinović, et al., 2011)	156
Equation 3.2: Differential equation for motion in the y-direction (Stojadinović, et al., 2011)	156

## LIST OF SYMBOLS, ABBREVIATIONS AND ACRONYMS

°	Degree
$\theta$	Theta used to indicate an angle
$\lambda$	Lamda used as Wavelength
$\mu\text{m}$	Micrometre
%	Percentage
$\rho_e$	Density of the explosives
$\rho_r$	Density of the rock
A	Cross-sectional area
AEL	African Explosives Limited
AI	Artificial Intelligence
ANFIS	Adaptive Neuro-Fuzzy Inference System
ANFO	Ammonium Nitrate Fuel Oil
ANN	Artificial Neural Networks
B	Burden
$C_1$	Drag constant (equal to $\rho_{\text{air}} \cdot A \cdot C_D$ )
$C_D$	Drag coefficient
CAD	Computer-Aided Design
cm	Centimetre
CNN	Convolutional Neural Network
D	Hole diameter
$\bar{D}$	Drag force vector
DA	Dimensional Analysis
$d_e$ or $d$	Charge diameter
DC	Direct Current
DE	Differential Evaluation
DEM	Digital Elevation Model
DIAL	Differential Absorption LiDAR
dist.	Distance
DoF	Depth of Field
DTM	Digital Terrain Model
DSLR	Digital Single-lens Reflex
EEZ	Exclusive Economic Zone
e.g.	Example
EO/IR	Electro-optical and Infrared
et.al.	Et Alia (which means “and others”)

FoS	Factor of Safety
FoV	Field of View
fps	Frames per second
g	Gravitational acceleration (equal to 9.81 m/s <sup>2</sup> )
g/cc	Gram per cubic centimetre
$\bar{G}$	Gravitational force vector
GA	Genetic Algorithm
GCP	Ground Control Point
GIS	Geographic Information System
GNSS	Global Navigation Satellite System
GPS	Global Positioning System
H	Bench Height or Hole depth
HD	High Definition
i.e.	Id Est (which means “in other words”)
ICA	Imperialist Competitive Algorithm
IMU	Inertial Measurement Unit
IR	Infrared
ISEE	International Society of Explosives Engineers
kg	Kilogram
km	Kilometre
kph	Kilometres per hour
L	Charge length
$\bar{L}$	Lift force vector
LED	Light Emitting Diode
LiDAR	Light Detection and Ranging
m	Metre
m (SDoB)	Contributing charge mass
m <sup>2</sup>	Square metre
m <sup>3</sup>	Cubic metre
max.	Maximum
MHT	Multiple Hypothesis Tracking
min.	Minimum
mm	Millimetre
ms	Millisecond
MLR	Multiple Linear Regression

MP	Mega-pixel
MRA	Multiple Regression Analysis
mV	Millivolt
N	Newton
N/A	Not applicable
Nd	Neodymium-doped
nm	Nanometre
O <sub>2</sub>	Oxygen
PF	Powder Factor
Q (or Ch)	Charge Mass per Delay
RADAR	Radio Detection and Ranging
RES	Rock Engineering Systems
RMR	Rock Mass Rating
RNN	Recurrent Neural Network
RoT	Rule of Thumb
RTD	Resistance Temperature Detector (Sensor)
s	Second
S	Spacing
SD	Specific Drilling
SDoB	Scaled Depth of Burial
SveDeFo	Swedish Detonic Research Foundation
SVM	Support Vector Machine
t	Time
T	Stemming length
U	Sub-drill
UV	Ultra-violet
$\bar{v}$	Velocity vector
V	Volt
ViDAR	Visual Detection and Ranging
VoD	Velocity of Detonation
vs.	Versus
W	Watt
WWI	World War 1
WWII	World War 2
YAG	Yttrium-Aluminium-Garnet

## LIST OF APPENDICES

Appendix A	Additional research and relevant literature .....	180
Appendix B	Supportive results .....	212



MOTIVATION FOR THIS STUDY

---

# 1. INTRODUCTION

## 1.1. GENERAL INTRODUCTION AND PROJECT BACKGROUND

Drilling and blasting remain essential phases in the production cycles of most mining operations and even with recent technological advances, still endure as the preferred method of rock breaking. In order to break a rock mass using explosives, a significant amount of energy is required to be charged and released almost instantaneously, often resulting in rock fragments thrown beyond expectation, i.e. flyrock.

Flyrock is the main cause of exterior damage to equipment or infrastructure resulting from a blast and has fatally injured people in the vicinity of the blast (Bajpayee, et al., 2003). Injury to mine employees as well as injury or damage to surrounding community's residents, livestock, structures, and/or equipment carry a high financial- and reputational penalty for the mine. Raina et al. (2015) summarise reported flyrock accidents cited by several sources in Table 1.1.

**Table 1.1: Accident Statistics of Reported Flyrock cited by Different Authors (Raina, et al., 2015)**

Reference	Period	Blasting Injuries	% of Flyrock Injuries in Blasting related Accidents
<b>Mishra and Mallick (2013)</b>	1996 - 2011	30	24 %
<b>Verakis (2011)</b>	2010 – 2011	18	38 %
<b>Bajpayee et al. (2004)</b>	1978 – 1998	281	41 %
<b>Verakis and Lobb (2007)</b>	1994 – 2005	168	19 %
<b>Little (2007)</b>	1978 – 1998	412	68 %
<b>Kecojevic and Radomsky (2005)</b>	1978 – 2001	195	28 %
<b>Adhikari (1999)</b>	-	-	20 %

Table 1.1 supports the statement that flyrock can pose a significant risk to the health and safety of employees or person in the mine's vicinity and can result in injuries ranging from minor to fatal. In addition, a study by Tose (2013) titled "*A practical approach to managing control of flyrock*", was motivated by recent flyrock incidents. Flyrock should, therefore, be mitigated or ideally eliminated, in order to avoid these penalties.

There are a number of approaches used on mines in an attempt to mitigate the risk of flyrock and protect their own assets and resources, as well as surrounding communities against the risk of flyrock. One such control is implementing a clearance radius or also known as the blast area. The clearance radius (or blast area) is defined by (ISEE, 2011) as “*the area surrounding the blast beyond which there should not be a risk of flyrock to the mine’s employees, equipment and infrastructure*”. This clearance radius dictates the minimum distance from the blast to which the blaster must evacuate the blasting team and every other team working within that perimeter.

This project follows initial research that began in 2016 on the validity of using a fixed minimum clearance distance, i.e. 500m for people and 300m for equipment (Glencore, 2017). The main focus of the research was to determine whether any technical theory or mathematical predictive formula exists that supports this (fixed) clearance distance. This project serves as an extension based on the outcome of that research.

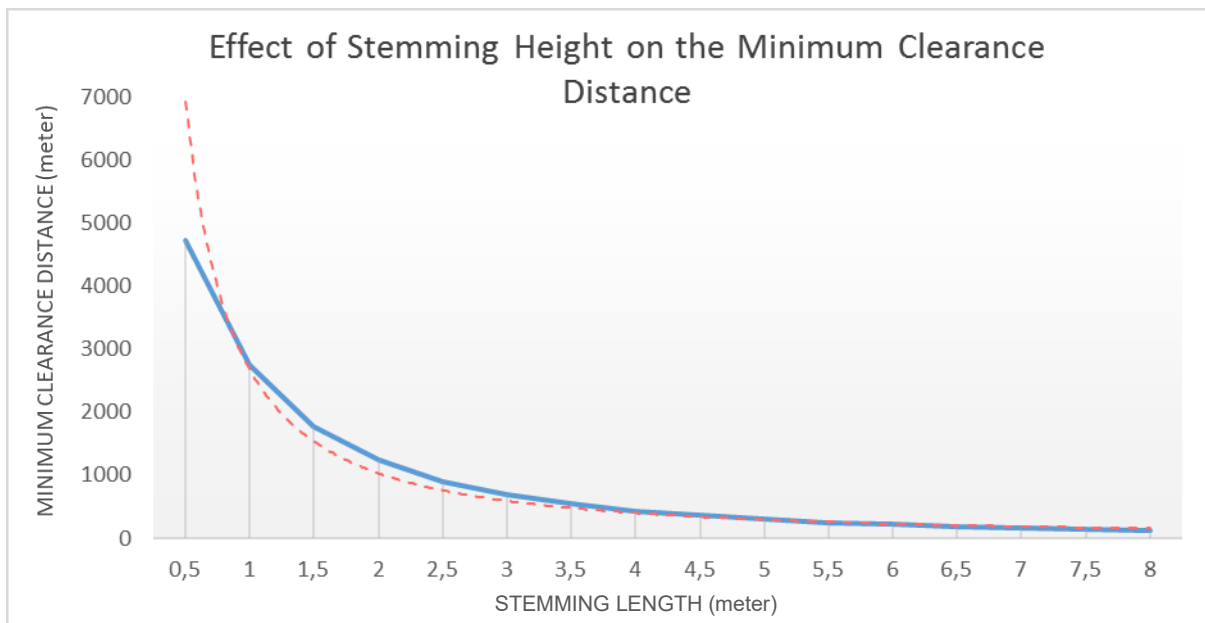
The initial research included a review of available literature on the industry standards on clearance radii, flyrock predictive models and the theoretical flyrock causative factors. This literature review yielded four potential predictive models, given in Table 1.2, that may be used to determine the maximum flyrock projection distance, also termed the minimum clearance distance.

Table 1.2: Summary of the available Flyrock Predictive Models and Equations

Source	Deliverable	Inputs	Input Symbol	Input Unit	Equation Number	Equation	Reference	
SveDeFo (Swedish Detonic Foundation)	Maximum Projection Range (m)	Charge Diameter	d	mm	(1)	$Max.Projection\ Range = FoS \times 30 \times d^{0.667}$ (FoS = Factor of Safety)	Blasters' Handbook	
ISEE Blasters' Handbook	Minimum Clearance Distance (m)	Stemming Length	T	m	(2) Input to Equation (3)	$SDoB = \frac{T + (0.0005 \times m \times D)}{0.00923 \times (m \times D^3 \times \rho)^{0.333}}$	Blasters' Handbook	
			Hole Diameter	D				mm
		SDoB	Contributing Charge Length	m				m = 10 for D > 100mm; m = 8 for D < 100mm
								Explosives Density
		Hole Diameter	D	mm	(3)	$Min.Clearance\ Distance = FoS \times 11 \times SDoB^{-2.167} \times D^{0.667}$		
AEL	Maximum Throw (m)	Hole Diameter	D	mm	(4)	$Max.Throw = 35 \times (d \times Pf_a)^{0.667}$	AEL Field guide recommendation	
		Actual Powder Factor	Pf <sub>a</sub>	g/cc				
Sasol	Maximum Throw (m)	Hole Diameter	D	mm	(5)	$Max.Throw = 35 \times \left(\frac{D}{Pf_a}\right)$	Sasol's Explosives Engineers' Surface Field Guide	
		Actual Powder Factor	Pf <sub>a</sub>	g/cc				

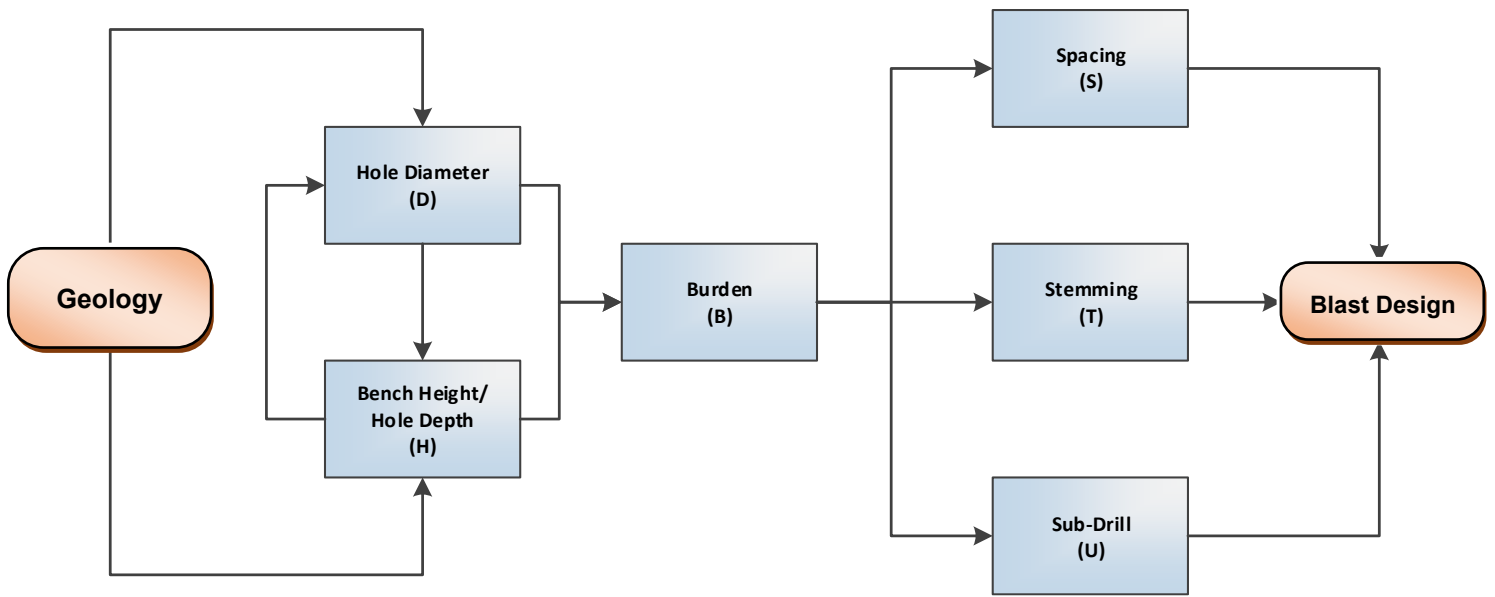
Of these available predictive models, the Scaled Depth of Burial (SDoB) approach, Equation 1, proved to be the best method of calculating an acceptable clearance distance. The main reason is the number and variety of factors considered in the development of this model, which will be discussed in further detail in Chapter 2.

Using Equation (2) in Table 1.2, an exponential relationship between the stemming length and calculated clearance distance was determined and is illustrated in Figure 1.1. This exponential relationship, although based on a specific hole diameter, demonstrates that: if the stemming length is less than the minimum value recommended by expert companies' field guides and rules-of-thumb, the clearance distance will increase significantly.



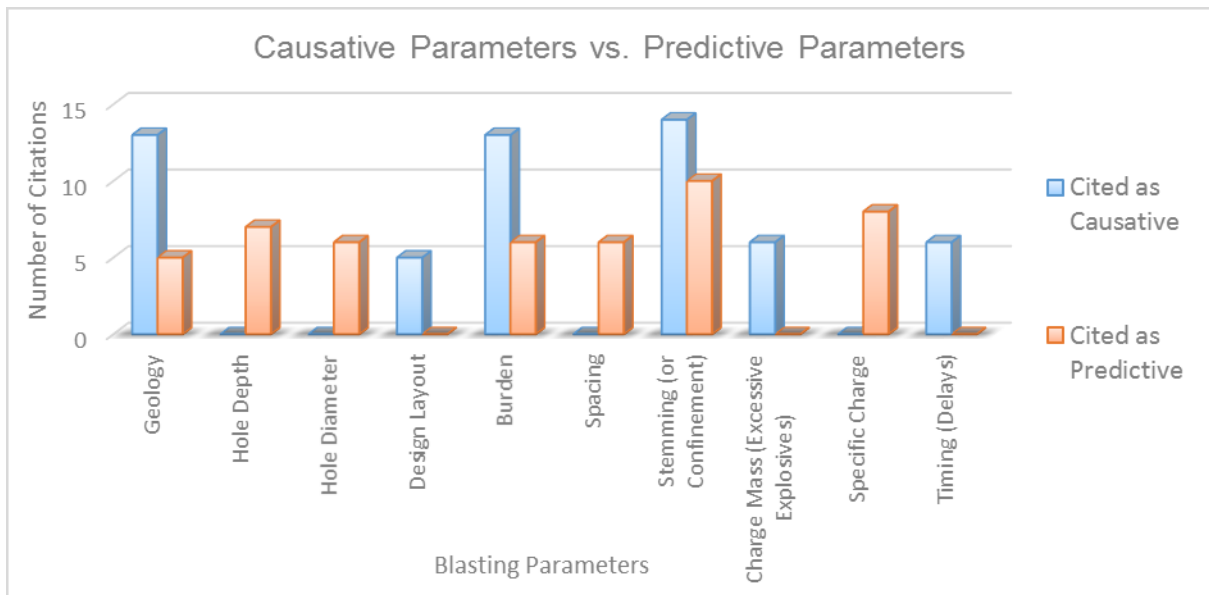
**Figure 1.1: The influence of stemming height on the maximum projection range (or minimum clearance distance)**

This caution can be linked to other blast parameters as well since the construction of the design rule-of thumbs, inherently, create interdependency between the parameters, illustrated in Figure 1.2. Therefore, it is essential that special attention is given to the blast design and the consequence of any change to a single design parameter, without adapting the other blasting parameters.



**Figure 1.2: Flow Diagram indicating the inter-dependency of the Blast Design Parameters (based on the industry rules-of-thumb published in various field guides)**

Ultimately, the research substantiated the conclusions reached by multiple other studies, including Raina, et al. (2015), which concluded by stating that “there are major research gaps into the phenomena of flyrock and that this concept is not well understood” (Raina, et al., 2015). One of these “gaps” in understanding is illustrated in Figure 1.3, by graphically comparing the theoretically causative factors of flyrock to the predictive factors taken into account in the predictive models and equations.



**Figure 1.3: Causative Parameters vs. Predictive Parameters**

Figure 1.3 illustrates the disconnect between the theoretical causative factors and the factors considered in the available predictive models, highlighting the lack in understanding of the concept of flyrock as a whole as well as the need for further investigations. In addition, the various predictive models do not take into account flyrock originating from a vertical free-face (i.e. face-burst), due to under-burdened free-face, angled blast holes and/or geological abnormalities.

The initial research concluded by recommending that the predictive models should ultimately be reviewed and the effect of the causative factors on the projection ranges of flyrock must be investigated and supported by actual field data. Only once the realistic effect of the blast parameters on the risk of flyrock is determined, can a new and revised prediction model be developed to increase the accuracy of the (predicted) maximum flyrock distances calculated in different environments.

In order to efficiently investigate the realistic effect of the various causative factor and achieve this new and revised prediction model, a large data-set is required. During a brief follow-up literature review, no specific method of quantitatively measuring flyrock could be identified.

For this reason, as well as the degree of technological advances in recent years, it was proposed to conduct an investigation focussing on the development of a concept that can be used to accurately (quantitatively) measure debris projected from a blast. Only once flyrock and its flight properties are quantitatively measured, can an accurate predictive model be developed and implemented in the mining industry.

## **1.2. RESEARCH PROBLEM STATEMENT AND RESEARCH OBJECTIVES**

### **1.2.1. Problem Statement**

Blasting, although as the preferred method of rock breaking, still pose significant safety risks to employees, communities and surrounding infrastructure. One such a risk is known as flyrock, defined as the undesirable throw of debris from a blast. Previous studies concluded that flyrock is not well understood and have identified gaps in how various blasting parameters relate to the risk of flyrock.

The focus of this project was not to invent new technology but rather to develop a concept. This concept should be able to quantify the flight path of the flyrock resulting from a blast. The initial aim of the investigation was to identify a viable concept and obtain sufficient proof of feasibility. It is important to note that this concept is not linked to a specific technology, therefore, the use of new and emerging technologies, like drones, were not eliminated in this project. The end goal was to develop a concept that is potentially compatible with various technologies, depending on the mine's preferences, budget and limitations.

### **1.2.2. Research Objectives**

- i. Investigate the recent work done (i.e. 2010 to the present) in an attempt to predict flyrock.
- ii. Investigate available and relevant monitoring (and measuring) techniques and technologies used in the mining industry, as well as other relative fields and industries.
- iii. Conduct a comparative analysis between the techniques and technologies investigated based on the applicability to this project.
- iv. Develop a concept that is able to quantify the motion (trajectory) of flyrock.
- v. Test and evaluate the concept and determine whether this concept can be used to calculate the trajectory of flyrock.

### **1.2.3. Research Questions**

- i. How effective are the recently proposed prediction models and strategies as a universal solution to predict flyrock?
- ii. Which existing technology or technique is the most suitable to quantitatively measure flyrock projected from blasting activities?
- iii. Can flyrock be effectively recorded and measured?
- iv. Can the developed concept be used to determine the trajectory of random rock fragments coming from a blast?



#### 1.2.4. Limitations and Assumptions of the Study

No main assumptions were made at the start of this project. The specific assumptions will be discussed further in Chapter 3 (Results and Analysis).

The two main limitations of this project are:

- i. The project was only aimed at developing a concept that can be used to quantify the motion of flyrock, i.e. the trajectory of flyrock, and
- ii. The analysis and interpretation of the field data, based on physics and statistics principles will not be included. This may be recommended as future work.

#### 1.2.5. Research Methodology

The proposed research approach and project flow are shown in Figure 1.4.

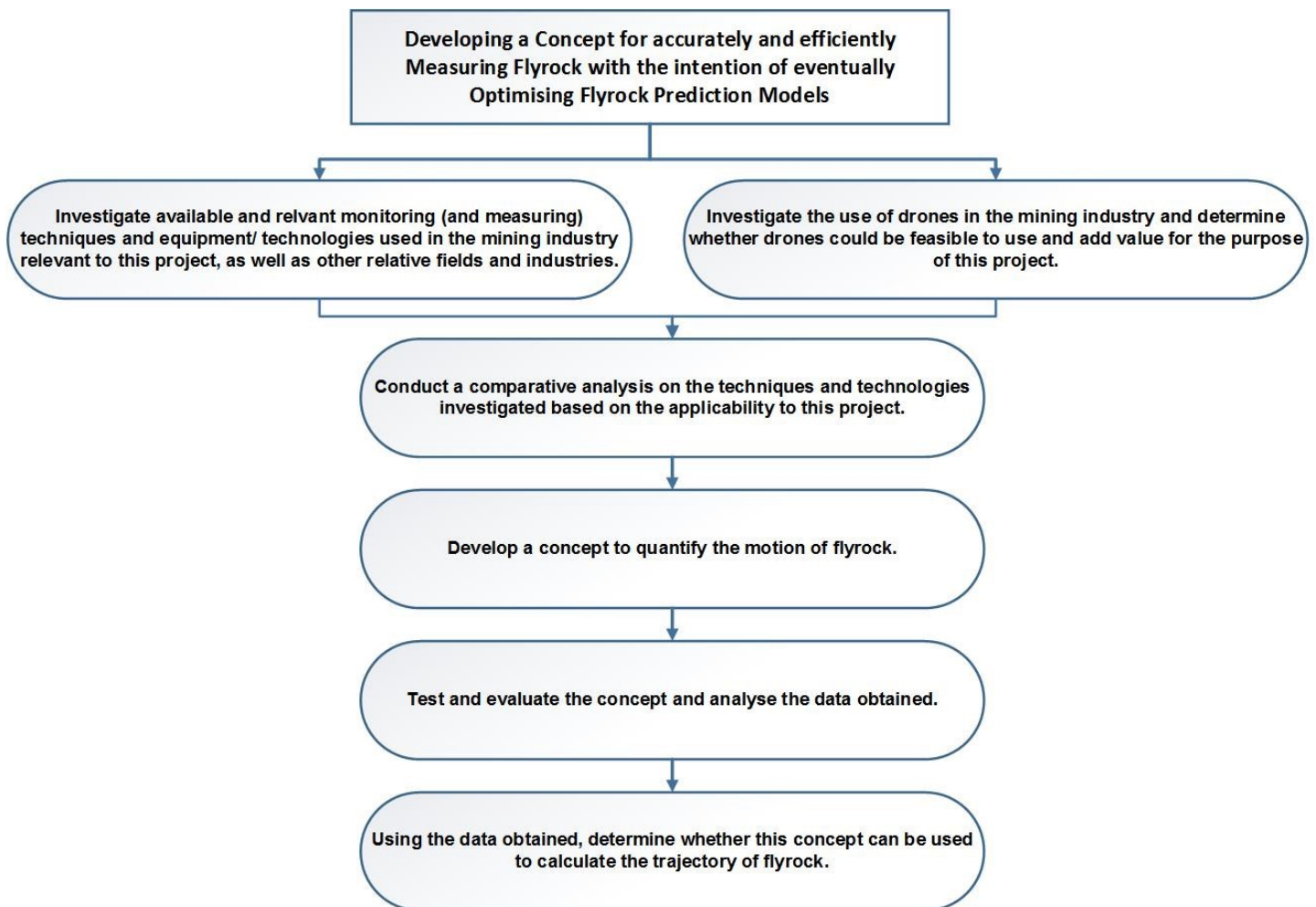


Figure 1.4: Proposed Research Approach and Project Flow

Table 1.3 indicates the objectives for this project and how each objective related to the next. Table 1.3 combines each research objective with the associated research methodologies used to successfully complete each of the project's objectives.

**Table 1.3: Research Objectives and related Methodology**

<b>Objective</b>	<b>Research Methodology</b>
<p>i. Investigate available and relevant monitoring (and measuring) techniques and equipment/ technologies used in the mining industry relevant to this project, as well as other relative fields and industries.</p>	<p><i>Information Gathering</i></p> <p>Information was collected by reviewing the literature available in the public domain. This purpose of this literature review was to identify methods that have already been used to measure flyrock in the mining industry as well as the measurement of projectiles in other industries.</p> <p>These methods include the measuring and analysis techniques and methodologies as well as the applicable technologies and equipment used.</p>
<p>ii. Conduct a comparative analysis of the techniques and technologies investigated based on the applicability to this project.</p>	<p><i>Comparative Analysis of Summarised Literature</i></p> <p>The information gathered during the literature review was summarised in order to ease the process of critically analysing the information contributing to the project. The various methods and technologies were directly compared to assist the subsequent evaluation between these methods and technologies, in order to identify the most viable approach.</p> <p><i>Evaluation and Comparative Analysis of the Techniques and Technologies in terms of relevance to this Project</i></p> <p>The summarised comparison was evaluated using a decision matrix based on specific criteria, which will be discussed in this report. The results of this evaluation were used to conduct a comparative analysis in order to identify the most viable approach for further investigation.</p>
<p>iii. Develop a concept that is</p>	<p><i>Consultation with Experts</i></p>

<p>able to quantify the motion (trajectory) of flyrock.</p>	<p>Since some of the topics and fields investigated in this project were unfamiliar, numerous experts had to be consulted in order to ensure that important information and data did not get lost in interpretation.</p> <p>These experts are acknowledged and thanked for their contributions.</p> <p><i>Critical Analysis of Information Gathered and Data generated from Previous Analyses.</i></p> <p>The results from the literature review and comparative analysis were used to develop a feasible concept that can be used to quantitatively measure flyrock.</p>
<p>iv. Test and evaluate the concept and analyse the data obtained.</p>	<p><i>Concept Tests (Controlled Tests in Controlled Environment)</i></p> <p>The concept tests are controlled tests in a controlled environment where variables can be managed and adjusted when needed. These concept tests were developed and executed with the assistance of Premier Mapping in order to develop the data collection and analysis section of the concept. Premier Mapping is a surveying- and mapping company, based in Cullinan (Premier Mapping (Pty) Ltd., 2015), with expertise in terrestrial surveying, photogrammetry and aerial survey techniques.</p> <p>It was important to identify key areas that could determine the success or failure of the application of the concept.</p> <p><i>Data Collection and Analysis</i></p> <p>Data was collected and analysed during these concept tests and was evaluated in order to prove or disprove whether the concept will be effective in the field.</p> <p><i>Software Development</i></p> <p>Since no existing software was available to process and</p>

		interpret the results obtained from the concepts test, new software needed to be written for this project.
v.	Using the data obtained, determine whether this concept can be used to calculate the trajectory of flyrock.	<p><i>Computations</i></p> <p>Once the concept was proven and the analysis process had been successfully developed, the resulting data could be used in computations using projectile motion principles and physics. These computations form the final step in obtaining the final coordinates of fragments thrown from a blast (and captured with the developed technique).</p> <p><i>Consultation with Experts</i></p> <p>Since some of the topics and fields investigated in this project were unfamiliar, numerous experts had to be consulted in order to ensure that important information and data did not get lost in interpretation.</p> <p>These experts are acknowledged and thanked for their contributions.</p>

### **1.3. PROJECT MOTIVATION SUMMARY**

Flyrock remains a major concern in blasting operations across the globe and holds the potential to result in significant financial and reputational penalties for mining companies. It is therefore imperative that the risk of flyrock be minimized and, ideally, entirely eliminated.

However, previous research studies have shown that the concept of flyrock is generally not well understood and the understanding of the effect of various blasting (causative) parameters in different circumstances is also limited. These previous investigations ultimately concluded by recommending that the prediction models should be reviewed and that the effect of the causative factors on the projection ranges of flyrock should be investigated further, in order to gain a detailed understanding of how these various parameters can affect the risk of flyrock.

Only once the effects of the causative factors are determined, can a new and revised predictive model be developed. The accuracy of the predicted maximum flyrock distances can then be increased by considering the various applicable factors specific to each blast and the impact of each factor.

In order to efficiently achieve this new predictive model, a large data-set is required. During a brief literature review, no specific method of quantitatively measuring flyrock could be identified. Flyrock have, to date, only been monitored through blast video footage and visual observation by observers of the blast. Some of these techniques are discussed further in Chapter 2.

For this reason, as well as the degree of technological advances in recent years, this investigation was aimed at developing a concept to accurately measure flyrock resulting from a blast. Only once flyrock, its origins and contributing factors can be accurately measured, will it be possible to develop an accurate predictive model that can be implemented in the mining industry.

Therefore, the main aim of this project was to develop a concept that can be used to quantitatively measure flyrock and its trajectory, in order to ultimately predict the final landing position of the fragments relative to the blast and its origins on the bench.

#### 1.4. REFERENCES

- Bajpayee, T. S. et al., 2003. Fatal Accidents Due to Flyrock and Lack of Blast Area Security and Working Practices in Mining. *Journal of Mines, Metals and Fuels*, November, 51(11/12), pp. 344-350.
- Chiappetta, R. F., 2014. *Optimizing your Drill and Blast Strategy*. Johannesburg, BAI: Blasting Analysis International Inc.
- de Graaf, W. W., 2016. *Blasting Engineering Programme: Module 5 (Flyrock)*. Pretoria, Enterprises (University of Pretoria).
- Glencore, 2017. *Blast Design and Flyrock monitoring* [Interview] 2017.
- IME, 1997. *Glossary of commercial explosives industry terms*. Safety Publication No. 12 ed. Washington DC: Institute of Makers of Explosives.
- ISEE, 2011. Chapter 15: Flyrock. In: J. F. Stiehr, ed. *Blasters' Handbook*. USA: International Society of Explosives Engineers, pp. 383-410.
- Olofsson, S. O., 1997. Bench Blasting: Throw, Flyrock. In: *Applied Explosives Technology for Construction and Mining*. Örebro: APPLEPLEX, pp. 110-114.
- Premier Mapping (Pty) Ltd., 2015. *Premier Mapping*. [Online] Available at: <http://www.premap.co.za/index.html> [Accessed 15 June 2018].
- Raina, A. K., Murthy, V. M. S. R. & Soni, A. K., 2015. Flyrock in Surface Mine Blasting: Understanding the Basics to Develop a Predictive Regime. *Current Science*, 108(4), pp. 660-665.
- Richards, A. B. & Moore, A. J., 2005. *Kalgoorlie Consolidated Gold Mines: Golden Pike Cut-Back - Flyrock Control and Calibration of a Predictive Model*, Eltham: Terrock Consulting Engineers.
- Tose, S. S. J., 2013. A Practical Approach to Managing Control of Flyrock. *ISEE 39th Annual Conference on Explosives and Blasting*, 10-13 February.



## 2. LITERATURE SURVEY

The main purpose of this project is to develop a concept that can be used to quantitatively measure flyrock resulting from a blast in order to determine the total travel distance of fragments from the blast. The importance of this distance is that it relates to the safety of the immediate area and its inhabitants. Damage to equipment, infrastructure, livestock and other company or community property will result in financial loss and potential penalties for the mine.

The motivation of this project is founded on the initial research conducted in 2016. A summary of this research has been presented in Chapter 1; however, key information is elaborated on in this chapter.

### 2.1. INITIAL RESEARCH AND MOTIVATION TO THIS PROJECT

#### 2.1.1. Sources of flyrock

“Sources of flyrock” refer to the specific areas of the bench or blast surface where the flyrock could originate from. Flyrock is often generated near any rock interfaces – i.e. along the free face or the collar area of the blast holes (ISEE, 2011). These rock interfaces are known as the source(s) of flyrock.

Three key mechanisms of flyrock are presented by Richards & Moore (2005) in a report published by Terrock Consulting Engineers. These three mechanisms are illustrated in Figure 2.1.

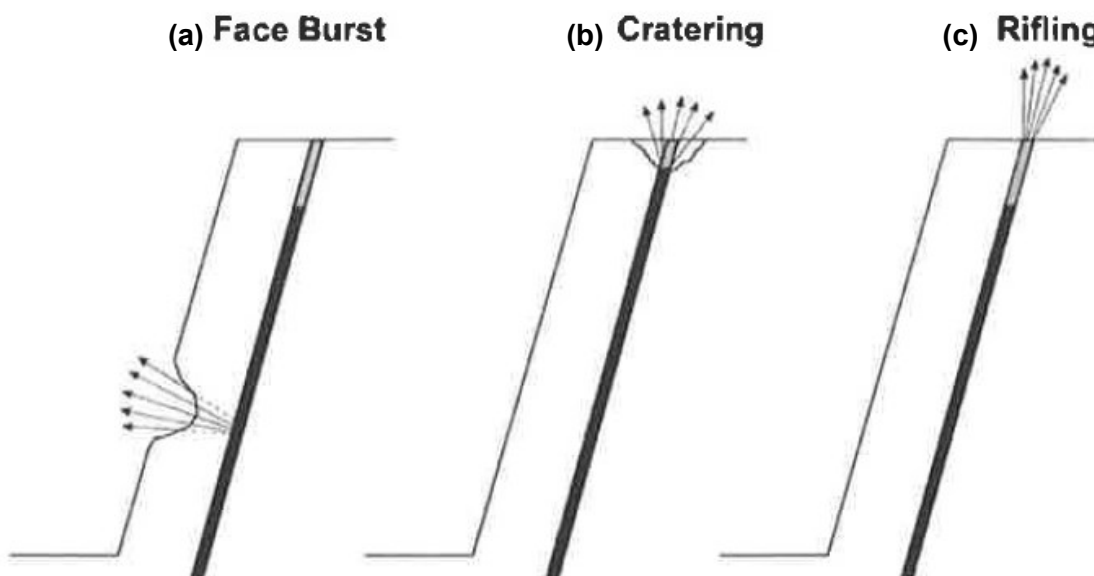


Figure 2.1: Three key mechanisms of flyrock (Richards & Moore, 2005)



(a) Face burst

This occurs at the free face of the blast surface and is directly linked to the burden conditions (Richards & Moore, 2005).

(b) Cratering

This occurs at the collar area of the blast hole. Cratering refers to the material thrown from the collar region due to insufficient stemming length or inadequate stemming material or weak rock around the collar area (Richards & Moore, 2005).

(c) Rifling

This occurs in the collar area when the stemming material is ejected from the blast hole or loose rocks on the collar surface is thrown by the blast (Richards & Moore, 2005).

Flyrock is also often generated during secondary blasting as well, i.e. when oversized rocks must be broken again by placing a charge on or in the boulder. Therefore, secondary blasting should be avoided by optimising the original blast fragmentation (ISEE, 2011).

### **2.1.2. Root causes of flyrock**

Flyrock is often referred to as being caused by a lack of adequate confinement of the explosives (ISEE, 2011). However, it is important to identify and understand all factors that may cause or contribute to flyrock in order to control it or eliminate the risk entirely.

These factors are divided into three main categories in the ISEE's Blasters' Handbook (2011), namely:

(1) Design Faults

Design faults refer to any error that may be present in the original blast design that is distributed to the drilling and blasting teams. Design factors such as Burden, Spacing, Hole Diameter, Powder Factor, Stemming Length, Stemming Material, Explosives Column Height, etc. are all included under this category or root cause (ISEE, 2011). The blast designs are executed according to industry rules-of-thumb, which have been determined through experimentation and "trial-and-error". However, these parameters can occasionally be manipulated as an attempt to optimise the blast design, seen during the initial field investigation. This could result in unwanted results such as poor fragmentation, excessive ground vibration, airblast, flyrock, back-break and over-break.

## (2) Deviations in Implementation

Deviations in implementation refer to the actual on-bench practice, i.e. how the blast plan or design is translated into practice (ISEE, 2011). A gap analysis can become significant at this point to determine how the “actual” deviates from the “ideal” i.e. blast design. The implementation of the blast design is not only linked to the discipline (or the human factor) of the teams on the bench but also the ability of the available equipment to execute the design, the specific bench conditions, the results of the previous blast and the communication of changes between the relevant parties.

## (3) Unforeseen Geological Conditions

Geology has a significant impact on the blast design as well as the blast results. A blast design is created according to the known geology and geological features or structures in the area that will be blasted. However, unknown or unforeseen geological conditions will influence the effectiveness of the blast (ISEE, 2011).

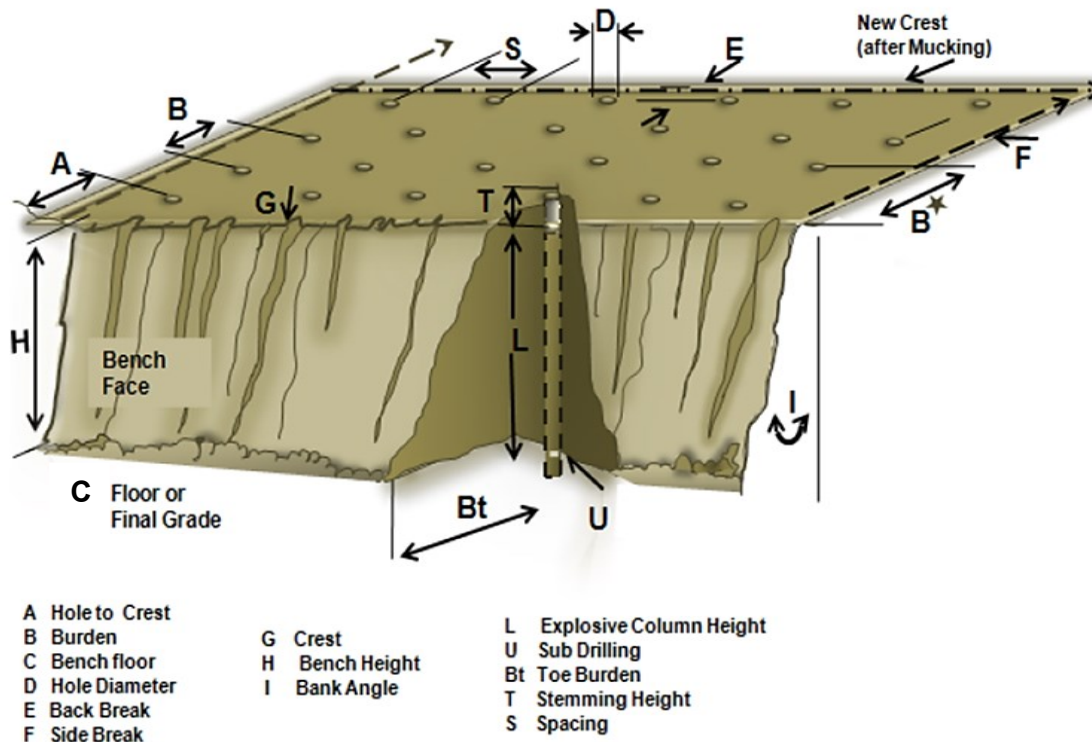
Some examples of the geological anomalies are (ISEE, 2011):

- Cavities in the blast hole, which can result in the hole being overcharged.
- Harder rock layers can result in oversized fragmentation or, depending on the location of these layers, could result in capping (if the layer is towards the bottom of the bench).
- Weaker or weathered rock material towards the top of the bench could result in excessive flyrock from the collar area.

These three root causes are only categories where errors may occur that could result in flyrock. These categories must be considered during each step of the drilling and blasting cycle.

### **2.1.3. Drilling and blasting factors that can contribute to flyrock**

The term “drilling and blasting factors” refers to the components of a blast design that needs to be calculated individually, typically according to the industry rules-of-thumb. A descriptive schematic of these blast design parameters is shown in Figure 2.2.



**Figure 2.2: Surface blast design parameters (de Graaf, 2016)**

The parameters illustrated in Figure 2.2 are the individual elements of any blast design. These parameters are described in the ISEE Blasters' Handbook (2011). A brief discussion on how specific blast parameters are generally expected to influence flyrock is given in Appendix A. The interdependency of these design parameter, inherently created through the rules-of-thumb, are illustrated in Figure 1.2. This relation between the parameters must be considered when altering one parameter in the design.

When evaluating a blast design, the desired results must be considered. The potential negative outcomes should also be considered as well as which design parameters contribute to which outcome and to what degree. Raina et al. (2015) summarised the possible blast results and categorised each according to its nature and mine-to-mill objective, presented in Table 2.1.

**Table 2.1: Blast outcomes, nature and objectives (Raina, et al., 2015)**

Blast Result	Nature	Comments	Mine-to-Mill Objective	Other Constraints
Fragmentation	Regular	Desired	Optimize	<ul style="list-style-type: none"> <li>• Geo-mining conditions</li> <li>• Presence of inhabitants in the area</li> <li>• Small working area</li> <li>• Production scheduling</li> </ul>
Throw (Heave)	Regular	Desired	Optimize	
Ground vibration	Regular	Undesired	Minimize	
Air overpressure and noise	Regular	Undesired	Minimize	
Toxic gasses and fumes	Regular	Undesired	Minimize	
Flyrock and excessive throw	Random	Undesired	Eliminate	
Back break	Random	Undesired	Minimize	

Flyrock is listed as an undesirable outcome which is random and should ultimately be eliminated as a blasting outcome. Since flyrock is considered to be random in nature, predicting when and how it will occur is a very difficult task. Thus, understanding these blast results and how the design parameters contribute to these results can ultimately improve the mine’s ability to optimize their blast design.

In addition to the factors discussed, Roth (1979) suggests that the type of explosives can influence the projection distance of material from a blast. Roth (1979) explains that “slurry-type” explosive can potentially generate higher projection distances. However, this is not necessarily due to the increased velocity of detonation (VoD) but rather due to the higher densities compared to ANFO.

#### **2.1.4. Flyrock predictive models**

Flyrock prediction models have been developed since the 1970s. The most well-known model for predicting the maximum throw resulting from a blast in an open-pit mine is presented by Lundborg, et al. (1975). Lundborg, et al. (1975) developed this model by observing and measuring a series of crater blasts and diligently documenting the results.

The resulting equation is known as the SveDeFo Equation and presented as (Lundborg, et al., 1975):

**Equation 2.1: SveDeFo Equation for predicting maximum projection range of flyrock (ISEE, 2011)**

$$\text{Maximum Projection Range} = 30 \times d_e^{0.667}$$

With:

Maximum projection range is given in meters [m]

$d_e$  = Charge diameter in millimeters [mm]

It is important to note that this model and equation is based on crater blasting. Crater blasting refers to the practice of charging shallow blast holes, using either very little stemming or none at all. Equation 2.1, therefore, presents a “worst-case” projection of material from a blast. These distances are not typical for normal bench blasting. (Bench blasting combines deeper blast holes and with increased stemming or confinement, resulting in an increased degree of burial of the explosives.) Due to the increased burial of the explosives charge as well as the increased confinement, Lundborg, et. al. (1975) emphasized that the maximum projection range during normal bench blasting would be approximately one-sixth ( $1/6^{\text{th}}$ ) of the range determined with the presented equation.

Additional versions of this model are often used by AEL and Sasol, presented in Chapter 1. However, the exact deduction from Lunborg, et. al. (1975)’s original equation is unclear.

Another recognised prediction model is presented by Chiappetta & Treleven (1997) and is known as the “Scaled Depth of Burial”. The ISEE (2011) defines the scaled depth of burial (SDoB) as *“the length of stemming plus half the length of charge contributing to the cratering effect, divided by the cube root of the weight of explosive contained within the portion of charge contributing to the cratering effect”*.

In essence, the SDoB is the relation between the confinement of the explosives (specifically stemming length) and the amount of explosives that will contribute to the cratering effect at the collar region of the blast hole, i.e. the top section of the hole up to a depth equal to 8 to 10 hole diameters (Chiappetta & Treleven, 1997).

The SDoB equation given by ISEE (2011) includes the stemming length, hole diameter, contributing charge length factor and explosive density as the inputs for the equation, given in Equation 2.2.

**Equation 2.2: Scaled Depth of Burial Equation (ISEE, 2011)**

$$SDoB = \frac{T + 0.0005 \times m \times d}{0.00923 \times (m \times d^3 \times \rho_e)^{0.333}}$$

With:

SDoB = Scaled Depth of Burial [m/kg<sup>1/3</sup>]

T = Stemming length [m]

d = Blast hole diameter [mm]

m = Contributing charge factor\* (8 x d, for d < 100 mm or 10 x d, for d > 100mm)

$\rho_e$  = Explosive's density [g/cc]

*(\*The contributing charge factor (m) has a maximum value of eight (8) hole diameters for blast holes with a diameter less than 100 mm; and a maximum value of ten (10) hole diameters for blast holes with a diameter greater than or equal to 100 mm (Chiappetta & Treleven, 1997))*

Chiappetta (2014) presents a simplified equation for the SDoB during a workshop at the IQPC Drill and Blast Africa seminar in 2014. This equation delivers the same value for the SDoB as Equation 2.3 and illustrated in Figure 2.3. This simplified SDoB equation is:

**Equation 2.3: Simplified Scaled Depth of Burial (Chiappetta, 2014)**

$$SDOB = \frac{D}{W^{1/3}}$$

With:

SDOB = Scaled Depth of Burial [m/kg<sup>1/3</sup>]

D = Distance from the surface to the centre of the stem charge [m]

W = Mass of explosives equivalent to 10 explosive diameters [kg]

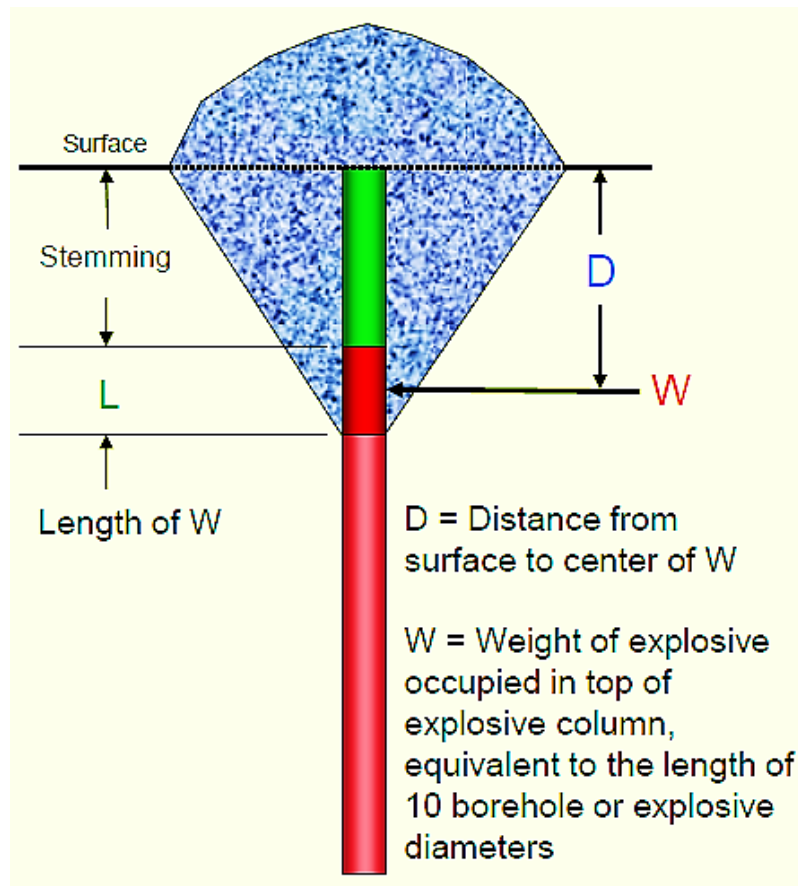


Figure 2.3: Illustration of Equation 2.3 (Chiappetta, 2014)

The effect of the SDoB is illustrated in Figure 2.4. The SDoB proves that deeper burial of an explosive charge will result in less energy available to move towards the top of the blast hole, resulting in lower projection velocities of ejected material. Lower projection velocities will reduce the projection range of the materials ejected during a blast and ultimately decrease the overall risk of flyrock.



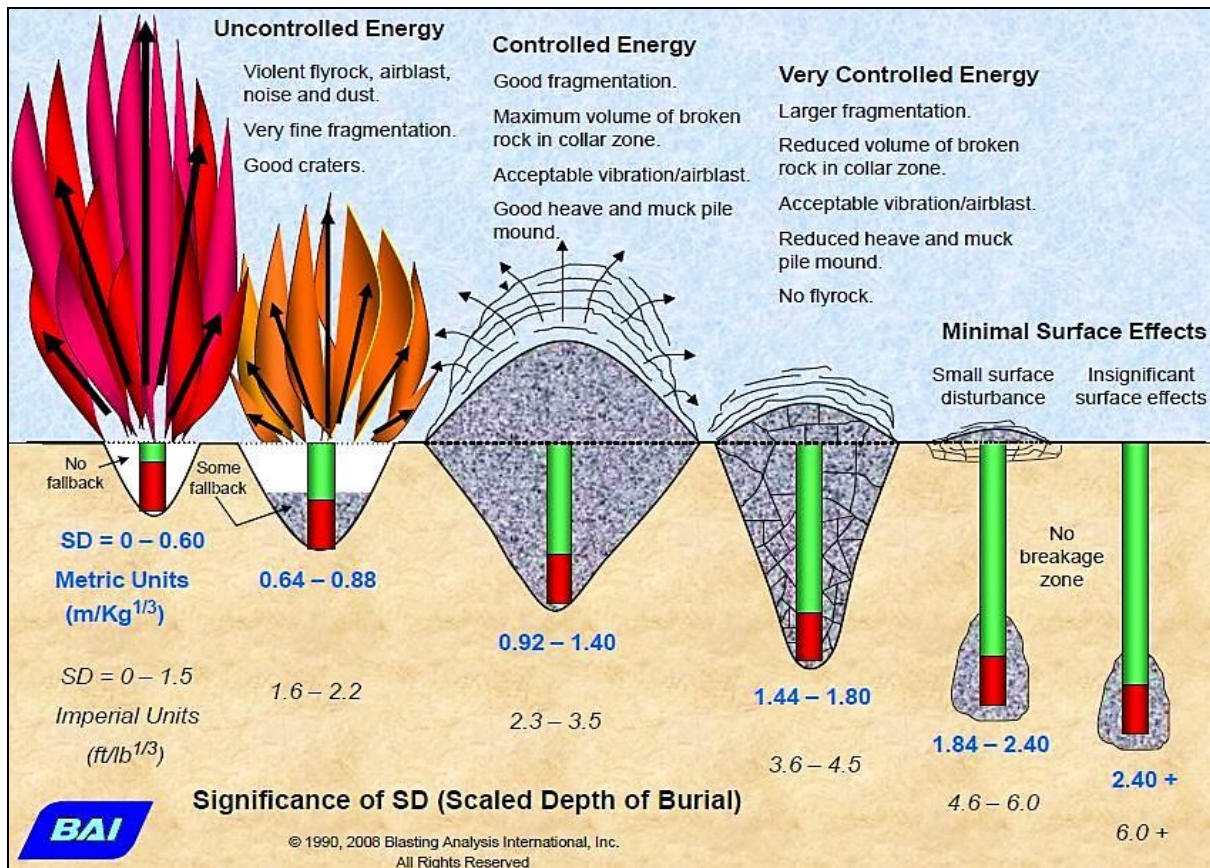


Figure 2.4: Scaled Depth of Burial (Chiappetta & Treleven, 1997)

ISEE (2011) suggest that the SDoB should always have a value greater than 1 m/kg<sup>1/3</sup> and should be increased when blasting operations approaches sensitive areas. However, when considering all the performance measurements are taken into account in a post-blast evaluation (i.e. fragmentation, throw, back-break, flyrock, etc.), the ideal SDoB value lies between 0.92 and 1.40, depending on the desired outcome of the blast.

The SDoB is only a factor indicating the relationship between the confinement of explosives and the contributing mass of explosives. Determining the projection range requires the consideration of additional factors. McKenzie (2009) used the SDoB concept and replaced the original equation for the maximum projection range, the SveDeFo Equation (Equation 2.1), by considering the launch velocity, rock properties and size. McKenzie (2009) presents a more universally applicable equation, Equation 2.4.

Equation 2.4: Maximum projection range including Scaled Depth of Burial (McKenzie, 2009)

$$\text{Maximum projection range} = 11 \times SDoB^{-2.167} \times d^{0.667}$$



These models are ultimately used to determine the safe blast area of the blast.

The prediction models have, however, been developed based on field observation and the measurement and analysis of observed blasts. These models are still not an exact science and should be used with particular care given to the specific blast site's characteristics since a number of "causative" blast parameters are still not linked to any prediction model.

Raina et al. (2015) demonstrated this disconnection between the predictive models and the flyrock causative factors. These causative parameters and parameters considered in the predictive models are compared in Table 2.2 and are graphically represented in Chapter 1 (Figure 1.3).

**Table 2.2: Comparison between causative factors and their use in flyrock distance prediction (Raina, et al., 2015)**

Causative parameters		Predictive parameters	
Parameter	Citations	Parameter	Citations
Burden	13	Stemming	10
Geology	13	Specific charge	8
Stemming	10	Hole depth	7
Excessive explosives	6	Burden	6
Inadequate delay	6	Spacing	6
Improper layout	5	Blast hole diameter	6
Poor confinement	4	The density of the rock	5

Raina et al. (2015) concluded that there are major research gaps in flyrock prediction and questions the overall understanding of the flyrock-concept. This conclusion supports the motivation for this project.

## **2.2. TECHNIQUES OR CONCEPTS THAT HAVE PREVIOUSLY BEEN USED TO MEASURE, ESTIMATE OR MODEL (PREDICT) FLYROCK**

Most of the work done in the field of flyrock since 2010, has focussed on the prediction of flyrock. The techniques used in these studies and the conclusions reached are discussed in this section. The outcome of some of these studies contributed to the final analysis of the various concepts and technologies that are available for use in this project.

### **2.2.1. Artificial intelligence (AI)**

Artificial intelligence (AI) is a term that has been used since the 1950s but has only recently become a popular subject among the general public. AI is defined as “*the science of training machines to perform human tasks*” (SAS Institute Inc., 2019).

AI techniques (specifically artificial neural networks (ANN) and adaptations thereof) have been implemented to study and predict flyrock resulting from a blast, however, any AI system is dependent on the quality of its input data. Further discussion on AI principles is given in Appendix A.

Since this input data is only qualitative, the accuracy of the output will still vary. However, the techniques used in these studies were investigated and are briefly discussed in the following sections.

#### **2.2.1.1. Flyrock research based on AI principles**

Numerous authors have presented concepts and techniques to predict or estimate flyrock or flyrock-related factors with AI principles. The main consistency between these proposed concepts or techniques is that the output or result of the system is highly dependent on the quality of the input parameters and the accuracy of the estimation of these parameters. Note that the details pertaining to the algorithms used in these concepts or techniques are not discussed in detail. This section only serves as an overview of the work conducted as an attempt to predict flyrock.

- (1) Monjezi, et al. (2010) published a paper titled “*Prediction of flyrock and back-break in open pit blasting operation: a neuro-genetic approach*” with the main objective being to develop a neuro-genetic model to predict flyrock and back-break. The motivation for this study was the poor predictions resulting from the existing empirical models at that time. The authors used a feed-forward ANN (with a 9-16-2 architecture) as the

basis for their model and incorporated a genetic algorithm (GA) as an attempt to optimise the network parameters (Monjezi, et al., 2010).

The input parameters and their ranges that were considered in the proposed model are presented in Table 2.3 (Monjezi, et al., 2010):

**Table 2.3: Model input parameters and their ranges (Monjezi, et al., 2010)**

Input Parameter	Symbol	Unit	Range
Hole diameter	D	mm	75 - 115
Hole length	L	m	6 - 16
Spacing	S	m	3 - 6.5
Burden	B	m	2.5 - 5
Stemming length	T	m	2 - 4.5
Powder factor	Pf	kg/ton	0.11 - 0.95
Specific drilling	SD	m <sup>3</sup> /m	0.01 - 0.29
Charge mass per delay	Ch	kg	14.5 - 296
Rock mass rating	RMR	-	36 – 47

The study concluded that the prediction results from the proposed model correlated with the measured flyrock distances. However, the methodology on how these measurements were taken and the accuracy thereof was not discussed in the article. The neuro-genetic ANN model proved to be superior to the existing empirical and statistical models. Stemming length and powder factor were concluded to be the most influential parameters (Monjezi, et al., 2010).

- (2) In 2012, an article titled “*Evaluation of the effect of blast design parameters on flyrock using ANN*” was published by Monjezi, et al. (2012). The main purpose of this study was to develop an ANN that is able to predict flyrock and compare the outcomes with existing empirical and statistical models, as well as investigate the influential input parameters. The motivation behind this study is the insufficient prediction capabilities of these existing models (Monjezi, et al., 2012).

A model was developed using a feed-forward ANN with a 9-5-2-1 architecture. Similar input parameters were used compared to the aforementioned study.

However, since the objective was to identify the influential parameters, some of the parameters were designed to be outputs of the system, along with flyrock (Monjezi, et al., 2012). These parameters are summarised in Table 2.4.

**Table 2.4: Input and output parameters of the proposed system (Monjezi, et al., 2012)**

<b>Input Parameter</b>	<b>Symbol</b>	<b>Unit</b>	<b>Range</b>
<b>Burden</b>	B	m	2 – 5
<b>Spacing</b>	S	m	2.5 - 6.5
<b>Charge mass per delay</b>	Ch	kg	10 – 71.33
<b>Hole diameter</b>	D	mm	76 - 152
<b>Hole depth</b>	L	m	3 – 18
<b>Output Parameter</b>			
<b>Stemming length</b>	T	m	1.6 – 4
<b>Specific drilling</b>	SD	m <sup>3</sup> /m	0.09 - 0.23
<b>Powder factor</b>	Pf	kg/ton	0.1 - 1.29
<b>Rock mass rating</b>	RMR	-	37 – 47

The study concluded by comparing the predicted flyrock with the measured flyrock. Again, the methodology followed to obtain these measurements or the accuracy thereof were not discussed in the article. Similar to the 2010 publication, the ANN model was determined to be superior to the existing empirical and statistical models. Finally, the key influential parameters, based on this model, were identified as the powder factor, blast-hole diameter, stemming length and charge mass per delay (Monjezi, et al., 2012).

- (3) In 2013, Raina, et al. (2013) published an article investigating the influence of the shape on the travel distance of flyrock. The motivation for the study is that kinematic equations can be difficult to apply to flyrock in different environments due to the uncertainty of air resistance based on the weight, size and shape of a fragment (Raina, et al., 2013). Air resistance or drag form an essential component of motion analysis based on kinematic principles and can, therefore, not be neglected.

The main objective in this study was to analyse the effect of the shape of a fragment on the travel distance of flyrock using ANN's.

The developed ANN model was made up of a 7-20-14-8-1 architecture. This model was developed based on the data collected from 75 test blasts, i.e. 75 concrete blocks were blasted with a single hole and varying blast parameters in an attempt to identify the influence of these parameters (Raina, et al., 2013). The input parameters to this model were the initial velocity of the fragment, launch angle, sphericity and the weight, length, width and thickness of the fragment.

The initial velocity, launch angle and weight of individual fragments were considered key parameters in this investigation. However, it was concluded that these are difficult to estimate in field conditions and further research and investigations were required (Raina, et al., 2013).

Ultimately, Raina, et al. (2013) mentioned that the effect of external factors such as the velocity of the air and specific weather conditions should also be investigated to determine the effect thereof on the flyrock travel distance.

- (4) Ghasemi, et al. (2014) published an article titled "*Application of artificial intelligence techniques for predicting the flyrock distance caused by blasting operation*" with the same motivation as the previous two publications. The aim of the study was to develop and compare two predictive models based on AI concepts (Ghasemi, et al., 2014).

The first model, based on ANN, was a feed-forward network with a 6-9-1 architecture (Ghasemi, et al., 2014).

The second model, based on ANFIS, is described as consisting of "triangular, trapezoidal membership functions" and is based on a Mamdani algorithm (Ghasemi, et al., 2014).

Both models were presented with six input parameters, i.e. blast-hole length, burden, spacing, stemming length, powder factor and charge mass per delay. The results showed that both models are able to yield accurate predictions when compared to the measured flyrock (Ghasemi, et al., 2014). This is, however, dependant on the accuracy and reliability of the measured flyrock. Similar to the previous two

publications, there is no discussion relating to the measurement methodology. The ANFIS method proved to be a better method, but the ANN still produced accepted results and was concluded to be a “good tool to minimise uncertainties” (Ghasemi, et al., 2014).

- (5) Marto, et al. (2014) conducted a study titled “*A novel approach for blast-induced flyrock prediction based on an imperialist competitive algorithm (ICA) and artificial neural network*”. The main objective was to predict flyrock by combining ANN’s and ICA to produce a novel ICA-ANN prediction model.

Seven input parameters were identified and determined to be influential to the system. These parameters are the blast-hole depth, burden-to-spacing ratio, stemming length, maximum charge mass per delay, powder factor, rock density and the Schmidt hammer rebound number (Marto, et al., 2014).

The data from 113 blasts were recorded and the flyrock measured, but no discussion on the measurement methodology was presented. Predictions were first evaluated against the measured flyrock. The prediction results from the developed ICA-ANN model was compared to that of other pre-developed ANN models and multiple regression analysis (MRA) results (Marto, et al., 2014).

The proposed ICA-ANN model did yield a tighter scatter of data points, which implies that it presents an improved prediction capability compared to the other models. Marto, et al. (2014) concluded their study by stating that the models are dependent on the accuracy of the input parameters.

- (6) In 2015, a study titled “*Prediction of blast-induced flyrock in open-cast mines using ANN and ANFIS*” was conducted by authors Trivedi, R; Singh, T N; and Gupta, N. the main objective for this study was to predict flyrock using ANN and ANFIS approaches. Both approaches were given the same input parameters, namely linear charge mass, burden, stemming length, specific charge, unconfined compressive strength and rock quality (Trivedi, et al., 2015).

The proposed models are evaluated with data collected from 125 blasts. Similar to the previous publications, the predictions from the proposed models were evaluated against the measured flyrock. Trivedi, et al. (2015) described the measurement process as visual observation of the blast and measuring the landing positions with a

hand-held GPS. High-speed cameras were used to record the blasts and estimate parameters such as initial velocities and launch angles (Trivedi, et al., 2015).

Trivedi, et al. (2015) concluded that the ANFIS approach produced better results compared to the ANN model.

- (7) Armaghani, et al. (2016) proposed a method to predict flyrock using an empirical approach. The motivation for conducting this study was that the existing empirical models are not sufficient due to the complex nature of flyrock (Armaghani, et al., 2016). ANN and ANFIS models were also developed in an attempt to reduce the uncertainties and solve the complex, non-linear functions derived by an empirical approach.

In the investigation, Armaghani, et al. (2016) presented two empirical formulas that have been published by other authors. However, these empirical equations are often site-specific and can not be used as a universal prediction model.

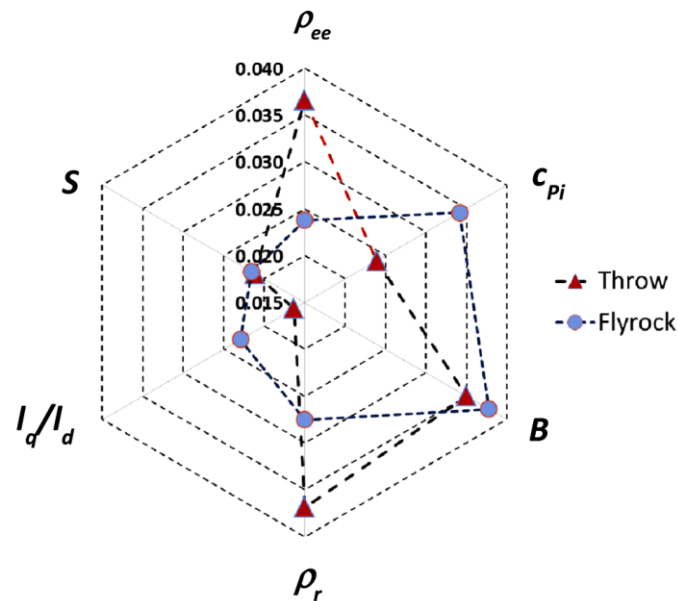
Armaghani, et al. (2016) developed an empirical graph, with the maximum charge per delay and powder factor as the two main influential parameters. However, this study also concluded in favour of AI techniques, such as ANN and ANFIS, as superior methods when developing a prediction model (Armaghani, et al., 2016).

- (8) Raina & Murthy (2016) presented their study titled "*Importance and sensitivity of variables defining throw and flyrock in surface blasting by ANN method*", with the aim of identifying the significance of the different parameters used in flyrock prediction.

Blasts data was collected from ten mines and a database was created. This database was analysed by means of ANN software, EasyNN-Plus®, in order to design, train and validate a suitable ANN model (Raina & Murthy, 2016). A feed-forward ANN model with a 20-16-6-4-1 architecture was suggested as an optimised network.

The key input parameter for this model was identified as burden (B), spacing (S), P-wave (primary wave) velocity ( $c_{pi}$ ), the density of the rock ( $\rho_r$ ), the effective in-hole density of the explosives ( $\rho_{ee}$ ) and the charge length to hole depth ratio ( $l_q/l_d$ ) (Raina & Murthy, 2016).

The study concluded with a spider graph illustrating the relative importance and sensitivity of the various input parameters. This graph is given in Figure 2.5.



**Figure 2.5: The relative importance and sensitivity of the variables for throw and flyrock (Raina & Murthy, 2016)**

A number of studies have been briefly summarised. The main conclusion drawn from all of these investigations is that implementing AI principles in prediction models yielded improved results compared to the existing empirical models. However, it is very important to note that any of the aforementioned ANN or ANFIS models are highly dependent on the quality and accuracy of the input parameters.

The methodologies followed to measure the “actual” flyrock distance are not elaborated on in any of the publications. Since each proposed method was evaluated against these measurements, some of the presented results and conclusions come into question based on the uncertainty regarding the accuracy of these measurements.

### 2.2.2. Rock engineering systems-based model

Rock engineering system (RES) was first presented by Hudson (1992) and is described as a methodology capable of simultaneously analysing various parameters (Faramarzi, et al., 2014).

Faramarzi, et al. (2014) describes this as an interaction matrix that represents the various relevant parameters and their relations. Hudson (2014) mentions that the effective



parameter that drives specific circumstances are selected and the interaction between these parameters are considered in the matrix. The purpose is to reduce the uncertainty in the system by evaluating the interaction of these parameters to determine the degree of influence of each parameter on the overall system.

This degree of influence of each parameter is described by allocating weights, also known as coding, to the matrix. This can ultimately be used to derive a cause-and-effect graph from the system. Additional detail regarding RES is redundant relative to the scope of this project, however, this approach may hold some potential in minimising the uncertainties relating to flyrock and flyrock prediction.

#### **2.2.2.1. Flyrock research based on rock engineering principles**

Only one publication could be identified implementing this method to predict flyrock. Faramarzi, et al. (2014) published an article titled “*Development of rock engineering systems-based models for flyrock risk analysis and prediction of flyrock distance in surface blasting*”. The aim of modelling the risk associated with flyrock and attempt to predict flyrock based on the RES methodology.

In this study, the authors used the data collected from 57 blasts and applied 13 parameters as inputs to the system. These input parameters are the burden, the maximum instantaneous charge, powder factor, spacing-to-burden ratio, stemming-to-burden ratio, stiffness factor, time delay, blast-hole diameter, the velocity of detonation (VoD), blast-hole deviation, burden-to-hole diameter ratio and RMR (Faramarzi, et al., 2014). Most of these parameters were measured on the bench with a measuring tape.

Flyrock travel distance was the only output of the system. These distances were measured after each blast which was used to evaluate the performance of the proposed RES against. Faramarzi, et al. (2014) explained the measuring methodology as properly cleaning the mine area prior to the blast, visually observing the flight path of the rock fragments and measuring the landing positions with a hand-held GPS.

The paper was concluded by stating that the RES methodology is superior to other methods such as the multivariable regression analysis model, and performed better in its predictive capability. However, similar to most of the proposed predictive models, the RES model presented in this study was site-specific and cannot be used as a generalised solution (Faramarzi, et al., 2014).

### **2.2.3. Empirical- and statistical analysis**

Empirical and statistical analysis have been the foundation of most of the prediction approaches since the 1980s. Lundborg, et al. (1975) published one of the first papers that considered an empirical approach in an attempt to predict the maximum throw resulting from a blast. Unfortunately, due to the vast number of variables and uncertainties that influence flyrock, modelling based on empirical approaches have not been favoured in recent studies. However, some researchers still conduct studies based on this approach.

#### **2.2.3.1. Flyrock research based on an empirical- and statistical analysis**

Empirical and statistical approaches to develop flyrock prediction models have been proposed since the early 1980s. However, due to the significant progress in technology development over the past two decades, only recent concepts and techniques proposed (i.e. publications from 2010) are summarised for the purpose of this project.

- (1) Ghasemi, et al. (2012) published an article titled "*Development of an empirical model for predicting the effects of controllable blasting parameters on flyrock distance in surface mines*" with the goal of developing an empirical prediction model for flyrock. The authors used data collected from 150 blasts and analysed this data based on a dimensional analysis approach (Ghasemi, et al., 2012). The large dataset (150 blasts) presented the advantage of improving the overall accuracy of the system. However, all of the blasts were from a single mining operation and the results of this study can be considered to be very site-specific.

The data collected formed the input parameters to the dimensional analysis and include the burden (B), spacing (S), stemming length (St), blast-hole length (H) and diameter (D), powder factor (P) and mean charge mass per delay (Q). The measurements of these input parameters were taken on the bench using a measuring tape (Ghasemi, et al., 2012).

The flyrock distances were also measured as evaluation criteria for the proposed model. The measurement data was acquired through visually observing the flyrock thrown from a blast and measuring the landing positions with a hand-held GPS. The fragments that were thrown the farthest distance from the blast, based on this measuring technique, were measured to be 10cm in diameter (Ghasemi, et al., 2012).

Ghasemi, et al. (2012) proposed a model based on the assumptions that the influential parameters discussed above, resulting in a flyrock function:

- Flyrock distance ( $F_d$ ) =  $f(B, S, St, H, D, P, Q)$

This function resulted in the empirical formula for predicting flyrock distance given in Equation 2.5 (Ghasemi, et al., 2012)

**Equation 2.5: Empirical equation for predicting flyrock proposed by Ghasemi, et al. (2012)**

$$F_d = 6946.547 [B^{-0.796} \cdot S^{0.783} \cdot S_t^{1.994} \cdot H^{1.649} \cdot D^{1.766} \cdot \left(\frac{P}{Q}\right)^{1.465}]$$

With      B = burden  
               S = Spacing  
               St = Stemming length  
               H = Blast-hole length  
               D = Blast-hole diameter  
               P = Powder factor  
               Q = Mean charge mass per delay

It is important that, again, this model is very site-specific. The validity of this equation was evaluated by means of Monte Carlo simulations. However, the authors noted that the validity of this prediction model is dependent on the range of the data and the quality of the samples and measurements taken (Ghasemi, et al., 2012).

Ghasemi, et al. (2012) concluded by stating that, based on the sensitivity analysis conducted, the stemming length, spacing, blast-hole length and diameter and the powder factor showed a direct influence relationship to the flyrock distance. Whereas, the burden and mean charge mass per delay showed an indirect influence relationship to flyrock distance. This was a confusing result since the logical argument would be that burden and charge mass per delay should directly influence the distance travelled by rock fragments (Ghasemi, et al., 2012). This confusion can potentially indicate a flaw in the proposed system.

- (2) Armaghani, et al. (2016) conducted a study titled "*Risk assessment and prediction of flyrock distance by combined multiple regression analysis (MRA) and Monte Carlo simulations of quarry blasting*". The main purpose of this study was to develop a prediction model based on MRA and simulate flyrock using Monte Carlo (or probability) simulations (Armaghani, et al., 2016).

The study included data collected from 62 blasts and input parameters were measured by means of a measuring tape. These input parameters are the burden (B), spacing (S), stemming length (ST), blast-hole depth (HD), maximum charge mass per delay (MC), the powder factor (PF) and RMR (Armaghani, et al., 2016). Similar to the paper summarised previously, the flyrock was measured by cleaning the blast area prior to the blast, visually observing the flyrock thrown from the blast and recording the landing positions with a hand-held GPS (Armaghani, et al., 2016).

In order to run simulations of flyrock using Monte Carlo simulations, an empirical equation is required to describe the relationship between the input parameters and the output. Armaghani, et al. (2016) therefore used software (SPSS, version 16) to generate this empirical equation, based on MRA. The resultant equation is given in Equation 2.6.

**Equation 2.6: Empirical flyrock equation presented by Armaghani, et al. (2016) using MRA**

$$F_d = 177.81 - (3.33 \times HD) - (2.55 \times S) - (3.49 \times B) - (13.93 \times ST) + (0.47 \times PF) + (1 \times MC) - (2.58 \times RMR)$$

With

- $F_d$  = Flyrock distance
- B = Burden
- S = Spacing
- ST = Stemming length
- HD = Blast-hole depth
- MC = Maximum charge mass per delay
- PF = Powder factor
- RMR = Rock Mass Rating

The primary goal of the Monte Carlo simulations is to quantitatively determine the uncertainties and variabilities when exposed to certain risks. The secondary goal is to investigate the major drivers of this uncertainty and variability (Armaghani, et al., 2016).

The results in this study are presented in favour of the empirical equation based on MRA above previously published empirical models. The Monte Carlo simulations presented promising results; however, the credibility of these results is highly dependent on the quality of the input parameters. Finally, the authors concluded that the powder factor was the most influential parameter (Armaghani, et al., 2016).

It is important to note that, similar to the previously proposed models, this model remains site-specific and is not a generalised solution.

- (3) In 2017, a study titled “*Prediction of blast-induced flyrock using differential evolution algorithm*” was published by authors Dehghani & Shafaghi. The motivation for this study was the insufficient predictive capability of the existing empirical models. Therefore, the main objective of this study was to predict flyrock using a combination of differential evaluation algorithms (DE) and dimensional analysis algorithms (DA) (Dehghani & Shafaghi, 2017).

DA is defined as an engineering method that is used to create equations that will satisfy the analysis of complex multivariable systems (Dehghani & Shafaghi, 2017). An example of this algorithm is given in Appendix A.

DE is defined as an optimization algorithm based on the evolution strategy of individuals in a population (Dehghani & Shafaghi, 2017). An example of this algorithm is given in Appendix A.

The methodology of this study was to collect data from 300 blasts and measure and record both the input parameters and the flyrock resulting from the blast (Dehghani & Shafaghi, 2017). The input parameters considered were the blast-hole diameter (D) and length (L), number of blast-holes (NB), spacing (S), burden (B), ANFO charge mass (Q), stemming length (St), powder factor (PF) and specific drilling (SD) (Dehghani & Shafaghi, 2017). Data collection is conducted in the same manner as in the previous studies discussed.

The resulting equation obtained from DA is presented in Equation 2.7.

**Equation 2.7: Empirical equations developed using DA (Dehghani & Shafaghi, 2017)**

$$F_d = \exp(-16.569) \left( \frac{Q}{PF} \right)^{2.457} . D^{1.484} . L^{-2.315} . NB^{-2.453} . S^{-4.057} . B^{109.606} . St^{-117.001} . SD^{-3.523}$$

- With
- F<sub>d</sub> = Flyrock distance
  - D = Blast-hole diameter
  - L = Blast-hole length
  - NB = Number of blast-holes

S = Spacing  
 B = Burden  
 Q = ANFO charge mass  
 St = Stemming length  
 PF = Powder factor  
 SD = Specific drilling

The resulting equation obtained from DE is presented in Equation 2.8.

**Equation 2.8: Empirical equations developed using DE (Dehghani & Shafaghi, 2017)**

$$F_d = \exp(0.394) \left( \frac{Q}{PF} \right)^{0.06} \cdot D^{0.59} \cdot L^{0.26} \cdot NB^{0.4} \cdot S^{0.39} \cdot B^{0.51} \cdot St^{-0.32} \cdot SD^{0.33}$$

With  $F_d$  = Flyrock distance  
 D = Blast-hole diameter  
 L = Blast-hole length  
 NB = Number of blast-holes  
 S = Spacing  
 B = Burden  
 Q = ANFO charge mass  
 St = Stemming length  
 PF = Powder factor  
 SD = Specific drilling

Both of these equations are site-specific.

Dehghani & Shafaghi (2017) concluded the study by stating that the DE equation yielded more accurate results than the DA equation. However, a sensitivity analysis showed that the powder factor and stemming length are the most influential parameters for both models. Dehghani & Shafaghi (2017) recommends further research to investigate the principles of physics, incorporation of the pressure measured in the rock, trajectory motion in the air and the influence of flyrock size and shape on the travelling distance.

(4) The final article in this section was published in 2017 and is titled “*Development of a precise model for prediction of blast-induced flyrock using regression tree technique*”. The regression tree technique is broadly defined as a simple and understandable

structure for decision-making. An example of a developed regression tree is given in Appendix A. The purpose of this study was to predict flyrock in an attempt to reduce its environmental impact (Hasanipanah, et al., 2017).

Data were collected from 65 blasts with the measured parameters important to the study being blast-hole length (HD), spacing (S), burden (B), stemming length (ST), maximum charge mass per delay (MC) and the powder factor (PF) (Hasanipanah, et al., 2017). The measurement methodology of the input parameters and the output (flyrock distance) was similar to that of previous studies.

The developed regression tree model consisted of 52 nodes with the powder factor as the root node. A multiple linear regression (MLR) model was also created, using SPSS (version 16) software, in order to conduct a brief comparative analysis between the performance of both models (Hasanipanah, et al., 2017). The equation created during the development of the MLR model is given in Equation 2.9.

**Equation 2.9: Equation created during MLR model development (Hasanipanah, et al., 2017)**

$$F_d = (-90.62 \times HD) - (7.76 \times S) - (4.31 \times B) + (53.99 \times ST) + (0.62 \times PF) + (8.38 \times MC) + 5.23$$

With       $F_d$  = Flyrock distance  
            HD = Blast-hole diameter  
            S = Spacing  
            B = Burden  
            ST = Stemming length  
            PF = Powder factor  
            MC = Maximum charge mass per delay

Hasanipanah, et al. (2017) concluded the study by stating that the regression tree model produced more accurate predictions when compared to the MLR model, but both models were able to predict flyrock travelling distance. A sensitivity analysis of the models showed that the powder factor and the burden were the most influential parameters in the proposed models.

In each of the publication summarised, it is emphasised that the proposed models are site-specific and cannot be used as universal models. The important thing to notice in each paper

is that the empirical equations presented differ significantly from the next. This can relate to the site-specific input parameters used in each model, however, it does bring into question the validity of the proposed models.

#### **2.2.4. A forensic approach based on ballistics principles**

In terms of the basic principles of physics and natural laws that are accepted globally, flyrock should follow the same principles that apply to projectile motion. Flyrock is fragments of rock propelled by a force from an external energy source. The energy exerted onto these rock fragments is converted into kinetic energy that these fragments now possess, based on the law of conservation of energy. According to Newton's second law of motion, the fragment maintains its motion unless an external force is applied onto it. Therefore, developing a system that is based on a physics or ballistics approach may possess the potential to accurately estimate flyrock distance.

##### **2.2.4.1. Flyrock research based on ballistics principles**

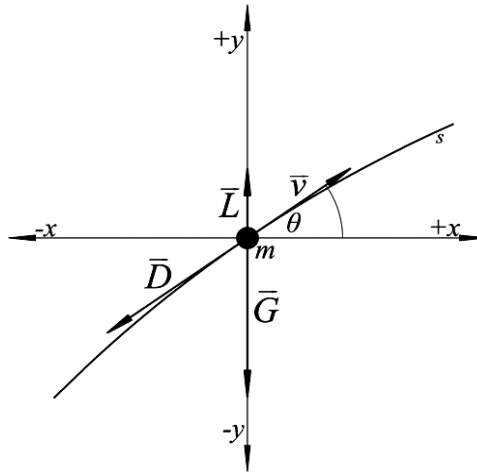
A series of three consecutive articles were published from 2011 to 2015 by research teams led by Saša Stojadinović driven by the need to develop a prediction model based on a forensic analysis approach. Stojadinović, et al. (2011) highlighted that the SDoB approach of estimating flyrock is favoured across the mining industry, but it only applies to normal or expected flyrock. Wild or unexpected flyrock due to bad blasting practices or unexpected geology was never considered and require a forensic analysis (Stojadinović, et al., 2011).

These three articles are summarised chronologically in this section.

- (1) Stojadinović, et al. (2011) published the first article in the series titled "*Prediction of flyrock trajectories for forensic applications using ballistic flight equations*". The objective of this study was to develop a method of determining the maximum throw of flyrock and to be able to estimate safe distances (Stojadinović, et al., 2011).

Flyrock was considered to be a projectile in this study (Figure 2.6), allowing Stojadinović, et al. (2011) to derive a numerical solution from ballistics flight principles (also known as projectile motion principles).





**Figure 2.6: Basic forces that act on flyrock fragments during its flight (Stojadinović, et al., 2011)**

This numerical solution is presented for motion in the x- and y-direction and is given in Equation 2.10 and Equation 2.11 respectively.

**Equation 2.10: Differential equation for motion in the x-direction (Stojadinović, et al., 2011)**

$$m\ddot{x} = -D_x = -C_1 v^2 \cos\theta$$

**Equation 2.11: Differential equation for motion in the y-direction (Stojadinović, et al., 2011)**

$$m\ddot{y} = -mg - D_y = -mg - C_1 v^2 \sin\theta$$

With  $\ddot{x}$  and  $\ddot{y}$  = acceleration in the x- and y-direction (m/s<sup>2</sup>)

$C_1$  = constant equal to the product of the density of air, the cross-sectional area of the projectile and the drag coefficient ( $\rho_{air} \cdot A \cdot C_D$ )

$v$  = velocity of the projectile (m/s)

$\theta$  = angle between the velocity vector and the horizontal axis (degree or °)

$m$  = mass of the projectile (kg)

$g$  = gravitational force (N)

Data was collected from a mining operation by measuring the blast design and bench conditions as input parameters. The flyrock (output) was measured by means of visual observation of the blast, measuring of landing positions and recording damage to surrounding structures and equipment (Stojadinović, et al., 2011).

The assumptions applied to this analysis were (Stojadinović, et al., 2011):

- The launch angle of 45° for a maximum throw;
- Launch velocity was calculated based on an equation presented by past publications. According to the equation, the launch velocities are dependent on the size of the fragment and ranged from 55m/s (for a 0.5m diameter fragment) to 150m/s (for a 0.05m diameter fragment).

Stojadinović, et al. (2011) concluded that this forensic approach is better suited for post-incident analysis since it is highly dependent on the accuracy of the input parameter such as actual launch velocity and launch angle. In a final comment, the authors noted that the influence of drag forms a crucial component of the trajectory and overall motion of flyrock fragments. Therefore, further research is required for incorporating an accurate drag coefficient into the presented equations.

A key discussion in the conclusion of this article describes the relationship between the size of the fragment and the drag force exerted onto it. Stojadinović, et al. (2011) highlighted that the acceleration of the fragment is dependent on the drag and the mass of the fragment and the drag is dependent on the cross-section area of the fragment and its velocity squared. But, the acceleration is also inversely dependent on the mass of the fragment due to its inertia (Stojadinović, et al., 2011).

Therefore, a smaller fragment with a smaller cross-sectional area and higher velocities will experience larger a drag force and due to its smaller mass, will not be able to overcome these drag forces. This means that smaller fragments will not be able to travel long distances (Stojadinović, et al., 2011). Larger fragments, with more mass, have the potential to overcome the drag forces exerted onto it and travel further. However, lower travel velocities will also limit their travel distances (Stojadinović, et al., 2011). It can, therefore, be assumed that there is an ideal fragment size that can travel the maximum flyrock distance, which is the focus os most of the studies conducted.

(2) In 2013, Stojadinović, et al. published a sequel article titled “*A new model for determining flyrock drag coefficient*”. By comparing previous prediction models proposed throughout the years, Stojadinović, et al. (2013) argues that implementing ballistics principles to predict flyrock is the most precise approach. However, the

drag exerted onto the rock fragments plays a significant role in the total travelled distance of the fragments. The main objective of this study was, therefore, to improve the ballistic approach by increasing the accuracy of the drag coefficient (Stojadinović, et al., 2013).

From the previous article (published in 2011), Stojadinović, et al. (2013) deduced the following:

- The fragment sizes that will result in a maximum travel distance of the flyrock range between 20cm and 35cm in diameter.
- Launch velocity is the most influential factor considering a ballistics approach and can be up to 150m/s. Launch velocities of 350m/s and 430m/s have been recorded but, in support of the final argument in the previous article, the maximum recorded launch velocity would not result in the maximum travel distance.
- Launch angle resulting in maximum throw ranges from between 35° to 43°, taking the effect of drag into account.

Initially, it was considered to use a wind tunnel to evaluate the drag forces but this idea was abandoned due to a complicated procedure (Stojadinović, et al., 2013). Therefore, the methodology followed in this study involved recording the blast with high-speed cameras (480 x 360 resolution). The known blast design parameter in the footage was used as control points and equipment in the field of view were used as scaling items (Stojadinović, et al., 2013).

Once the footage was obtained, it was divided into individual frames and imported into CAD software in order to measure the flyrock. The exact measuring technique is not discussed in the article. A key problem with this methodology was that the image quality was extremely poor, especially when magnified. The authors decided to measure the estimated centre points of the pixelated clouds thought to be the rock fragments (Stojadinović, et al., 2013). The initial purpose of this technique was to gather data on the launch velocity of the flyrock. However, the data could be used for the purpose of this study as well (Stojadinović, et al., 2013).

The drag coefficient was calculated by measuring the movement of the fragment at terminal velocity. The main problems experienced by the research team were

determining the size and trajectories of the individual fragments (Stojadinović, et al., 2013).

The equations presented in the 2011 paper were used to test the results of the measurements, using the following initial conditions for a vertical shot (Stojadinović, et al., 2013):

- $t_0 = 0$  seconds;
- $v_0 = 200\text{m/s}$ ; and,
- $\theta_0 = 90^\circ$ .

A vertical shot was considered since it was the most likely situation to measure a fragment's motion at terminal velocity.

The final expectation was that the same or similar drag coefficient would have been calculated for different rock fragments (Stojadinović, et al., 2013). However, this was not the case. The drag coefficient results did not yield a unique value. This could have been due to the influence of the shape of the fragment (Stojadinović, et al., 2013). Measurement error could also have contributed to the unexpected results due to the poor quality of the images.

Stojadinović, et al. (2013) concluded by stating that since the drag coefficient is considered to be a very important input parameter to the ballistics equations, this drag coefficient should vary with changes in launch angle and fragment size.

- (3) The final article published in this series is titled "*Prediction of flyrock launch velocity using artificial neural networks*" and was published in 2015. The motivation behind this study was that most prediction models require accurate launch velocity calculation as a key input. All of the previously proposed models are highly dependent on the quality and accuracy of the input parameters. The main objective of this study was, therefore, to develop a concept of an adaptive system application capable of predicting the launch velocities of flyrock (Stojadinović, et al., 2016).

Data were collected from a total of 36 blasts from three mining operations. The methodology followed to measure and record the input parameters as well as the output (flyrock) was the same as that presented in the previous paper (Stojadinović,

et al., 2016). The input parameters considered in this study are divided into technical and natural parameters.

- Technical input parameters (Stojadinović, et al., 2016):
  - Blast-hole diameter, length and inclination;
  - Stemming length;
  - Stemming factor;
  - Specific stemming;
  - Burden;
  - Spacing;
  - The volume of rock broken per blast-hole;
  - Inter-hole delay;
  - Number of free faces;
  - Charge mass per delay;
  - Powder factor;
  - Explosives density;
  - The velocity of detonation; and,
  - The volume of the gaseous product of detonation.
  
- Natural input parameters (Stojadinović, et al., 2016):
  - Rock density;
  - Compressive and tensile strength; and,
  - The presence of groundwater.

An ANN model was developed using a Peltarion Synapse, described as a fuzzy algorithm for used optimization (Stojadinović, et al., 2016). The proposed ANN model consists of a 19-8-6-1 architecture. The predictor that formed part of this system demonstrated the potential for predicting the initial velocity of flyrock fragments. However, Stojadinović, et al. (2016) emphasised that the predictor in this system was only a concept and not fully developed. The authors motivated that this was due to the similar geology between the three mining sites, resulting in a lack of diverse data.

Stojadinović, et al. (2016) concluded the study by stating that this lack of diverse data should be viewed as an opportunity for future research towards the ultimate goal of developing a universal prediction model.

Since 2010, numerous prediction models have been proposed based on various approaches and concepts. However, all have proven to be primarily site-specific and the accuracy of the results are highly dependent on the quality and accuracy of the input parameters.

### **2.3. EXISTING TECHNOLOGIES THAT CAN BE CONSIDERED DURING THE DEVELOPMENT OF THE CONCEPT OR TECHNIQUE**

In order to (quantitatively) measure the overall movement or the physical input parameters necessary to conduct an analysis of the motion of an object (or particle), a specific tool or technique is required. Sensors are devices commonly used for this purpose, i.e. measuring and quantifying physical parameters. Sensors and the applicability thereof in this investigation are discussed further in section 2.3.1.

#### **2.3.1. Sensor technology**

Different types of sensors have been used in various industries for a number of years. Sensors are defined as devices that record and converts physical parameters into a signal that can be processed and analysed, like an electrical signal (Sobhan, 2005).

Sensors are integrated with various technologies and combined with other sensors to create multi-sensor systems, including everyday devices such as a cell phone or smartwatch (Rowe, 2013). The need for sensors of everyday life is extensive. With the development of new technology and technological concepts, sensors and the communication between different sensory systems have become indispensable.

Sensors' function is based on four main principles of physics, namely (Sobhan, 2005):

(1) Ampere's Law

"A current-carrying conductor in a magnetic field experiences a force (e.g. galvanometer)."

(2) Curie-Weiss Law

"There is a transition temperature at which ferromagnetic materials exhibit paramagnetic behaviour."

(3) Faraday's Law of Induction

"A coil resists a change in the magnetic field by generating an opposing voltage or current (e.g. transformer)."

#### (4) The Photoconductive Effect

“When light strikes certain semiconductor materials, the resistance of the material decreases (e.g. photo-resistor).”

Sensors are therefore able to detect, record and measure certain physical phenomena and convert it into a signal suitable for processing, analysis and interpretation. These detectable physical phenomena are summarised by Sobhan (2005) and presented in Table 2.5. In addition to the physical phenomenon that must be measured, other criteria that are often considered when selecting a sensor include (Engineers Garage, 2012):

- (1) Accuracy of the measurement required,
- (2) Environmental condition,
- (3) Range of measurement,
- (4) Calibration of the sensor,
- (5) Resolution (i.e. smallest increment that can be detected by the sensor),
- (6) Cost, and
- (7) Repeatability of results under similar conditions.

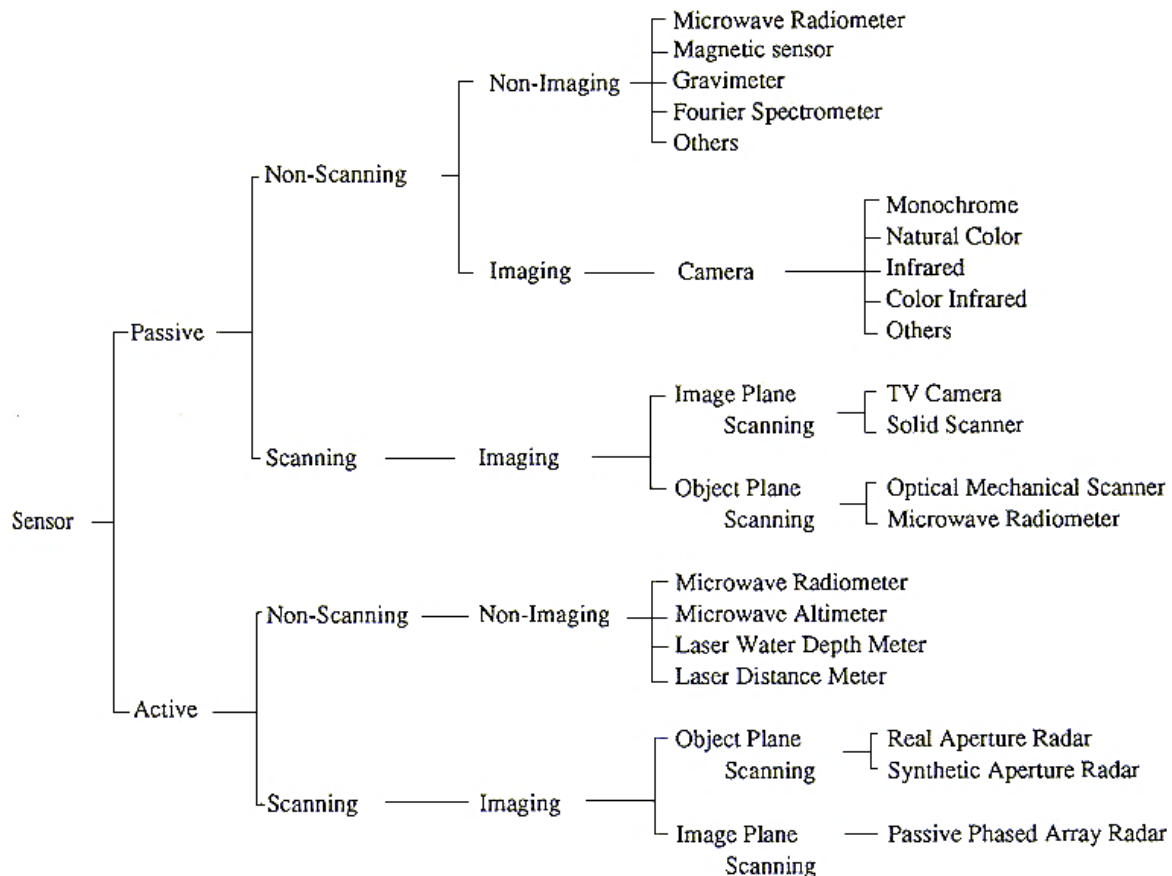
**Table 2.5: Detectable physical phenomena with sensor systems (Committee on New Sensor Technologies, 1995), (Sobhan, 2005)**

Category (Energy)	Physical phenomenon measured
Acoustic	Wave (amplitude, phase, polarization), Spectrum, Wave Velocity
Biological & Chemical	Composition, Concentration, Reaction rate, pH, Fluid Concentrations (Gas or Liquid)
Radiant	Intensity, Phase, Wavelength, Polarization, Reflectance, Transmittance, Refractive index
Electric	Charge, Voltage, Current, Electric field (amplitude, phase, polarization), Conductivity, Permittivity
Magnetic	Magnetic field (amplitude, phase, polarization, intensity), Flux density, Magnetic moment, Permeability
Optical	Refractive Index, Reflectivity, Absorption
Thermal	Temperature, Entropy, Specific Heat, Thermal Conductivity, Flux
Mechanical	Length, Area, Volume, Position, Velocity, Acceleration, Force, Strain, Stress, Pressure, Torque,

For more information on the specific types of sensors available, refer to Appendix A.

### 2.3.1.1. Remote sensing technology

It is important to note that only remote sensing or non-contact units are applicable to this project since the origin of the flyrock is an extremely hazardous activity, i.e. blasting. A summative diagram is presented by Bouzgou (2006) in Figure 2.7.



**Figure 2.7: Classification of sensors (Bouzgou, 2006)**

The main or first classification in Figure 2.7 divides sensors into either active or passive sensors. Active sensors are defined as sensors that create their own electromagnetic energy which is emitted towards the target object or area, resulting in an echo received by the sensor's receiver unit (Pramoda, 2017). Passive sensors are the opposite, able to detect and respond to a specific input without emitting an electromagnetic wave, i.e. it detects the naturally occurring electromagnetic energy (Pramoda, 2017).

Both active and passive sensor technologies are often used in remote sensing systems, able to observe and take measurements at a distance (Rouse, 2014). Pramoda (2017) compares active and passive sensors in Table 2.6.



**Table 2.6: Key differences between active and passive sensors (Pramoda, 2017)**

Active Sensors	Passive Sensors
Active transducers generate an output in the form of an electric current or voltage directly in response to echoed data received.	Passive transducers produce an output in the form of a change in some passive electrical quantity, i.e. capacitance, resistance or inductance. These outputs usually require additional electrical energy prior to interpretation.
Active sensors provide their own internal energy source for illumination.	Passive sensors can only be used to naturally occurring energy is available.
Active sensors are able to obtain measurements anytime, i.e. during the day or night.	Passive sensors can only obtain measurements only during the day.

### 2.3.1.2. Smart sensor technology

Smart technology is becoming a lot more apparent in everyday life and includes everyday objects such as cell phones, televisions, computers and watches.

A smart sensor is defined by Rouse (2019) as “*a device that takes input from the physical environment and uses built-in compute resources to perform predefined functions upon detection of specific input and then process data before passing it on*”. Therefore, smart sensors can be considered as a system more than just simply a device, including sub-systems such as (Committee on New Sensor Technologies, 1995):

- (1) The primary sensing element (transducer)
- (2) Excitation control
- (3) Amplification
- (4) Data filtering
- (5) Data conversion
- (6) Digital processing of information and communications
- (7) Inherent power supply

A smart sensor allows for more accurate and automated data collection and interpretation without the man-hours typically associated with data analysis. This technology is ideal for monitoring and controlling mechanism within a wide variety of industries and environments,

from battlefield reconnaissance (military) to geological exploration (minerals exploration) (Rouse, 2019).

In the new technological era and with concepts such as the 4<sup>th</sup> Industrial Revolution and the Internet of Things (IoT), the smart sensor has certainly become the “go-to” sensing technology for any new developments. The IoT is defined as: “*a network of devices that are connected via the Internet, which facilitates interchange and exchange of data* (Engineers Garage, 2012).” Thus, having smart sensors functioning within systems that are connected to networks that are ultimately connected to a global hub, allow organisations and systems to update data and processes in real-time, monitor performances of various areas within the organisation, improve workflows and ultimately optimise the entire operation or system (Engineers Garage, 2012).

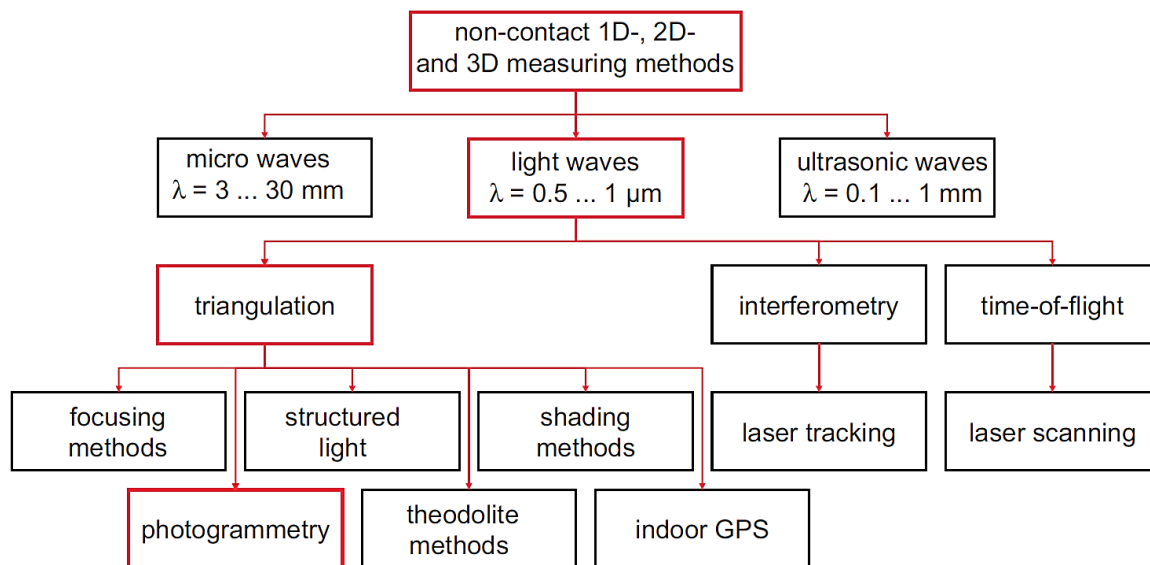
### **2.3.2. Measuring and monitoring techniques and technologies**

Monitoring-systems and -processes within an operation and measuring task deliverables within these systems and processes have become common practice in most industries across the globe. In some industries, such as manufacturing and mining, continuous (and even real-time) monitoring systems and technologies have become critical components to the success and safety of the operation.

Monitoring software is defined by Technopedia Inc. (2019) as “*software that observes and tracks the operations and activities of users, applications and network services on a computer or an enterprise’s systems*”. The software can be integrated into other operating systems and technologies to form an overall operating system, capable of tracking and measuring the function, productivity and wear of each component in the process and alert the operator of any malfunction as soon as it occurs.

There are various techniques and technologies available to monitor processes and measure performance or deterioration within the process.

Since the aim of this project is to develop a concept that can be used to quantify the motion of “random” flyrock, it can be assumed that a non-contact technique would form the basis of the final result. The reason for this assumption is due to the very dangerous activity, i.e. blasting, from which the flyrock originate. Existing non-contact, measuring techniques or technologies are typically driven by some form of electromagnetic energy to detect and measure a specific object or target (Luhmann, et al., 2006). These techniques are summarised by Luhmann, et al. (2006) and are presented in Figure 2.8.



**Figure 2.8: Non-contact measuring techniques (Luhmann, et al., 2006)**

In practice, the specific classification of these techniques can often be distorted due to the complex, multi-sensor systems these techniques typically form part of (Luhmann, et al., 2006). Most of these techniques or technologies have primarily been developed for specific purposes or industries, but will however form the foundation of this project.

The following technologies will, therefore, be discussed in more detail:

1. High-speed photography;
2. Photogrammetry;
3. RADAR (Radio Detection and Ranging);
4. LiDAR (Light Detection and Ranging); and,
5. ViDAR (Visual Detection and Ranging).

### 2.3.2.1. High-speed photography

Even though photography is still a relatively new technology, some significant advances have been made since its invention in the 1830s, including high-speed photography (The Atomic Heritage Foundation, 2017). High-speed photography is defined by Ohnsman (2017) as “the ability to manipulate the exposure of a photograph so that all movement is frozen and things can be seen that could not be seen with the eye alone” (Ohnsman, 2017).

Fuller (2007) divides the concept of high-speed photography into four main areas, which is summarised in Table 2.7.

**Table 2.7: High-speed photography definition classification (Fuller, 2007)**

<b>Classification</b>	<b>Frame rate (fps)</b>
<b>High speed</b>	50 to 500 fps ( $1/50$ seconds to $1/500$ seconds)
<b>Very high speed</b>	500 to 100,000 fps ( $1/500$ seconds to $1/100,000$ seconds)
<b>Ultra high speed</b>	100,000 to 10 million fps ( $1/100,000$ seconds to $1/10$ million seconds)
<b>Super high speed</b>	More than 10 million fps ( $< 1/10$ million seconds)

High-speed photography, therefore, allows the photographer to capture fast-moving objects or events that are too fast to see with the human eye, allowing for a frame-by-frame breakdown of motion or a specific event (The Atomic Heritage Foundation, 2017; Gabriel, 2019).

High-speed photography can also be divided into (Fuller, 2009):

- High-speed cine photography, relating to the frame rate of the recording (i.e. a series of images taken which create the illusion of motion when played back), and
- High-speed still photography, relating to the exposure time rather than frame rate (i.e. images taken at a specific point in time).

Developments and advances in high-speed photography are taking place at an exponential rate, but the foundation of the working of these cameras remain similar. However, in order to understand the working of high-speed cameras, it is essential to understand the basic concepts in photography.

### **Basic principles of photography**

In photography, the most important and fundamental concept to understand is exposure. Exposure is the key to taking quality images (Dunlop, 2011). It is defined by photographer Spencer Cox as “*the amount of light that reaches the camera’s sensor or film*” (Cox, 2017). This, therefore, relates to the brightness and clarity of the images taken with a camera.

Exposure forms the foundation of photography, mirroring the how a cameras work (Figure 2.9), and is built on three pillars, namely (1) aperture, (2) shutter speed and (3) ISO (the sensor of the camera).

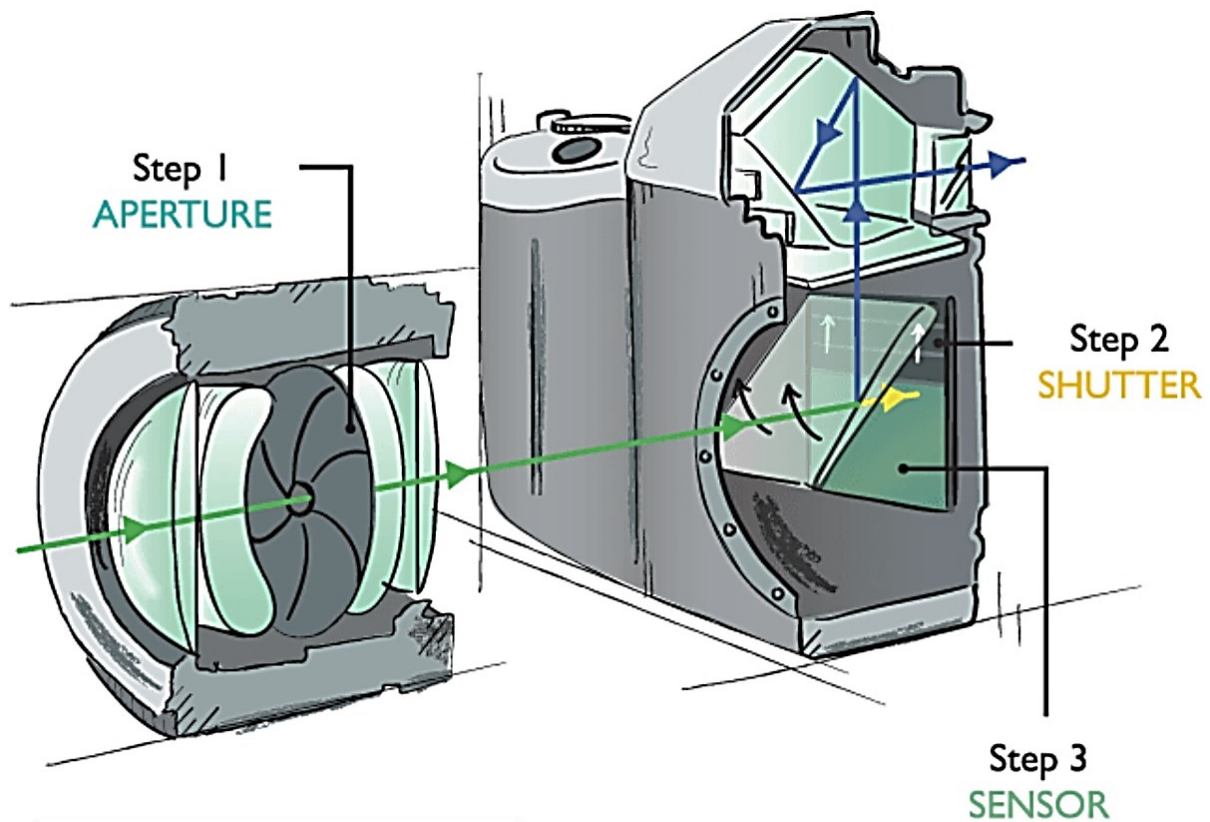


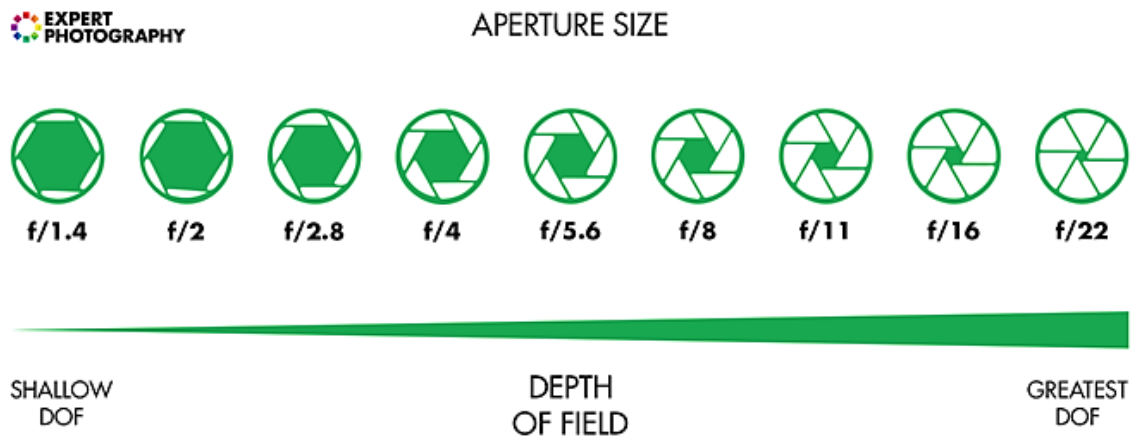
Figure 2.9: The working of a camera, illustrating the three pillars of exposure (Dunlop, 2011)

### (1) Aperture

Aperture is the first “gate” light needs to pass when an image is being captured with a camera (Figure 2.9). Blades in the lens of the camera forms an opening (known as the aperture), which works similar to the pupil of a human eye, controlling the amount of light entering the camera (Cox, 2017). A bigger the opening or wider aperture will allow a larger amount of light to pass through, typically used for darker settings. The reverse is also true, a smaller opening or narrow aperture will reduce the amount of light that can pass through, typically used for brighter scenes (Dunlop, 2011).

Aperture is expressed as an f/number, for example, f/1.4, f/2, f/2.8, f/4, f/5.6, f/8, and f/11. When comparing the f/number relating to a specific aperture setting, it is often easier to think of the f/number as a fraction. In other words, comparing f/2 and f/8 is similar to comparing  $\frac{1}{2}$  and  $\frac{1}{8}$ . This relates to the size of the opening of the aperture (Cox, 2017). An f/2 aperture

indicates a bigger opening, whereas an  $f/8$  aperture setting indicates a smaller opening. This aperture scale is illustrated in Figure 2.10.



**Figure 2.10: Aperture scale including depth of field (Dunlop, 2011)**

Dunlop (2011) also specifies that with each step down the aperture scale (i.e. to the right of the scale) indicates that the aperture surface area is exactly half the surface area of the previous setting.

Unfortunately, the aperture is not just as simple as how bright the image will turn out. The aperture setting also influences the depth of field in the image.

The depth of field is defined as the amount of the scene captured in an image, front to back, that appears clear and sharp (Cox, 2017). Typically, with a landscape image, one would prefer that the entire scene is in focus and sharp so that all the features are clearly visible. Oppositely, with a portrait image, it is preferred to have the subject of the image is clear and in focus with the background being slightly blurred (Cox, 2017).

Aperture directly influences the depth of field captured in the image, also shown in Figure 2.10. A wide aperture will result in a short depth of field, which is ideal when the focus of the image is on a specific subject, and a narrow aperture will result in a longer depth of view, ideal for landscape images.

Therefore, since the aperture setting is the first filter for the amount of light allowed to pass when capturing an image, and directly influences the depth of field of the image, it should be the first setting fixed before using any camera (Dunlop, 2011). (Note: if some form of motion

blur is desired in an image, the aperture should be set second to the shutter speed of the camera.)

## **(2) Shutter speed**

Once light passes through the lens, it will reach the shutter of the camera (Figure 2.9). Now, the shutter speed setting becomes important, i.e. how much light should pass through into the camera or, in other words, how much time spent taking the image (Dunlop, 2011). Therefore, understanding shutter speed and how it works is essential to capturing quality images.

Shutter speed is expressed in seconds or commonly as a fraction of a second, e.g.  $\frac{1}{250}$  seconds. Different cameras offer different ranges in shutter speed settings. A typical shutter speed range of  $\frac{1}{8,000}$  seconds to 30 seconds is very common for most entry-level cameras. High-speed cameras offer significantly faster shutter speeds, such as 5,000 to 500,000 frames per second (fps) or  $\frac{1}{5,000}$  seconds to  $\frac{1}{500,000}$  seconds.

Cox (2017) explains that the two main reasons why shutter speed is noteworthy in photography.

The first reason is that shutter speed directly relates to the brightness of the image. Therefore, if an image is taken in daylight with a shutter speed of 30 seconds, the image will just be white. And, if a fast shutter speed is used to capture an image in a dark setting, the image will only be black (Cox, 2017). Note: If an image is too dark, the term “underexposed” is used and if an image is too bright, the term “overexposed” is used.

The second reason is that the shutter speed relates to motion blur visible in an image. Slow shutter speed will allow the camera to capture any movement in front of the lens while the image is being captured. This motion will appear as a blurred streak across the image. A faster shutter speed captures a better “frozen in time” image, even if an object is moving across the lens while the image is being captured (Cox, 2017). This means that all the features in the image will be clear and visible.

Motion blur can be sub-divided into two categories, that is:

- Camera blur, i.e. the camera moves while the image is captured.
- Subject blur, i.e. the subject in the image move the image is captured.

In order to obtain a clear image, any motion blur should be eliminated.

### **(3) ISO**

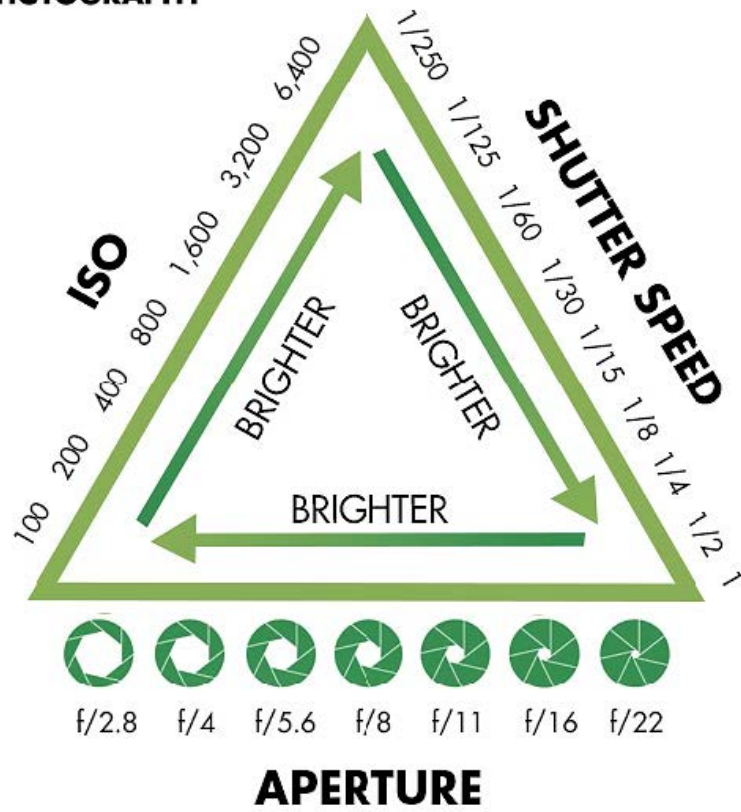
Once the light has passed through the lens, through the aperture and filtered through the shutter speed, it reaches the sensor within the camera. The ISO setting of the camera is applicable to the sensor of the camera and the processing of the image within the camera.

Cox (2017) describes the ISO as “not part of the luminous exposure setting”. This means that the ISO does not filter the amount of light entering the camera, like the previous two pillars. The ISO setting brightens the image after the light has passed through the sensor (Cox, 2017). Therefore, the brightness contributed by ISO setting to the image, is not determined by the external light but can rather be thought of as synthetic.

The major disadvantage of using a higher ISO setting to brighten an image is that by increasing the ISO, the amount of noise in the image is also increased. Higher ISO settings may be necessary if there is no other way to brighten an image, but the quality of the image will decrease. Cox (2017) advises that the ISO be kept as low as possible to achieve the best quality images.

With each component discussed briefly, it is important to understand how they work together in different environments. Unfortunately, a complete understanding only comes with experience through trial-and-error. The three pillars are often represented in the form of a triangle named the “Exposure Triangle”, to illustrate the relationship between each camera setting, shown in Figure 2.11.





**Figure 2.11: Exposure triangle**

Cox (2017) does make some recommendations, summarised in Table 2.8. However, these should only be considered as a starting point.

**Table 2.8: Exposure recommendations for different photographic genres (Cox, 2017)**

Photographic Genre	Aperture	Shutter speed	ISO
<b>Landscape photography</b>	An f/8 setting is generally preferred, but an f/11 to f/16 setting can also be used if a larger depth of field is required. (Aperture is the priority)	Allow the camera to select the shutter speed automatically, based on the selected aperture setting.	Use the base value setting. With most cameras, this is 100.
<b>Portrait photography</b>	Require a shallow depth of field, i.e. an f/1.4 to f/2.8 setting. (Aperture is the priority)	Select shutter speed based on the desired motion blur in the image.	Use a low ISO, but ISO can be increased if the image needs to be brightened.
<b>Sport and wildlife photography</b>	Require a wide aperture, typically an f/1.4 to f/2.8 setting. (Aperture is the priority)	High shutter speed is required since high-speed motion will be captured. Typically, a shutter speed of $1/500$ to $1/1,000$ is used.	A higher ISO is typically used than the other genres since some light and brightness is lost due to the high shutter speed. In essence, noise in an image is better than blur.

There are more complex settings and features in the camera that are useful in the field of photography, but these are not particularly relevant to this investigation.

### **Key elements or considerations in high-speed photography**

High-speed photography allows one to capture an event that occurred within a fraction of a second and is often difficult to see with the human eye. However, some key elements must be considered in order to successfully achieve the desired (or satisfactory) result. These elements or considerations include:

- Lighting or light source

Since the exposure time is extremely short in high-speed photography, a significant amount of good lighting is required to ensure quality images. Bright sunlight (outdoor scenes) can be sufficient but is not always available (Fuller, 2009). Additional light is often necessary and can be achieved in one of two ways, i.e. (1) constant light

source or (2) a pulsed light synchronised to the shutter speed of the camera (Fuller, 2009).

The choice of a light source is dependent on the existing ambient light or natural lighting, the characteristics of the subject in the image and the desired outcome (Fuller, 2009).

- Shutter speed

High-speed photography is typically used when fast-moving objects are recorded for later viewing or analysis. Therefore, the correct shutter speed must be selected in order to ensure that the specific outcome is achieved (Gabriel, 2019). It is important to remember that higher shutter speeds will reduce the amount of light entering the camera sensor, therefore, additional light sources should be considered.

- Type of camera

Different types of cameras with different features are commercially available. Some have higher shutter speeds (often classified as high-speed cameras), but entry-level DSLR cameras also have high shutter speeds, up to  $1/4000$  or even  $1/8000$  seconds (Mansurov, 2010).

- Trigger system

The trigger system used to initiate the camera is essential in high-speed photography, especially if the photographer cannot be in the vicinity of the event being photographed (Fuller, 2009). Trigger systems also allow for some delay between activating the camera's "firing sequence" and the camera actually capturing the images. This is very helpful when the event occurs faster than the photographer's response time (Fuller, 2009).

Fuller (2009) presented the following examples of the classification of some trigger system:

- Simple "make or break" contact triggers
- Detection of radiation emitted or reflected from the subject in the photo
- Detection of the interruption of external radiation because the subject passed in-front of it
- Detection of sound emitted by the subject in the image
- Detection of pressure changes or shock waves

- Detection of changes in surrounding electrical- or magnetic fields with the presence of the subject.

### **Applications of high-speed photography**

High-speed photography is a very versatile technique and has applications across several industries. Fuller (2009) lists the following focus areas (or applications) where high-speed photography is commonly used:

- Fluid flow and combustion research
- Aero-ballistic ranges
- Ballistics and general arming research
- Machining and tool design
- Manufacturing processes
- Physical and chemical processes
- Sporting and physiological studies
- Behaviour and movement of animals, birds and insects
- Lighting and electrical engineering research
- Medical research
- Astrophysics research
- Space sciences research
- Accident research
- Racing timing
- Transport and vehicle research
- Materials research
- Atomic energy research
- Educational studies
- Advertising and entertainment
- Wind tunnel research

High-speed photography is mostly used for qualitative analysis of systems, processes, designs, research concepts, etc. However, once this technique is combined with other techniques or software, some quantitative quality can be generated for a more robust deliverable.

### 2.3.2.2. Photogrammetry

Photogrammetry is a technique used for centuries in various applications with the purpose of obtaining information and data from photographs (Premier Mapping, n.d.). The history of photogrammetry is vast and is briefly summarised as a timeline in Table 2.9.

**Table 2.9: History of photogrammetry (Premier Mapping, n.d.)**

<b>Date or Period</b>	<b>Event</b>
<b>350 B.C.</b>	Aristotle (Optical projection of images)
<b>1600 (approx.)</b>	Dr B Taylor (Linear perspective) Lambert (Use of perspective in map preparation)
<b>1839</b>	Daguerre (Photographic process, i.e. plates made to be light-sensitive with a coating of silver iodide)
<b>1840</b>	Arago (Use of photography in topography surveying)
<b>1849</b>	Laussedat, “the Father of Photography” (Aerial photography using kites and balloons, as well as terrestrial photography)
<b>1861</b>	Three colour photographic process
<b>1886</b>	Captain Deville, Surveyor General of Canada (Topographic mapping of the mountains in Canada)
<b>1891</b>	Roll film
<b>1894</b>	US Coast and Geodetic survey
<b>1902</b>	Wright brothers (The aeroplane is invented)
<b>1904</b>	Fourcade, Cape Town (Stereo mapping of Devil’s Peak)
<b>1909</b>	Dr Pulfrich, Germany (Experimented with stereo pairs)
<b>1913</b>	An aeroplane was used for the first time to obtain photos and mapping purposes.
<b>WWI</b>	Aerial photography for reconnaissance purposes
<b>1920’s to 1940s</b>	Mass production of topographic maps from aerial photographs
<b>WWII</b>	Military mapping and photo interpretation for reconnaissance and intelligence

In addition to the timeline presented in Table 2.9, Schenk (2005) mentions four distinct generations of photogrammetry. The first generation was originated by Daguerre and

Niepce in 1839 through the development of the photographic process. The first generation includes the revolutionary photogrammetric work done through terrestrial and aerial photogrammetry using balloons and kites (Schenk, 2005).

The second generation started from the early 1900s when Dr Pulfrich invented stereophotogrammetry that leads to the invention of the stereo-plotter by Orel in 1908 (Schenk, 2005). The second generation is often also referred to as “*analogue photogrammetry*”. During the first world war, aeroplanes and cameras were combined to take aerial photographs and conduct aerial surveys using analogue photogrammetry (Schenk, 2005).

The third generation came into being with the arrival of computers during the 1950s and is commonly referred to as “*analytical photogrammetry*” (Schenk, 2005). During this generational period, Schmidt developed the foundation of analytical photogrammetry in the 1950s through matrix algebra and computer programs. In the late 1960s, Brown developed the first block adjustment program that ultimately improved the accuracy of aerial triangulation, determined from aerial survey photographs (Schenk, 2005). In addition to the aerial triangulation developed during the third generation, the analytical plotter was also a significant invention during this period (Schenk, 2005).

The fourth generation is also known as “*digital photogrammetry*”. The main difference is that digital photographs are used instead of aerial photographs, in order to create the required models or outputs (Schenk, 2005). Digital photogrammetry is currently still in development and is still a continuously improving system.

Photogrammetry can be defined as “a *three-dimensional measurement technique which uses central projection imaging as its fundamental mathematical model*” (Luhmann, et al., 2006).

Another definition of photogrammetry is presented by Schenk (2005): “*Photogrammetry is the science of obtaining reliable information about the properties of surfaces and objects without physical contact with the objects, and measuring and interpreting this information*”.

The term “photogrammetry” comprises of three Greek words, namely (Schenk, 2005):

- (1) “phos” or “phot” which means light,
- (2) “gramma” which means letter or draw, and
- (3) “metrein” which means measure.

Therefore, Geodetic Services, Inc. (2017) divides the photogrammetry into two main phases:

- (1) Photography, the same principles discussed in section 2.3.2.1 is relevant in this section, and
- (2) Metrology, i.e. the technique used to convert the two-dimensional image or photograph into a three-dimensional object or surface from which specific measurements can be taken.

Photogrammetry is a speciality discipline that falls within the broad field of remote sensing (Premier Mapping, n.d.). Premier Mapping defines remote sensing as “*the technique of obtaining information about objects through the analysis of data collected by instrumentation which is not in physical contact with the object being studied*” (Premier Mapping, n.d.). Remote sensing uses electromagnetic radiation to detect and measure objects within the range of the system, by transferring the energy between the bodies. In photogrammetry, the object of interest is captured as a photograph (or onto film). Therefore, energy transfer is from the object to the film or photographic medium (Premier Mapping, n.d.).

Photogrammetry is, therefore, an optical technique used to obtain physical measurements and data. Other optical techniques often used for the same purpose are (Luhmann, et al., 2006):

- Triangulation techniques  
Examples: Photogrammetry (single, stereo and multiple imaging), angle measuring systems (theodolites), indoor GPS, structured light (light section procedures, fringe projection, phase measurement, moiré topography), focusing methods, shadow methods, etc.
- Interferometry (often used in association with radar technology)  
Examples: Optically coherent time-of-flight measurement, holography, speckle interferometry, coherent radar
- Time-of-flight measurement  
Examples: Distance measurement by optical modulation methods, pulse modulation, etc.

## Types of photogrammetry

Photogrammetry can be categorised into multiple groups, depending on the need for the classification. The categories are presented by (Luhmann, et al., 2006) and are summarised in Table 2.10.

**Table 2.10: Categories of photogrammetry (Luhmann, et al., 2006)**

<b>Categorised according to:</b>	<b>Category</b>	<b>Typical application</b>
<b>Camera position and object distance</b>	Satellite photogrammetry	Processing of satellite images (distance to object > approx. 200km)
	Aerial photogrammetry	Processing of aerial photographs (distance to object > approx. 300m)
	Terrestrial photogrammetry	Measurements from a fixed terrestrial location
	Close range photogrammetry	Imaging distances < approx. 300m
	Macro photogrammetry	Microscope imaging
<b>By number of measurement images</b>	Single image photogrammetry	Single image processing, mono-plotting, rectification, ortho-photographs
	Stereophotogrammetry	Dual image processing, stereoscopic measurement
	Multi-image photogrammetry	More than two images, bundle triangulation
<b>By the method of recording and processing</b>	Plane table photogrammetry	Graphical evaluation, until about 1930
	Analogue photogrammetry	Analogue cameras, optomechanical measurement systems, until about 1980
	Analytical photogrammetry	Analogue images, computer-controlled measurement
	Digital photogrammetry	Digital images, computer-controlled measurement



	Video-grammetry	Digital image acquisition and measurement
	Panorama photogrammetry	Panoramic imaging and processing
	Line photogrammetry	Analytical methods based on straight lines and polynomials
<b>By the availability of measurement results</b>	Real-time photogrammetry	Recording and measurement completed within a specified time period particular to the application
	Off-line photogrammetry	Sequential, digital image recording, separated in time or location from measurement
	On-line photogrammetry	Simultaneous, multiple, digital image recording, immediate measurement
<b>By application or specialist area</b>	Architectural photogrammetry	Architecture, heritage conservation, archaeology
	Engineering photogrammetry	General engineering (construction) applications
	Industrial photogrammetry	Industrial (manufacturing) applications
	Forensic photogrammetry	Applications to diverse legal problems
	Biostereometrics	Medical applications
	Motography	Recording moving target tracks
	Multi-media photogrammetry	Recording through media of different refractive indices
	Shape from stereo	Stereo image processing (computer vision)

These categories will be further analysed and utilised in Chapter 3, based on the applicability to this project and the potential outcome.

## The photogrammetric process

Schenk (2005) describes photogrammetry as a system. The purpose of taking this systems approach to explain photogrammetry is to simplify a general complex technique. In his explanation, Schenk (2005) considers photogrammetry as a “black box”. The inputs to this “black box” are largely photographic images obtained through some form of electromagnetic energy. The output of the system refers to the desired photogrammetric result (Schenk, 2005).

By considering this systems approach, Schenk (2015) divides the photogrammetry process into three phases summarised in the diagram in Figure 2.12.

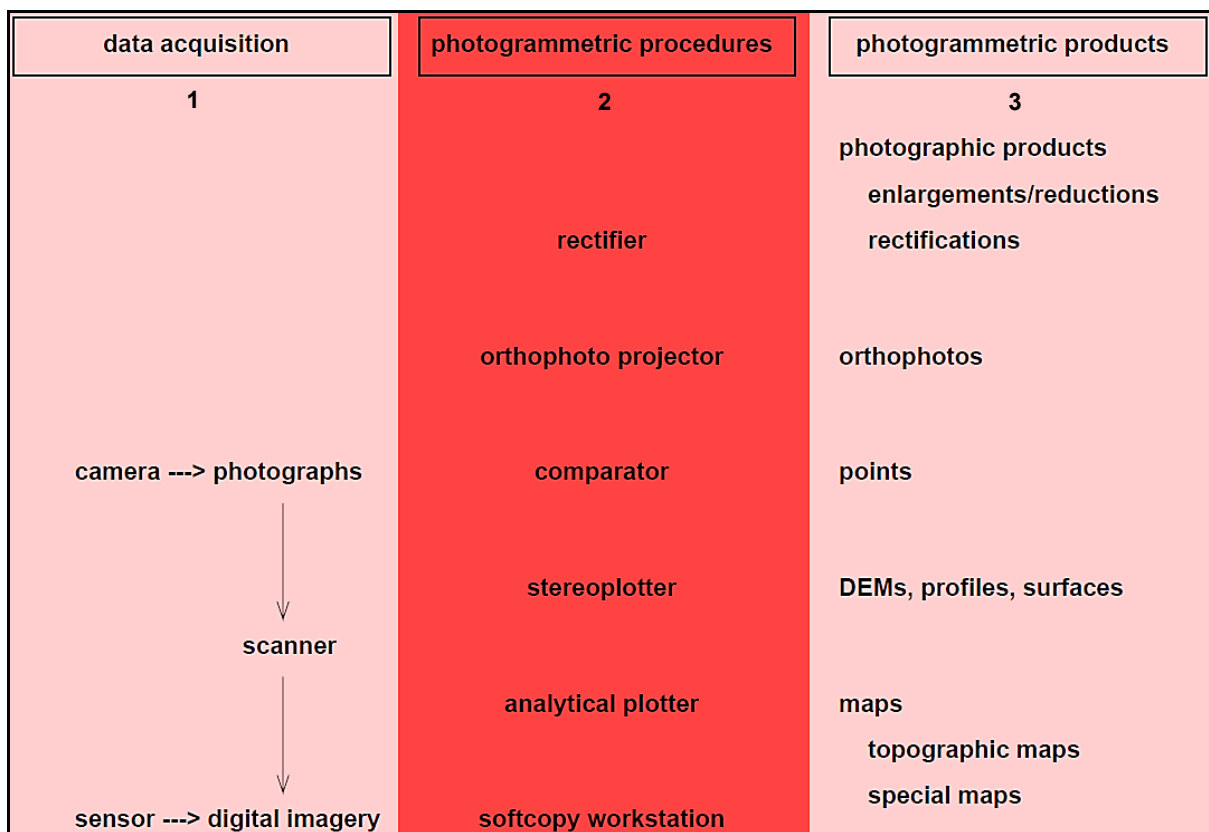
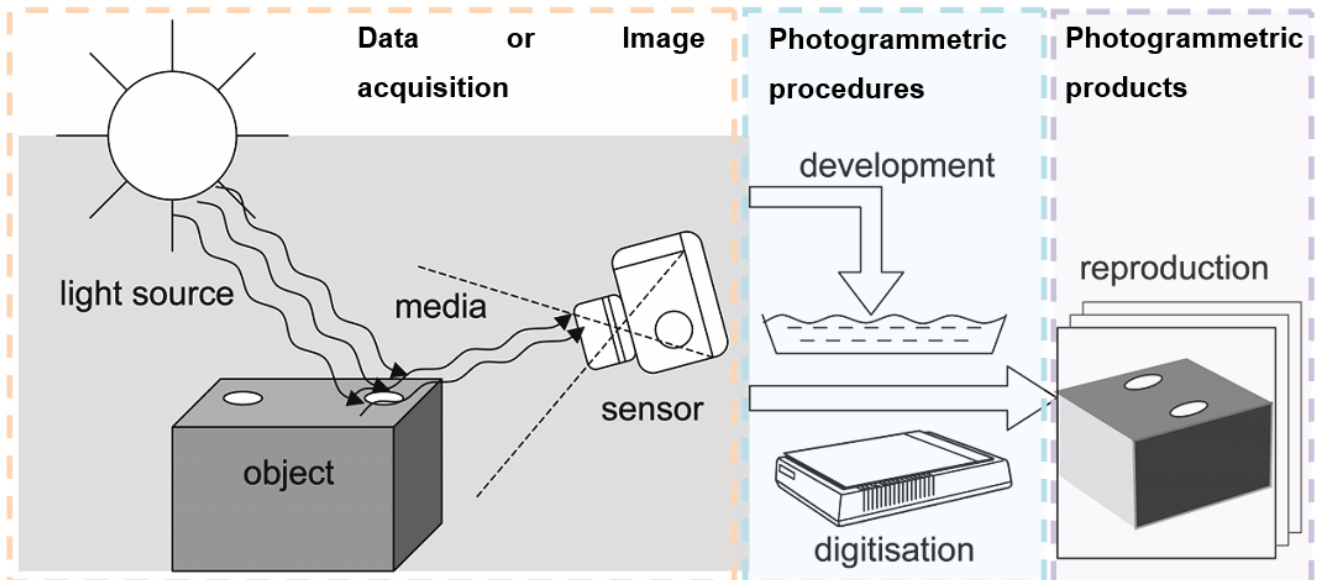


Figure 2.12: Photogrammetry portrayed as a system (Schenk, 2005)

Luhmann, et al. (2006) illustrated this process in Figure 2.13.



**Figure 2.13: Photogrammetry from an object (or surface) to a three-dimensional digital model (Luhmann, et al., 2006)**

### **(1) Data (or image) acquisition**

The data or inputs to the photogrammetric system is the photographs taken with a camera. These photographs are typically captured using specific photogrammetry cameras, but can also be captured using digital sensor cameras (National Institute of Building Technology Nashik, 2018). These photographs can either be mounted on a tripod on the ground (i.e. terrestrial photogrammetry) or can be a fixed tool mounted on an aircraft, helicopter or even a satellite (National Institute of Building Technology Nashik, 2018).

These photographs or the data acquired through these images are divided into four main categories by Schenk (2005), namely:

- Geometric information, which refers to the position and shape of specific objects of interest. This is key information when implementing photogrammetry.
- Physical information, which relates to electromagnetic radiation properties such as wavelengths and polarisation.
- Semantic information, which relates to the interpretation of the data within the image and its meaning.
- Temporal information, which relates to any change in an object or landscape over time. This is seen when comparing multiple images that were captured at different times.

In order to take precise measurements and create an accurate and representative model of the object or surface of interest, five main areas of focus must be considered during the data or image acquisition phase (illustrated in Figure 2.14). These five focus areas are:

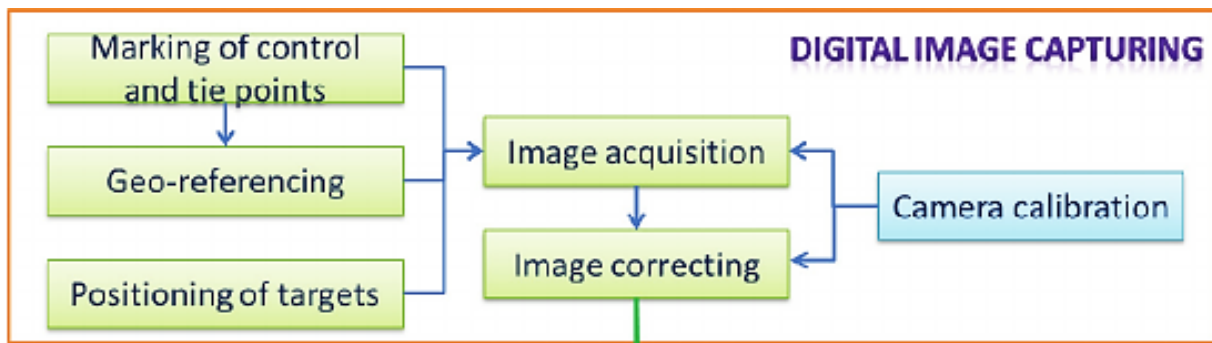


Figure 2.14: Pipeline for digital image capturing process (Sužiedelytė-Visockienė, et al., 2015)

- **Selecting the correct hardware to achieve the desired quality images.**

The term “hardware” only includes the sensor unit, i.e. the camera used to capture the images. There are cameras that are classified as photogrammetry camera, but some terrestrial cameras (e.g. typical DSLR cameras) can be used as well. The sensor requirement for these terrestrial cameras is that the sensor must have a minimum sensor resolution of 12 megapixels (MP) (Sužiedelytė-Visockienė, et al., 2015). Most modern digital cameras are typically available with a 24-megapixel sensor resolution. Top of the range cameras contains up to 60MP sensor resolution (Sužiedelytė-Visockienė, et al., 2015).

In addition to the camera itself, the selected lens is also a critical element (if the selected camera has a removable lens). The lens should be selected according to the desired field of view. However, while wider angle lenses do offer a greater field of view, it also creates significant distortion along the edges of the image (Kock, 2019). This can result in greater errors during the measurement phase of the process and can ultimately yield an inaccurate model ((SmartTech), 2019; Kock, 2019).

Finally, it is essential to calibrate the lens of the camera in order to process and analyse the images captured further (Kock, 2019). Calibration can be done in a laboratory (photogrammetry cameras with fixed lenses). For basic DSLR cameras, with interchangeable lens, a site calibration is required each time the lens is used ((SmartTech), 2019). The main purpose of the site calibration is to determine the

internal and external parameters of the lens on the day of capturing the images (Luhmann, et al., 2006).

- **Considering photographic principles (discussed in section 2.3.2.1).**

Since photogrammetry is based on photographs captured and dependent on the quality of these photographs, the relevant photographic principles must be considered and implemented. The basic principles of photography are discussed in section 2.3.2.1 and applies to this discussion as well. In order to determine distinct edges and features in an image, the focus and lighting in the image are critical. This relates to the exposure of the images and the camera setting for specific conditions.

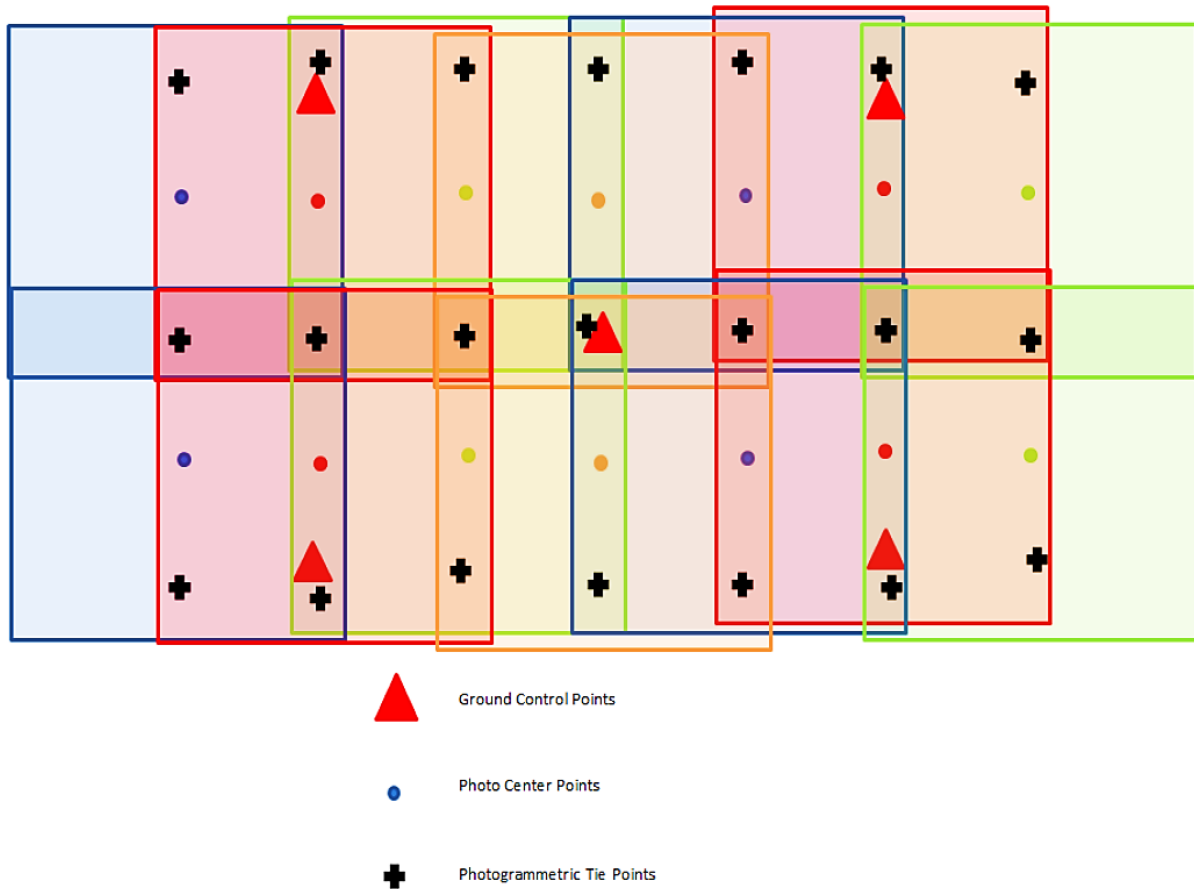
- **Field of view and determining the target area.**

Determining the field of view of the lens is critical in order to capture high-quality images. The field of view of the lens used should not be much wider than the target area or object ((SmartTech), 2019). The reason for this is that the camera sensor captures higher resolution images when the distance between the camera and the target area is small. Using the photogrammetry processes (that are discussed in the following section), the images were taken must overlap enough to identify and measure identical features in more than one image (Kock, 2019). These features are used in the overlapping images to create a three-dimensional representation of the target area or object. The camera or tripod positions (terrestrial photogrammetry) or flight path (aerial photogrammetry) is predetermined to achieve this overlap.

- **Planning flight path (aerial photogrammetry) or camera positions (terrestrial photogrammetry).**

The flight path of aircraft or drones, typically flown in a grid pattern, must be designed in such a way that the photos were taken overlap in both the x- and y-directions of the grid. According to Karen Bester, this overlap should ideally be a minimum of 60% ((SmartTech), 2019). If the overlap between adjacent is less than 60%, the accuracy of the measurements and final product may be at risk, illustrated in Figure 2.15.

### Aerial Triangulation Block Concept



**Figure 2.15: Overlap of photogrammetry images including ideal GCP placement (Colorado Department of Transportation, 2015)**

Another key consideration is the orientation of the camera in each position. With aerial photogrammetry, the aircraft or drone should remain stable when images are captured. This results in parallel images which are easier to orientate during analysis ((SmartTech), 2019). With terrestrial photogrammetry, the camera should be strategically placed to ensure the field of view in each image is parallel to that of the previous image ((SmartTech), 2019). This ensures less variability in the images during the analysis phase of the technique.

- **Positioning and surveying of ground control points.**

The ground control points (GCPs) are known features placed in the target area or around the target object, within the field of view of the camera. These points are critical to the accuracy of the remainder of the process since it creates an easily identifiable and known point in the images (Kock, 2019). The coordinates of these GCPs are accurately surveyed before the photogrammetric images are captured.

These coordinates are used in the downstream processes in photogrammetry, i.e. measuring positions and creating a point-cloud or three-dimensional model of the area or object (Colorado Department of Transportation, 2015). More GCPs will increase the accuracy of the final model. A general rule-of-thumb is that a minimum of five to ten GCPs are required in the field of view and must be visible in at least ten overlapping images ((SmartTech), 2019). Note: two overlapping photos, taken from different positions, are known as a stereo pair or a single stereo model (Colorado Department of Transportation, 2015).

## **(2) Photogrammetric processes**

The photogrammetric processes refer to the processing and analysing of the images taken in phase one. This discussion only includes the basic outline and is not linked to any specific photogrammetry workstation or software.

Modern photogrammetric processes (digital photogrammetric systems) are computerised and various software or computer programmes are commercially available. These software programs are based on the mathematical models and algorithms developed during each generation of photogrammetry. The software simplifies and accelerates the process and analysis phase. These specific mathematical models and algorithms will not be discussed in detail.

If a site calibration of the lenses is required, software (such as Pix4D) can be used. The calibration is done by importing the calibration images taken prior to the actual photogrammetric images and marking as many of the GCPs as possible in each of the images. This is done to enable the software to reference each image, as well as the features in each image, to known coordinates (Pix4D, 2017). Once these GCP points are marked and the project is processed (i.e. the software orientates the images according to the selected points), the software will generate the internal and external parameters for the lens on that specific job or project. Once the lenses are calibrated, the actual photogrammetric images can be processed.

Once the photogrammetric images are imported into the software, the first step is to create or add a referencing component, which will allow the software to geo-reference each photograph (Colorado Department of Transportation, 2015). Typically, this refers to selecting a specific coordinate system (global or local) which is combined with correctly marking the known GCPs on each image. By geo-referencing the images, the software is

able to build a digital, three-dimensional representation by creating tie-points between the photographs (Kock, 2019).

The geo-referenced images are used to generate a point-cloud of the area or object (Pix4D, 2017). It is during this step that erroneous points or data can be identified, investigated and excluded if necessary. This point-cloud is used to create some of the photogrammetric products by triangulating between the point-data to create surfaces (Kock, 2019). More point-data will increase the accuracy of the final product, i.e. less (or smaller) assumptions or interpolations is required.

Additional measurements and analysis of these data sets follow, depending on the desired outcome or photogrammetric product. These measurements and analysis include (Luhmann, et al., 2006):

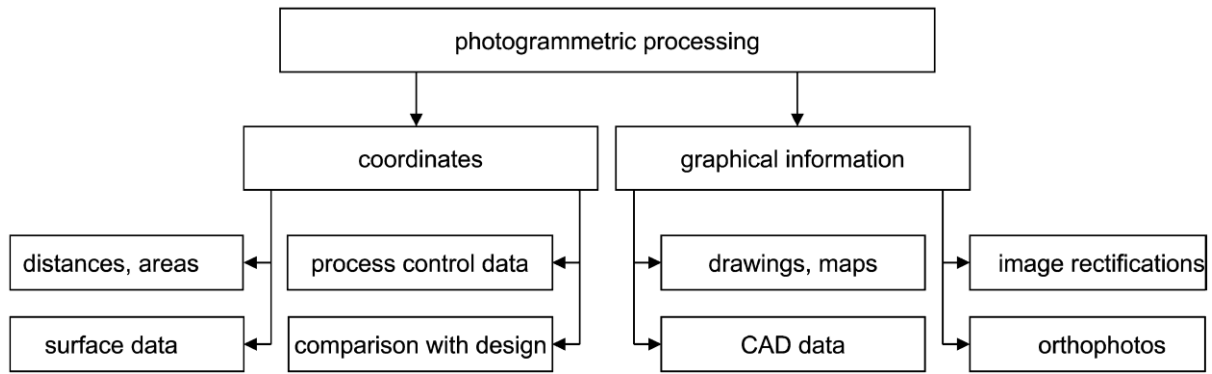
- Single point measurements, i.e. creating three-dimensional point coordinates for further analysis.
- Graphical plotting, i.e. creating scaled maps for CAD (computer-aided design) models or GIS (geographic information system) purposes.
- Rectification or Orthophoto, i.e. creating transformed images by removing the effects of tilt relative to a specific reference frame (rectification) or removing the effects of perspective (orthophoto).

Other photogrammetric hardware, such as stereo plotters and softcopy workstations, can be incorporated in this process.

### **(3) Photogrammetric products**

Various photogrammetric products (or deliverables) can be generated for different purposes. These products are summarised in Figure 2.16:





**Figure 2.16: Common photogrammetric products resulting from the processing and analysis of images (Luhmann, et al., 2006)**

### The factors affecting the accuracy of photogrammetry

PhotoModeler Technologies defines six main factors that affect the accuracy of the photogrammetric product or deliverable (summarised in Figure 2.17). These six factors are (PhotoModeler Technologies, n.d.):

- **Photo resolution (pixels per image)**

A higher resolution will result in better quality images and more accurate measurements.

- **Camera calibration**

The calibration of the camera lens will yield the parameters, both internal (the lens's exact focal length, format size and distortion) and external (deviation from a level orientation due to rotation). A better-calibrated lens (i.e. more specific details are known about the lens), will result in a higher accuracy of the photogrammetric product and measurements.

- **Angles**

This refers to the angle between the camera and a specific point. If this angle is too shallow, it implies that a specific point does not appear in enough images taken from different positions. This means that processing software has a limited sample of what that specific feature looks like and need to assume and interpolate the missing information. This results in larger errors between the actual surface or object and the three-dimensional representation

- **Photo orientation quality**

The orientation of the camera can result in larger errors if there are significant rotation and movement of the camera between positions. This can lead to a reduced overlap between images, reducing the accuracy of the end product.

- **Photo redundancy**

More photographs or images decreases the software's need to interpret missing information, risking the accuracy of the final product or model.

- **Marking precision**

Marking GCPs and other tie points correctly will ensure that the correct position or coordinate is allocated to a specific feature in the photogrammetric model.

	Camera Resolution	Camera Calibration Method	Point Angles *	Photo Orientation Quality	Photo Redundancy	Targets
<p><b>Lowest Accuracy</b> 1 part in 100</p>	<p>Low (eg Video) 640x480</p>	<p>No calibration ↓ Inverse Camera</p>	<p>15 degrees or less</p>	<p>Few points per photo, low point coverage</p>	<p>Points mostly on only 2 photos</p>	<p>No circular targets, all user marked points</p>
<p><b>Average Accuracy</b> 1 part in 5,000</p>	<p>Medium (eg basic/older digital camera) 8MP 3264x2468</p>	<p>PhotoModeler Camera Calibrator (good solution) ↓</p>	<p>20-90 degrees</p>	<p>15+ points per photo, up to 60% coverage</p>	<p>Most points on 3 or more photos</p>	<p>Some points marked on naturally lit targets at key locations</p>
<p><b>Highest Accuracy</b> 1 part in 30,000+</p>	<p>High (eg good quality digital camera) 20MP+ 5400x3600 or higher</p>	<p>Field Calibration</p>	<p>Close to 90 degrees</p>	<p>35+ points per photo, up to 60% coverage</p>	<p>Most points on 8 or more photos</p>	<p>Many points marked on standard target points  All points marked on well-defined targets</p>

Figure 2.17: Photogrammetry accuracy factors (PhotoModeler Technologies, n.d.)

## Applications of photogrammetry

Digital photogrammetry is a relatively simple technique that has numerous applications across several industries. These applications (and industries) include:

- Land surveying

Photogrammetry is a very common land surveying technique that has been used for centuries. All four generations of photogrammetry have contributed to surveying site and large topographical areas. Modern land surveying includes site planning, topographical mapping and modelling, earthwork volume estimations, creation of digital elevation models (DEM's) and image-based mapping or orthophotography (National Institute of Building Technology Nashik, 2018).

- Engineering

Photogrammetry is ideal for engineering purposes since it is reliant on accurate measurements. Photogrammetry is used in the field of civil engineering to evaluate the progress of construction projects and visualise this progress to the clients (GIS Resources, 2018). In the automotive industry, photogrammetry is typically used to evaluate the BIW (body in white) structure movement when the vehicle is put through various test cycles. Photogrammetry is also a faster technique than equivalent scanning technology and it is much easier to set up and implement (Lipman, 2018).

- Mining

In mining, orthophotographs and DEM's are often used for design and planning purposes. These photogrammetry products or outputs assist the mines to control their footprint on the environment, monitor production outputs (by measuring the stockpile volumes on a monthly basis) and identify potential areas of concern with topographical and terrain modelling (Lipman, 2018).

- Energy (Wind, Oil and Gas)

Considering that wind turbine blades are continuously exposed to the elements, it can be expected that it suffers significant wear and tear. Photogrammetry is used to identify any wear and faults that may weaken the structure or lead to failure (Lipman, 2018). This optical or visual technique also assist with future research and design to increase the life of these blades (Lipman, 2018).

In the oil and gas industry, aerial photogrammetry can assist companies when designing the pipelines and assist in the detection of leaks or damages when combined with remote sensor systems (Lipman, 2018).

- Architecture and Real estate

Detailed images taken of homes and properties can be used to create three-dimensional models for potential buyers to review when considering a purchase (GIS Resources, 2018).

- Forensics

Photogrammetry, although not typically associated with crime scene investigation (CSI) or forensics, add significant value to these investigations. Photogrammetry can be used to reconstruct crime- or accident scenes for further detailed analysis and interpretation (GIS Resources, 2018). It allows investigators to identify and study the smaller details, that may have been overlooked at the scene, and take precise measurements that may be vital to a case and can be used in a court of law (GIS Resources, 2018).

- Archaeology

In archaeology, photogrammetry is used to survey historical and three-dimensional reconstruction of these sites as well as historical artefacts. This will ensure that a detailed digital copy of these sites and artefacts are available for future analysis and investigations. It also allows the public to view these sites without physically visiting the site. (Mearmanand & Roberts, 2014)

- Film and Entertainment

In film and gaming, photogrammetry is commonly used to create detailed three-dimensional models and landscapes that can be used in the virtual gaming environment or as computer-generated imagery in cinematography (GIS Resources, 2018). Photogrammetry allows developers to produce high-quality models and representations to increase the authenticity of the experience (GIS Resources, 2018).

- Sport

Photogrammetry is commonly used by athletes, both professionals and amateurs, to record, visualise and analyse their movements while practising their specific sport.

By tracking and evaluating their movements, the athletes are able to make small changes that will improve their overall performance (GIS Resources, 2018).

### **Advantages and disadvantages of photogrammetry**

As with any technique and technology, advantages and disadvantages are applicable. However, these advantages and disadvantages often add significant value during the decision-making process.

#### **Advantages**

- The photos taken is a precise and permanent record of the environment, terrain or object at the specific point in time when the photo was taken (Colorado Department of Transportation, 2015). These images not only hold visual information but quantitative and measurable information as well (National Institute of Building Technology Nashik, 2018).
- These photos can be used to communicate information to various stakeholders, including the general public and the government (Colorado Department of Transportation, 2015).
- The photos taken for photogrammetry can be used for multiple purposes other than photogrammetry including reconnaissance, design and environmental concerns (Colorado Department of Transportation, 2015).
- Photogrammetry is often used to present a wide project field, both topographical and cultural features (National Institute of Building Technology Nashik, 2018). DTM's and mapping of large topographical areas can be done quicker and cheaper than other ground survey methods (Colorado Department of Transportation, 2015).
- If certain aspects need to be re-surveyed or re-measured, it is not necessary to re-do the fieldwork. The same images are used to re-do some measurements (National Institute of Building Technology Nashik, 2018).
- Photogrammetry can be implemented in hard to reach areas or difficult and dangerous terrains (Colorado Department of Transportation, 2015).
- Coordinates of each point in the survey or mapping field can be determined without any additional cost or effort (National Institute of Building Technology Nashik, 2018).

#### **Disadvantages**

- Since photogrammetry is an optical or visual technique, environmental factors such as weather, shadows and vegetation can result in poor quality photographs which lead to

weaker data sets or measurements (National Institute of Building Technology Nashik, 2018).

- If the area or object of interest is blocked from view, either by trees or building overhangs or roofs, this blocked area will not be recorded and cannot be measured (Colorado Department of Transportation, 2015).
- The accuracy of the measurements is dependent on the quality of the camera and the distance to the area of interest, i.e. ground surveys are more accurate compared to aerial surveys due to the distance between the topography and the camera (National Institute of Building Technology Nashik, 2018).
- Identifying planimetric features can be difficult or even impossible in some cases (National Institute of Building Technology Nashik, 2018).
- Underground features cannot be detected or measured (National Institute of Building Technology Nashik, 2018).

### **2.3.2.3. RADAR (Radio Detection and Ranging)**

Radar is an acronym that stands for Radio Detection and Ranging system. Radar is an electromagnetic system used to detect the position of an object of interest and measure the distance between such an object and the radar system (Elprocus, 2019).

Radar first became a significant detection technology during the 1930s, when its military application became the focus of related research and development.

The first component of radar is based on the theoretical work, conducted by James C Maxwell in the 1880s, that concluded by stating that light- and radio waves are examples of electromagnetic waves, which can be reflected off metallic surfaces and refracted by dielectric mediums (Encyclopædia Britannica, Inc., 2019). This theoretical work was later supported by Heinrich Hertz's experimental work, proving that light- and radio waves behave according to these properties. Hertz's experimental work formed some of the foundations of radar technology (Encyclopædia Britannica, Inc., 2019).

The Doppler principle was first named in 1842 when Christian J Doppler published a paper on determining motion using the frequency of light while studying the movement of the stars (Decatur Electronics, 2019). The properties of radio waves, combined with the Doppler principle, created a stable foundation for radar's ultimate development and implementation as detection and ranging technology in industries such as aviation, maritime and military.

## Working of the system

A basic radar system (or radar set) consists of six main components, namely (Elprocus, 2019):

- **Transmitter**  
The transmitter is the origin of the radio (wave) signal, generated by a waveform generator and amplified in the power amplifier.
- **Waveguides**  
The waveguides are transmission lines for the radio waves emitted from the transmitter.
- **Antenna**  
The antenna can be a parabolic reflector, planar arrays or electronically steered phased arrays.
- **Duplexer**  
The duplexer allows one antenna to be used, alternately, as a transmitter and a receiver. It is typically in the form of a gaseous device that would produce a short-circuit at the input to the receiver when the transmitter is working. This is important since the high energy pulse from the transmitter would destroy the receiver if allowed to pass through the receiver unit.
- **Receiver**  
The receiver unit receives the return signal after it has been reflected (or echoed) by the object of interest. It includes a processor that detects and processes the signal and provides video signals as an output.
- **Threshold decision**  
The output of the receiver is compared with a threshold to detect the presence of any object. If the output is below any threshold, the presence of “noise” is assumed.

The basic working of a radar system, illustrated in Figure 2.18, follows the sequence of the components as listed. The electromagnetic signal generated by the transmitter unit and emitted through the antenna. Once the signal makes contact with an object, it is reflected (or echoed) back towards the receiver or deflected onto various directions, depending on the surface of the object. Once the signal is received by the antenna, it is delivered to the



receiver unit. The received signal is then processed and converted into a video output (Elprocus, 2019).

The output data can be used to determine the position and range (or distance between the radar system and the object of interest) by considering the angle of the returned signal and the time it took for the signal to travel to the object and back to the receiver. The position and distance of moving objects can be measured using the Doppler principle.

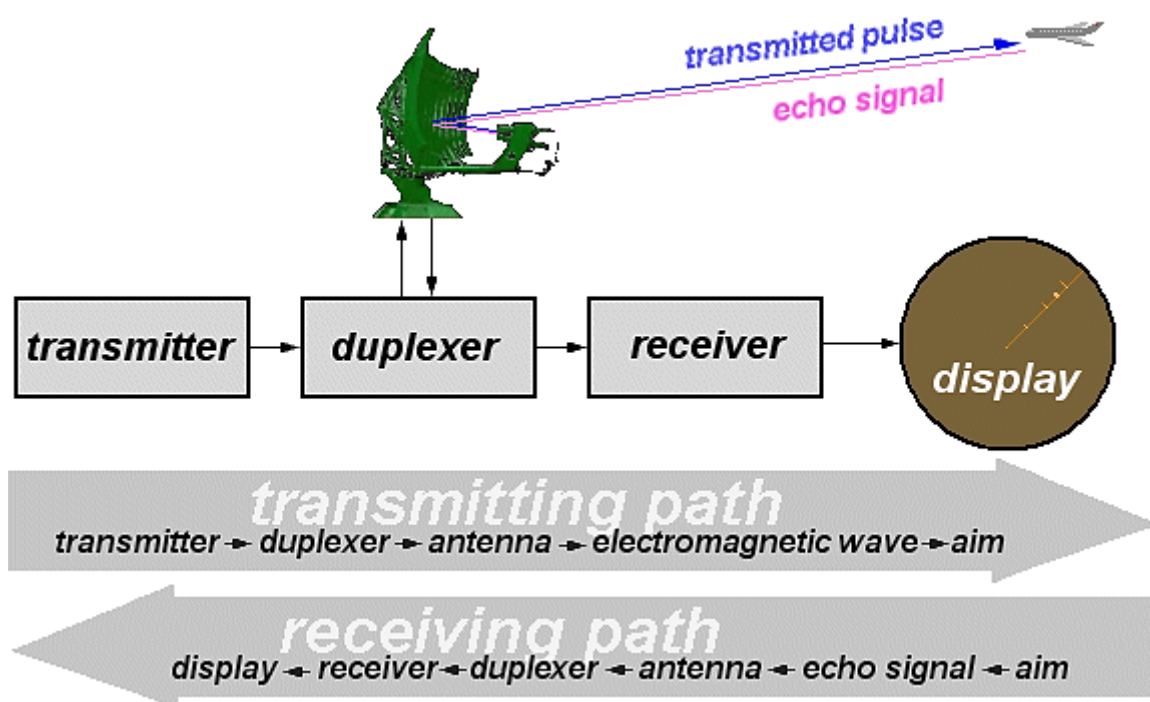


Figure 2.18: Basic working of a radar system (Wolff, 2019)

Radar is typically used in order to achieve one of three goals, namely (Brain, 2019):

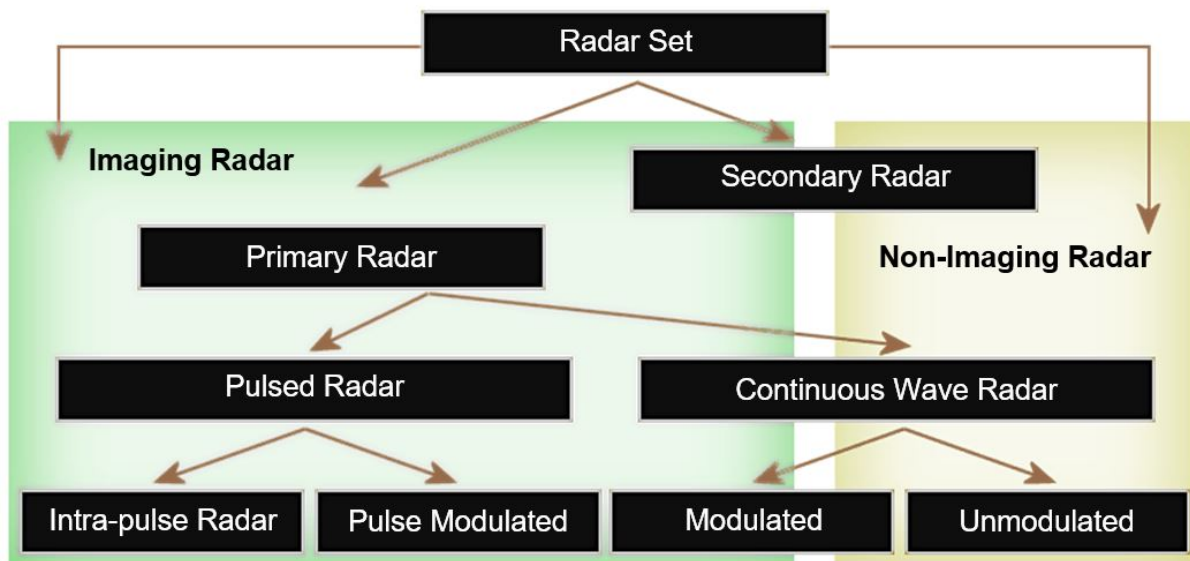
- Detect the presence and position of an object.  
This includes both moving objects, such as aeroplanes, and stationary objects, such as underground (buried) objects.
- Detect and determine the velocity of moving objects.
- Map surfaces, such as topographies.

### Types of radar systems

Radar systems (sets) can be roughly categorised into two main groups, i.e. imaging and non-imaging radar, illustrated in Figure 2.19.

Imaging radar converts the received data into a visual, map-like image, with typical applications include weather radar and military air surveillance radar (Wolff, 2019).

Non-imaging radar produces an output in the form of pure numerical values. Typical applications include some radar altimeters and speedometers, with a non-imaging secondary radar application being an immobilizer system in modern cars (Wolff, 2019).



**Figure 2.19: Classification of radar sets (Wolff, 2019)**

The primary radar emits high-frequency signals that are reflected at targets. In contrast to secondary radars, primary radars receive their own emitted signals reflected off an object's surface (Wolff, 2019). Secondary radar is typically associated with surveillance systems such as an air traffic control system. In other words, the aircraft is equipped with a transponder (transmitting responder) which receives a signal from the radar interrogator, typically a ground station combined with primary radar. A response is generated within the transponder, which is then sent back to the secondary radar. The run time can also be used to measure the distance to the target object, as with primary radar. However, this reply often contains more information, e.g. altitude, identification or technical problems on board, than what can be achieved with primary radar (Wolff, 2019).

Pulse radars are the most common type. Pulse radars emit a high power and high-frequency pulsed signal, followed by a pause in which the reflected signal can be received before a new transmission is sent out (Wolff, 2019). The location and distance of the target

can be determined from the antenna position and return time of the signal, based on the Doppler principle (Elprocus, 2019).

A continuous-wave radar emits a transmitting signal without interruption. The returned signal is received and processed simultaneously and continuously, with the receiver is not necessarily in the same location as the transmitter. Any powerful broadcasting transmitter can function as a transmitter if a remote receiver compares the propagation times of the direct signal with the reflected signal (Wolff, 2019).

An unmodulated continuous wave radar's transmitted signal remains constant in amplitude and frequency. These radar systems are mainly used for speed measurements using the Doppler principle, i.e. locations and distances cannot be measured (Wolff, 2019).

Frequency modulated continuous wave radar's transmitted signal remains constant in amplitude but changes in frequency. The distance to the object of interest can be determined from the frequency shift, which has the advantage that assessment of the data can take place without disrupting the incoming or returning signal (Wolff, 2019).

An intra-pulse modulated radar transmits a signal with lower power but longer pulse duration. Similar to frequency modulated continuous wave radar, these radars control the transmitted signal pulse in order to use the compression signal wave to determine the distance (Wolff, 2019).

Bi-static radars consist of a transmitter and receiver that are separated by a significant distance (equal to the distance between the radar and the target object), while a monostatic radar refers to a system consisting of a transmitter and receiver located in the same place (Elprocus, 2019).

### **Applications of radar**

Elprocus (2019) mentions 5 main industries and applications of radar. These industries and applications are:

- **Military applications**

In the military, radar fulfils three major roles, namely:

- (1) Target detection, recognition and weapons control in air defence,
- (2) Missile guidance systems, and
- (3) Detecting enemy locations.

- Air traffic control
 

Radar fulfils three major roles in air traffic control as well, namely:

  - (1) Controlling air traffic around airports, by detecting and track aircraft flying in the vicinity,
  - (2) Guiding the aircraft onto the runway in bad weather, and
  - (3) Monitor the runways for vehicles and aircraft in order to prevent collisions.
  
- Remote sensing
 

Radar is used to monitor the weather. It can also be used to detect and track ice in the ocean in order to ensure safe routes for ships. Radar can also be used to identify and track rock falls next to roads.
  
- Ground traffic control
 

Radar is often used by police to monitor the speeds at which motorist travel on the roads. It is also used in vehicles to locate obstacles and other vehicles in the proximity of the operating vehicle and alert the driver to it.
  
- Space
 

Radar fulfils four major roles in astronomy and other space-related studies, namely:

  - (1) Guidance systems for space crafts,
  - (2) Observing planetary systems and movement,
  - (3) Detect and track satellites, and
  - (4) Monitor meteors.

### **Advantages and disadvantages of radar**

The following advantages and disadvantages are presented on a website by LIDAR and RADAR Information (2019).

#### **Advantages (LIDAR and RADAR Information, 2019)**

- Radar can penetrate mediums such as clouds, mist and snow.
- It can penetrate insulators.
- It can give the exact position of an object.
- It can determine the velocity of a target.
- It can measure the distance to an object.
- It can distinguish between stationary and moving targets.

- Radar signals do not require a specific medium of transportation.
- Radar signals can target several objects simultaneously.
- Radar allows for 3D imaging based on the various angles of return.
- High operating frequency allows for storage of large amounts of data.
- It covers a wider geographical area.
- It allows for repetitive coverage.
- Easy data acquisition at different scales.
- Data acquisition is fast if the area is not too large.
- A cheap and fast method of calculating base maps when no detailed survey is required.
- It can acquire data from some of the remotest areas of the planet.
- It is economical when doing small-scale map revision.

#### **Disadvantages (LIDAR and RADAR Information, 2019)**

- Radar takes more time to lock on an object.
- Radar has a wider beam range.
- It has a shorter range.
- It cannot track if an object is decelerating at more than 1.6kph/s.
- Large objects that are close to the transmitter can saturate the receiver.
- Readings can be falsified if the object is handheld.
- Radar can be interfered by multiple objects and mediums in the air.
- It cannot differentiate between multiple targets.
- It cannot differentiate the colour of the object.
- It cannot detect targets that are deep in the sea.
- It cannot detect targets that are obstructed by a conducting material.
- It cannot detect the type of the object.
- It is not very accurate.
- It can be interrupted by other signals.
- It is not very stable and is susceptible to external interference.
- It can be oversensitive.
- It cannot be used beyond the ionosphere.
- It can be expensive if used in small areas especially if it is a one-time use.
- It requires specialized training to analyse the data.
- The data provided by radar systems are usually not complete.

#### 2.3.2.4. LiDAR (Light Detection and Ranging)

LiDAR is an acronym for light detection and ranging and is often referred to as 3D laser scanning. Geospatial Consulting, Inc. (2018) defines lidar as “a remote sensing method that uses light in the form of a pulsed laser to measure distances to objects or surfaces”.

LiDAR is considered to be a relatively new technology with most of the initial development taking place in the early 1960s and 1970s (Elprocus, 2019). LiDAR is conceptually similar to a radar system, with the main difference being the type of energy or wave transmitted (3D Laser Mapping, 2019).

Wheeler (2017) compares LiDAR and radar technologies, specifically referring to how the technology or system functions. As discussed in section 2.3.2.3, radar functions by emitting radio waves, which is echoed and received by the system’s receiver. LiDAR functions by emitting laser (light) pulses to generate point data of the characteristics of an object, surface or landscape (Wheeler, 2017).

Marcoe (2007) summarised the main differences between radar and LiDAR in Table 2.11.

**Table 2.11: Differences between LiDAR and RADAR**

LiDAR	RADAR
Uses optical signals (approaching infrared spectrum, with wavelengths $\approx 1\mu\text{m}$ )	Uses microwave signals, with wavelengths $\approx 1\text{cm}$ . (Approximately 100,000 times longer than infrared spectrum)
Shorter wavelengths, i.e. allow detection of smaller objects such as cloud particles, dust and other airborne particles.	Size of the target object or surface is limited by longer wavelength.
High three-dimensional resolution due to focused beam and high frequency of a wave.	Three-dimensional resolution is limited by the (Synthetic aperture techniques reduce antenna length requirements.)
Limited to clear atmospheric conditions.	Can operate in the presence of clouds.

LiDAR technology is an active system that allows scientists, engineers and designers to accurately examine and analyse natural and man-made objects and surfaces (National Oceanic and Atmospheric Administration, 2018). A set of data points (also referred to as a

point cloud) can consist of millions of points, each encompassing its own spacial information, i.e. longitude, latitude and elevation (Geospatial Consulting, Inc., 2018). Similar to photogrammetry, discussed in section 2.3.2.2, this point cloud can be used to generate a three-dimensional representation or model of the target object or area (AOC Archaeology Group, n.d.).

### **Working of the system**

As previously mentioned, LiDAR technology functions conceptually similar to radar technology (3D Laser Mapping, 2019). Similar to the radar system, LiDAR also consists of a transmitting unit, emitting a type of energy wave. Data is collected when this energy wave is echoed (reflected by an object or surface) and received by a receiver unit. However, there are distinct differences between these two technologies (some are highlighted in Table 2.11).

LiDAR emits laser pulses in rapid succession, up to 150,000 pulses per second, toward a target area (Elprocus, 2019). An internal sensor unit measures the time of each reflected wave (echo) which allows the system to interpret other data since the speed of light (laser pulse) is known (Elprocus, 2019).

A typical LiDAR system consists of four main components, namely (National Oceanic and Atmospheric Administration, 2018; Elprocus, 2019):

#### **(1) Laser**

A variety of lasers are available in different LiDAR systems. Elprocus (2019) explained that a 1,064 nm diode-pumped Nd (neodymium-doped): YAG (yttrium-aluminium-garnet) laser is typically used in airborne LiDAR systems and a 532 nm double diode-pumped Nd:YAG laser is typically used in Bathymetric LiDAR systems. A laser using shorter pulses yield greater resolution if the receiver unit has sufficient capacity to process the increased data flow (Elprocus, 2019).

#### **(2) Scanner (or Optics)**

The scanning capability of the LiDAR system determines the speed that the images (data) can be developed. The type of optic determines the range and resolution of the system (Elprocus, 2019).

(3) The receiver unit (Photodetector)

The receiver unit or photodetector is a device that reads and records the echoed signal to the system (Elprocus, 2019).

(4) GPS (Global Positioning/Navigation System)

The GPS in the LiDAR unit generate accurate coordinates of the LiDAR sensor and an inertial measurement unit (IMU) records the orientation of the LiDAR unit (Elprocus, 2019).

Figure 2.20 illustrates the basic schematic of a LiDAR unit. The infrared diode generates the laser beam that is transmitted towards the target object or area. This beam is then reflected by the target object or surface and received by the receiver in the LiDAR as data points. These data points are georeferenced by LiDAR's GPS (Elprocus, 2019). The data collected is imported into specialised software and processed. After processing, the data points are presented as an accurate, georeferenced point cloud that is for further processing and analysis (LiDAR-UK, 2019).

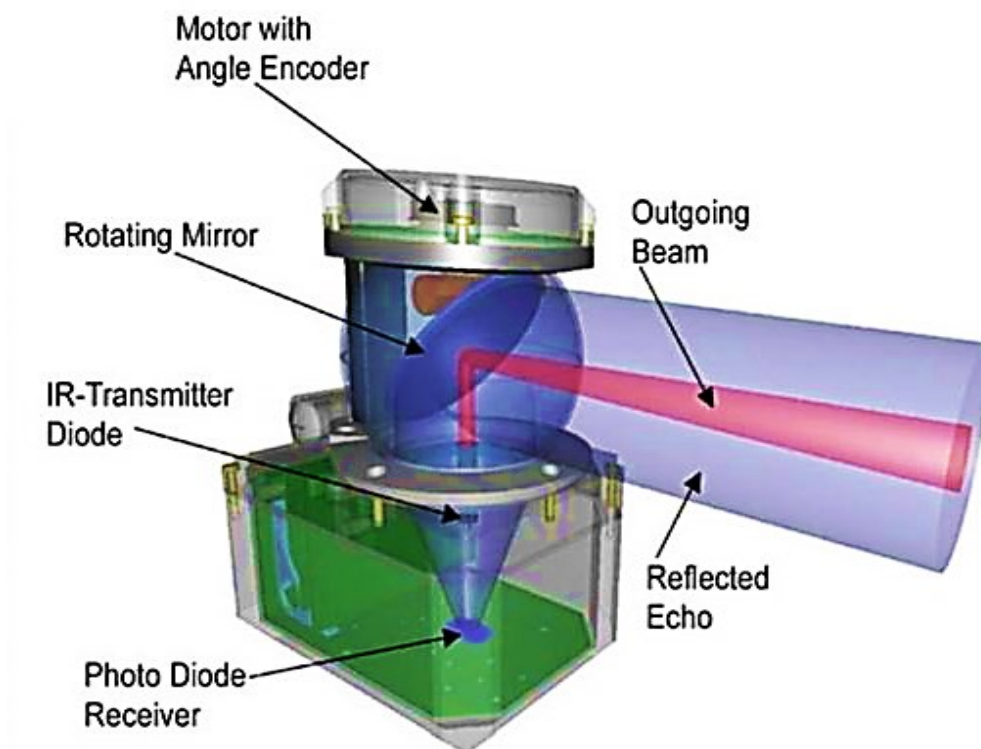


Figure 2.20: Schematic of a LiDAR system (Elprocus, 2019)

Similar to photogrammetry, the point cloud output can be used to generate accurate three-dimensional representations or models of the target area or object, including engineering design models and survey outputs such as volume measurements and elevation contours. If



data (of the same area or object) is collected at different GPS positions, the resulting point clouds can be “stitched” together to form one dataset (Geospatial Consulting, Inc., 2018). This process is known as registration (Geospatial Consulting, Inc., 2018).

### **Types of LiDAR**

There are different types of LiDAR systems available and are typically implemented for different purposes. LiDAR is often classified differently, depending on the purpose of the classification. Elprocus (2019) classifies LiDAR according to:

(1) Platform or Mounting, i.e.:

- Ground-based LiDAR
- Airborne LiDAR
- Spaceborne LiDAR

(2) Physical process, i.e.:

- Rangefinder LiDAR
- DIAL LiDAR
- Doppler LiDAR

(3) Scattering process, i.e.:

- Mie
- Rayleigh
- Raman
- Fluorescence

For the purpose of this project, the platform or mounting classification will be sufficient.

### **Applications of LiDAR**

Geospatial Consulting, Inc. (2018) lists the industries and circumstances where LiDAR can add value as:

- Engineering  
Processes and system in manufacturing can be monitored and visualised using LiDAR systems. Existing design layouts can be digitised and used to conduct deviation analysis and clash detection (Geospatial Consulting, Inc., 2018). Engineering of autonomous vehicles includes the use of LiDAR sensors as the

vehicles main method of identifying and manoeuvring around obstacles (Geospatial Consulting, Inc., 2018).

Civil engineers use LiDAR technology to conduct topographical surveys to use in infrastructure designs such as buildings, roads and bridges. LiDAR is also used in the monitoring of dams' and tunnels' structural integrity (deformation analysis) (Geospatial Consulting, Inc., 2018).

- **Architecture**  
Architects use LiDAR to create as-built drawings of existing buildings and generate three-dimensional models. LiDAR is also often used to conduct land boundary surveys according to regional laws and regulations (Geospatial Consulting, Inc., 2018).
- **Urban planning**  
Urban planners use LiDAR to map city layouts and existing structures. Three-dimensional models can be created and existing water supply lines, waste drainage lines and electrical power lines can be mapped and incorporated in these models (LIDAR and RADAR Information, 2019). Sub-stations and powerplants are also mapped for planning purposes (Geospatial Consulting, Inc., 2018).
- **Road safety**  
Law enforcement uses LiDAR to measure the speeds of vehicles travelling on public roads (LIDAR and RADAR Information, 2019).
- **Space exploration**  
Astronomers use LiDAR technology to estimate the size and shape of celestial bodies in space, as well as the distance between these bodies and earth (LIDAR and RADAR Information, 2019).
- **Meteorology and Atmospheric physics**  
Meteorologists use LiDAR to study clouds and the behaviour thereof. The LiDAR beam strikes the particles in the cloud and the density of the cloud can be determined and investigated (Elprocus, 2019). LiDAR can also be used to determine the concentration of specific gas particles (such as O<sub>2</sub>, nitrogen and sulphur) in the middle and upper atmosphere (Elprocus, 2019).

- Mining

In the oil and natural gas industry, LiDAR is commonly used to map and study topographical areas in order to identify potential mineral-rich areas (LIDAR and RADAR Information, 2019).

Operational mines use LiDAR to map operations (layout) and track movement in the rock mass that can pose a significant safety risk to the employees (LIDAR and RADAR Information, 2019). This allows early identification of high-risk areas so that additional support can be installed or, if necessary, operations evacuated.

- Military

LiDAR is used to determine the precise location of a target and estimate the size of the target (which is beyond the capability of radar technology) (LIDAR and RADAR Information, 2019). Aerial mapping allows the military command to understand the geographical terrain before sending their teams into an area (Elprocus, 2019).

Drones and stealth aircraft use LiDAR sensors for orientation and to ensure accurate weapon strikes (LIDAR and RADAR Information, 2019).

- Forensics and expert witness

Criminologists and other forensic experts use LiDAR to map a crime scene, to create an accurate digital representation, for further investigation and analysis. This digital representation help investigators to re-create the specific event, including arson, bombings, and other catastrophic incidents (Geospatial Consulting, Inc., 2018).

- Archaeology

LiDAR is used by archaeologists to determine potential locations of historical value or historical artefacts buried below the earth's surface (LIDAR and RADAR Information, 2019).

- **Agriculture and Forestry**

LiDAR is used to map the location and pattern of a set of crops for agricultural purposes. Aerial LiDAR is often used to monitor the health of these crops as well as the soil conditions prior to planting (LIDAR and RADAR Information, 2019).

Aerial LiDAR surveillance is often used to monitor and manage forests. Managing forests include tracking forest fires, deforestation and illegal logging activities (LIDAR and RADAR Information, 2019).

River systems (i.e. depth and width of rivers, flow strength and underwater properties) is also monitored and studied using LiDAR (Elprocus, 2019).

- **Oceanography**

LiDAR is used to measure the depth of the oceans (also known as bathymetry), as well as study and calculate the phytoplankton fluorescence and biomass in the ocean (Elprocus, 2019).

### **Advantages and disadvantages of LiDAR**

The following advantages and disadvantages of LiDAR are presented on a website by LIDAR and RADAR Information (2019).

#### **Advantages (LIDAR and RADAR Information, 2019)**

- Data can be collected fast and with high accuracy.
- Surface data has a higher sample density, i.e. dense point cloud.
- Capable of collecting elevation data in a dense forest.
- Can be used day and night.
- Does not have any geometry distortions.
- It can be integrated with other data sources.
- It has minimum human dependence.
- It is not affected by extreme weather.
- Can be used to map inaccessible and featureless areas.

#### **Disadvantages (LIDAR and RADAR Information, 2019)**

- High operating costs in some applications.
- Ineffective during heavy rain or low hanging clouds.
- Degraded at high sun angles and reflections.
- Unreliable for water depth and turbulent breaking waves.

- Very large datasets that are difficult to interpret.
- Elevation errors due to the inability to penetrate very dense forests.
- The laser beams may affect the human eye in cases where the beam is powerful.
- Inability to penetrate thick vegetation.
- Requires skilled data analysis techniques.
- The low operating altitude of between 500 to 2,000m.

#### **2.3.2.5. ViDAR (Visual Detection and Ranging)**

ViDAR, i.e. visual detection and ranging, is a relatively new “optical radar” technology developed by the Australian research and development company, Sentient Vision (Sentient Vision Pty Ltd, 2016). With successful trials conducted in September 2016 in the United States of America, this technology is reportedly “*challenging radar as the sensor of choice in airborne search and rescue*” (Sentient Vision, 2017). During these 2016 trials, the following detection capabilities were demonstrated (Sentient Vision Pty Ltd, 2016):

- Detection of a person in water: more than 1.7 nautical miles (or 3.15 km)
- Detection of a six-person raft: more than 3.5 nautical miles (or 6.48 km)
- Detection of a 12 m boat: more than 17.5 nautical miles (or 32.41 km)
- Detection of a 6 m boat: more than 9.1 nautical miles (or 16.85 km)
- Detection of a large ship: more than 30 nautical miles (or 55.56 km)

ViDAR is formally defined as “*an airborne wide-area maritime search system that autonomously detects objects on the ocean surface and provides the operator with a detailed image of objects that other search methods often miss*” (Sentient Vision Pty Ltd, 2016).

Day (2017) explains that this system uses one or more commercially available, high-resolution video- or infrared cameras, typically mounted on a small UAV (unmanned aerial vehicle or drone), that scans 180° in front of the aircraft. If this system is required for function on a larger, manned aircraft, three to five cameras are typically used (Day, 2017). This system allows search and rescue team to search across the ocean surface with significantly greater coverage, up to 80 times the capability of other EO/IR (electro-optical and infrared) sensor systems (Electronic Sub-Systems, 2018).

ViDAR has the potential to significantly reduce the timeline and man-power required in a search and rescue operation, which can potentially be the difference between “search and rescue” or “recovery” (Sentient Vision, 2017).

## **Working of the system**

As briefly mentioned in the previous paragraphs, the ViDAR system consists of (Sentient Vision Pty Ltd, 2016):

- One to five high-resolution commercially available cameras
- An onboard processor per camera
- Integration system into the aircraft mission system

Video feed from the cameras is automatically processed (in real-time) by means of the onboard processing units. The algorithms written in the processing software analyses each pixel in each frame and evaluates it against the background of the ocean's surface (Day, 2017). The goal is to detect objects on the water's surface. The software is also designed to differentiate between a potential object of interest and environmental features such as white tops from waves, sun glare and mist (Day, 2017).

Once a potential target is autonomously identified by the software, a georeferenced still photo is sent to the operator for review (Day, 2017). The operator determines whether a target requires further investigation or not. If further investigation is required, the aircraft's "spotter sensor" is alerted, enabling the cameras to zoom in on the target (Day, 2017).

The developers of the ViDAR system, Sentient Vision (Pty) Ltd. (2016), lists the following as the capabilities of the system:

- Real-time detection of small objects
- Autonomous detection
- Wide area coverage
- Sensor cross-cue
- Passive search
- Up to sea state 6 (i.e. very rough seas, with wave heights of up to 6 meters)
- Reduces operator workload

## **Applications of ViDAR**

Sentient Vision Pty Ltd (2016) lists the applications of the ViDAR system as:

- Marine search and rescue
- Anti-piracy on the oceans
- Counter-narcotics
- Illegal immigration across the sea

- Persistent oceanic surveillance
- Maritime security
- Exclusive Economic Zone (EEZ) patrol

#### **2.3.2.6. Other potential projectile tracking technologies**

The following techniques or technologies are briefly presented as an indication of specialised work done in the field of projectile or object tracking. Some specific information regarding the tracking, processing and analysis algorithms may not be available. Therefore, only a basic overview of other potential techniques or technologies is discussed in this section.

##### **Hawk-eye**

Hawk-eye is a technology and innovations company that forms part of the Sony group. Hawk-eye is currently the leading innovations company in sports technology with their main focus and core objective to make sport fairer, safer and more engaging for spectators (Hawk-Eye Innovations Ltd., 2018). Initial research began in February 1999 and Hawk-eye officially launched as a company in September 2001 (Hawk-Eye Innovations Ltd., 2018). The following timeline (Table 2.12) of major milestones are presented by Hawk-Eye Innovations Ltd. (2018):

**Table 2.12: Hawk-eye timeline (Hawk-Eye Innovations Ltd., 2018)**

<b>Date</b>	<b>Milestone</b>
<b>Feb 2002</b>	Hawk-eye is first used in a tennis match as a part of the BBC network's coverage of the Davis Cup.
<b>Jan 2003</b>	Hawk-eye debuts in the Australian Grand Slam tournament.
<b>March 2006</b>	The first tournament (Nasdaq 100 in Miami) officially adopt the Hawk-eye system.
<b>Feb 2007</b>	Development starts on Hawk-eye's goal-line technology for football, which is initially approved by the IFAB (international football association board), which is later withdrawn.
<b>June 2007</b>	Hawk-eye technology is adopted at Wimbledon.
<b>Aug 2008</b>	Hawk-eye technology gets involved in the Olympic Games for the first time.
<b>March 2011</b>	Sony acquires Hawk-eye as a flagship company for its sports business
<b>July 2012</b>	IFAB officially approves Hawk-eye's goal-line technology and Hawk-eye becomes an official license holder of the technology.
<b>Aug 2012</b>	Hawk-eye's video replay technology is used in Major League Baseball and the Olympic Games.
<b>May 2013</b>	The Premier League confirms the official use of Hawk-eye's goal-line technology.
<b>2014 - 2015</b>	Hawk-eye's technology is adopted in other sport such as badminton, horse racing, athletics, volleyball and rugby.

Currently, Hawk-eye's technology is part of more than 20 sports in over 90 countries (Hawk-Eye Innovations Ltd., 2018).

Hawk-eye is commonly associated with ball sports, due to their mm-accuracy ball-tracking technology and software. However, Hawk-eye's visual processing technology is also capable of tracking larger objects such as cars (Nascar) and the movements of individual athletes (Hawk-Eye Innovations Ltd., 2018). This makes the technology beneficial to coaches.

The Hawk-eye system consists of a minimum of six high-performance cameras (Figure 2.21) that are positioned around a stadium to ensure adequate coverage of the field or target area (Vijayakumar & Anand, 2016 ). The video feed from the cameras and the advanced visual processing technology are combined with Hawk-eye's intelligent IT-based software to

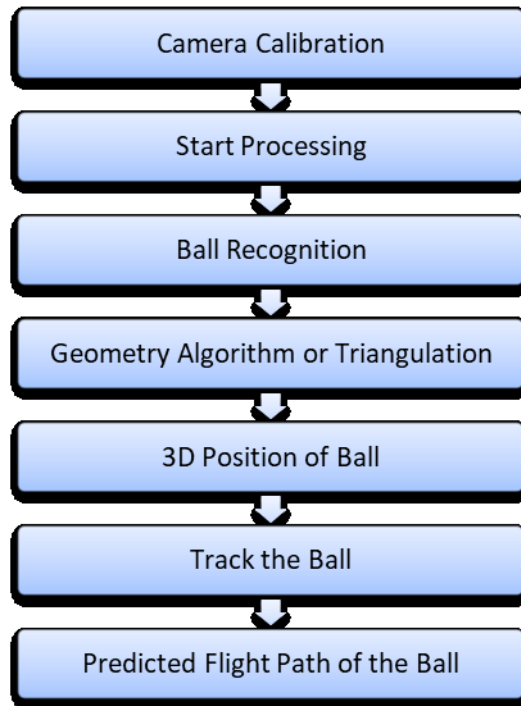


generate a number of different output, depending on the results required at that point (Hawk-Eye Innovations Ltd., 2018).



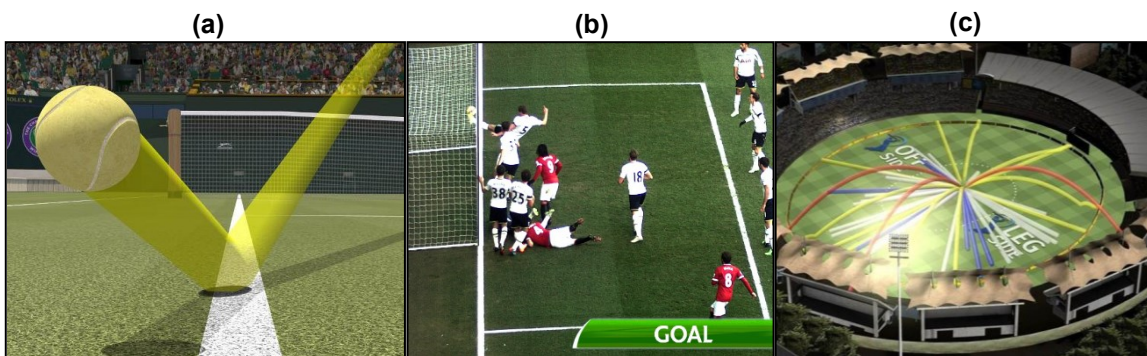
**Figure 2.21: Hawk-eye technology camera layout in a stadium (the focus of the system is the target area) (Bandaru, 2016)**

A ball is tracked by the system based on the calibration of the cameras in the stadium, which is very controlled and remains the same through the use of the system, and the triangulation between the cameras and the ball (Vijayakumar & Anand, 2016 ). The workflow of the system is summarised by Vijayakumar & Anand (2016) and given in Figure 2.22.



**Figure 2.22: Workflow of the Hawk-eye ball tracking system (Vijayakumar & Anand, 2016 )**

Hawk-eye has made a significant impact on sport officiating and broadcasting. Sports such as tennis (Figure 2.23 (a)), soccer or football (Figure 2.23 (b)), cricket (Figure 2.23 (c)), badminton, snooker, baseball, rugby and volleyball have implemented hawk-eye as a standard system (Bandaru, 2016). This system can automatically calculate the speed the ball is travelling, the specific movement and spin of the ball, the origin of the ball and finally predict the expected flight path (trajectory) of the ball.



**Figure 2.23: Hawk-eye in sports, (a) Tennis, (b) Soccer or Football, (c) Cricket (Hawk-Eye Innovations Ltd., 2018)**

It is important to note the controlled environment required with the Hawkeye system and that only one projectile is tracked at any point in time. In addition, the dimensions of the target object (i.e. the ball that is being tracked) must be within a predetermined range (typically 5mm (Bandaru, 2016)). When the target object exceeds this tolerance, the accuracy of the predicted trajectory will decrease.

Note: the detection and tracking algorithms are not available in the public domain, however, can potentially contribute to the concept developed in this project.

### Visual or optical detection and tracking

Visual or optical detection and tracking systems are based on a visual sensor, typically a camera, which records the setting through which an object moves. This visual sensor records the observation area as a video which can be analysed manually or through specially designed software. Once the data is captured and recorded, it is analysed based on video object and motion segmentation principles (Hu, et al., 2015; Anthwal & Ganotra, 2019).

Trambadiya & Varnagar (2015) illustrates the basic analysis steps in Figure 2.24 and divides the analysis of video data into three main phases, (1) Object Detection, (2) Object Classification and (3) Object Tracking.

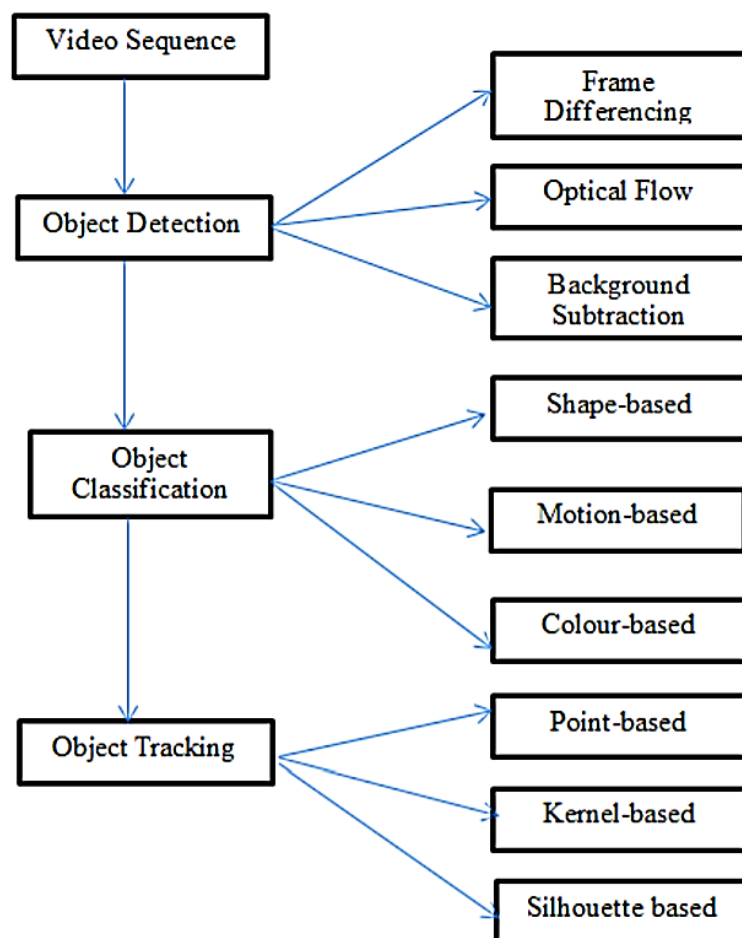


Figure 2.24: Basic steps for detecting and tracking an object (Trambadiya & Varnagar, 2015)

(1) Object Detection (Trambadiya & Varnagar, 2015)

Object detection is the first step in the data analysis process and is based on one of three methods, namely:

- Frame differing, i.e. comparing two successive video frames or images and calculating the differences. This is typically considered to be a simple calculation that is easy to implement, but it can be difficult to find the correct outline of the object of interest which will ultimately reduce the overall accuracy of the detection method.
- Optical flow, i.e. the calculation of the optical flow, defined as the apparent motion of objects in a scene, based on the motion between the scene and the observer or sensor (Science Direct, 2013). Group or clustering processing is conducted according to the calculated (optical flow) characteristics within the frame or image. This method extracts better or more complete motion data from the background but is very sensitive to noise in the image.
- Background subtraction, i.e. an object segmentation technique that requires an accurate model of the background information in the scene prior to applying the detection and tracking technique. This model is used to subtract all the background information from the video frames or images to identify and track any new information or objects in view. This method renders very accurate result but is very sensitive to external variations, in other words, if the background changes during the detection and tracking process, the subtracted background model will not remain an accurate representation. Background subtraction is commonly based on one of two approaches, namely Recursive algorithms and Non-recursive algorithms.

(2) Object Classification (Trambadiya & Varnagar, 2015)

Object classification is the second step in the data analysis process and is based on one of three methods, namely:

- Shape-based;
- Motion-based; and,
- Colour-based.

### (3) Object Tracking (Trambadiya & Varnagar, 2015)

Object tracking is the final step in the data analysis process and is based on one of three methods, namely:

- Point-based, i.e. once an image structure is created, the motion of an object is tracked based on the feature points identified on the object. This means that the software algorithms recognise the object through these feature points and tracks the motion of the objects by identifying the same point in successive frames or images. Tracking objects using the point-based method is achieved by three algorithms or approaches, namely the Kalman filter, the Particle filtering algorithm and the Multiple hypothesis tracking (MHT) algorithm.
- Kernel-based, i.e. the motion of an object is calculated from one frame or image to the next by assigning and tracking a geometric shape that closely resembles the objects, represented by the embryonic region of the object. One restriction is that portions of the object may fall outside of this geometric shape and some portions of the background may fall within it. Tracking objects using the kernel-based method is achieved by three algorithms or approaches, namely Template matching, the Mean shift method and the Support vector machine (SVM).
- Silhouette-based, i.e. generating an accurate object model (shape description) based on finding the object outline from prior frames or images. This is done by considering the contours and shadows visible in the images. This method is often implemented when a complex shaped object is considered, such as hands and fingers, i.e. when a general geometric shape cannot be associated with the shape of the object. Tracking objects using the silhouette-based method is achieved by two algorithms or approaches, namely Contour tracking and Shape matching.

Numerous other algorithms and models exist that can be used for the analysis and interpretation of the information collected using visual or optical detection and tracking systems, but these are outside of the scope of this project. However, analysing the data captured and interpreting the results are still a subject of active research across several industries (Hu, et al., 2015).

Visual or optical systems are used in numerous fields such as detection and tracking of moving or stationary objects or people through video surveillance or still images in (Akshay, et al., 2016):

- Security and protection services (intelligent surveillance);
- Traffic surveillance services;
- Military guidance systems;
- Navigation systems in robotics and drones;
- Artificial Intelligence (AI); and
- Numerous medical applications.

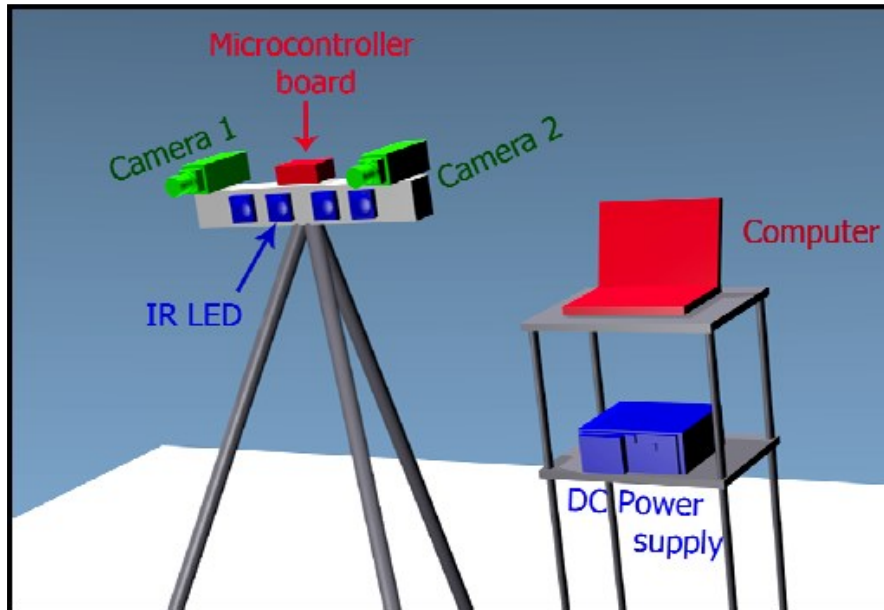
### **Active infrared system**

Detection and tracking of supersonic projectiles (artillery rounds) have been effective using a combination of acoustic sensors and techniques. These systems identify and track supersonic projectile by detecting the shockwaves created by the projectile through a medium, typically air, or the shockwave originating from the muzzle of the weapon (Stančić, et al., 2017). However, silenced weapons and subsonic rounds are often difficult to detect with acoustic sensors.

Other techniques, such as optical and optical-electrical techniques, detects the visible “flash” from the muzzle of the weapon (Kastek, et al., 2010). However, modern muzzle suppression technology reduces this visible “flash” as well as the audible “blast”, increasing the challenges experienced by acoustic and optical techniques (Stančić, et al., 2017).

Stančić, et al. (2017) proposed an active infrared detection and tracking system, that is potentially able to identify and track subsonic artillery fire. The basic design layout (Figure 2.25) of this system consists of two high-speed cameras, set up in a stereo configuration (i.e. the cameras have overlapping fields of view across the target area allowing the conversion from two-dimensional images into a three-dimensional space). An external power source is included to provide constant power to the system and a computer is used to control and stream the footage obtained from both cameras.

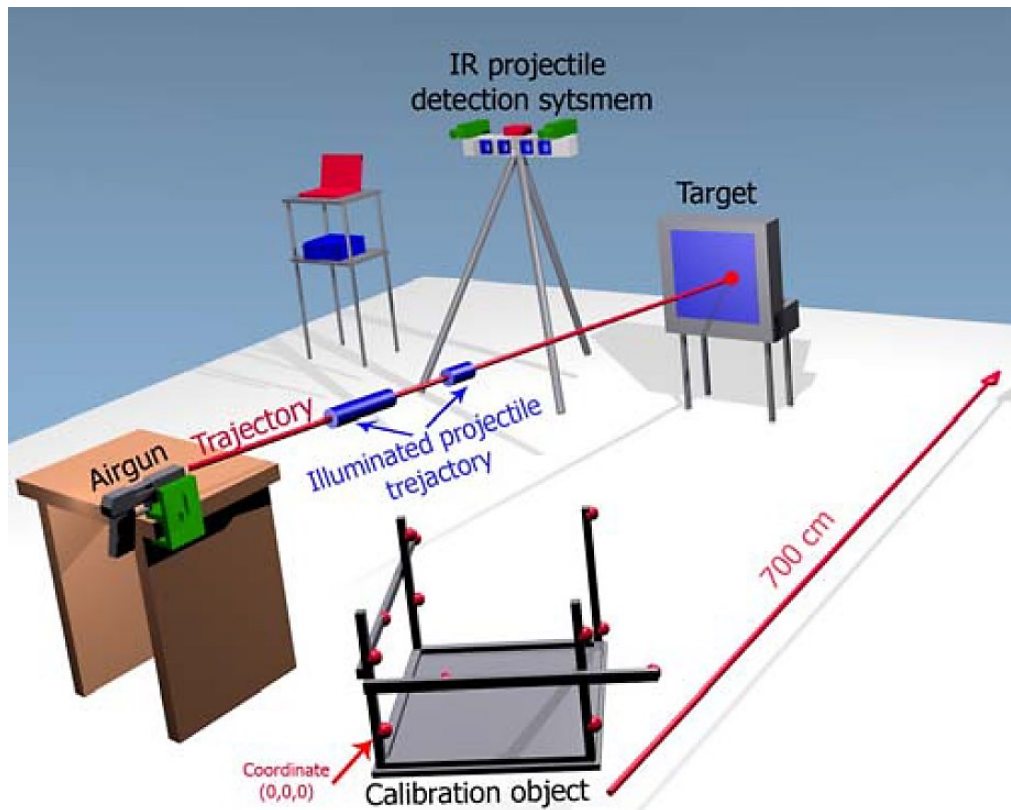




**Figure 2.25: Layout and components of the active infrared system (Stančić, et al., 2017)**

The proposed system (similar to a visual or optical system) consists of two main phases, i.e. (1) detect and (2) track a projectile, and is designed to use an infrared light source to illuminate the field of view of the cameras, through which the projectile will move. Algorithms are used to detect a moving projectile through the illuminated field by comparing background images or frames with subsequent images or frames (Stančić, et al., 2017). The constant infrared illumination of the cameras' fields of view allows the cameras to capture the projectile's trajectory trail, a line across the captured images that illustrates the positions of the projectile from which data can be collected (Stančić, et al., 2017).

It is important to note that the calibration of the cameras is essential to the accuracy of the data obtained. The cameras are calibrated by placing a known control or reference in the fields of view of the cameras prior to and while capturing the projectile in motion (Stančić, et al., 2017). This setup is illustrated in Figure 2.26.



**Figure 2.26: Concept test setup of the active infrared system for detecting and tracking a projectile (Stančić, et al., 2017)**

Following 20 trials, using the setup shown in Figure 2.26, a projectile and its trajectory were successfully detected and reconstructed with acceptable accuracy. Stančić, et al. (2017) did note that the detection and tracking accuracy is higher for projectiles within a range of 1m from the infrared detector system (i.e. the infrared LED and two cameras) compared to those moving further away from the system.

Considering that the main objective of this system was to detect and track subsonic projectiles, which have proven to be challenging using existing acoustic techniques, this system does have some potential. However, there are some significant limitations that require additional research and development, namely (Stančić, et al., 2017):

- The field of view or target area is limited to the effective range of the infrared illuminator;
- The effective range or target area of the system is small, i.e. 4m width, 3m height and 8m depth;
- The tracking component is dependent on the infrared illumination and the creation of the trajectory trail of the projectile; and,



- The authors also suggest that further work should be done on refining the algorithms used in order to increase the accuracy of the system.

There are several techniques and technologies available that may assist in this project. The work that has previously been conducted in the field of flyrock prediction have also added value to the success of this project. These previously proposed models, techniques and technologies are analysed and evaluated in Chapter 3 according to the desired outcomes of this project.

## 2.4. REFERENCES

- Bester, K., 2019. *SmartTech: Photogrammetry and Stereo Mapping* [Interview] 2019.
- 3D Laser Mapping, 2019. *What can you use LiDAR for?*. [Online] Available at: <https://www.3dlasermapping.com/what-is-lidar-and-how-does-it-work/> [Accessed 11 April 2019].
- Akshay, S., Sajin, T. & Ram, P. A., 2016. Improved Multiple Object Detection and Tracking Using KF-OF Method. *International Journal of Engineering and Technology (IJET)*, 8(2), pp. 1162-1168.
- Anthwal, S. & Ganotra, D., 2019. An overview of optical flow-based approaches for motion segmentation. *The Imaging Science Journal*, 67(5), pp. 284-294.
- AOC Archaeology Group, n.d. *3D Laser Scanning and Aerial Lidar*. [Online] Available at: <http://www.aocarchaeology.com/services/archaeology/survey/3Dscanning/> [Accessed 11 April 2019].
- Apogee Instruments Incorporated, 2019. *Applications and Uses of UV Sensors*. [Online] Available at: <https://www.apogeeinstruments.com/applications-and-uses-of-uv-sensors/> [Accessed 27 February 2019].
- Armaghani, D. J. et al., 2016. Risk Assessment and Prediction of Flyrock Distance by Combined Multiple Regression Analysis and Monte Carlo Simulation of Quarry Blasting. *Rock Mechanics and Rock Engineering*, 49(9), pp. 3631-3641.
- Armaghani, D. J. et al., 2016. Evaluation and prediction of flyrock resulting from blasting operation using empirical and computational methods. *Engineering with Computers*, 32(1), pp. 109-121.
- Avnet Inc., 2019. *Pressure Sensors: The Design Engineer's Guide*. [Online] Available at: <https://www.avnet.com/wps/portal/abacus/solutions/technologies/sensors/pressure-sensors/> [Accessed 07 May 2019].
- Bandaru, A., 2016. *Hawk-Eye Technology - An Understanding*. [Online] Available at: <https://www.slideshare.net/AbhinayBandaru2/hawk-eye-technology-an-understanding> [Accessed 23 April 2019].
- Beg, S. M., 2017. *A cloud-integrated wireless garbage management system for smart cities - Scientific Figure on ResearchGate..* [Online] Available at: [https://www.researchgate.net/figure/Sketch-of-working-principle-of-the-Ultrasonic-Sensor-C-Smoke-Sensor-MQ2-Gas-Sensor\\_fig2\\_3213481](https://www.researchgate.net/figure/Sketch-of-working-principle-of-the-Ultrasonic-Sensor-C-Smoke-Sensor-MQ2-Gas-Sensor_fig2_3213481) [Accessed 27 February 2019].
- Bouzgou, H., 2006. *Development of Multiple Regression Systems for Hyperdimensional Spectral Spaces*, Batna: University of Batna.

Brain, M., 2019. *How Radar Works*. [Online] Available at: <https://science.howstuffworks.com/radar.htm> [Accessed 21 May 2019].

Chiappetta, R. F., 2014. *Optimizing your Drill and Blast Strategy*. Johannesburg, BAI: Blasting Analysis International Inc.

Chiappetta, R. F. & Treleven, T., 1997. *Expansion of the Panama Canal*. Allentown, PA, Blasting Analysis International Inc. (BAI), p. 967.

Colorado Department of Transportation, 2015. Chapter 4: Aerial Surveys. In: *Survey Manual*. Colorado: Colorado Department of Transportation.

Committee on New Sensor Technologies, 1995. Chapter 1: Introduction to Sensors. In: *Expanding the Vision of Sensor Materials*. Washington D.C.: National Academy Press, pp. 9-18.

Coulton.com, 2019. *Beginner's guide to the ultrasonic level transmitter*. [Online] Available at: [https://www.coulton.com/beginners\\_guide\\_to\\_ultrasonic\\_level\\_transmitters.html](https://www.coulton.com/beginners_guide_to_ultrasonic_level_transmitters.html) [Accessed 27 February 2019].

Cox, S., 2017. *What is Exposure? (A Beginner's Guide)*. [Online] Available at: <https://photographylife.com/what-is-exposure> [Accessed 22 May 2019].

Cruise, J. A., 2011. *Rock Breaking - A Science, not an Art*. s.l., Southern African Institute of Mining and Metallurgy.

Day, S., 2017. *ViDAR Optical Radar Provides New Maritime Search Capability*. [Online] Available at: <https://www.techbriefs.com/component/content/article/tb/features/application-briefs/26476> [Accessed 11 April 2019].

de Graaf, W. W., 2016. *Blasting Engineering Programme: Module 5 (Flyrock)*. Pretoria, Enterprises (University of Pretoria).

Decatur Electronics, 2019. *History of Radar*. [Online] Available at: <https://www.decaturelectronics.com/information-center/history-of-radar> [Accessed 21 May 2019].

Dehghani, H. & Shafaghi, M., 2017. Prediction of blast-induced flyrock using differential evolution algorithm. *Engineering with Computers*, 33(1), pp. 149-158.

Doctor, R., 2019. *Feature/Science: World's Fastest Camera Captures Speed of Light in Slow Motion*. [Online] Available at: <https://www.techtimes.com/articles/240692/20190401/worlds-fastest-camera-captures-speed-of-light-in-slow-motion.htm> [Accessed 22 May 2019].

- Dunlop, J., 2011. *Photography for Beginners: A Complete Guide*. [Online] Available at: <https://expertphotography.com/a-beginners-guide-to-photography/#Focal Length> [Accessed 22 May 2019].
- Electronic Sub-Systems, 2018. *Sentient Vision to Showcase ViDAR Optical Radar*. [Online] Available at: <https://www.uasvision.com/2018/04/12/sentient-vision-to-showcase-vidar-optical-radar/> [Accessed 11 April 2019].
- Elprocus, 2019. *All You Know About LIDAR Systems and Applications*. [Online] Available at: <https://www.elprocus.com/lidar-light-detection-and-ranging-working-application/> [Accessed 11 April 2019].
- Elprocus, 2019. *RADAR: Basics, Types and Applications*. [Online] Available at: <https://www.elprocus.com/radar-basics-types-and-applications/> [Accessed 21 May 2019].
- Encyclopædia Britannica, Inc., 2019. *Electronics: History of Radar*. [Online] Available at: <https://www.britannica.com/technology/radar/Advances-during-World-War-II> [Accessed 21 May 2019].
- Engineers Garage, 2012. *Blogs: Sensor Types used in IoT*. [Online] Available at: <https://www.engineersgarage.com/blogs/sensor-types-used-iot> [Accessed 27 February 2019].
- Engineers Garage, 2012. *Insight: Learn the Working of Ultrasonic Sensors*. [Online] Available at: <https://www.engineersgarage.com/insight/how-ultrasonic-sensors-work> [Accessed 27 February 2019].
- Engineers Garage, 2012. *Sensors: Different Types of Sensors*. [Online] Available at: <https://www.engineersgarage.com/articles/sensors> [Accessed 27 February 2019].
- Faramarzi, F., Mansouri, H. & Farsangi, M. A., 2014. Development of Rock Engineering Systems-Based Models for Flyrock Risk Analysis and Prediction of Flyrock Distance in Surface Blasting. *Rock Mechanics and Rock Engineering*, 47(4), pp. 1291-1306.
- Fargo Controls Inc., 2018. *Operating Principles for Proximity Sensors*. [Online] Available at: <http://www.fargocontrols.com/sensors.html> [Accessed 25 February 2019].
- Fuller, P. W. W., 2007. Definition of High-Speed Photography. In: *Focal Encyclopedia of Photography (4th Edition)*. Woburn, MA: Focal Press, p. 539.
- Fuller, P. W. W., 2009. An introduction to high-speed photography and photonics. *The Imaging Science Journal*, 57(6), pp. 293-302.

Future of Life Institute, 2016. *Benefit and Risks of Artificial Intelligence*. [Online] Available at: <https://www.futureoflife.org/background/benefits-risks-of-artificial-intelligence/?cn-reloaded=1>  
[Accessed 3 September 2019].

Gabriel, M., 2019. *Articles: High-Speed Photography 101*. [Online] Available at: <https://contrastly.com/high-speed-photography-101/>  
[Accessed 22 May 2019].

GeeksTips.com, 2019. *Arduino Snow Depth Remote Sensing with Ultrasonic Sensor and ESP8266*. [Online] Available at: <https://www.geekstips.com/arduino-snow-depth-remote-sensing-with-ultrasonic-sensor/>  
[Accessed 27 February 2019].

Geospatial Consulting, Inc., 2018. *Terrestrial LiDAR / 3D Laser Scanning*. [Online] Available at: <http://www.cbcgeospatial.com/terrestrial-lidar.html>  
[Accessed 11 April 2019].

Ghasemi, E., Amini, H., Ataei, M. & Khalokakaei, R., 2014. Application of artificial intelligence techniques for predicting the flyrock distance caused by the blasting operation. *Arabian Journal of Geosciences*, 7(1), pp. 193-202.

Ghasemi, E., Sari, M. & Ataei, M., 2012. Development of an empirical model for predicting the effects of controllable blasting parameters on flyrock distance in surface mines. *International Journal of Rock Mechanics and Mining Sciences*, Volume 52, pp. 163-170.

Gillespie, K., 2018. *12 Ultrasonic Sensor Applications*. [Online] Available at: <https://www.maxbotix.com/articles/ultrasonic-sensor-applications.htm>  
[Accessed 22 April 2019].

GIS Resources, 2018. *Most Common Business Uses of Photogrammetry*. [Online] Available at: <http://www.gisresources.com/common-business-uses-photogrammetry/>  
[Accessed 22 March 2019].

Gudino, M., 2018. *How Touch Sensors Work*. [Online] Available at: <https://www.arrow.com/en/research-and-events/articles/how-touch-sensors-work>  
[Accessed 25 February 2018].

Harrod Sport, 2018. *Hawk-Eye - Technology in Sport*. [Online] Available at: <https://www.harrod sport.com/advice-and-guides/hawkeye-technology-in-sport>  
[Accessed 7 August 2018 ].

Hasanipanah, M. et al., 2017. Development of a precise model for prediction of blast-induced flyrock using regression tree technique. *Environmental Earth Sciences*, Volume 76, p. 27 (10).

Hawk-Eye Innovations Ltd., 2018. *Hawk-Eye Innovations*. [Online] Available at: <https://www.hawkeyeinnovations.com/index.html> [Accessed 7 August 2018].

HBM, n.d. *Definition of a Pressure Sensor*. [Online] Available at: <https://www.hbm.com/en/7646/what-is-a-pressure-sensor/> [Accessed 07 May 2019].

Hudson, J. A., 2014. A review of Rock Engineering Systems (RES) applications over the last 20 years. In: X. Feng, J. A. Hudson & F. Tan, eds. *Rock Characterisation, Modelling and Engineering Design Methods*. Chichester: Ellis Horwood, pp. 419-424.

Hu, W.-C. et al., 2015. Moving object detection and tracking from video captured by moving camera. *Journal of Visual Communication and Image Representation*, Volume 30, pp. 164-180.

Intelliplate.com, 2019. *What is Artificial Intelligence?* [Online] Available at: <https://www.intelliplate.com/blog/what-is-artificial-intelligence/> [Accessed 6 October 2019].

ISEE, 2011. Chapter 14: Blast Design Principles. In: J. F. Stiehr, ed. *Blasters' Handbook*. USA: International Society of Explosives Engineers, pp. 341-382.

ISEE, 2011. Chapter 15: Flyrock. In: J. F. Stiehr, ed. *Blasters' Handbook*. USA: International Society of Explosives Engineers, pp. 383-410.

Jang, J.-S. R., 1993. ANFIS: Adaptive-Network-Based Fuzzy Inference System. *IEEE Transactions on Systems, Man and Cybernetics*, 23(3), pp. 665-685.

Kastek, M., Dulski, R., Trzaskawka, P. & Brieszczad, G., 2010. Sniper detection using an infrared camera: technical possibilities and limitations. In: E. M. Carapezza, ed. *Proceedings of SPIE (Volume 7666)*. s.l. SPIE.

Kock, R. (. M., 2019. *Photogrammetry* [Interview] 2019.

Kukreja, H., Bharath, N., Siddesh, C. S. & Kuldeep, S., 2016. An Introduction to Artificial Neural Network. *International Journal of Advance Research and Innovative Ideas in Education*, 1(5), pp. 27-30.

LIDAR and RADAR Information, 2019. *Advantages and Disadvantages of LiDAR*. [Online] Available at: <http://lidarradar.com/info/advantages-and-disadvantages-of-lidar> [Accessed 11 April 2019].

LIDAR and RADAR Information, 2019. *Advantages and Disadvantages of Radar Systems*. [Online] Available at: <http://lidarradar.com/info/advantages-and-disadvantages-of-radar-systems> [Accessed 21 May 2019].

LIDAR and RADAR Information, 2019. *Uses of LIDAR sensor*. [Online] Available at: <http://lidarradar.com/apps/uses-of-lidar-sensor> [Accessed 22 March 2019].

- LiDAR-UK, 2019. *LiDAR*. [Online] Available at: <http://www.lidar-uk.com/index.php> [Accessed 11 April 2019].
- Lipman, A., 2018. *5 Industrial Photogrammetry Applications*. [Online] Available at: <https://industrytoday.com/article/5-industrial-photogrammetry-applications/> [Accessed 22 march 2019].
- Luhmann, T., Robson, S., Kyle, S. & Harley, I., 2006. *Close Range Photogrammetry: Principles, techniques and applications*. Scotland: Whittles Publishing.
- Lundborg, N., Persson, P. A., Ladegaard-Pedersen, A. & Holmberg, R., 1975. Keeping the Lid on Flyrock in Open-pit Blasting. *Engineering and Mining Journal*, Volume 176, pp. 95-100.
- Mansurov, N., 2010. *Introduction to Shutter Speed in Photography*. [Online] Available at: <https://photographylife.com/what-is-shutter-speed-in-photography> [Accessed 22 March 2019].
- Marto, A. et al., 2014. A Novel Approach for Blast-induced Flyrock Prediction based on Imperialist Competitive Algorithm and Artificial Neural Network. *The Scientific World Journal*, Volume 5.
- McKenzie, C. K., 2009. *Flyrock Range and Fragment Size Prediction*. Denver, CO, International Society of Explosives Engineers (ISEE).
- Mearmanand, J. W. & Roberts, J. C., 2014. *The application of photogrammetry for the visualization of complex heritage environments*. s.l., Eurographics Conference on Visualization (EuroVis).
- Mehta, A., 2019. *A Comprehensive Guide to Types of Neural Networks*. [Online] Available at: <https://www.digitalvidya.com/blog/types-of-neural-networks/> [Accessed 3 September 2019].
- Merriam-Webster Incorporated, 2019. *Merriam-Webster: Dictionary*. [Online] Available at: <https://www.merriam-webster.com/dictionary> [Accessed 05 March 2019].
- Monjezi, M., Amini Khoshalan, H. & Yazdian Varjani, A., 2010. Prediction of flyrock and back-break in open pit blasting operation: a neuro-genetic approach. *Arabian Journal of Geosciences*, 5(3), pp. 441-448.
- Monjezi, M., Mehrdanesh, A., Malek, A. & Khandelwal, M., 2012. Evaluation of the effect of blast design parameters on flyrock using artificial neural networks. *Neural Computing and Applications*, 23(2), pp. 349-356.
- National Institute of Building Technology Nashik, 2018. *Photogrammetry Surveying, Its Benefits and Drawbacks*. [Online] Available at: <https://medium.com/@nibtnashik/photogrammetry-surveying-its-benefits-drawbacks->



[afc47c34f1d7](#)

[Accessed 22 March 2019].

National Oceanic and Atmospheric Administration, 2018. *What is LIDAR?*. [Online] Available at: <https://oceanservice.noaa.gov/facts/lidar.html>

[Accessed 11 April 2019].

Ohnsman, R., 2017. *A Beginner's Guide to High-Speed Photography*. [Online] Available at: <https://improvephotography.com/49616/a-beginners-guide-to-high-speed-photography/>

[Accessed 22 May 2019].

OMEGA Engineering, 2019. *What is an RTD Sensor?*. [Online] Available at: <https://www.omega.com/prodinfo/rtd.html>

[Accessed 25 February 2019].

PhotoModeler Technologies, n.d. *Factors affecting accuracy in photogrammetry*. [Online] Available at: [https://www.photomodeler.com/kb/factors\\_affecting\\_accuracy\\_in\\_photogramm/](https://www.photomodeler.com/kb/factors_affecting_accuracy_in_photogramm/)

[Accessed 22 March 2019].

Pix4D, 2017. *Support: Manual*. [Online] Available at: <https://support.pix4d.com/hc/en-us/articles/204272989-Offline-Getting-Started-and-Manual-pdf>

[Accessed 8 August 2018].

Prakash, A., 2014. *ANFIS (Adaptive Neural Fuzzy Inference Systems)* [Interview] (14 September 2014).

Pramoda, R., 2017. *Slideshare: Active and Passive Sensors*. [Online] Available at: <https://www.slideshare.net/pramodgpramod/active-and-passive-sensors>

[Accessed 22 April 2019].

Premier Mapping, n.d. *Photogrammetry for Mine Surveyors*. Cullinan: Premier Mapping.

Raina, A. K. & Murthy, V. M. S. R., 2016. Importance and sensitivity of variables defining throw and flyrock in surface blasting by artificial neural network method. *Current Science*, 111(9), pp. 1524-1531.

Raina, A. K., Murthy, V. M. S. R. & Soni, A. K., 2013. Relevance of shape of fragments on flyrock travel distance: An insight from concrete model experiments using ANN. *Electronic Journal of Geotechnical Engineering*, Volume 18, pp. 899-907.

Raina, A. K., Murthy, V. M. S. R. & Soni, A. K., 2015. Flyrock in Surface Mine Blasting: Understanding the Basics to Develop a Predictive Regime. *Current Science*, 108(4), pp. 660-665.

Richards, A. B. & Moore, A. J., 2005. *Kalgoorlie Consolidated Gold Mines: Golden Pike Cut-Back - Flyrock Control and Calibration of a Predictive Model*, Eltham: Terrock Consulting Engineers.



Roth, J., 1979. *A model for the determination of flyrock range as a function of shot conditions*, California: United States Department of the Interior Bureau of Mines.

Rouse, M., 2014. *Internet of Things: Active Sensor*. [Online] Available at: <https://internetofthingsagenda.techtarget.com/definition/active-sensor> [Accessed 13 August 2018].

Rouse, M., 2019. *Smart Sensor*. [Online] Available at: <https://internetofthingsagenda.techtarget.com/definition/smart-sensor> [Accessed 15 March 2019].

Rowe, M., 2013. *Sensor Basics: Types, Functions and Applications*. [Online] Available at: <https://www.edn.com/design/test-and-measurement/4420987/Sensor-basics--Types--function-and-applications> [Accessed 27 February 2019].

SAS Institute Inc., 2019. *Artificial Intelligence: What is it and why it matters*. [Online] Available at: [https://www.sas.com/en\\_za/insights/analytics/what-is-artificial-intelligence.html](https://www.sas.com/en_za/insights/analytics/what-is-artificial-intelligence.html) [Accessed 03 September 2019].

Schenk, T., 2005. *Introduction to Photogrammetry*. [Online] Available at: <http://www.mat.uc.pt/~gil/downloads/IntroPhoto.pdf> [Accessed 22 March 2019].

Science Direct, 2013. *Optical Flow*. [Online] Available at: <https://www.sciencedirect.com/topics/engineering/optical-flow> [Accessed 01 July 2019].

Sentient Vision Pty Ltd, 2016. *ViDAR - The world's first Optical Radar*. [Online] Available at: <http://www.sentientvision.com/products/vidar-2-2/> [Accessed 11 April 2019].

Sentient Vision, 2017. *ViDAR "Optical Radar" changes the SAR game*. [Online] Available at: <https://sentientvision.wordpress.com/2017/12/04/vidar-optical-radar-changes-the-sar-game/> [Accessed 11 April 2019].

Sharma, R., 2019. *Top 15 Sensor Types being used in IoT*. [Online] Available at: <https://www.finoit.com/blog/top-15-sensor-types-used-iot/> [Accessed 27 February 2019].

Sobhan, S., 2005. *Introduction to Sensors*. [Online] Available at: [http://engineering.nyu.edu/gk12/Information/RAISE Workshop PowerPointFiles/Introduction%20to%20Sensors.ppt](http://engineering.nyu.edu/gk12/Information/RAISE%20Workshop%20PowerPointFiles/Introduction%20to%20Sensors.ppt) [Accessed 27 February 2019].

- Stančić, I., Burgarić, M. & Perković, T., 2017. Active IR System for Projectile Detection and Tracking. *Advances in Electrical and Computer Engineering*, 17(11), pp. 125-130.
- Sterling Sensors, 2018. *How does a thermocouple device work? What's its principle?*. [Online] Available at: <https://www.quora.com/How-does-a-thermocouple-device-work-Whats-its-principle> [Accessed 27 February 2019].
- Stojadinović, S. et al., 2016. Prediction of flyrock launch velocity using artificial neural networks. *Neural Computing and Applications*, 27(2), pp. 515-524.
- Stojadinović, S. et al., 2013. A new model for determining flyrock drag coefficient. *International Journal of Rock Mechanics and Mining Sciences*, Volume 62, pp. 68-73.
- Stojadinović, S., Pantović, R. & Žikić, M., 2011. Prediction of flyrock trajectories for forensic applications using ballistic flight equations. *International Journal of Rock Mechanics and Mining Sciences*, 48(7), pp. 1086-1094.
- Sunpower Electronics Ltd., 2014. *Glossary: Capacity Coupling*. [Online] Available at: <https://www.sunpower-uk.com/glossary/what-is-capacitive-coupling/> [Accessed 27 February 2019].
- Sužiedelytė-Visockienė, J., Bagdžiūnaitė, R., Malys, N. & Maliene, V., 2015. Close-range photogrammetry enables documentation of environment-induced deformation of architectural heritage. *Environmental Engineering and Management Journal*, 14(6), pp. 1371-1381.
- TCI.de, 2019. *FAQs*. [Online] Available at: <https://www.tci.de/tci-kompetenz/faq/> [Accessed 28 February 2019].
- The Atomic Heritage Foundation, 2017. *History: High-Speed Photography*. [Online] Available at: <https://www.atomicheritage.org/history/high-speed-photography> [Accessed 22 May 2019].
- ThermocoupleInfo.com, 2011. *What is a Thermocouple?*. [Online] Available at: <https://www.thermocoupleinfo.com/> [Accessed 25 February 2019].
- Trambadiya, D. & Varnagar, C., 2015. A Review on Moving Object Detection and Tracking Methods. *International Journal of Advanced Engineering and Research Development*.
- Trivedi, R., Singh, T. N. & Gupta, N., 2015. Prediction of Blast-induced Flyrock in Opencast Mines using ANN and ANFIS. *Geotechnical and Geological Engineering*, Volume 33.
- Vijayakumar, A. M. & Anand, H., 2016. Survey on Hawkeye Technology. *International Journal of Advanced Research in Computer Science and Software Engineering*, 6(10), pp. 43-47.
- Wheeler, A., 2017. *3D Scanning: Understanding the Differences In LIDAR, Photogrammetry and Infrared Techniques*. [Online] Available at: <https://www.engineering.com/Hardware/ArticleID/14541/3D-Scanning-Understanding->

[the-Differences-In-LIDAR-Photogrammetry-and-Infrared-Techniques.aspx](#)

[Accessed 11 April 2019].

Wolff, C., 2019. *Basics: Radar Principles*. [Online]

Available at: <http://www.radartutorial.eu/01.basics/Radar%20Principle.en.html>

[Accessed 21 May 2019].

Yigiter, E., 2018. *What is High-Speed Photography?*. [Online]

Available at: <https://www.miops.com/blogs/news/what-is-high-speed-photography?>

[Accessed 22 May 2019].



### **3. RESULTS AND ANALYSIS**

The results in this discussed chapter are presented according to the research objectives prescribed in Chapter 1. The results per objective are first presented and discussed according to its relevance to this project. It is then analysed according to the project's main objective.

#### **3.1. RECENT WORK (SINCE 2010) CONDUCTED IN THE FIELD OF FLYROCK PREDICTION**

Several recent (i.e. in the past decade) publications focussed on flyrock and flyrock prediction were reviewed in the literature survey. These publications proposed concepts and models that are mainly based on one of the following five approaches:

- Artificial neural networks (ANN);
- Adaptive neuro-fuzzy inference system (ANFIS);
- Rock engineering systems (RES);
- Empirical- and statistical analysis; and,
- Forensic or ballistics approach.

Each of these methods is briefly described in Chapter 2. These studies are summarised chronologically in Table 3.1, in terms of the aim or focus of the study, the authors' approach and the outcome.

**Table 3.1: Summary of work conducted relative to flyrock and flyrock prediction since 2010**

Author	Date	Main objective	Approach	Outcome	Input parameters	Key conclusions
<b>Monjezi, et al.</b>	2010	To develop a neuro-genetic model to predict flyrock and back-break.	ANN	A feed-forward ANN model with a 9-16-2 architecture that is combined with a GA. This model produced better predictions compared to the existing empirical models at that time.	<ul style="list-style-type: none"> <li>• Blast-hole diameter and length;</li> <li>• Spacing;</li> <li>• Burden;</li> <li>• Stemming length;</li> <li>• Powder factor;</li> <li>• Specific drilling;</li> <li>• Charge mass per delay; and,</li> <li>• RMR</li> </ul>	The presented models are highly dependent on the quality and accuracy of the input parameters. The most influential input parameters were stemming length and powder factor.
<b>Stojadinović, et al.</b>	2011	To develop a method of determining the maximum throw of flyrock.	Ballistics	A numerical solution in the form of two differential equations (i.e. x- and y-direction) was presented based on ballistics equations. Data were collected to determine the values of the input parameters. Two key assumptions were made, (1) a maximum launch angle of 45° and (2) a launch velocity was calculated based on past publications.	<ul style="list-style-type: none"> <li>• Drag coefficient;</li> <li>• Size and mass of the fragment;</li> <li>• The velocity of the fragment; and,</li> <li>• Launch angle.</li> </ul>	The authors concluded that this approach was better suited as a post-incident investigation. The results are dependent on the input parameters and relative assumptions. The influence of drag or air resistance is uncertain and require additional research.

Author	Date	Main objective	Approach	Outcome	Input parameters	Key conclusions
Ghasemi, et al.	2012	To develop an empirical prediction model for flyrock.	Empirical	Data were collected from 150 blasts and analysed using dimensional analysis (DA) approach. The proposed empirical equation (Equation 2.5) was validated using Monte Carlo simulations. However, the author noted that the equation is dependent on the range of data collected and the accuracy of the measured input parameters.	<ul style="list-style-type: none"> <li>• Burden;</li> <li>• Spacing;</li> <li>• Stemming length;</li> <li>• Blast-hole length and diameter;</li> <li>• Powder factor; and,</li> <li>• Mean charge per delay.</li> </ul>	The presented empirical equation was very site-specific. From the field data, the fragments that were continuously thrown the furthest were 10cm in diameter. Based on the equation, the parameters that directly influenced flyrock were identified as stemming length, spacing, blast-hole length and diameter and the powder factor. The parameters that had an indirect influence on flyrock was the burden and charge mass per delay.
Monjezi, et al.	2012	To develop an ANN model to predict flyrock and compare it against available empirical and statistical models.	ANN	A feed-forward ANN model with a 9-5-2-1 architecture. Both the input parameters and results obtained were very similar compared to the 2010 publication from the same authors.	<ul style="list-style-type: none"> <li>• Blast-hole diameter and length;</li> <li>• Spacing;</li> <li>• Burden; and</li> <li>• Charge mass per delay.</li> </ul>	The quality and accuracy of the input parameters dictate the success of this model. The most influential parameters were determined as powder factor, blast-hole diameter, stemming length and charge mass per delay.

Author	Date	Main objective	Approach	Outcome	Input parameters	Key conclusions
Stojadinović, et al.	2013	To improve on the previously proposed ballistic model by increasing the accuracy of the drag coefficient.	Ballistics	A high-speed camera was used to record various blasts, which was analysed in CAD software. Some measurements were taken at the point where the rock fragment reached terminal velocity. These measurements were used to determine the drag coefficient, but the resulting calculations produced contradicting results that resulted from errors in the methodology and uncertainty regarding the influence of the shape of the fragment.	<ul style="list-style-type: none"> <li>• Fragment size;</li> <li>• Launch velocity; and,</li> <li>• Launch angle.</li> </ul>	<p>Prior to presenting the results in this publication, the authors made three important deductions from their previous study in 2011. These are:</p> <ol style="list-style-type: none"> <li>(1) Fragment sizes that travel the maximum distance range between 25cm and 35cm.</li> <li>(2) Maximum launch velocity is typically 150m/s for fragments approximately 5cm in diameter.</li> <li>(3) Launch angles for maximum distance range between 35° and 43° when drag is taken into account.</li> </ol> <p>A number of difficulties were identified in this study. The main problem was the inaccuracy of the measuring process. Low-resolution images resulted in uncertainty regarding the exact position of the fragment in the image. Ultimately, the authors conclude that the drag coefficient is an essential factor in ballistics analysis and should vary along with the fragment size and launch angle.</p>



Author	Date	Main objective	Approach	Outcome	Input parameters	Key conclusions
Raina, et al.	2013	To analyse the effect of the shape of flyrock on its travel distance.	ANN	A feed-forward ANN model with a 7-20-14-8-1 architecture developed based on 75 test blasts (concrete blocks). However, it was difficult to replicate in actual field conditions and required more research.	<ul style="list-style-type: none"> <li>• Initial velocity;</li> <li>• Launch angle;</li> <li>• Sphericity; and,</li> <li>• Weight, length, width and thickness of the fragment.</li> </ul>	The key parameters were determined to be the initial velocity of a fragment, the launch angle and the weight of a fragment. The effects of external factor and weather conditions were recommended as important future research.
Ghasemi, et al.	2014	To develop and compare two predictive models based on AI principles.	ANN and ANFIS	A feed-forward ANN model with a 6-9-1 architecture and an ANFIS model based on a Mamdani algorithm. Both models can be used to “minimise uncertainties”, but the ANFIS model produced better predictions.	<ul style="list-style-type: none"> <li>• Blast-hole length;</li> <li>• Burden;</li> <li>• Spacing;</li> <li>• Stemming length;</li> <li>• Powder factor; and,</li> <li>• Charge mass per delay.</li> </ul>	The results from both methods were highly dependent on the accuracy and validity of the input parameters. Both ANN and ANFIS are good tools to attempt to minimise uncertainties associated with flyrock.
Marto, et al.	2014	To predict flyrock through a novel model created by combining ANN and ICA.	ANN	An ICA-ANN model that produced better prediction results compared to previously proposed ANN models, based on data obtained from 113 blasts.	<ul style="list-style-type: none"> <li>• Blast-hole length;</li> <li>• Burden-to-Spacing ratio;</li> <li>• Stemming length;</li> <li>• Powder factor;</li> <li>• Maximum Charge mass per delay;</li> <li>• Rock density; and,</li> <li>• Schmidt hammer rebound number.</li> </ul>	The proposed model was (similar to the previous models) highly dependent on the accuracy and validity of the input parameters.

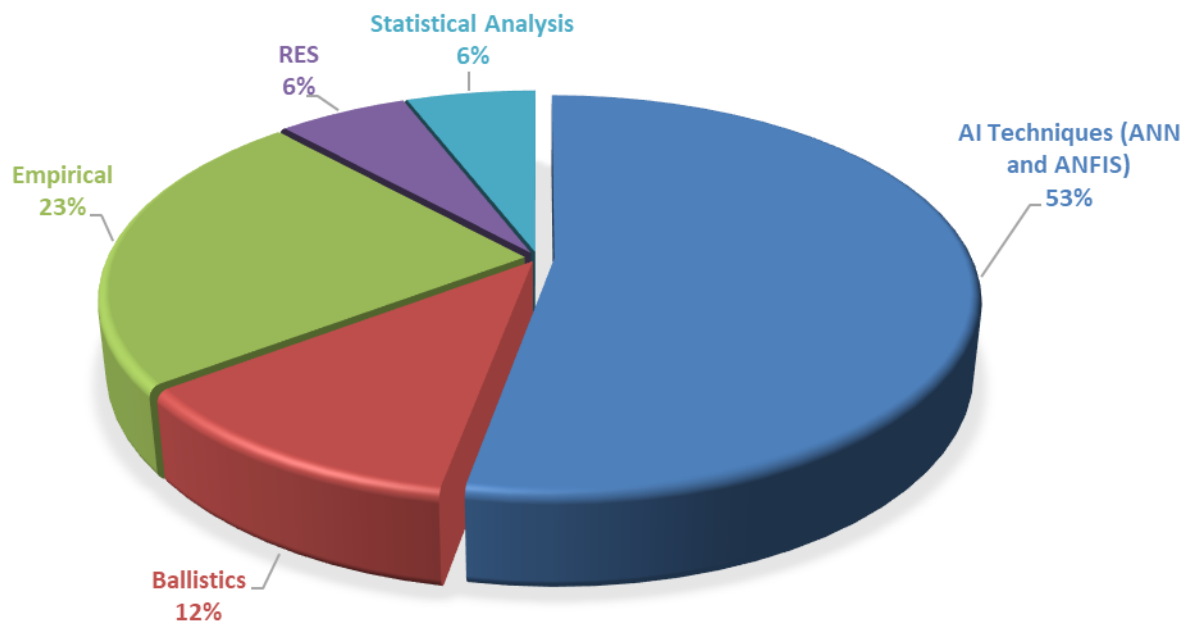
Author	Date	Main objective	Approach	Outcome	Input parameters	Key conclusions
Faramarzi, et al.	2014	To model the risk associated with flyrock and predict flyrock based on RES principles.	RES	Blast data from 52 blasts were collected and used to develop the RES system, using 13 input parameters. The RES model presented superior prediction results compared to other methodologies such as multivariable regression analysis (MRA) models.	<ul style="list-style-type: none"> <li>• Burden;</li> <li>• Maximum instantaneous charge;</li> <li>• Powder factor;</li> <li>• Spacing-to-burden ratio;</li> <li>• Stemming-to-burden ratio;</li> <li>• Stiffness factor;</li> <li>• Time delay;</li> <li>• Blast-hole diameter;</li> <li>• VoD;</li> <li>• Blast-hole deviation;</li> <li>• Burden-to-Hole diameter ratio; and,</li> <li>• RMR.</li> </ul>	Similar to the empirical prediction models, the RES model was site-specific. Therefore, the technique could be used to develop separate models for different sites, but this specific model cannot be used as a universal solution for predicting flyrock.
Trivedi, et al.	2015	To predict flyrock based on the ANN and ANFIS approaches.	ANN and ANFIS	An ANN and an ANFIS model were created using the same input parameters and field data from 125 blasts. The ANFIS model proved the produced better prediction results compared to the ANN model.	<ul style="list-style-type: none"> <li>• Linear charge mass;</li> <li>• Burden;</li> <li>• Stemming length;</li> <li>• Specific charge;</li> <li>• Unconfined compressive strength; and,</li> <li>• Rock quality.</li> </ul>	The proposed models were (similar to the previous models) highly dependent on the accuracy and validity of the input parameters.

Author	Date	Main objective	Approach	Outcome	Input parameters	Key conclusions
<b>Stojadinović, et al.</b>	2015	To develop a concept capable of predicting the launch velocities of flyrock.	ANN	Data were collected from 36 blasts at three mining operations. An ANN model with a 19-8-6-1 architecture was developed and a fuzzy algorithm was used for its optimization.	<ul style="list-style-type: none"> <li>• Several input parameters were considered. Refer to section 2.4.1 for additional information.</li> </ul>	The three mining operations had similar geology and blast parameters and did, therefore, not yield a diverse dataset. The authors highlighted that the lack of diverse data was an opportunity for additional work and research.
<b>Armaghani, et al.</b>	2016	To develop a model, based on an empirical approach, to predict flyrock.	Empirical (The authors later included ANN and ANFIS)	An empirical graph was created based on data obtained from 232 blasts. However, this graph was purely site-specific. ANN and ANFIS models were developed as an attempt to solve these equations and minimise uncertainties.	<ul style="list-style-type: none"> <li>• Maximum charge per delay, and</li> <li>• Powder factor.</li> </ul>	The most influential parameters during the development of the model were the two input parameters. Empirical solutions remain to be very site-specific. ANN and ANFIS were recommended as a better approach to developing a more universal predictive model.
<b>Raina &amp; Murthy</b>	2016	To identify the significance of different blasts parameters on throw and flyrock.	ANN	An ANN model was designed, trained and validated using EasyNN-Plus© software, based on blast data obtained from 10 mines. The resulting ANN models consisted of a 20-16-6-4-1 architecture.	<ul style="list-style-type: none"> <li>• Burden;</li> <li>• Spacing;</li> <li>• P-wave velocity (primary shock wave);</li> <li>• Rock density;</li> <li>• The effective in-hole density of the explosives; and,</li> <li>• Charge length-to-hole depth ratio.</li> </ul>	Implementing AI concepts in flyrock prediction presented better predictive capability compared to empirical approaches. However, models based on AI concepts (i.e. ANN and ANFIS) remain very dependent on the quality of the estimation of the input parameters.

Author	Date	Main objective	Approach	Outcome	Input parameters	Key conclusions
Armaghani, et al.	2016	To develop a prediction model based on MRA and Monte Carlo simulations.	MRA (Empirical)	An empirical equation was generated based on MRA to describe the relationship between flyrock and the input parameters, using SPSS (ver.16) software. The Monte Carlo simulations produced results in favour of the presented equation, but the credibility of the results remain dependent on the validity of the input parameters.	<ul style="list-style-type: none"> <li>• Burden;</li> <li>• Spacing;</li> <li>• Stemming length;</li> <li>• Blast-hole depth;</li> <li>• Maximum charge mass per delay;</li> <li>• Powder factor; and,</li> <li>• RMR.</li> </ul>	The proposed equation was specific to the test site and its parameters and can, therefore, not be used as a universal solution. Powder factor was determined to be the most influential input parameter in this model.
Dehghani & Shafaghi	2017	To predict flyrock based on a combined DE and DA approach	DE and DA (Empirical)	Data were collected from 300 blasts and analysed to present one DA-equation (Equation 2.7) and one DE-equation (Equation 2.8). Based on the prediction results, the DE-equation produced more accurate results than the DA-equation.	<ul style="list-style-type: none"> <li>• Blast-hole length and diameter;</li> <li>• Number of blast-holes;</li> <li>• Spacing;</li> <li>• Burden;</li> <li>• ANFO charge mass;</li> <li>• Stemming length;</li> <li>• Powder factor; and,</li> <li>• Specific drilling.</li> </ul>	Powder factor and stemming length were determined to be the most influential parameters in both equations. The authors recommended that further research should be conducted into the principles of physics, trajectory motion in the air and the influence of the size and shape of a fragment on its travelling distance.

Author	Date	Main objective	Approach	Outcome	Input parameters	Key conclusions
Hasanipanah, et al.	2017	To predict flyrock using the regression tree technique in order to reduce its environmental impact.	Regression Tree Analysis	A regression tree model was developed using data from 65 blasts. The model consisted of 52 nodes. An empirical equation (Equation 2.9) was produced and compared to a separately generated MLR model. The results proved that the regression tree technique produced better prediction results.	<ul style="list-style-type: none"> <li>• Blast-hole length;</li> <li>• Spacing;</li> <li>• Burden;</li> <li>• Stemming length;</li> <li>• Maximum charge mass per delay; and,</li> <li>• Powder factor.</li> </ul>	The authors commented that both the MLR and regression tree technique had the potential to predict flyrock. Powder factor and burden were determined to be the most influential input parameters.

The approaches or techniques implemented in the recent flyrock prediction and flyrock related studies are summarised in Figure 3.1.



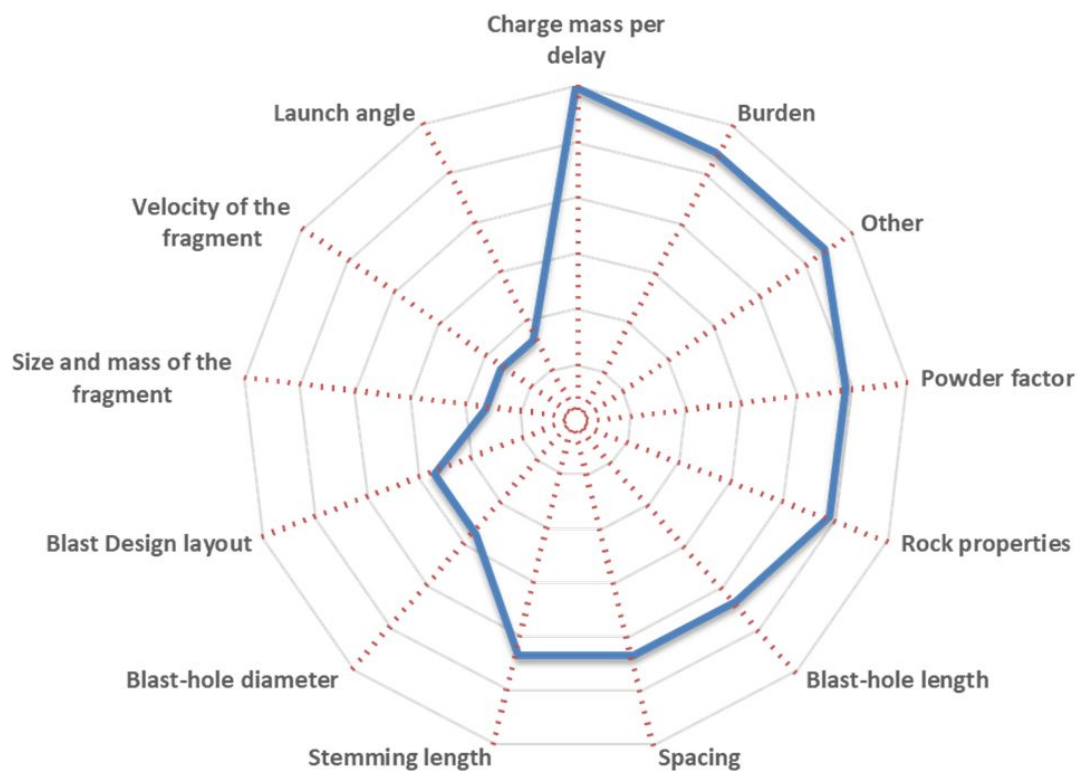
**Figure 3.1: Approaches or Techniques used in the recent flyrock prediction studies**

Although the proposed models in these publications and the related approaches are not specifically used in this project, some important information can be deduced from the results in each publication. These key points are:

- i. Empirical approaches have been proposed since the early 1980s, but even recent empirical approaches have proven to be insufficient. Empirical models tend to be site-specific and these models can, therefore, not be used as a general approach to predicting flyrock.
- ii. ANN and AI concepts have proven to assist in minimising the uncertainties related to flyrock. However, considering the ANN models proposed in chronological order, it is apparent that the architecture of these ANN models has increased significantly with time. This means that the networks have become increasingly complex, i.e. taking more input parameters into account and processing it over more hidden layers. This indicates that there still are several uncertainties related to flyrock, as well as which blast parameters directly influence the risk of flyrock and to what degree.

Finally, all of these ANN prediction models are highly dependent on the input parameter and the estimation thereof. Considering the level of uncertainty regarding these input parameters and how much they contribute to flyrock, errors can be expected in these models.

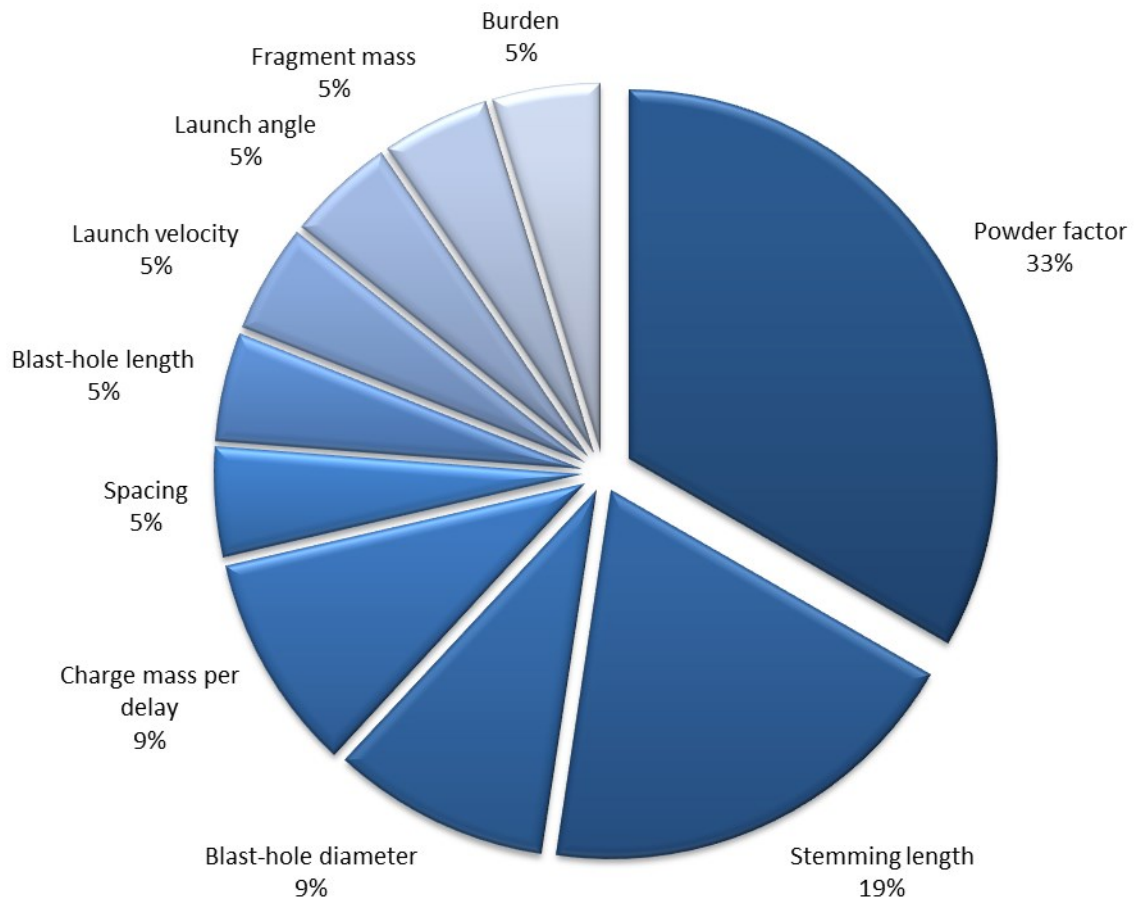
- iii. The input parameters taken into account throughout all 16 publications are included in Table 3.1. It is clear that some of these input parameters are considered in most of the publications, while others are unique to certain studies. The frequency of these parameters being used as an input is illustrated in Figure 3.2. Charge mass per delay, powder factor, burden, spacing, stemming length and blast-hole length are shown to be the most popular input parameters (based on these 16 publications).



**Figure 3.2: Frequency of input parameters used in the proposed flyrock (or flyrock-related) prediction models discussed in the aforementioned publications**

In most of these studies, a sensitivity analysis was conducted to identify the most influential input parameter(s), based on the proposed model. These influential parameters are presented in Figure 3.3 as a percentage of the total influential parameters discussed in all 16 publications. It is important to note that since some of these models incorporated different input parameters, the sensitivity analyses and,

therefore, the mentioned influential parameters may be indicated as outliers in Figure 3.3. However, this is just an overview of which parameters are interpreted as essential by the authors of the papers.



**Figure 3.3: Most influential input parameters (frequency) based on the proposed models in the aforementioned publications**

Based on Figure 3.3, the powder factor and stemming length seem to be the key parameters relating to flyrock, based on the proposed models, which aligns with what one would expect. However, the burden is not highlighted as a critical parameter which is contradicting to the face burst mechanism of flyrock.

This summary of the fundamental parameters that could potentially influence flyrock and the contradiction of the importance of burden support the argument that the effect of blast parameters on flyrock is not fully known or understood.

- iv. The application of ballistics on flyrock prediction may not be ideal, however, using ballistics principles to analyse flyrock present exciting new opportunities. According



to the laws of physics, a fragment of rock moving through the air will behave according to Newton's laws of motion. The ballistics formulae are based on these laws. Ballistics should, therefore, be a viable and accurate method of analysing the motion of flyrock. The work done using ballistics have been based on a data collection technique that leaves room for significant error. Subsequently, it can be concluded that the proposed models are flawed.

There are some key points emphasised in the studies implementing ballistics principles, namely:

- The influence of drag or air resistance is significant but is often neglected.
- The effect of the shape of the fragment on the drag force experienced is unknown.
- The influence of external factor such as weather conditions has not been researched.
- The fragment size that will likely travel the furthest distance (i.e. small enough to experience a large launch velocity but big enough to overcome some of the drag force) range between 10cm and 35cm in diameter.
- The launch angle that will allow a fragment to travel a maximum distance is not  $45^\circ$  as would be expected, but rather range between  $35^\circ$  and  $43^\circ$  when taking the drag force into account.

Considering the recent work conducted in flyrock prediction or investigating the effect of certain parameters on the flyrock travel distance, it can be concluded that implementing ballistics principles to analyse flyrock motion is the best method to understand its behaviour. However, a lot of uncertainty exists in terms of how external forces, such as drag, impacts the travelling distance of flyrock. The effect of the shape of a fragment on the drag force it could experience can be investigated through wind tunnel tests. The effect of various weather conditions can also be investigated by means of a wind tunnel.

ANN and ANFIS approaches hold significant potential for further refining (i.e. minimising the related uncertainties) of a flyrock prediction model, however, the impact and relevance of input parameters must be estimated accurately in order to achieve accurate predictions.

## **3.2. EXISTING TECHNIQUES AND TECHNOLOGIES**

Various techniques and technologies were investigated during the literature review and initial research for this project. These techniques and technologies are summarised and discussed in this section.

### **3.2.1. Sensors**

Sensors are devices that are able to detect and record physical parameters and convert these measurements into a signal that can be interpreted. Sensors form the foundation of all detection, monitoring or measuring technologies available at this time. Therefore, the various types of sensors and the associated capabilities and applications were investigated prior to the available technologies in order to support the discussion on the available techniques and technologies. The sensors considered in this project are summarised in Table 3.2.

**Table 3.2: Summary of various sensors**

Type of Sensor	Active or Passive	Use	Applicable Industries
<b>Temperature Sensor</b>	Passive	Detect and measure changes in temperature.	Mainly in refrigeration and air-cooling systems, as well as manufacturing, agriculture and health care.
<b>IR Sensor</b>	Active	Detect electromagnetic radiation or thermal energy emitted in the infrared spectrum and not visible to the human eye.	Thermography, Spectroscopy, Meteorology, Climatology and Optical fibre- and short-range communications.
<b>UV Sensor</b>	Passive	Detect and measure ultra-violet radiation, i.e. sunlight and similar radiation.	Measuring UV radiation outdoors and in laboratories using artificial lighting.
<b>Ultrasonic Sensor</b>	Active	Measure the distance from the sensor to the object of interest by emitting ultrasonic waves.	Liquid level sensing; Trash level sensing; Production lines; Vehicle detection for car washes, automotive assembly, and parking garage applications; Anti-collision detection; People detection; Contouring or profiling and Presence detection.
<b>Touch Sensor</b>	Passive	Control and manipulate a system or control unit without the requirement of distinct push buttons.	Commercial, Appliances, Transportation, Industrial automation and Consumer electronics.
<b>Pressure Sensor</b>	Passive	Record and measure pressure applied onto a surface or object.	Industrial and Manufacturing
<b>Proximity Sensor</b>	Active	Detects the presence or absence of nearby objects.	Retail and Security

Sensors are divided into two main categories, also indicated in Table 3.2, namely active and passive sensors.

- Active sensors or systems emit some form of an electromagnetic wave or signal from an internal power source. This wave or signal is echoed from the surface of the target object or area and is received by the receiver unit within the sensor. Active sensors can be used during the day or at night

In general, active sensors are often favourable in most applications since it contains its own internal source of illumination. However, the setup and functioning between

components (i.e. transmitter, receiver, etc.) can be complex. Finally, since the output of active sensors is primarily dependent on the echoed signal received from an object or topography, the reflectivity of the object's surface or topography becomes a critical property. If the reflectivity of the surface of the object or topography is low, the signal may not be sufficiently echoed back towards the sensor's receiver unit. This means that the sensor will not detect or record the object or topographical surface.

- Passive sensor or systems detects and records the natural electromagnetic energy that surrounds the sensor or system. Passive sensors can only be used during the day since it is dependent on natural illumination. These sensors are often not very dependent on the physical properties of the surface of the target object or topography. Passive sensors often consist of a simpler configuration compared to active sensor or systems since it does not include an internal energy source.

As previously stated, sensors form the foundation of all detection and monitoring technologies currently available. Therefore, even if sensors are not specifically detailed in the outcome of this project, understanding the function and application of each sensor is a critical component of developing a credible concept.

### **3.2.2. Available techniques and technologies**

Numerous techniques and technologies are available for the purpose of monitoring systems and processes or measuring physical phenomena. As previously stated, the sensors discussed in section 3.2.1, form the basis of these technologies. Some of these technologies may consist of a combination of multiple sensors to achieve their desired outcome. The combination of sensors used in each of the investigated techniques or technologies is not discussed in this project since it exceeds the scope of this project. However, it may be a necessary topic to investigate as a suggestion for further study.

The main assumption that guided the investigation on the existing techniques and technologies that may aid the outcome of this project was that a non-contact technique or technology is required. This is due to the inherent danger or risk associated with blasting activities. Therefore, in order to measure flyrock resulting from a blast and quantify the motion of the fragments, it is essential that the equipment and the operator are positioned at a safe distance from the blast.

The following techniques and technologies were investigated as a part of this project, i.e.:

- High-speed photography;
- Photogrammetry;
- RADAR;
- LiDAR;
- ViDAR; and,
- Other systems including Hawk-eye, visual or optical detection and tracking and active infrared systems.

The outcome of this investigation is summarised in Table 3.3.

**Table 3.3: Summary of the existing techniques and technologies that can support this project's objective**

Technique or Technology	Basic principles	Active/Passive	Application	Advantages	Disadvantages
<b>High-speed photography</b>	Still images or video taken at high frame rates, able to capture events that occur too fast for the human eye to perceive.	Passive	<ul style="list-style-type: none"> <li>• Ballistics;</li> <li>• Manufacturing;</li> <li>• Medicine;</li> <li>• Astrophysics and space studies;</li> <li>• Sport-related studies;</li> <li>• Movement of animals, birds and insects; and,</li> <li>• Entertainment and cinematography.</li> </ul>	<ul style="list-style-type: none"> <li>• It is a non-contact system.</li> <li>• Remote triggering options are available.</li> <li>• High-speed processes and phenomena can be recorded.</li> <li>• Delayed triggering is possible, i.e. the system is not reliant on the reaction time of the operator to capture or record an event.</li> </ul>	<ul style="list-style-type: none"> <li>• Often only used for qualitative analysis.</li> <li>• High shutter speeds can result in lower quality images or footage.</li> <li>• Good natural lighting is required is no artificial illumination is available.</li> <li>• High shutter speeds require amplified illumination from external sources.</li> </ul>
<b>Photogrammetry</b>	Physical measurements are taken from multiple still images taken of a single object or surface. The overlap between these multiple images is used to create a stereo model of the object or area of interest, from which measurements are taken.	Passive	<ul style="list-style-type: none"> <li>• Land surveying;</li> <li>• Engineering;</li> <li>• Mining and Energy;</li> <li>• Forensics;</li> <li>• Archaeology;</li> <li>• Film and entertainment; and,</li> <li>• Sport.</li> </ul>	<ul style="list-style-type: none"> <li>• It is a non-contact system.</li> <li>• Images hold both visual and quantitative data.</li> <li>• Data is collected cheaper and faster compared to ground survey techniques.</li> <li>• If errors occur during the analysis of the data, it is not necessary to re-do the data acquisition in the field. It is easy to use in hard-to-reach and dangerous terrains.</li> </ul>	<ul style="list-style-type: none"> <li>• Data collection is susceptible to environmental factors and changes in the weather.</li> <li>• Visibility of the object or area can be obstructed by structures or vegetation.</li> <li>• The accuracy of measurements is dependent on the control points in the field as well as the quality of the images or camera.</li> </ul>

Technique or Technology	Basic principles	Active/Passive	Application	Advantages	Disadvantages
<b>RADAR</b>	The RADAR system transmits radio waves towards a determined area. These waves are echoed from the surface of the target object and are received by the RADAR system. The output data from the RADAR can be used to determine the position and range of the target.	Active	<ul style="list-style-type: none"> <li>• Military;</li> <li>• Air traffic control;</li> <li>• Remote sensing;</li> <li>• Ground traffic control; and,</li> <li>• Space research, guidance and monitoring.</li> </ul>	<ul style="list-style-type: none"> <li>• It is a non-contact system.</li> <li>• Radio waves can penetrate various media such as clouds, snow and soil.</li> <li>• Data can be used to determine positions of a target object, the distance to that object and if the object is moving, its velocity.</li> <li>• RADAR can target several objects simultaneously.</li> <li>• It can cover a wide area.</li> <li>• RADAR allows for repetitive scanning.</li> </ul>	<ul style="list-style-type: none"> <li>• Data is less accurate and often incomplete compared to similar technologies such as LiDAR.</li> <li>• RADAR is dependent on the reflectivity of the target's surface.</li> <li>• Analysis of data requires specialised training.</li> <li>• It is very susceptible to external interference.</li> <li>• RADAR cannot be used to identify the type of object or any specific physical property of the object.</li> </ul>
<b>LiDAR</b>	The basic concept if LiDAR is very similar to RADAR. LiDAR emits laser pulses towards the target area in order to obtain data from the echoed laser pulses. LiDAR is used to	Active	<ul style="list-style-type: none"> <li>• Engineering;</li> <li>• Architecture;</li> <li>• Urban planning;</li> <li>• Road safety;</li> <li>• Space exploration;</li> <li>• Meteorology;</li> <li>• Atmospheric physics;</li> <li>• Mining;</li> </ul>	<ul style="list-style-type: none"> <li>• It is a non-contact system.</li> <li>• LiDAR generates high accuracy data and high-density data points.</li> <li>• Data acquisition is fast.</li> <li>• Data acquisition is not dependent on illumination, i.e. scanning can take place</li> </ul>	<ul style="list-style-type: none"> <li>• LiDAR scanners are very expensive.</li> <li>• Very large datasets can be collected which can complicate the analysis thereof and its interpretation.</li> <li>• LiDAR is not able to penetrate physical barriers</li> </ul>

	generate point data of the features of an object or surface area.		<ul style="list-style-type: none"> <li>• Military;</li> <li>• Forensics;</li> <li>• Archaeology;</li> <li>• Agriculture;</li> <li>• Forestry; and,</li> <li>• Oceanography.</li> </ul>	<p>during the day or night.</p> <ul style="list-style-type: none"> <li>• Datasets do not have any geometric distortions.</li> <li>• LiDAR is not susceptible to weather changes.</li> </ul>	<p>such as dense vegetation.</p> <ul style="list-style-type: none"> <li>• The laser in the system poses a health and safety risk to humans.</li> <li>• The analysis and interpretation of the data require a specialised skill set.</li> </ul>
<b>VIDAR</b>	ViDAR is a visual detection system designed to detect objects on the surface of large bodies of water. Video footage from the drone cameras is automatically processed by onboard processing units. Processing software to analyse each frame and evaluates it against the background of the ocean's surface.	Passive	<ul style="list-style-type: none"> <li>• Marine search and rescue;</li> <li>• Anti-piracy on the oceans;</li> <li>• Counter-narcotics;</li> <li>• Illegal immigration; and,</li> <li>• Oceanic surveillance and maritime security.</li> </ul>	<ul style="list-style-type: none"> <li>• It is a non-contact system.</li> <li>• Processing of the recorded footage is done in real-time.</li> <li>• Wide area coverage.</li> <li>• The system helps ocean search and rescue services.</li> </ul>	<ul style="list-style-type: none"> <li>• ViDAR is dependent on natural illumination.</li> <li>• The system is designed to function as a part of a manned or unmanned aircraft.</li> <li>• It is susceptible to sudden weather changes.</li> </ul>



Technique or Technology	Basic principles	Active/Passive	Application	Advantages	Disadvantages
<b>Other systems:</b>					
<b>Hawk-eye</b>	Hawk-eye is a system that is commonly associated with live sports events and broadcasting. Hawk-eye is a specialist visual detection and tracking system that incorporates algorithms that automatically detects the ball on the field or court and tracks its movement, while it moves within the controlled area of the system.	Passive	<ul style="list-style-type: none"> <li>• Predominantly live sports events, broadcasting and fair refereeing during events.</li> </ul>	<ul style="list-style-type: none"> <li>• It is a non-contact system.</li> <li>• The system is fully established in professional sport environments.</li> <li>• Tracking algorithms are trusted to ensure fairness in sport.</li> <li>• Tracking is done in real-time.</li> </ul>	<ul style="list-style-type: none"> <li>• The system is designed to track single projectiles only.</li> <li>• Hawk-eye is designed to work in a highly controlled environment.</li> <li>• Six or more high-speed cameras are needed for this system.</li> <li>• Hawk-eye is not a flexible system that can simply be employed in other environments.</li> </ul>
<b>Visual or optical detection and tracking</b>	Visual or optical detection and tracking system use a visual sensor that records a target area as a video which can be analysed manually or through specially designed	Passive	<ul style="list-style-type: none"> <li>• Security and protection services;</li> <li>• Traffic surveillance services;</li> <li>• Military guidance systems;</li> <li>• Navigation systems in robotics and drones;</li> </ul>	<ul style="list-style-type: none"> <li>• It is a non-contact system.</li> <li>• This system is flexible, with various algorithms available to apply in different scenarios.</li> <li>• Wide area coverage (depending on the which cameras are used).</li> </ul>	<ul style="list-style-type: none"> <li>• The system is dependent on natural or artificial lighting.</li> <li>• The analysis and interpretation of the recorded data are still the subjects of active research, i.e. the technique is still developing.</li> <li>• The system is susceptible to</li> </ul>

	software. The recorded data is analysed based on video object and motion segmentation principles		<ul style="list-style-type: none"> <li>• AI; and</li> <li>• Several medical applications.</li> </ul>		external factors such as changes in the weather.
<b>Active infrared systems</b>	An active infrared system is a system proposed by Stančić, et al. (2017). The purpose of this system is to record and measure the movement of objects travelling at subsonic speeds. Cameras, set up in stereo, are used to record the object. Infrared LEDs are used to create an illuminated area through which the object will move, enabling the designed software to analyse the footage.	Active	<ul style="list-style-type: none"> <li>• The proposed system is still new but is designed to detect and track subsonic projectiles.</li> </ul>	<ul style="list-style-type: none"> <li>• It is a non-contact system.</li> <li>• Simple visual tracking algorithms are sufficient.</li> <li>• Only two cameras are required, i.e. only one stereo model is generated.</li> </ul>	<ul style="list-style-type: none"> <li>• The system is limited by the range of the infrared LED (short-range).</li> <li>• It is highly dependent on the infrared lighting in order to track the movement of an object.</li> <li>• The system is still very conceptual and significant research is still required.</li> </ul>

These techniques and technologies are evaluated in a comparative analysis in order to identify which, if any, would be the best approach or foundation of the proposed concept.

### **3.2.2.1. Comparative analysis**

The purpose of this project is to develop a concept that can be used to quantify the flight path of the flyrock resulting from a blast. The focus of this project was not to invent new technology but only develop a conceptual technique that can be employed in the rough terrain of a mining site.

The recent work conducted in the field of flyrock prediction was investigated in Chapter 2 and evaluated in section 3.1. The main conclusion drawn was that while an empirical approach has not yet produced any reliable predictions, the application of physics and ballistics remain a valuable method of analysing the trajectory of flyrock. The use of AI concepts has proven to add value by allowing researchers to minimise the uncertainties associated with flyrock. However, these concepts are highly dependent on the input parameters and their estimated influence on the risk of flyrock. It is very important to note that some gaps still exist with regards to what parameters are considered inputs and to what degree these parameters contribute to the risk of flyrock.

The existing techniques and technologies that are used for monitoring purposes or the measurement of physical parameters were investigated in Chapter 2 and are summarised in section 3.2.2. This comparative analysis is conducted in order to evaluate these existing techniques and technologies to establish which would form a stable foundation that will, in all probability, lead to a successful outcome of this project.

The comparative analysis will be evaluated against the following criteria.

i. Non-contact:

Due to the safety risk associated with blasting activities, the proposed method should be able to acquire data from a safe distance. Therefore, a non-contact approach or sensor system is a necessity.

ii. Passive:

The flight path and physical properties of flyrock are typically random in nature. Therefore, a passive system is essential in order to minimise the implication of varying physical properties since a passive system records the existing, natural electromagnetic energy.

- iii. Remote triggering system:  
Similar to the motivation for a non-contact system, initiating the proposed method should be possible from a safe distance. This means that the operator may not always be positioned near the relevant equipment.
- iv. Multiple projectile detection  
Multiple fragments are projected simultaneously from a blast, each with the potential of causing damage. It is, therefore, essential that the proposed method is able to record the data from multiple fragments concurrently.
- v. Flexible system  
Due to the different topographies and layouts of various mining operations, the proposed method should be flexible enough to adapt to these varying layouts.
- vi. Dependent on the physical properties of the target  
The physical properties of flyrock fragments are often unknown and cannot accurately be estimated due to the unknowns associated with geology and blasting.
- vii. Quantitative Data  
The purpose of the study is to quantify the flight path of flyrock. Therefore, the proposed concept must include a technique of obtaining quantitative measurements from the acquired field data.

The different techniques and technologies are evaluated by means of a weighting system that is assigned to each criterion, shown in Table 3.4.

**Table 3.4: Weighting matrix used to evaluate the comparative criteria**

Criterion	Rating				
	1	2	3	4	5
<b>Non-contact</b>	Full contact is required	Contact is not required but advised for accurate data.	Non-contact	Non-contact, short range (<50m)	Non-contact, long range (>100m)
<b>Passive</b>	Active	N/A	N/A	N/A	Passive
<b>Remote triggering</b>	Not available	Remote triggering is not	Remote triggering is possible	Short-range triggering (<50m) or continuous recording	Long-range triggering (>100m)
<b>Detect multiple projectiles</b>	Not possible	Unlikely	Neutral	Possible	Multiple projectiles can be detected
<b>Flexibility</b>	Not flexible	Less flexible	Neutral	Flexible	Very Flexible
<b>Dependency on physical properties</b>	Highly dependent	Dependent	Neutral	Fairly independent	Completely independent
<b>Quantitative data</b>	Not possible	Unlikely	N/A	Possible	Definitive

These ratings are applied to each available option, in Table 3.5, in order to identify which option will, in all probability, support the outcome of this project.

Table 3.5: Comparative analysis between the existing techniques and technologies

	Criteria							Total:
	Non-contact	Passive	Remote triggering	Multiple projectiles	Flexibility	Dep. on physical properties	Quantitative data	
High-speed photography	5	5	4	3	4	4	1	26
Photogrammetry	5	5	5	4	3	4	5	31
RADAR	5	1	5	4	3	1	4	23
LiDAR	5	1	5	1	3	3	5	23
ViDAR	5	5	5	3	4	3	3	28
Hawk-eye	4	5	4	1	2	4	4	24
Optical detection and tracking	5	5	4	4	3	4	2	27
Active infrared system	3	1	3	2	1	3	2	15

Based on the comparative analysis in Table 3.5, the top three available technologies are:

1. Photogrammetry;
2. LiDAR; and,
3. Optical detection and tracking.

Based on this analysis, it is apparent that a visual or optical approach is the best option to acquire flyrock flight data that can be analysed quantitatively. An essential criterion is to obtain quantitative data or measurements from the field data collected. Considering the ratings in Table 3.5, the technique or technology that has a well-established quantitative element is photogrammetry. The main draw-back is that photogrammetry is often not very flexible in terms of the commercially available software.

However, the purpose of this comparative study is to identify a technique or technology that can establish a foundation only. Photogrammetry was, therefore, chosen as the base technology that will, most likely, produce a successful outcome in terms of the objectives of this project.

Initially, it was considered to use drones to fly over the blast area and scan the surface, either photographically or using LiDAR, before and after a blast in an attempt to identify new fragments on the ground. This would have been done by overlaying the point data generated from the image data or scans and identifying the topographical differences. Control points would have been placed within this area to ensure that the acquired data could be geo-referenced.

However, critical problems became apparent whilst exploring this option further.

These problems included:

- The blast area must be properly cleaned prior to the fly-over, i.e. no loose materials should lay on the ground. This is very time-consuming and not viable if data should be acquired in a producing mine.
- The blast area is very large and would require the drone to fly high at a high altitude in order to timeously acquire the necessary data. An increase in altitude will result in lower resolution scans or image data.
- No equipment can move in the area before the drone has completed the data acquisition. Moving equipment, especially after the blast, may result in loose rock

fragments on the ground that was not a result of the blast. This would increase the re-entry time for teams after the blast and, therefore, delay production.

- If there is a lot of vegetation within the target area, rock fragments from the blast could move between the vegetation and would not be recorded by the drone. Therefore, the data acquired may be incomplete.
- Finally, if successful, the data acquired with this technique could only be used to determine the final landing positions and overall travelling distance of a rock fragment. No other information can be deduced from the data.

### **3.3. DEVELOPMENT OF A NEW PHOTOGRAMMETRIC CONCEPT THAT CAN BE USED TO QUANTIFY THE MOTION OF RANDOM FLYROCK RESULTING FROM A BLAST**

The purpose of this new concept is to enable researchers or mines to quantify the flight path of random flyrock caused by surface blasting activities. The desired output of this tool is a trajectory calculation that quantifies the motion of fragments, in order to ultimately determine the landing position of these flyrock fragments as well as its origin on the bench. (Note: determination of the origin of a rock fragment will also not be possible using the drone technique discussed in the previous section.)

Photogrammetry was identified as an existing technique that presented the highest probability of success in terms of the desired outcomes and predetermined criteria. Photogrammetry is a technique that incorporates multiple still images, taken in a stereo configuration that ensures the development of a stereo model. This means that the environment captured in the images can be transformed into a three-dimensional environment, relative to the surveyed control points.

Based on the previous studies investigated and summarised in section 3.1, it was established that empirical approaches have not produced reliable prediction results and were concluded to be only applicable to site-specific applications. However, the laws of physics and principles applied through ballistic principles remain true and relevant for objects moving through a medium. For this reason, a ballistic and projectile physics approach was determined to be the best approach in terms of quantifying the trajectory of a projectile, i.e. a flyrock fragment.



The developed tool concept is presented in Figure 3.4. The proposed model consists of three main components or phases and is designed to incorporate photogrammetry techniques and ballistics principles.

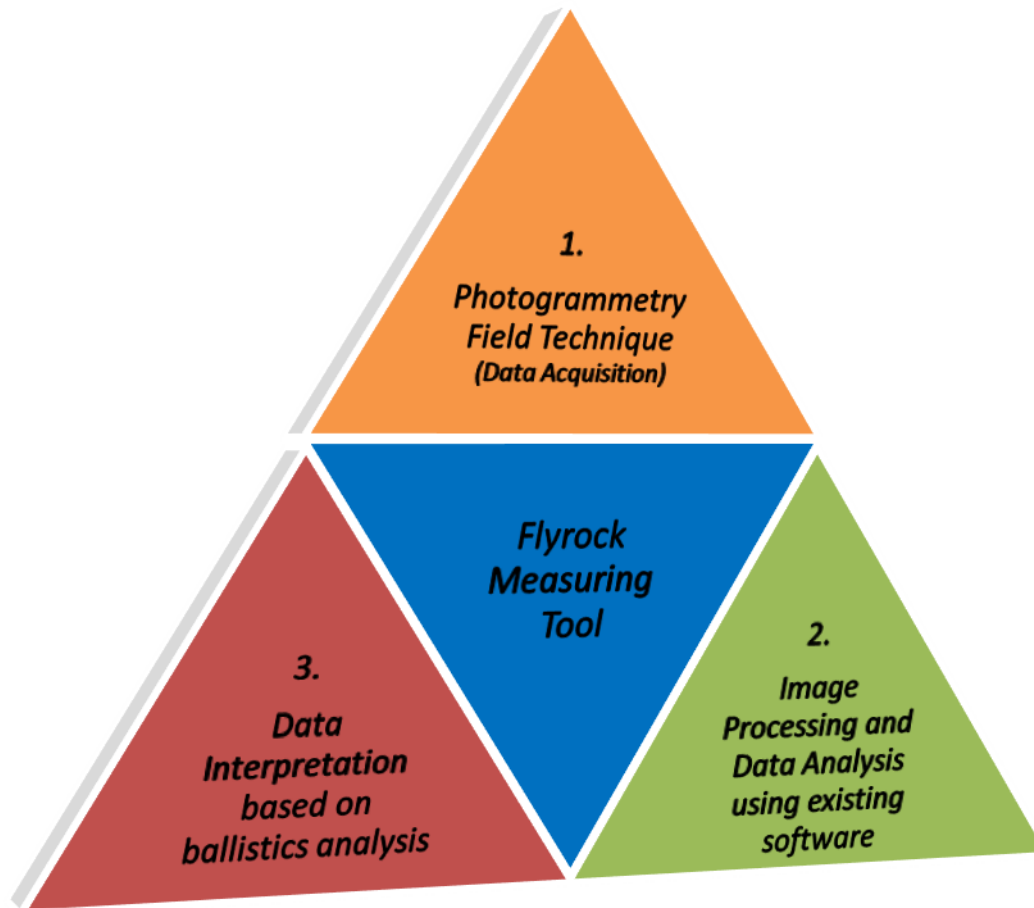


Figure 3.4: Model of the developed tool concept

Each phase or component of this model is discussed.

### 3.3.1. Phase 1

The field technique is designed with photogrammetry as its foundation. In order to maintain the accuracy of the technique, high quality still images are required. High-speed video footage cannot be converted into the required high quality still images because, according to photography experts, even a 4K HD video will only produce approximately 6MP still images or frames. Consequently, it was decided that the necessary still images should be acquired using DSLR cameras, i.e. Canon 77D DSLR cameras. The high-speed burst shot function in these cameras offer the opportunity to capture the maximum number of still images at the full quality available from the camera and lens.

The critical components within phase 1 include:

**(1) The placement and orientation of the cameras in the field.**

Since photogrammetry form the foundation of the field technique and existing photogrammetry software are used in phase 2, the specific camera orientation and placement required by the software should be adhered to in order to successfully process the image data.

In order to use photogrammetry software during phase 2, the following field considerations are essential:

- Images must be taken in a landscape orientation, which also allows one to capture the maximum field of view (i.e. information) in each image.
- The software also requires that the images are taken parallel to one another, i.e. the cameras' field of view must be positioned parallel to the other. The angle of view of the lenses was used to ensure the required overlap between neighbouring cameras (a minimum of 60%). The overlapping images will allow the generation of a stereo model of the site or the event.

The angle of view of various lenses can be obtained from the product specifications. Schematics of the fields of view for three Sigma lenses are given in Appendix B. The calculation of the relationship between the distance to the target area (D) and the width of the lens's field of view (FoV) is also given in Appendix B and is summarised in Table 3.6.

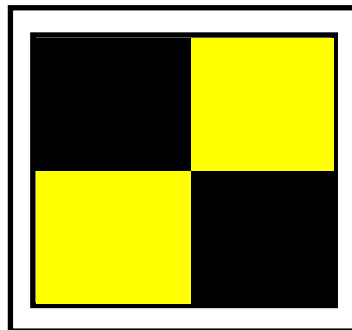
The spacing between neighbouring cameras (d) is given as a ratio of the distance to the target area (D) in Table 3.6.

**Table 3.6: Summary of essential considerations relating to the placement of the cameras in the field**

Lens	FoV : D	d : D
<b>Sigma 35mm</b>	$FoV = 1.2352(D)$	$d = 0.49408(D)$
<b>Sigma 50mm</b>	$FoV = 0.8655(D)$	$d = 0.3462(D)$
<b>Sigma 85mm</b>	$FoV = 0.5098(D)$	$d = 0.20392(D)$

The relationship between the minimum distance between the bases of the camera or tripods is also presented in Table 3.6. This relationship was determined based on the minimum of 60% overlap between subsequent images required by photogrammetry software. Therefore, since identical cameras and lenses are used in this proposed field technique, it was determined that the maximum base distance between the cameras is 40% of the FoV width.

- A decision was made to use a minimum of three cameras to acquire the necessary image data. Three cameras with fixed focal lenses were used in the proof of concept tests. The reason for using fixed focal lenses are that the zoom of the lenses on each camera cannot be adjusted. This is essential to minimise variabilities in the system.
- Finally, in order to geo-reference the acquired images, surveyed ground control points must be placed within the fields of view of the cameras. Control points (Figure 3.5) must be placed within the FoV of all the cameras and accurately surveyed.



**Figure 3.5: An example of the GCPs (ground control points) used in the field**

These GCPs are essential to the site calibration of the lenses and will, ultimately, influence the accuracy of the final output of the system.

## **(2) The calibration of the cameras' lenses in the field.**

In order to accurately geo-reference the image data, it is essential to calibrate each lens to eliminate the influence of slight internal and external variables on the dataset. Even if identical cameras are used, manufacturing inherently result in minor internal differences in each camera. If cameras are used that is

compatible with interchangeable lenses, handling the camera will result in small changes in the internal camera/lens parameters.

It is, therefore, essential to calibrate each lens on-site, prior to the blast in order to eliminate small errors that may be magnified in subsequent phases. Several overlapping images are taken of the target area by walking across the camera placement area (i.e. from camera one to three and back) The process of calibration is discussed in phase 2.

### **(3) Triggering of the cameras from a safe distance.**

Due to the inherent risks associated with blasting activities as well as the safety protocols at the mines, triggering the cameras remotely was a key consideration. Most mines implement a minimum evacuation distance for people of 500m and 300m for equipment. If the cameras are placed within this 500m radius, a remote triggering method must be used to simultaneously trigger all of the cameras.

Existing remote triggers were used to initiate each camera's high-speed burst shot function. One trigger is connected to each camera in order to initiate that specific camera once a signal is received. The PocketWizard PlusX triggers (Figure 3.6) used in photography are currently the best and most reliable remote triggers on the market. These triggers offer the fastest communication between triggers with a maximum line-of-sight range of about 80m, based on field tests conducted to verify the manufacturer's specifications. These triggers were, therefore, used as the basis of the triggering system.



**Figure 3.6: PocketWizard PlusX trigger (PocketWizard, 2019)**

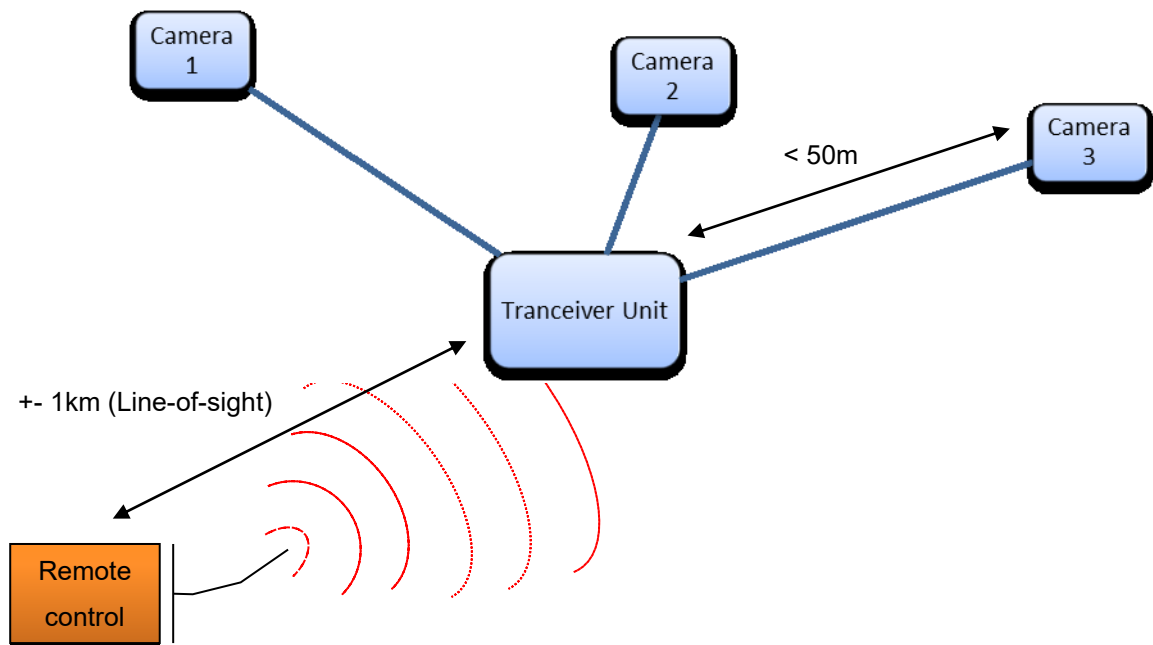
In order to initiate the triggers from a safe distance, a communication system was required to simultaneously trigger the receivers connected to each camera from a single transmitter unit. An expert communications company, Hennie's drone repair and maintenance, were commissioned to design and develop this long-distance trigger system using the PocketWizard PlusX triggers as its foundation.



**Figure 3.7: Long-range trigger system designed for this project.**

The final product is shown in Figure 3.7 and is capable of communicating with the receiving transmitter (or transceiver) at a line-of-sight distance in excess of 1km. In Figure 3.7, (a) and (c) indicates the front and the back of the transceiver, respectively, showing the connection into the PocketWizard PlusX

trigger which forms the foundation of the system. The centre image, (b), shows the transceiver with the remote trigger (a standard radio controller). The communication between these devices and the triggers connected to each camera is shown in Figure 3.8.



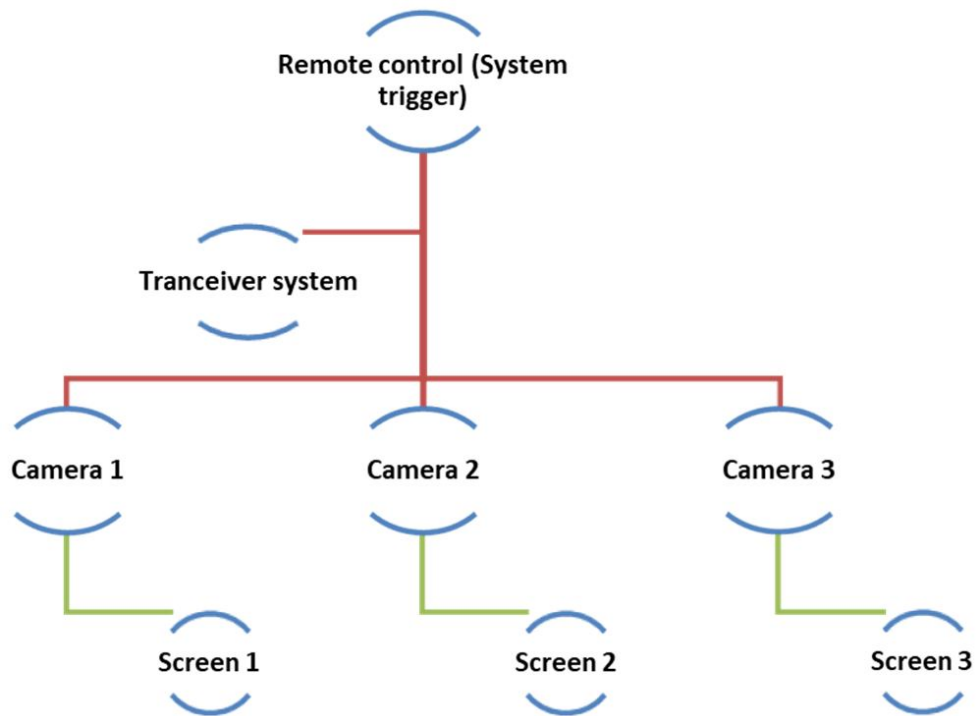
**Figure 3.8: Basic communication diagram between the remote control and the transceiver, and between the transceiver and the receiving triggers connected to each camera.**

**(4) The synchronisation between cameras to ensure the images align in terms of their timing.**

The synchronisation between the cameras, i.e. the point in time when each image is taken, is a critical element to this tool. The goal of the proposed tool is to capture the movement of each flyrock fragment through the air by creating a stereo model of each time step in this motion. Therefore, the accuracy of the measurements takes from these stereo models will significantly depend on the exact time each camera triggers. If two cameras trigger only seconds apart, the position of a fragment captured in each camera's image will be different and this error will transfer into the stereo model.

Another reason that supports the importance of synchronisation between the cameras, is that estimating the elapsed time between each measurement is an essential part of the ballistics analysis in phase 3 of this tool.

Due to this significance, various time studies were conducted to determine what the actual internal delays are between identical cameras' image capturing when separated by a distance of 5m to 25m. The layout or methodology that was followed is shown in Figure 3.9.




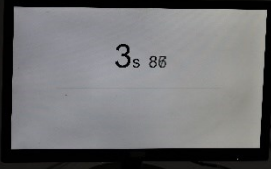
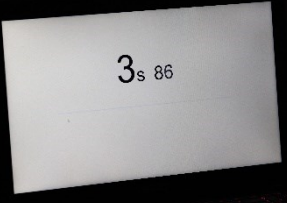

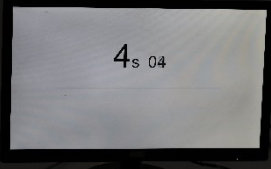
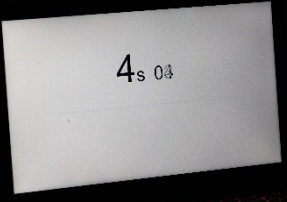

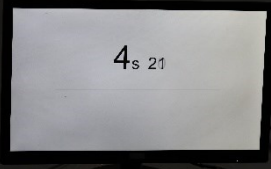
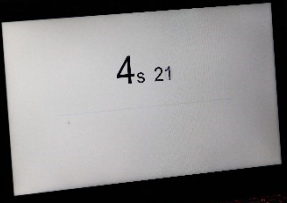
**Figure 3.9: Layout of timing or synchronisation tests**

The red lines indicate the radio communication between the triggering system and the green lines indicate the visual communication between the screens and the cameras. The screens were connected to a single source, i.e. a laptop, that projected a stopwatch. Any delay in the projection was determined to be negligible. This was also tested using a single camera capturing all three screens.

While the stopwatch is activated, the three cameras were triggered. The photographed times on each screen were analysed and compared to the other screens, shown in Table 3.7.

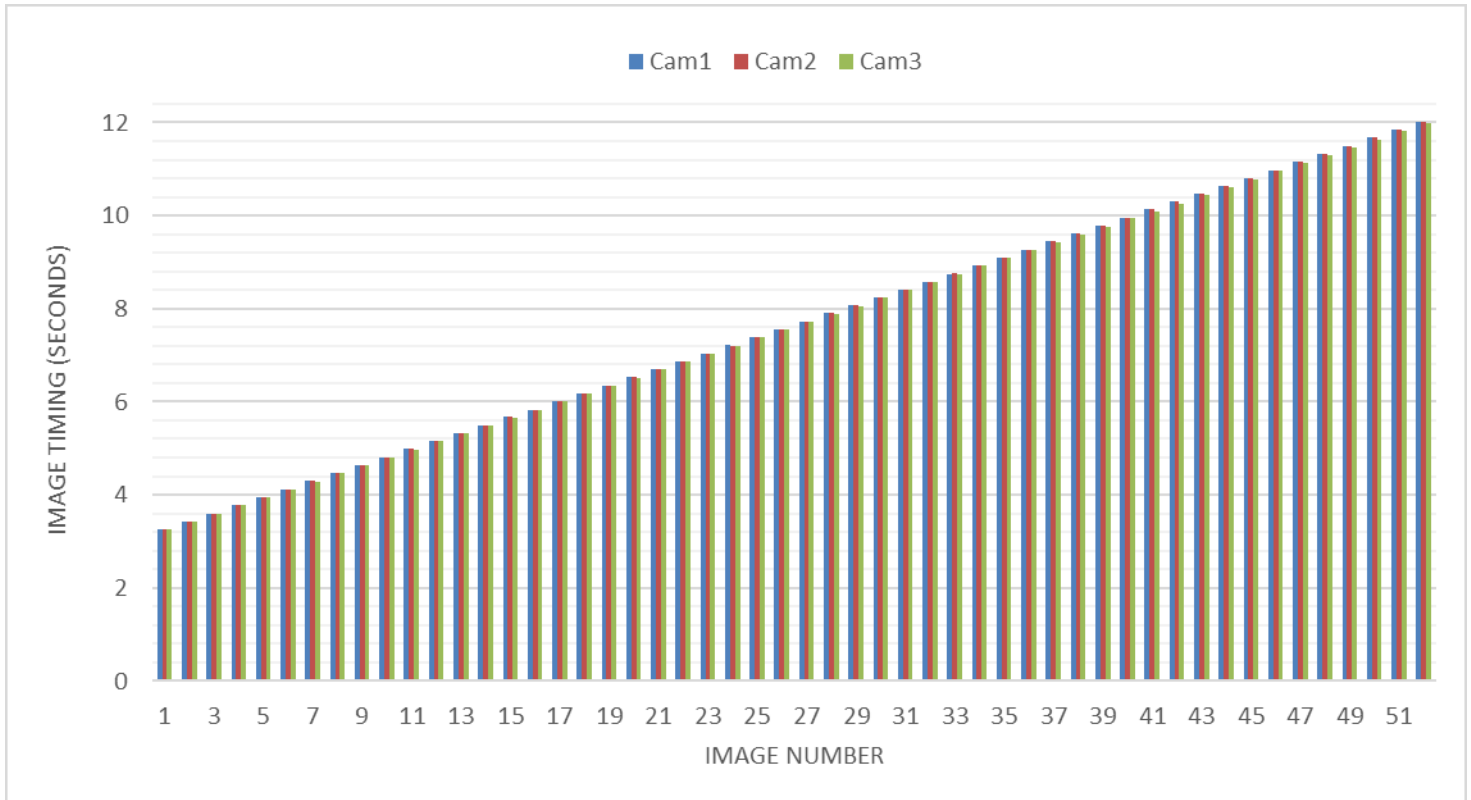


**Table 3.7: Camera timing or synchronisation tests' results**

Image no.	Camera 1	Camera 2	Camera 3
1			
2			
3			

For an example of the tabulated results, please refer to Appendix B. The average time elapsed between successive images were between 0.170s and 0.172s. This means that there is a maximum variation of 0.002s or 2ms between the cameras. It is important to note that this variation is not consistent throughout the image acquisition process, i.e. the error is not cumulative. This 2ms difference between images acquired from different cameras fluctuate. This is illustrated in Figure 3.10.





**Figure 3.10: Timing results from one test illustrating the fluctuation in the timings and that the error is not cumulative.**

This 2ms average error is insignificant at this point and can be minimised by averaging the positional measurements acquired from a combination of the stereo models (created by the multiple cameras) in phase 2.

Most of the challenges experienced throughout the development of the field technique to acquire acceptable data in phase 1 for subsequent processing and analysis have been discussed as key components of the field technique.

### 3.3.2. Phase 2

The image processing and data analysis phase include the identification of critical projectiles in the captured images and measuring the positions (i.e. x-, y- and z-coordinates) at different points in time using photogrammetry software. Obtaining the positional measurements are highly dependent on the site calibration of the cameras' lenses on the day of the blast.

The site calibration of the lenses was developed based on the calibration of aerial photogrammetry cameras. These principles were rotated to a horizontal perspective and applied to this project. Calibration is done by marking each GCP (Figure 3.5) in every image and linking the GCPs to their surveyed coordinates in the photogrammetry software (Pix4D), shown by the yellow markers in Figure 3.11. The key output of this process is to determine the internal and external parameters and orientation of the cameras.



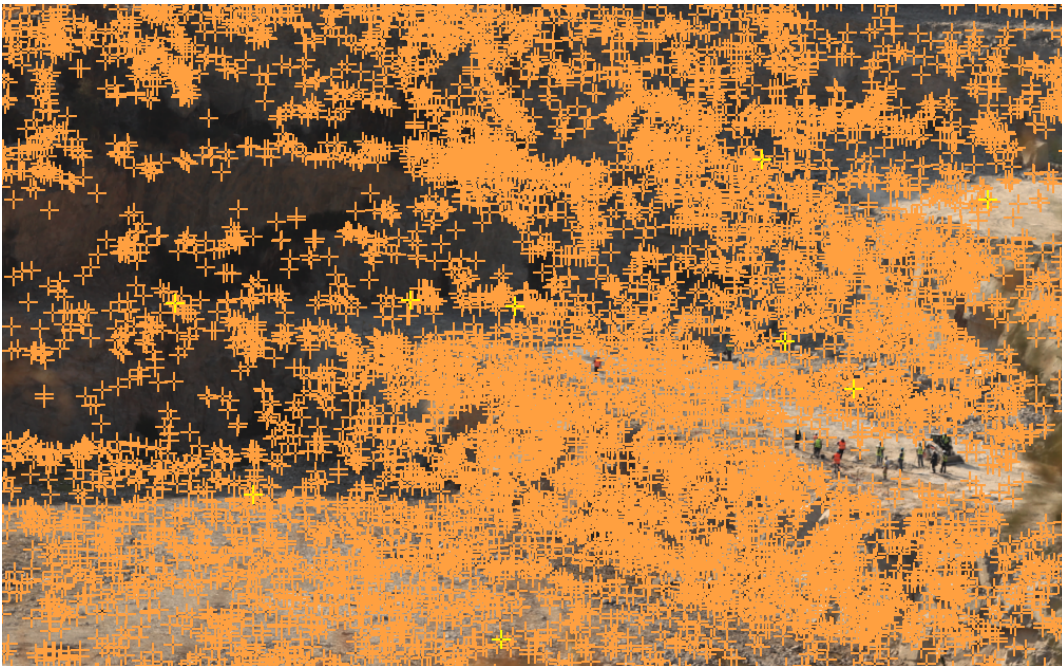
**Figure 3.11: Marked GCPs on a calibration image using Pix4D**

Once all the GCPs are marked and referenced to the relative coordinates, the software is allowed to process the data. During this processing stage, the software uses the marked GCPs on each image and the surveyed coordinates to create tie-points between the images. This is illustrated by the orange markers in Figure 3.12 and Figure 3.13.

These tie-points represent specific features that the software recognise in different images, creating a relation between the location where the image was taken, the specific feature in the image and the known GCPs. The creation of these tie-points will determine the accuracy of the point-data and three-dimensional representation of the scene. This will directly influence the error applicable when taking the positional (coordinate) measurements of the highlighted fragments or projectiles.



**Figure 3.12: Some of the tie-points shown in one image**



**Figure 3.13: All of the tie-points shown in one image**

If these tie-points are successfully created, the image data can be converted into a three-dimensional point cloud dataset. The calibration output and dataset are used, in conjunction with the stereo models of the event (blast), to obtain the positional measurements of various projectiles (fragments).



A key challenge was that photogrammetry software was not designed to be used for a horizontal perspective. Typically, photogrammetry software algorithms are developed to process and analyse aerial images that captured a specific topography with recognisable features. For this tool, the FoV is horizontal and need to capture fragments travelling through the air, which is often a very uniform background. The photogrammetry software, therefore, struggles to distinguish enough features in each image to create sufficient tie-points between the various images. These tie-points between images is what allows the software to create a three-dimensional representation of the scene or object.

It was proposed that the FoV's of the cameras should incorporate a majority of the benches or high-wall behind the blast area in order to capture these distinguishable features. Further research and development are required to eliminate this challenge.

The process of obtaining these measurements have been tested using stereo mapping software, SmartTech's uSMART Softcopy software. The concept tests, discussed in section 3.4, proved that is it possible to obtain positional coordinates of a projectile travelling through the air. However, this process is still in development and further investigation of this component form part of this project's recommendations in Chapter 5.

### 3.3.3. Phase 3

The data interpretation phase consists of combining the data collected in phases one and two and incorporating it into existing ballistics equations. These ballistics equations are based on the principles of projectile physics and Newton's laws of motion, which remain valid for all moving objects.

Previous studies, such as Stojadinović, et al. (2011), have investigated and applied these equations and principles to flyrock. The following equations (numerical solutions initially presented in Chapter 2) were derived in this study:

**Equation 3.1: Differential equation for motion in the x-direction (Stojadinović, et al., 2011)**

$$m\ddot{x} = -D_x = -C_1 v^2 \cos\theta$$

**Equation 3.2: Differential equation for motion in the y-direction (Stojadinović, et al., 2011)**

$$m\ddot{y} = -mg - D_y = -mg - C_1 v^2 \sin\theta$$

With  $\ddot{x}$  and  $\ddot{y}$  = acceleration in the x- and y-direction ( $\text{m/s}^2$ )

D = Drag force (N)

$C_1$  = constant equal to the product of the density of air, the cross-sectional area of the projectile and the drag coefficient ( $\rho_{\text{air}} \cdot A \cdot C_D$ )

v = velocity of the projectile (m/s)

$\theta$  = angle between the velocity vector and the horizontal axis (degree or  $^\circ$ )

m = mass of the projectile (kg)

g = gravitational force (N)

However, the authors concluded that a ballistics approach was best suited for a post-incident investigation. The significance of certain parameters within these ballistics equations that relate to specific circumstances or external factors must be considered and investigated.

The most important of these parameters is the drag force experienced by these flyrock fragments whilst travelling through the air. Estimating the vector quantity of the drag force is dependent on the drag coefficient (which relates to the size and shape of the fragment), the cross-sectional area of the fragment and the speed it is travelling. The cross-sectional area of the fragment and the velocity it is travelling can be calculated by means of the positions of a fragment at different points in time.

It is important to note that the effect of rotation or spin of the fragment has not been considered in any previous study relating to flyrock.

Therefore, in order to achieve accurate trajectory calculations of the recorded fragments, it is essential to investigate the following fields:

- An accurate estimation of the drag coefficient of different rock types;
- The effect of the shape of each rock type on its drag coefficient; and,
- The effect of rotation or spin of the fragment on the drag force experienced.

For this project, the ballistics principles will be used to analyse and interpret the data obtained from:

- Phase one, i.e. the field conditions and time elapsed between subsequent positions; and,
- Phase two, i.e. the x-, y- and z-coordinates of the flyrock fragments in motion.

The final measuring tool process flow is presented in Figure 3.14.

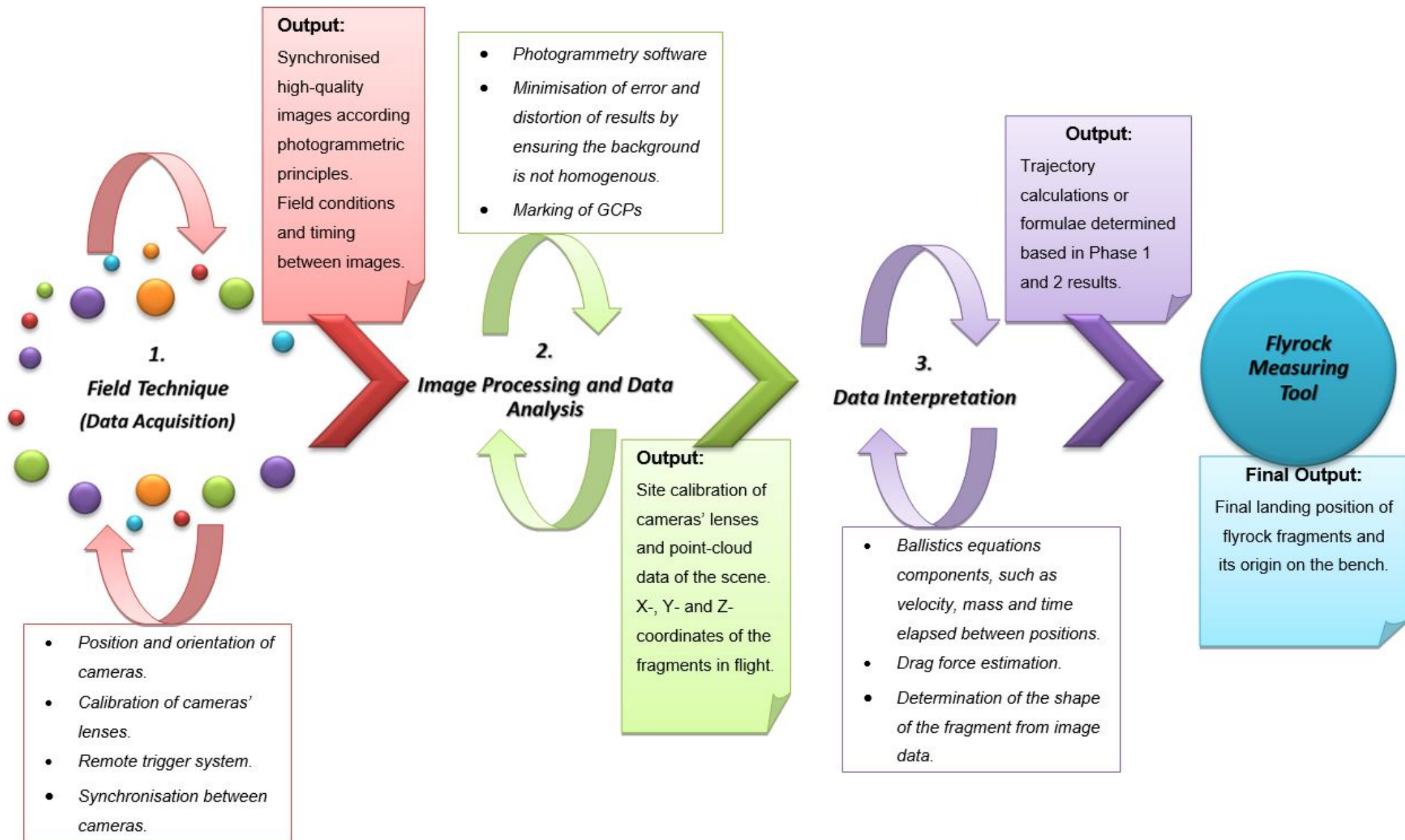


Figure 3.14: Full process flow of the proposed flyrock measuring tool

### 3.4. INITIAL PROOF OF CONCEPT TESTS

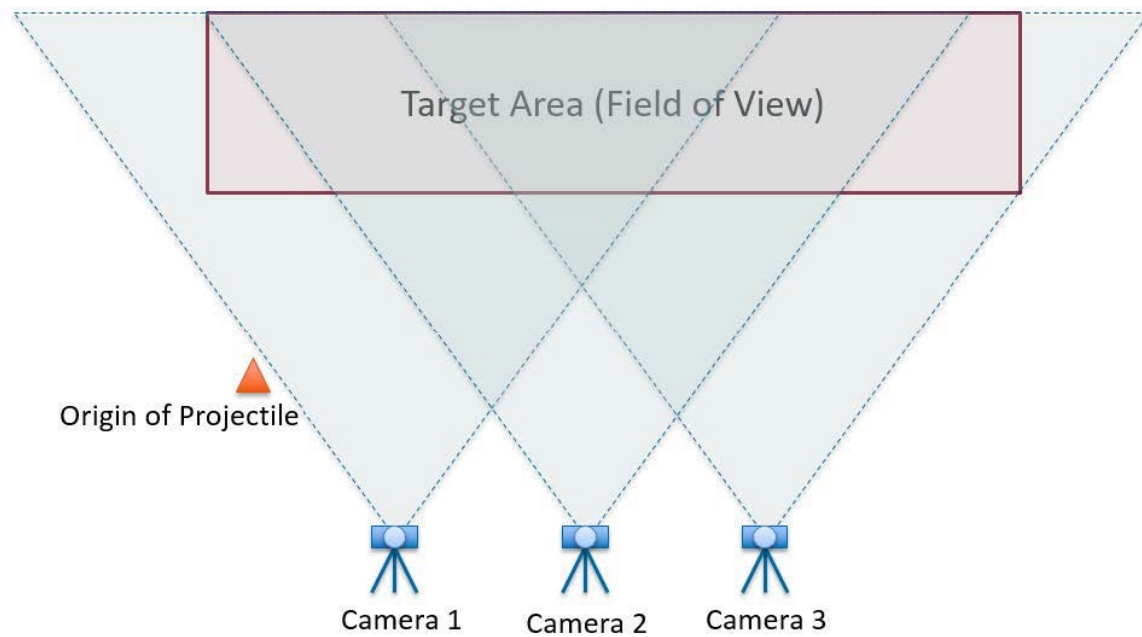
Initial proof of concept tests was conducted between October 2018 and January 2019. The motivation behind these initial tests confirmed that it is possible to achieve a specific outcome relative to key elements in phase one and phase two. These elements and the related desired outcomes are summarised in Table 3.8.

**Table 3.8: Initial concept tests' focus elements and desired outcomes**

	<b>Main element</b>	<b>Desired outcome</b>
<b>1</b>	Evaluate the horizontal (rotated “aerial”) calibration technique.	Internal and external camera parameters prior to the “blast” or event can be determined with the Pix4D software
<b>2</b>	Generation of point-cloud data of the scene.	Sufficient point-cloud data of the environment can be generated using the calibration images.
<b>3</b>	Capturing a high-quality image of a moving object.	High-quality images without significant motion blur will allow clear and accurate measurements to be taken.
<b>4</b>	Capturing a moving object in flight and visually tracking that object’s motion in successive images.	Identifying and “tracking” the same object in successive images. The physical characteristics of the object will assist with this.
<b>5</b>	Creating a stereo model of an object in motion from images taken from two separate cameras.	The point-cloud of the scene based on the calibration data are combined with the event data (“blast” images) to create stereo models (two cameras per model) for each camera-combination.
<b>6</b>	Obtaining positional measurements (x-, y- and z-coordinates) using existing stereo mapping software.	Once the stereo models are successfully generated, the coordinates of a point within the images can be acquired.

The methodology for these concepts tests was designed to simulate an environment where a projectile is moving air the air on an unknown (or even random) trajectory. In order to control as many variables as possible, it was decided that using clay pigeons launched from a clay trap will be the best approach. The clay pigeon launcher allowed the team to constantly launch the projectile into a specific target area while still keeping a degree of randomness of its flight path. Clay pigeons are designed to remain in the air for longer (i.e. it experiences higher lift forces) than a spherical projectile, prolonging the duration during which quality images can be acquired.

The setup of the proof of concept tests is illustrated in Figure 3.15.



**Figure 3.15: Concept tests setup**

The concept test methodology is shown in Figure 3.16.



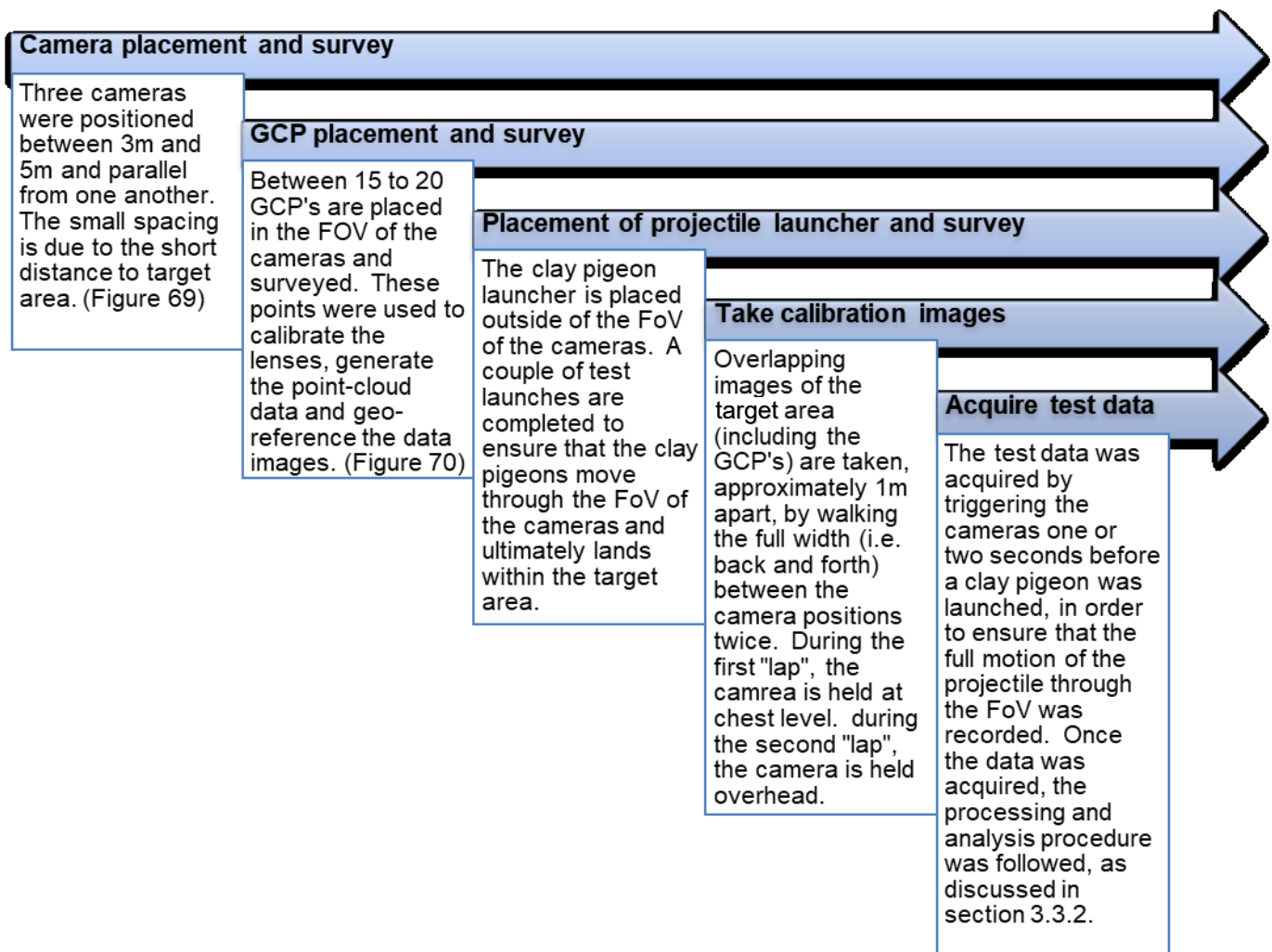


Figure 3.16: Proof of concept tests' methodology



Figure 3.17: Camera placement for the proof of concept tests



**Figure 3.18: GCP placement in the FoV of the cameras, within the target area**

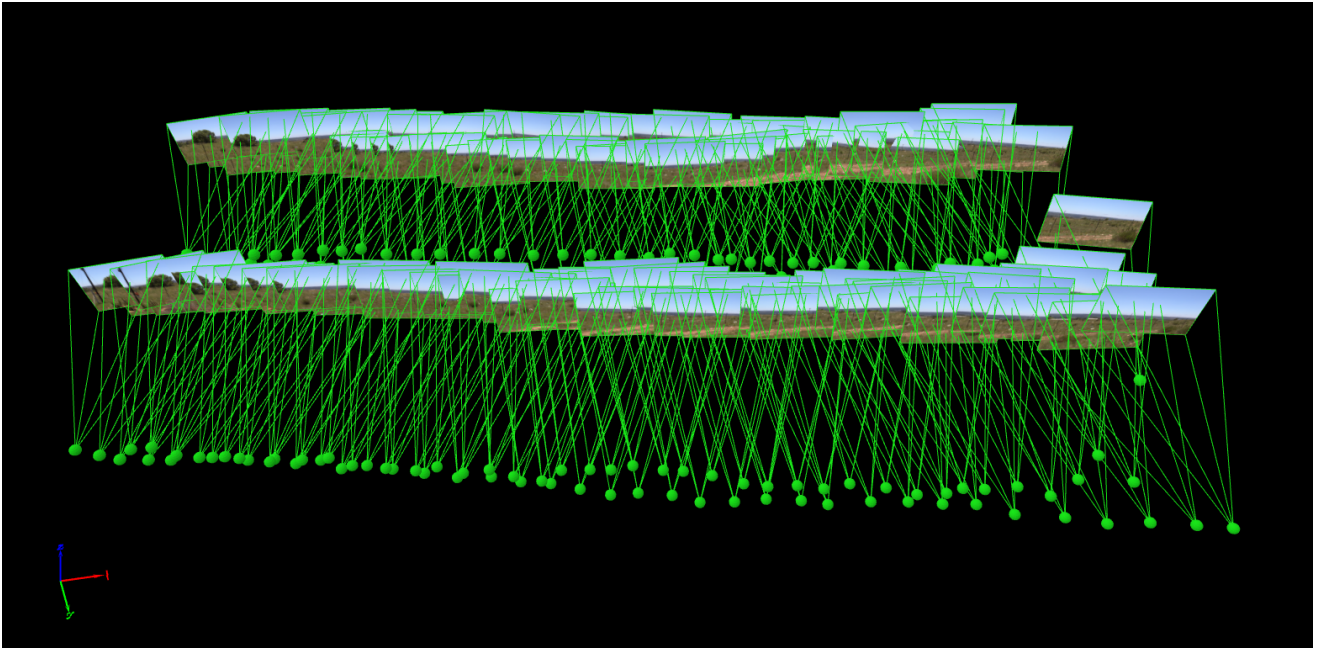
### **3.4.1. Proof of concept test results**

The results of the concept tests are discussed according to the predetermined elements and desired outcomes presented in Table 3.8.

#### **3.4.1.1. Evaluate the horizontal (rotated “aerial”) calibration technique.**

Calibration of aerial surveying camera lenses is typically done by flying over a target area with contain ground markers and taking overlapping images in succession. These images and ground markers are then used to determine the characteristics of the camera(s) on the day. This exact technique was used for the proposed tool, however, it had to be rotated by 90° to capture a horizontal target area.

The calibration data from the Pix4D software is exported in the form of external and internal camera parameters and are summarised in a .csv file that can be imported into the stereo mapping software. The calibration process was successful but time-consuming. This calibration process is still in the process of being improved and refined in order to reduce the amount of labour required in this phase. The calibration image data and the path followed to take these images are illustrated in Figure 3.19.



**Figure 3.19: Calibration image data and the path followed (green dots)**

The main challenge was that the software was never designed to process data with a homogenous background such as blue skies.

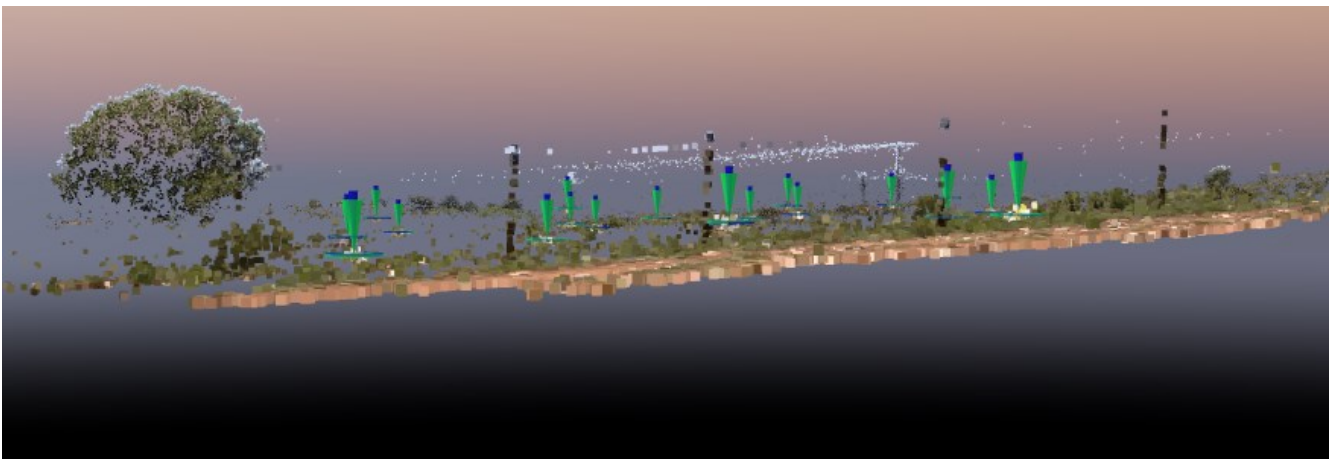
#### **3.4.1.2. Generation of point-cloud data of the scene.**

The calibration images were also used to generate a point-cloud of the environment prior to the event. The generation of the point-cloud data was the reconstruct the environment into a digital three-dimensional space. The point-cloud data also enables the images to be geo-referenced for the analysis phase (phase 2 of the proposed tool). A point-cloud was successfully generated and is given in Figure 3.20 and Figure 3.21.





**Figure 3.20: Point-cloud of the test environment (without GCPs)**



**Figure 3.21: Point-cloud of the test environment including the aligned GCPs (blue and green markers)**

This point-cloud can be used for further data processing and interpretation, as well as potential visualisation of the data in virtual reality. This was concluded to be a new potential application of the proposed tool.

#### **3.4.1.3. Capturing a high-quality image of a moving object.**

Being able to capture a high-quality image of a moving object without any motion blur is very important to obtain accurate measurements of the object's position at different times. This essentially means that the "guess-work" of the exact position of the object is eliminated. The only solution for this is to use good quality cameras and lenses and apply photographic

principles. However, these specific camera settings will vary with each environment and is not presented as results.

Capturing a high-quality image of a moving object was a successful outcome and is shown in Figure 3.22.



**Figure 3.22: High-quality image of a moving object while travelling through the air**

The distance between the concept test target area and the cameras were significantly smaller than it would be in a real blasting scenario. However, this result can still be achieved by using a lens with a higher focal length.

#### **3.4.1.4. Capturing a moving object in flight and visually tracking that object's motion in successive images.**

In addition to capturing and recording the position of a moving object while it is in flight, it was important to evaluate whether the same object can be identified and visually tracked in subsequent images taken from different cameras. This was another successful outcome based on the proof of concept test. This is illustrated in Table 3.9.



Table 3.9: Visually detecting and "tracking" a moving object through multiple cameras

Camera 1

Camera 2

Camera 3













In order to ensure that the same position of the projectile (clay pigeon) is observed and evaluated in each camera's images, the acquired images were evaluated in reverse. This means that the images taken last were viewed and evaluated first and, working backwards and considering surrounding features, corresponding images from different cameras were identified and grouped.

In the proof of concept tests, it was decided to only record the motion of a single projectile, in an attempt to simplify the test methodology and limit the potential variables. It is essential to continue testing this element considering the motion of multiple projectiles simultaneously.

#### **3.4.1.5. Creating a stereo model of an object in motion from images taken from two separate cameras.**

A stereo model is created by superimposing two overlapping images taken from two neighbouring cameras or two positions using the same camera. The two superimposed images are combined with the three-dimensional point data and camera calibration data generated using the Pix4D software.

The stereo model is created by aligning the projectile and other recognisable features in each image with that in the second image, in a three-dimensional space. If the alignment of the projectile and other features in the two images of the stereo model is flawed (i.e. when the images are taken out of the stereo, the measured point is in different locations), this error will be carried over to the positional measurements taken. If the stereo model is set up correctly and all features align, the error of the positional measurements could be as little as 1mm which is the maximum tolerance allowed for survey data and -models.

Therefore, it is important to ensure that these features (including the projectile) are aligned as closely as possible in order to minimise the error related to the coordinate measurements taken.

For the proof of concept tests, it was possible to create these stereo models in the mapping software, uSMART Softcopy, to within an accuracy of a couple of centimetres (as depicted by the powerline pole measurements in Table 3.10). For the purpose of proving the concept, this error was considered to be acceptable. Further testing and refining of the procedure will enable the reduction of this error to an acceptable margin for actual field tests.

#### **3.4.1.6. Obtaining positional measurements (x-, y- and z-coordinates) using existing stereo mapping software.**

Once the stereo model has successfully been created, measurement of any feature within this model can be acquired. This is simply done by marking the centre-point of a feature to measure

its position or using the measuring tool (similar to any CAD software) to measure distance or the circumference of an object. Table 3.10 demonstrates the results obtained for one of the proof-of-concept tests. For this test, only three positions could be measured within an acceptable error margin.

**Table 3.10: Results for three successive positions of the clay pigeon**

<b>Name</b>	<b>y</b>	<b>x</b>	<b>z</b>	<b>Survey Method</b>
<b>Puck(P1_S2_Photo2)</b>	47 158,573	2 843 249,409	1 512,449	Photogrammetry
<b>Puck(P1_S2_photo3)</b>	47 165,081	2 843 248,586	1 513,470	Photogrammetry
<b>Puck(P1_S2_Photo4)</b>	47 170,591	2 843 247,229	1 515,874	Photogrammetry
<b>Top of Powerline Pole</b>	47 056,919	2 843 279,453	1 516,384	Survey (Total Station)
<b>Top of Powerline Pole</b>	47 056,518	2 843 279,555	1 516,394	Photogrammetry

The powerline pole measurements were taken to give an estimate of the stereo model error since the powerline was stationary throughout the test. The error displayed varied between 1cm and 40cm. It is important to note that the powerline pole was not inside the control area, i.e. it was located beyond the last line of GCPs placed in the target field. Therefore, it can be assumed that the actual error was less than the measured error. The full report for this results that were exported from the uSMART software is given in Appendix B.

The process of creating an accurate stereo model is still under investigation. Further testing and investigating the improvement of the entire phase two process and its accuracy is still ongoing. However, in terms of proving the concept according to the desired outcomes presented in Table 3.8, it was concluded to be satisfactory and motivate dedicated further investigation.

A small-scale field test (or quarry test) was consequently carried out at a quarry to ascertain whether the cameras would capture flyrock in flight from an actual blast. Figure 3.23 shows that the flyrock was successfully captured and could be visually tracked in subsequent images taken by the cameras. The next step would be to convert the photographic data to point cloud information.



Figure 3.23: Quarry test blasts image data, showing the same projectiles at different time intervals.

CONCLUSIONS

---

## 4. CONCLUSIONS

Flyrock remains a significant risk to the health and safety of the mine's employees and infrastructure as well as the safety of the neighbouring communities and their property. Losses and damages can result in significant financial and reputation consequences. The lack of fundamental research in recent years and quantifiable data relating to the relationship between blast design parameters and the risk of flyrock motivated this project. A number of authors concluded that major gaps in knowledge relative to flyrock caused by its random nature still remain a weakness in the field.

Recent papers published (since 2010) proposed a wide range of potential approaches and techniques to predict or investigate flyrock. However, the majority of these papers concluded that the proposed results were site-specific and could not be applied to other environments. Several authors proposed viable qualitative solutions based on assumed causative parameters and their impact as inputs. Since the actual impact of blast design parameters on the risk of flyrock is debatable, based on the contradicting assumptions made in these publications, it can be concluded that the results presented in these publications may be flawed.

The focus of this project was to develop a concept that is able to quantify the flight path of the flyrock resulting from a blast. The motivation behind the development of this concept was to enable future researchers to quantify the impact of the different blast design parameters on the measured flyrock.

Various technologies were considered and investigated during this project. After a comparative analysis of these technologies, it was decided to use photogrammetry as the foundation of the proposed concept tool. The proposed concept consists of three main phases, namely (1) data acquisition, (2) image processing and data analysis and (3) data interpretation.

To date, progress has been achieved with phase one and phase two. In phase one, all objectives have been met. However, there are still areas which need refinement, specifically regarding the placement of the cameras in the field.

The key elements of phase one were concluded as:

- The positioning and orientation of the cameras relative to one another as well as the target area was determined by means of photogrammetric principles.

- The site calibration of the cameras was developed based on the calibration of aerial photogrammetry cameras. The same principles were rotated to a horizontal perspective and applied to this project.
- The remote triggering system was based on existing photography triggers. A long-range trigger was designed and manufactured in order to trigger the cameras from the same distance from the blast.
- The synchronisation between the cameras were also determined to be within acceptable ranges when using top-of-the-range triggers. Identical cameras were also used to minimise this variance.

Phase two has been tested to the point of on-site calibration of the camera lenses and creation of point-cloud data of the environment before the “blast”. The process of calibrating the lenses has been established, however, further optimization is possible. Initial proof of concept tests enabled the team to take reliable coordinate measurements of a moving projectile at different times. The measurements acquired are incorporated into existing ballistics equations to calculate the trajectory of the fragments.

Point-cloud data was successfully generated in the concept test, but converting the image data from subsequent quarry test blasts proved more challenging and is still a work in progress. Once phase two has been satisfactorily resolved, attention will focus on phase three.

The key components in phase three are the drag coefficient for each projectile (including the impact of the fragment’s shape) and the effect of the environment or weather on the day.

Therefore, in order to achieve accurate trajectory calculations of the recorded fragments, it is essential to investigate the following fields:

- An accurate estimation of the drag coefficient of different rock types;
- The effect of the shape of each rock type on its drag coefficient; and,
- The effect of rotation or spin of the fragment on the drag force experienced.

The proposed tool concept is developed to record, quantitatively measure and calculate reliable trajectories for fragments thrown from a blast. Initial concept tests proved that this concept is capable to quantify the motion of random projectiles that originated from a relatively unknown position. However, further development, testing and refining of phases two and three are essential before this tool is able to be used in general and practical flyrock research.

RECOMMENDATIONS

---

## 5. RECOMMENDATIONS

Based on the findings of this project, the main recommendation is that further investigation and research should be conducted to develop this concept into a comprehensive tool.

This tool can, ultimately, be used for one of three purposes, namely:

- (1) Mines can generate a database with accurate historical flyrock of their blasting operations. This database of historical information can be used to motivate clearance distances if it comes into question.
- (2) Research teams can implement this tool to conduct quantitative research and investigations into flyrock and the impact of different blast design parameters on the risk of flyrock.
- (3) Point-cloud data combined with ballistics calculations can be used to visualise blasts and flyrock in Virtual Reality for training and education.



SUGGESTIONS FOR FURTHER WORK

---

## 6. SUGGESTIONS FOR FURTHER WORK

Similar to Chapter 7, the main suggestion for further work is to develop phases two and three of the proposed tool concept.

The use of existing photogrammetry software has presented some challenges during phase two. The algorithms that make up the software are designed to process image data with non-homogenous backgrounds and distinguishable features. It is, therefore, suggested that further work should be focussed on incorporating visual detection and tracking techniques and algorithms for the purpose of this tool. This may imply that new or adapted software must be written specifically for this tool.

For phase three, it is recommended to investigate the drag coefficient and the impact of the size and shape of fragments on the drag force exerted onto it. Additional work should also be done to determine the breaking profiles of different rock types in an attempt to predict the shape of blasted rock.



---

**7. ADDITIONAL RESEARCH AND RELEVANT LITERATURE**

---

**7.1. BLAST DESIGN PARAMETERS AND OTHER FACTORS THAT INFLUENCE THE RISK OF FLYROCK**

“Parameters and factors that influence the risk of flyrock” refers to those causative factors that, when it is adjusted or manipulated, can cause a change in the probability and consequence of flyrock. Therefore, any change in any one of the factors discussed in this section can cause a change in the risk of flyrock.

The majority of the literature reviewed refers to the same design parameters and other drilling and blasting factors as causative to flyrock. These causative factors are:

**(1) Geology:**

The geology of the area should be the foundation of any blast design. The blast design parameters are determined according to the geology as well as the final result required by the operation. Geology can become a problem when unknown geological features or structures are present within the blast area (ISEE, 2011). These structures, for example, a highly jointed area, can result in the explosive energy escaping through the path of least resistance (i.e. the joints) and can cause excessive throw of the material. Weathered material toward the collar area of the blast holes will also likely be thrown further than expected.

The rock type can potentially also contribute to the risk of flyrock if the original blast design did not sufficiently consider the specific rock properties, especially when different rock types are blasted simultaneously. Roth (1979) suggests that softer rock types may be thrown further than harder rock types, however, this is contradicted later in his report by further graphs and diagrams. The ISEE (2011), therefore, concludes that there is not efficient field data or research to prove a correlation between rock type and flyrock. This conclusion is supported by Roth (1979).

**(2) Blast pattern or layout:**

The blast pattern refers to the layout of the holes in the blast design. Ideally, the blast holes are designed in a grid pattern where the relationship between the burden and spacing remains constant throughout the design (ISEE, 2011). The

reason for keeping the burden-to-spacing ratio constant is to ensure consistent fragmentation through the entire blast. The timing sequence should also support the blast pattern in order to achieve the desired heave or throw from the blast.

The geometry of each of these patterns allows for a uniform energy distribution throughout the blast. Any alteration to the geometry of any pattern will result in irregular distribution of energy and can result in unwanted movement of the rock mass, including flyrock (ISEE, 2011).

**(3) Burden:**

The burden refers to the distance between the individual rows of a blast design. If the burden is increased there will not be enough cumulative explosive energy to break the rock mass (ISEE, 2011). The opposite is true if the burden is reduced, resulting in a more violent blast with the possibility of excessive throw, including flyrock, and excessive ground vibrations. The burden is also a key parameter when designing a blast since the other design is calculated using the burden as an input, indicated by the interdependency of the blast parameters (Figure 1.2) in Chapter 1 and Appendix A. Therefore, the entire blast design should change accordingly when the burden is adjusted. Abiding by the rules-of-thumb ensures that the blast design parameters are related to each other according to the predetermined ratios.

**(4) Hole diameter:**

The hole diameter is generally determined by considering the geology, rock type, type of blasting desired and the available drilling equipment on the mine (ISEE, 2011).

If the hole diameter is smaller than designed, with the other design parameters remaining the same as originally designed (specifically the designed stemming), the explosives per hole will not be enough to break the required block of ground. This will result in poor fragmentation and the possibly require secondary breaking.

Similarly, if the hole diameter is larger than designed, with the other design parameters remaining the same as originally designed, there will be too many explosives charged per hole. This will result in undesired fines, excessive throw or flyrock, unwanted ground vibration, noise, dust, back-break and over-break. This, again, relates to the interdependency between blast design parameters.

**(5) Hole angle:**

Angled holes can increase the risk of flyrock due to potentially under-burdening at the free-face, especially if the final wall is vertical (i.e. 90°). Drilling angled holes is often dependent on the experience of the operator and, therefore, contributes to the variability in the actual burden of the blast.

**(6) Charge mass:**

The charge mass per hole refers to the mass of explosives in each blast hole. Similar to the discussion under heading (4) Hole diameter, excessive explosives charged per blast hole will result in undesired fines, excessive throw or flyrock and unwanted ground vibration, noise and dust (ISEE, 2011).

**(7) Powder factor:**

The powder factor refers to the mass of explosives required to break one cubic meter (1m<sup>3</sup>) of rock. If the powder factor is excessive, the blast will be extremely violent and flyrock will likely be a result of such a blast. If the powder factor is insufficient, the blast will not achieve the fragmentation required and secondary breaking will most likely become necessary (ISEE, 2011).

However, Roth (1979) illustrates that the powder factor cannot be used as a reliable indicator of flyrock. Roth (1979) argues that high powder factors can still be achieved in normal bench blasting if the confinement (stemming) of the charge is increased as well.

**(8) Stemming:**

The stemming refers to the confinement of the explosives in a hole (ISEE, 2011). The stemming keeps the explosives in the hole long enough so that most of the explosive energy actually moves through the rock mass and not straight out of the hole. The stemming is divided into two components, namely the stemming length and the stemming material. Both of these components are significant to the outcome of the blast and is indicative of the degree of confinement.

The stemming length (T) is calculated from the burden or the hole diameter, with a ratio of between 0.7 and 1.0 times the burden distance (Tose, 2007) or 20 to 40 times the hole diameter (ISEE, 2011). Increasing the stemming length means that more of the explosive energy will be forced through the rock mass, breaking it more efficiently. However, if the stemming length is too long, the explosive energy will be

confined towards the bottom of the blast hole, resulting in poor fragmentation towards the collar region of the blast hole.

It is therefore essential to optimise the stemming length for any blast design. ISEE (2011) presents some “stemming length performance factors”, namely:

- The strength of the rock at the top of the bench or area of decking
- The charge diameter
- The charge energy (higher energy will require more stemming)
- The burden
- Water in the stemming area will reduce the locking capacity of the stemming particles
- Flyrock considerations

The required or designed stemming length is site (and blast) specific and should be reviewed as soon as any change in the design and surrounding area occurs.

The stemming material also contributes to the success of the stemming. The physical properties of the stemming material will determine the efficiency of the stemming. ISEE (2011) and WorkSafe Victoria (2012) states that crushed, angular rock chippings, 20 to 30 times the blast hole diameter, should be used as stemming material and should be sized approximately  $\frac{1}{10}$  of the hole diameter. The reason for using crushed, angular rock chipping for stemming is that the angular chippings “interlocks and wedges against the sides of the blast hole” (WorkSafe Victoria, 2012). If there is water in the hole, the angular chippings will retain its friction against the side of the blast hole compared to rounded chippings.

If crushed, angular chippings are not available and normal drill chippings must be used, ISEE (2011) advises that the stemming length should be increased in order to compensate for the frictional loss and reduced locking capabilities. The stemming length should now be calculated to 30 to 40 times the blast hole diameter (ISEE, 2011).

Therefore, if the stemming length and material are not sufficient to confine the blast, the explosive energy will escape through the path of least resistance, which is often through the collar of the blast hole. This can result in flyrock and is often referred to

as the main mechanism of flyrock experienced, illustrated as cratering and rifling in Figure 2.1 (Richards & Moore, 2005).

**(9) Timing sequence:**

The timing of the blast refers to the delay between the detonation of a hole within a single row (inter-hole delay) as well as the detonation between the rows (inter-row delay) (ISEE, 2011). The purpose of the timing sequence of a blast is to allow the explosive energy of each hole to propagate far enough through the rock mass before the next hole detonates. Each hole that detonates should support the following detonation, ensuring the explosive energy propagates through the hole as efficiently as possible (Cruise, 2011).

There are various timing designs implemented in the mining industry, each designed to achieve a specific goal, i.e. fragmentation, muck-pile profile or throw. The timing sequence is, therefore, designed according to the mine's needs.

When blast holes detonate without any delay, the explosive energy will not adequately propagate through the rock before the successive holes detonate. This can result in a cumulative effect throughout the blast, which can result in excessive ground vibration, noise, flyrock and unacceptable fragmentation.

The opposite is also true, i.e. if the delays are too long, the explosive energy per hole will not support the next hole's detonation, resulting in poor fragmentation and potentially back-break.

However, the ISEE (2011) states that there are insufficient data and research on the effect of timing on the risk of flyrock to draw any correlation between the two. According to the ISEE (2011) and based on the work done by McKenzie (2009), it is more likely that short delays will promote the probability of flyrock (McKenzie, 2009).

**(10) Human factor:**

The human factor will always have an influence on any mining operation. Errors generally occur when employees are rushed and taking shortcuts in order to save time or speed up the process. In terms of blast results and flyrock, these shortcuts can often include (ISEE, 2011):

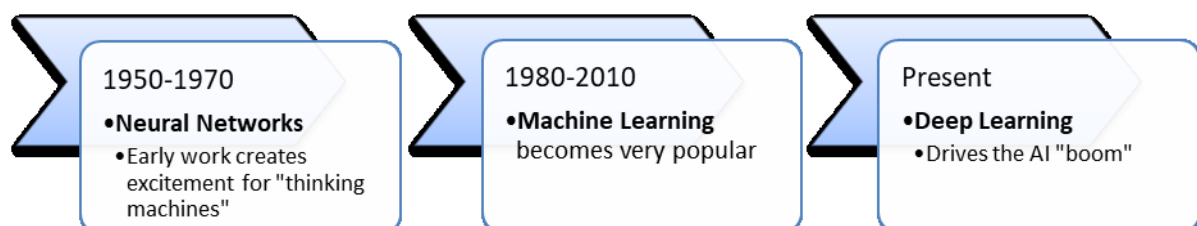


- Holes not measured for accuracy (i.e. position, diameter, depth, deflection or incorrect inclination),
- Primers or boosters are not positioned in the bottom portion of the blast hole,
- Overcharged holes are not corrected (i.e. excess explosives are not scooped out),
- Holes not measured after being charged, resulting in shorter or longer stemming lengths,
- Some holes can even be skipped during stemming,
- Improper tying up of the holes and rows, affecting the inter- and intra-row timing of the blast,
- Drill chippings covering the primer (before charging takes place) resulting in the primer not being in contact with the explosives,
- Incorrect explosives delivered into blast holes,
- Incorrect density or dead pressing in the toe of the hole, and
- Incorrect charging method (i.e. wet holes must be charged from the bottom or augured).

Therefore, even if a blast design is “flawless”, the effect of human error can still be significant and yield unwanted results.

## 7.2. ARTIFICIAL INTELLIGENCE (AI) PRINCIPLES

The SAS Institute Inc. (2019) present a broad timeline of the evolution of AI since the 1950s in Figure 7.1.



**Figure 7.1: Artificial Intelligence developmental timeline (SAS Institute Inc., 2019)**

The basic working of an AI system is described as a computer processing input data based on prescribed steps in the form of algorithms. Depending on the purpose of the AI system (i.e. the desired output), the developer will write algorithms that prescribes the “thinking” process and task execution to the computer (Intelliplateat.com, 2019). The computer processes and analyses the input data, based on these algorithms, and generates a specific

output. This output can range from a numerical prediction (such as weather forecast or the outcomes of sporting events) to a physical movement of a machine, as per the field of robotics.

However, AI is a very broad field and consist of several sub-fields that can be researched and developed separately. The six main sub-fields or components of AI are illustrated in Figure 7.2 and are described by Intelliplaat.com (2019) and SAS Institute Inc. (2019) as:

- **Cognitive computing**

Cognitive computing refers to programming a computer to imitate and simulate human processes, specifically the ability to recognise visual images and speech and respond through speech.

- **Computer vision**

Computer vision refers to programming a computer to recognise a feature in an image or video by means of pattern recognition algorithms and deep learning. This allows the computer to “see”, process, analyse and interpret images or visual surroundings.

- **Machine learning**

Machine learning refers to enabling a computer to “learn on its own”. This is achieved by presenting numerous examples (case studies) and past experiences against which the computer can automatically compare its outputs and adjust its algorithms to improve future outputs. Machine learning incorporates methods such as neural networks, statistics, physics and research regarding similar operations or systems to find additional insights on the relative input data.

- **Neural networks**

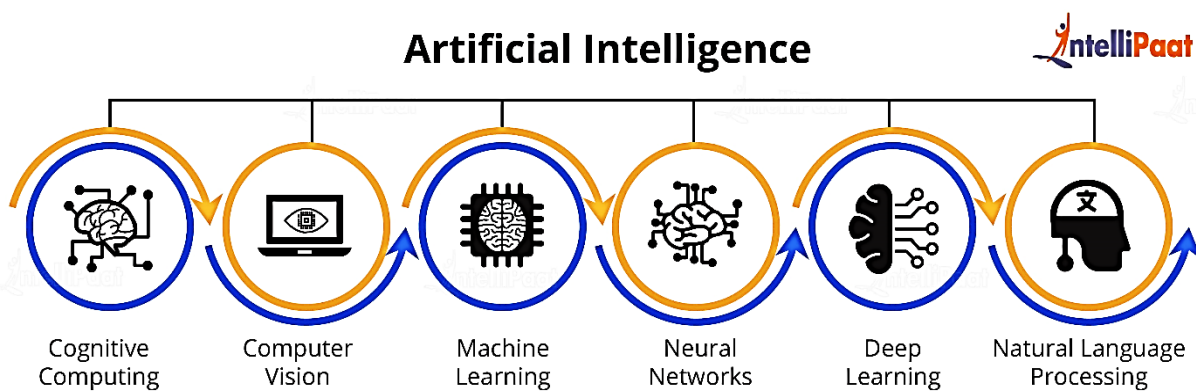
Neural networks (also known as artificial neural networks (ANN)) is defined as a system designed to imitate the function of the human brain. Neural networks consist of multiple input streams and processing units (neurons) that allow the system to process a set of data multiple times to find different connections and interpret vague data.

- **Deep learning**

Deep learning refers to an ANN on a much larger scale, consisting of multiple layers of processing units. This allows computers to process and analyse large and complex data sets, exploiting the recent advances in computing power and improved learning techniques and algorithms. Common applications include image and speech recognition technologies.

- **Natural language processing**

Natural language processing refers to programming techniques and algorithms that allow computers to analyse, understand and respond in human language, including speech.



**Figure 7.2: The six main sub-fields or categories of AI (IntelliPaat.com, 2019)**

AI has made a significant impact in several industries, including health care, retail, manufacturing and banking (SAS Institute Inc., 2019). Social media and marketing industries have also exploited AI algorithms to learn the behaviour of clients and adjust advertising strategies accordingly.

#### **7.2.1.1. Artificial neural networks (ANN)**

Artificial neural networks (ANN) are developed as an attempt to imitate the human brain and its functions. The human brain has the natural ability to learn and adapt to a changing environment. It is also able to identify and scrutinize incomplete or confusing information or data and draw conclusions from this information (Kukreja, et al., 2016). The human brain's more significant functions do not only include controlling the movement of the body's limbs and features, but also complex activities such as dreaming, thinking and learning (Kukreja, et al., 2016).

An ANN typically consists of the following components, and is illustrated in Figure 7.3 (Kukreja, et al., 2016):

- **Inputs**

The inputs to the ANN system are the raw data that needs to be processed into an output. The input layer refers to the initial layer where the input values or raw data are received into the system.

- **Weights**

A specific weight is allocated to the importance or contribution of a specific input to the desired output. This is often also referred to as the “strength of the signal” from a specific input and is often represented as links between each node in the system schematic (Figure 7.3).

- **Neurons**

The neurons are the processing units of the ANN system. The goal of the neuron in this system is to replicate the behaviour of the natural neuron in the human brain. The neurons are located in the hidden layers of the system, between the input and output layers. An ANN can be a single- or multi-layer system.

- **Outputs**

The output is the result yielded by the ANN system ranges between 0 and 1 and is based on the weightings and neurons prescribed. The output layer is usually only connected to a single neuron. An ANN system can, however, have multiple outputs.

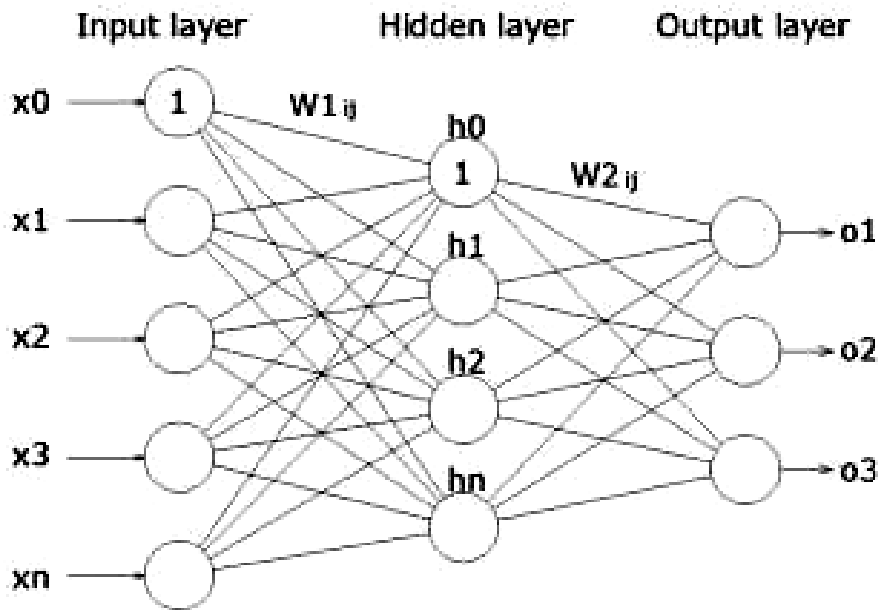


Figure 7.3: Neural network architecture (Kukreja, et al., 2016)

There are various types of ANN, each with a different architecture and purpose. Mehta (2019) summarised in the seven most important types in Table 7.1.

Table 7.1: Types of ANN (Mehta, 2019)

Type of ANN	Description	Diagram
<b>Feed-forward Neural Network</b>	<p>This is one of the simplest types of ANN. In a feed-forward ANN, the data passes through the different input neurons, through the hidden layer, and finally reaches the output layer.</p> <p>This type of ANN is typically written as:</p> $i - h(1) - h(2) - o$ <p>with</p> <ul style="list-style-type: none"> <li>• “i” as the number of input neurons;</li> <li>• “h(1)” as the number of neurons in the first hidden layer;</li> </ul>	<p>The diagram shows a feed-forward neural network with three layers. The input layer on the left has three nodes. The hidden layer in the middle has three nodes. The output layer on the right has three nodes. All nodes in one layer are connected to all nodes in the next layer.</p>

Figure 7.4: Feed-forward ANN (Mehta, 2019)

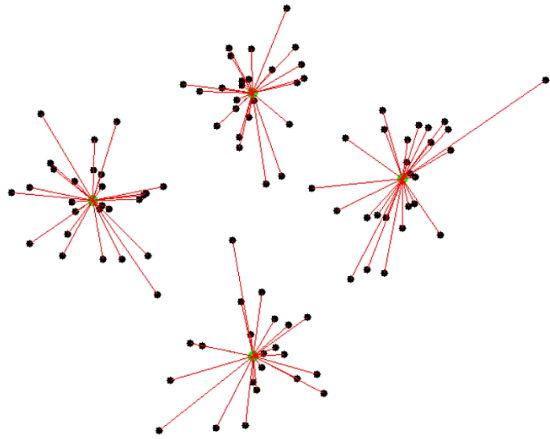
	<ul style="list-style-type: none"> <li>• “h(2)” as the number of neurons in the second hidden layer; and,</li> <li>• “o” as the number of neurons in the output layer.</li> </ul>	
--	---	--

**Radial Basis Function**

This type of ANN considers the distance of any point relative to the centre neuron. These ANN typically have two layers.

In the inner layer, the features are combined with the radial basis function.

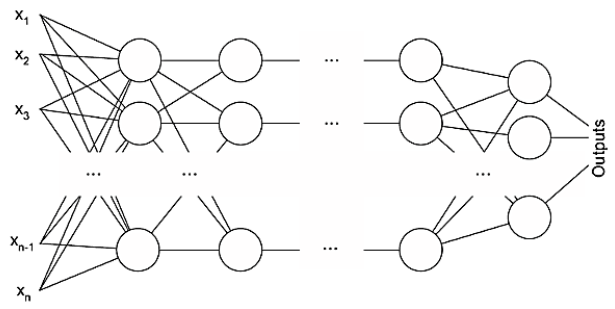
In the output layer, these features are taken into account when calculating the same output in subsequent processes.



**Figure 7.5: Radial Basis Function ANN (Mehta, 2019)**

**Multilayer Perceptron**

This type of ANN consists of three or more fully connected layers. This means that every single node in a layer is connected to each node in the following layer. It is typically used to classify data that cannot be separated linearly.

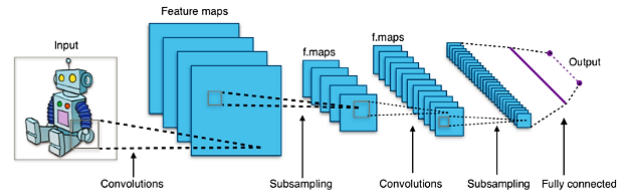


**Figure 7.6: Multilayer Perceptron ANN (Mehta, 2019)**

**Convolutional Neural Network (CNN)**

This type of ANN uses a variation of the multilayer “perceptrons” or linear binary classifier algorithm. A CNN contains one or more convolutional layers, which can either be completely inter-connected or grouped.

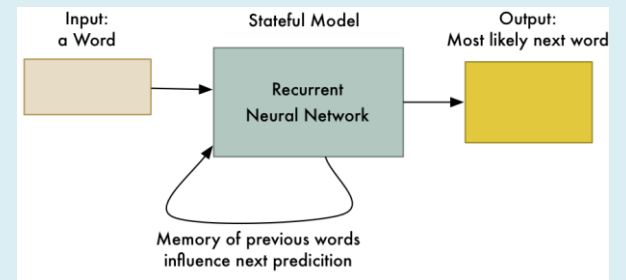
Before a result is passed through to the following layer, the convolutional layer uses a convolutional operation (specific mathematical operation) on the input, allowing the network to be deeper with much fewer parameters.



**Figure 7.7: Convolutional ANN (Mehta, 2019)**

**Recurrent Neural Network (RNN)**

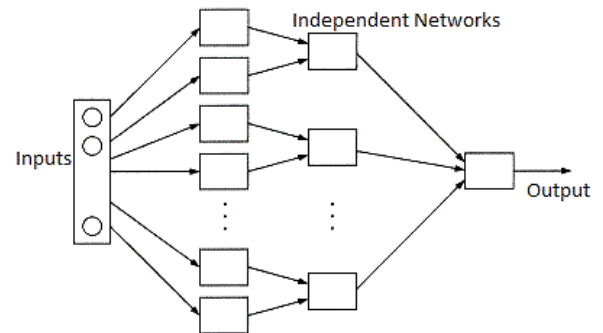
With this type of ANN, the output of a particular layer is saved and fed back to the input. This supports the prediction layer’s outcome.



**Figure 7.8: Recurrent Neural Network (Mehta, 2019)**

**Modular Neural Network**

This type of ANN consists of a number of different networks that function independently and perform sub-tasks. The different networks do not interact with or signal another during the process. They work independently towards achieving the output.



**Figure 7.9: Modular ANN (Mehta, 2019)**

<b>Sequence-To-Sequence Models</b>	<p>This type of ANN consists of two repeated neural networks. An encoder processes the input and a decoder processes the output. The encoder and decoder can use the same or different parameters. This model is particularly applicable in those cases where the length of the input data differs from the length of the output data.</p>	<p>—</p>
------------------------------------	--	----------

ANN is often the backbone of machine learning methodologies and can be combined with other systems such as the fuzzy inference system.

#### 7.2.1.2. Adaptive neuro-fuzzy inference system or Adaptive-network-based fuzzy inference system (ANFIS)

An Adaptive Neuro-Fuzzy Inference System (ANFIS) is based on the principles of ANN but incorporates the principles of fuzzy logic inference system. Prakash (2014) describes ANFIS as a system that *“combines the learning capability of Neural Networks with the capability of Fuzzy Logic to model uncertainty in expressiveness”* or *“the ability to model uncertain scenarios using Fuzzy Logic and create a Neural Network to learn that model”*.

Therefore, instead of just incorporating the input-output system flow of ANN, ANFIS combines the ANN and the if-then rules of the fuzzy logic algorithms allowing the system to model and interpret real-world scenarios (Prakash, 2014). The if-then rules in the fuzzy inference system are commonly explained in the form “If A, then B” (Jang, 1993).

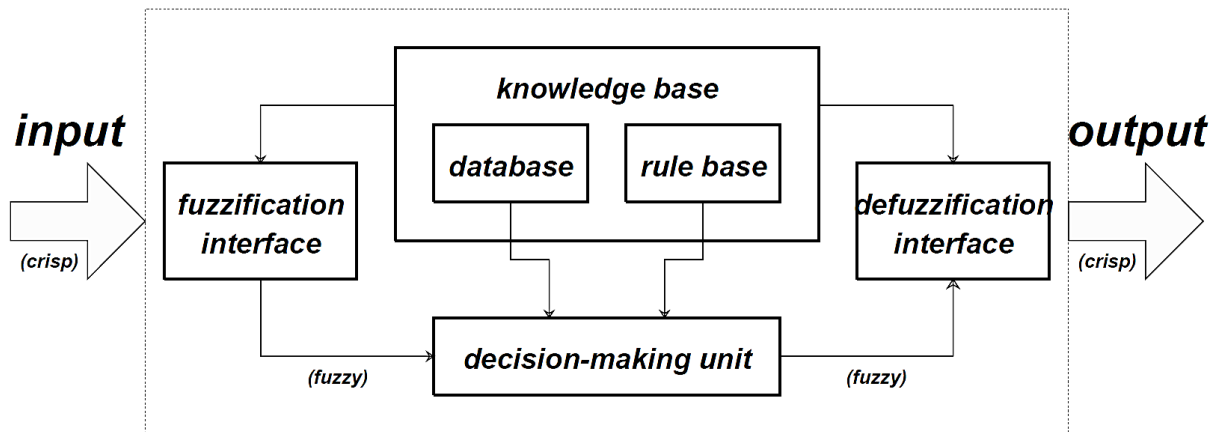
Example (Prakash, 2014): *“If a car drives slow, then do A. If a car drives at medium speed, then do B. If a car drives fast, then do C.”* Prakash (2014) describes A, B and C as tasks or actions represented by a mathematical value or algorithm that includes other variables such as value “X”, i.e. the pressure placed on the accelerator of the car.

Jang (1993) divides a fuzzy inference system into five components or functional blocks (Figure 7.10):

- (1) A rule-base that contains a number of if-then rules;
- (2) A database that defines the “membership functions” used in these if-then rules;



- (3) A decision-making unit that conducts the inference operations on these rules;
- (4) A fuzzification interface that transforms the input into degrees of truth with linguistic values; and,
- (5) A defuzzification interface that transforms the “fuzzy results” into a comprehensible output.



**Figure 7.10: Fuzzy inference system (Jang, 1993)**

The result or output from the fuzzy inference system can be evaluated by the ANN according to the final values prescribed to it and the ANN can begin to learn the defuzzification process of the system (Prakash, 2014).

### 7.3. ALGORITHMS RELATED TO DEGHANI & SHAFAGHI'S (2017) DIFFERENTIAL EVOLUTION ALGORITHM APPROACH TO PREDICT FLYROCK

#### 7.3.1. Dimensional Analysis Algorithm

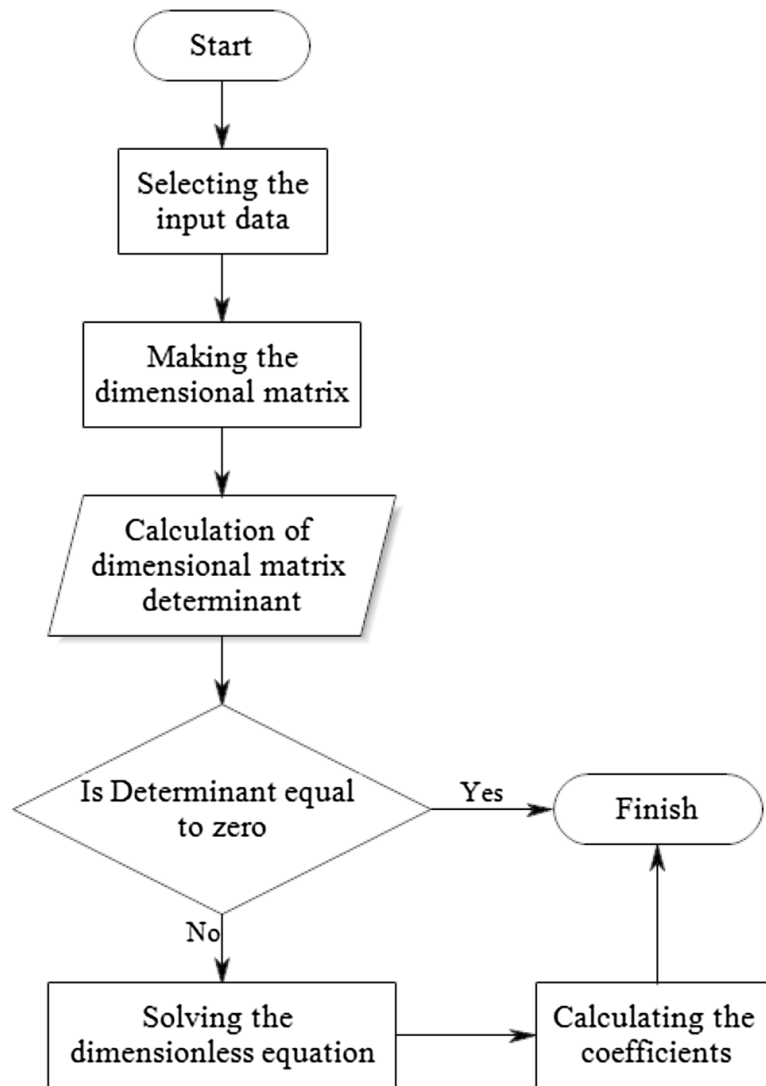


Figure 7.11: Dimensional analysis algorithm (Dehghani & Shafaghi, 2017)

### 7.3.2. Differential Evolution Algorithm

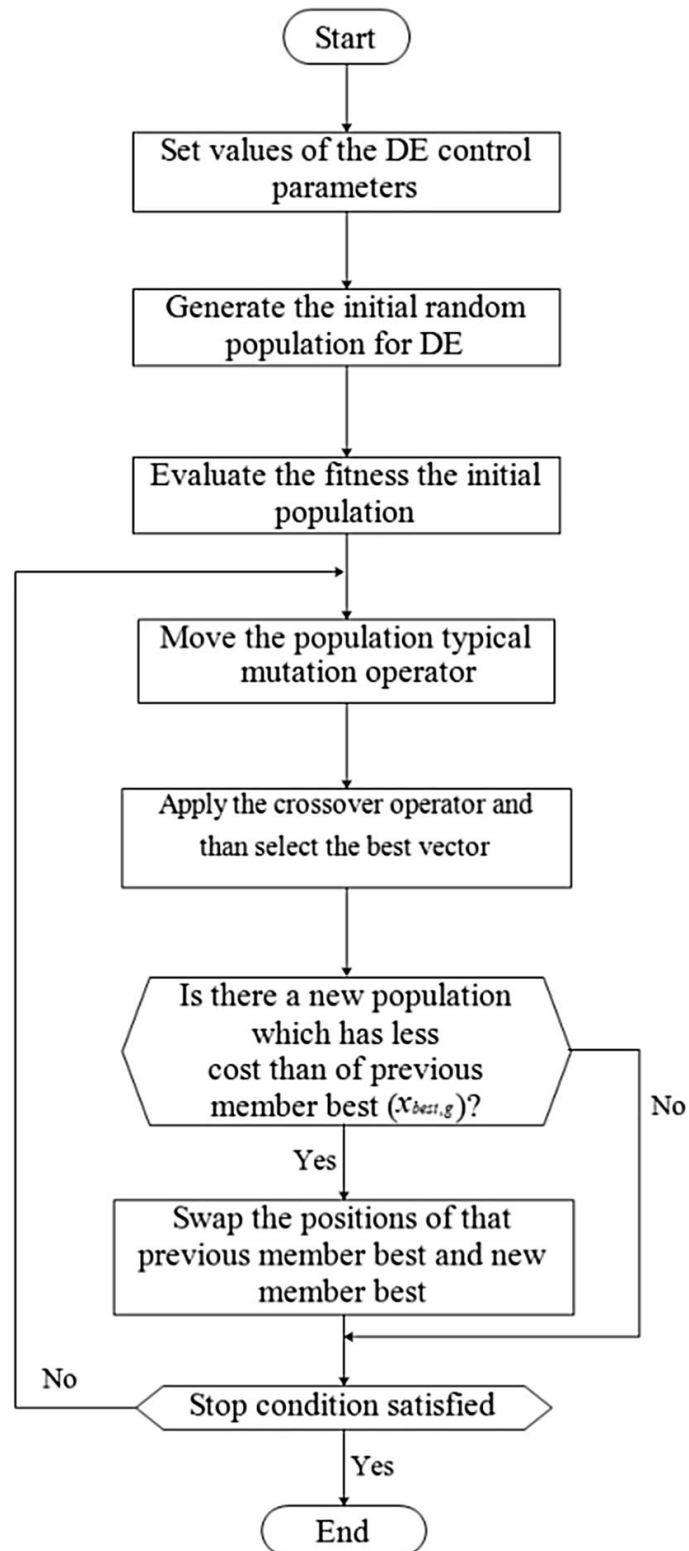


Figure 7.12: Differential evaluation algorithm (Dehghani & Shafaghi, 2017)

### 7.3.3. Regression tree analysis presented by Hasanipannah, et al. (2017)

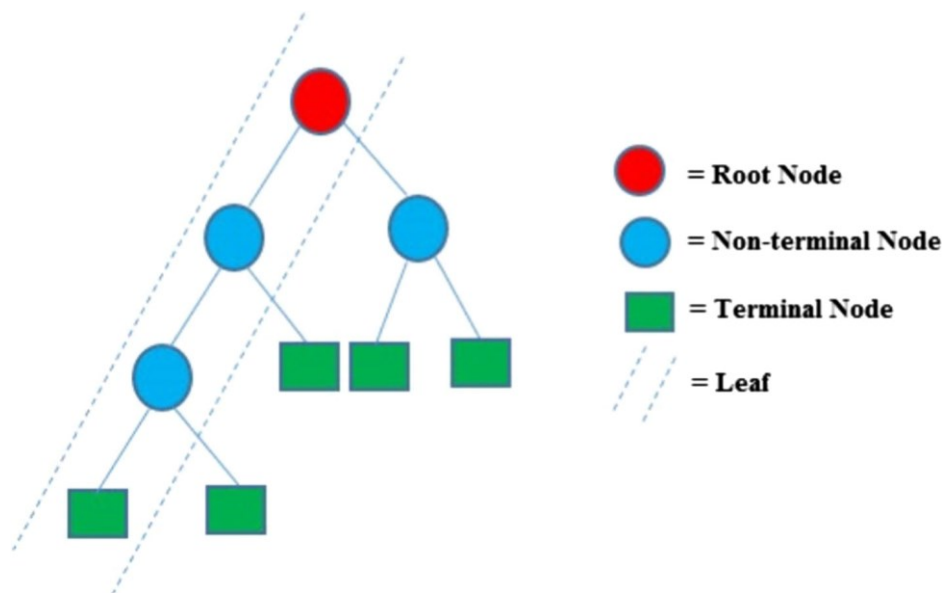


Figure 7.13: Simple decision tree structure (Hasanipannah, et al., 2017)

Using this simple structure presented in Figure 7.13, Hasanipannah, et al. (2017) developed the following regression tree structure (Figure 7.14) for the purpose of their study.

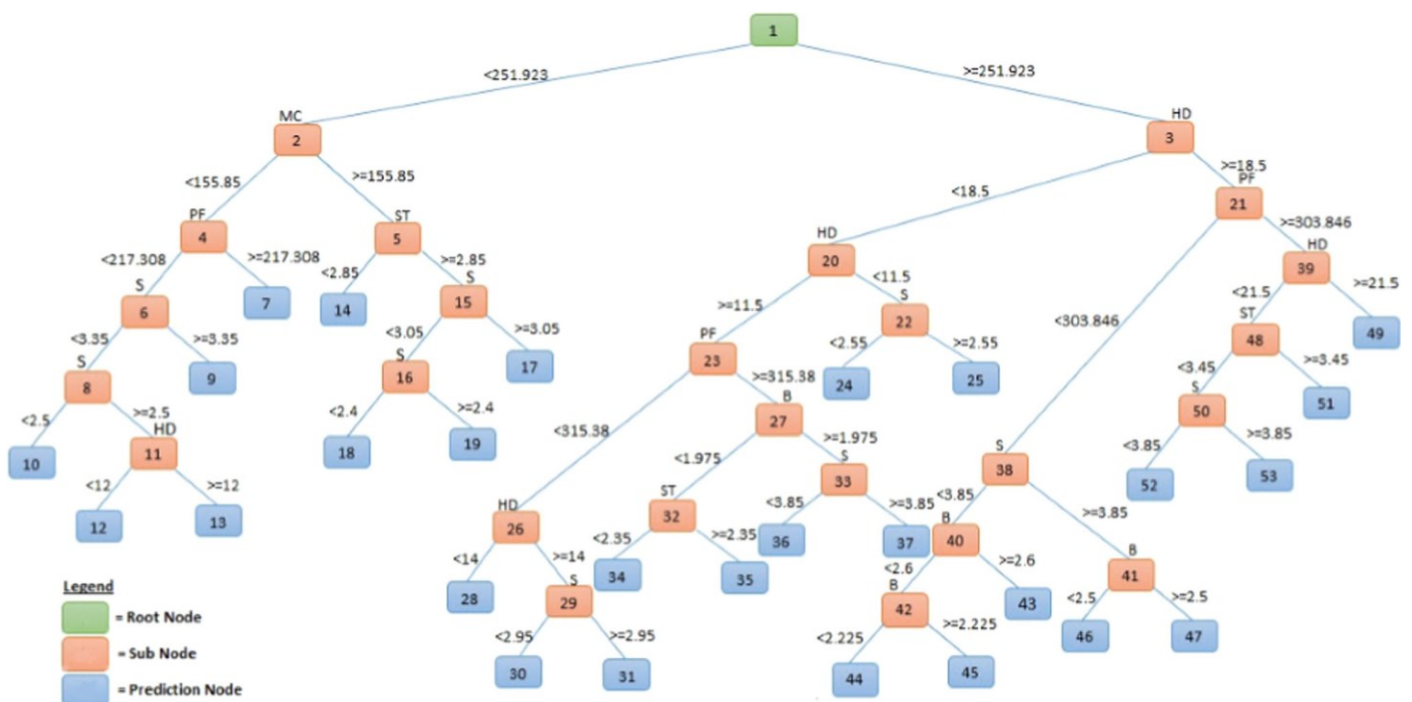


Figure 7.14: Structure of the developed regression tree model (Hasanipannah, et al., 2017)

## 7.4. SENSOR TECHNOLOGY

Sensors can be classified according to a number of criteria, including (Engineers Garage, 2012):

- (1) Primary input quantity (i.e. parameter being measured)
- (2) Transduction principles (physical or chemical effect)
- (3) Material and technology (typically selected by development engineering groups)
- (4) Property or use
- (5) Application
- (6) Energy supply required (Active or Passive)

The criteria according to which sensors are classified primarily depend on the purpose of using and/or classifying the sensors. For the purpose of simplicity, the types of sensors will be classified and briefly discussed based on its use and application.

### 7.4.1. Temperature sensors

A temperature sensor is defined as a device that is used to detect and measure changes in temperature and convert the measured changes into comprehensible data for the user (Engineers Garage, 2012). A common example is a mercury thermometer. Until recently, temperature sensors have mainly been used for refrigeration and air conditioning systems. However, temperature sensors have become applicable to other industries such as manufacturing, agriculture and health care (Sharma, 2019).

Temperature sensors can be sub-divided into two main categories, namely (Engineers Garage, 2012):

- (1) Contact sensors, i.e. sensors must make physical contact with the object/medium being measured (suitable to monitor temperature changes in solids, liquids and gasses).
- (2) Non-contact sensors, i.e. sensors do not need to be in physical contact with the object or medium in order to be effective and is not suitable to use with gasses due to the transparency thereof.

### Types of temperature sensors

- (1) Thermocouples

Thermocouples are devices that measure the change in temperature and convert it into a change in voltage, i.e. when the temperature increase, the voltage output

increases as well (Sharma, 2019). This device basically consists of two wires (made from different materials) joined at one end. Once this junction experiences a temperature change, a current will flow from one material to the next, resulting in a change in the voltage (output) (ThermocoupleInfo.com, 2011). This concept is illustrated in Figure 7.15.

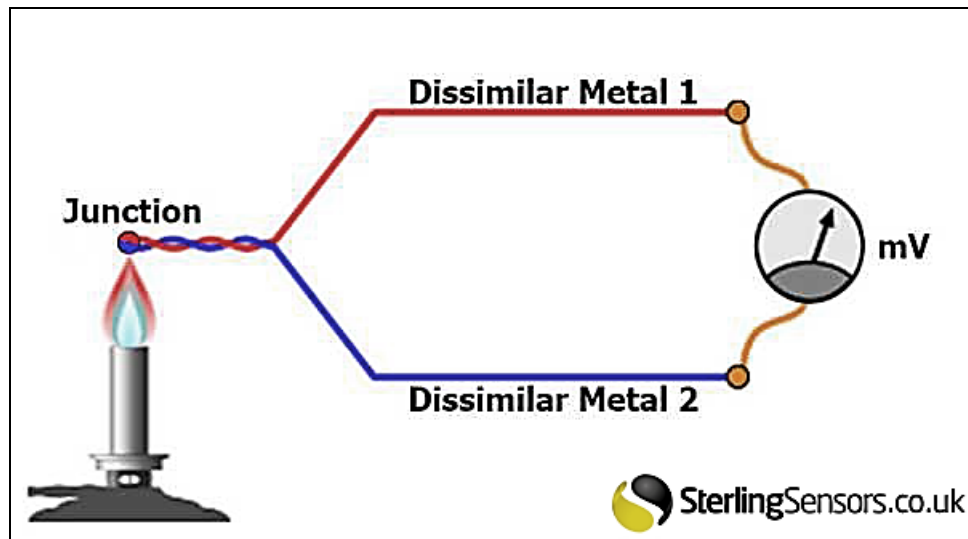


Figure 7.15: Thermocouple working principle (Sterling Sensors, 2018)

### (2) Resistor temperature detectors (RTD's)

RTD's are devices that contain a thermal resistor. The resistance value of the device changes with varying temperatures (OMEGA Engineering, 2019). RTD's are relatively expensive when compared to other temperature sensing devices (Engineers Garage, 2012), and are known to be quite sensitive to vibration.

### (3) Thermistors

Thermistors also contain thermal resistors but are more suitable to measure small temperature changes (Engineers Garage, 2012).

## 7.4.2. Infrared (IR) sensors

Infrared sensors detect electromagnetic radiation or thermal energy emitted in the infrared spectrum, which is not visible to the human eye (Engineers Garage, 2012). The basic function of an infrared sensor is based on emitting an infrared signal from a transmitter unit within the sensor and receiving the reflected signal with a receiver unit within the same device. The differences between these signals are converted into voltage readings as the sensor's output (Engineers Garage, 2012).

There are different applications of an infrared sensor since the device transmits an infrared signal and receives the same signal after it has been reflected from a surface. These applications include (Engineers Garage, 2012):

(1) Thermography

*“A technique for detecting and measuring variations in the heat emitted by various regions of the body and transforming them into visible signals that can be recorded photographically (as for diagnosing abnormal or diseased underlying conditions).”*  
(Merriam-Webster Incorporated, 2019)

(2) Spectroscopy

*“The technique used to identify the molecules by analysing the constituent bonds, using infrared radiation.”* (Engineers Garage, 2012)

(3) Meteorology

*“Cloud heights and calculation of land and surface temperature is possible if satellites are equipped with scanning radiometers (infrared sensors or detectors).”* (Engineers Garage, 2012)

(4) Climatology

*“Monitoring the energy exchange between the atmosphere and the earth.”*  
(Engineers Garage, 2012)

(5) Communications

*“Infrared lasers provide light for optical fibre communications, also used for short-range communications such as cell phone and computer peripherals.”* (Engineers Garage, 2012)

#### **7.4.3. Ultra-violet (UV) sensors**

UV sensors are used to detect and measure ultra-violet radiation (i.e. includes wavelengths longer than x-rays but shorter than visible radiation) (Engineers Garage, 2012). Majority of UV sensors are used for the purpose of measuring sunlight and the related radiation. The output signal is expressed as watts per square meter ( $W/m^2$ ) also known as energy flux (Apogee Instruments Incorporated, 2019).

The application of UV sensors includes (Apogee Instruments Incorporated, 2019):

- (1) Measurement of UV radiation (sunlight) in an outdoor environment,

- (2) Use in laboratories with artificial light sources, and
- (3) Monitoring the filtering ability and stability of various materials.

#### 7.4.4. Ultrasonic sensors

Ultrasonic sensors are devices used to measure the distance from the sensor to the object of interest. These devices function by emitting ultrasonic waves (i.e. higher frequency than what is audible to human) to measure the distance to the object of interest. These (ultrasonic) waves are classified as mechanical energy since it travels as successive compressions and rarefactions through a medium along the direction of wave propagation (Engineers Garage, 2012). These sensors, therefore, convert the mechanical energy from the sound wave into electrical energy (measured in Volts).

An ultrasonic sensor consists of a transmitter and receiver, which are identical in design (Figure 7.16) but function opposite to one another. The “horn” indicated in Figure 7.16 is also known as a resonator (which radiate the sound waves outward) and the “metal plate” is known as the vibrator (which generates the ultrasonic waves).

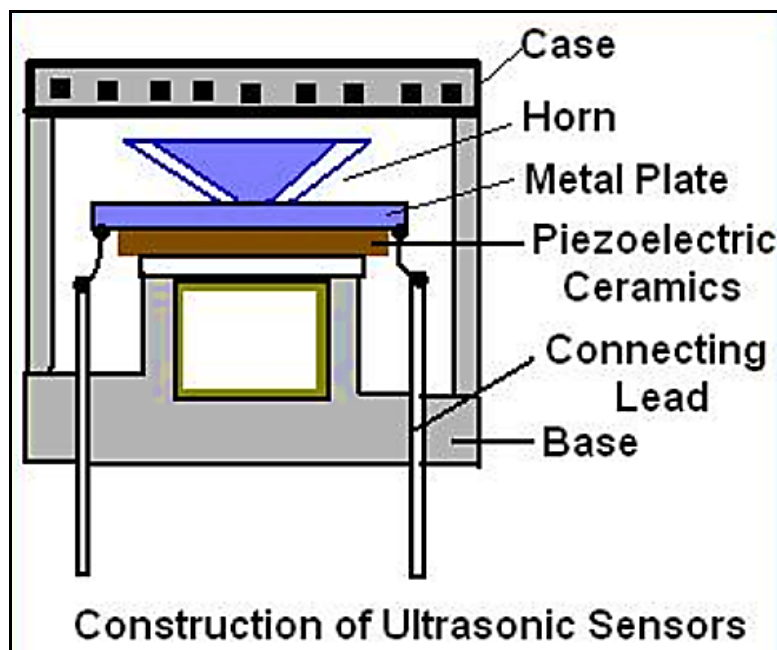


Figure 7.16: Construction of ultrasonic sensors (Coulton.com, 2019)

In order to emit an ultrasonic wave, an electrical voltage is applied to the transmitter unit's piezoelectric ceramic component through the connecting lead wires. As a result, the piezoelectric ceramics (along with the vibrator) will vibrate and generate ultrasonic waves due to its material properties (Engineers Garage, 2012). These ultrasonic waves are transferred through the vibrator (or metal plate) and are further propagated through the



resonator (Engineers Garage, 2012). Therefore, the vibrator does not generate the vibration (and ultrasonic waves), but rather assist the transfer of the vibration and ultrasonic waves due to its low resistive property.

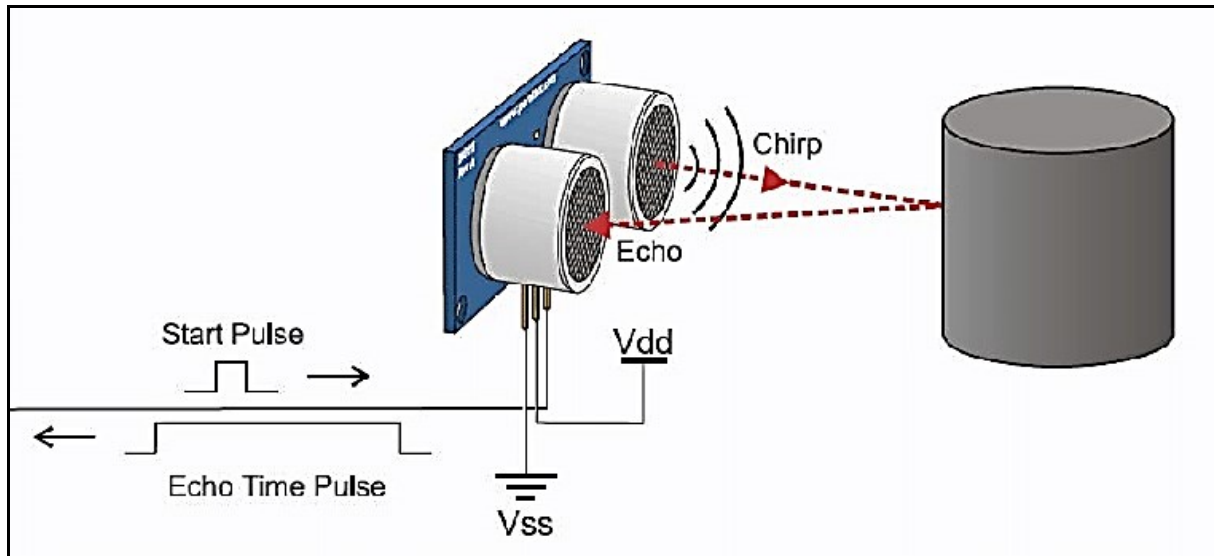


Figure 7.17: Working principle of an ultrasonic sensor (Beg, 2017)

The receiver unit of the device functions in reverse, i.e. the ultrasonic waves are received by the resonator, from the echo (Figure 7.17) due to the waves being reflected from the surface of the object. These waves are then transferred through the vibrator. The vibrations from the vibrator are transferred to the piezoelectric ceramic, resulting in the generation of an electric current (due to the material properties of the piezoelectric ceramic) across two wires.

The voltage taken over these two wires is the output recorded from the sensor, which relates to the distance measured (i.e.  $\text{Distance} = \text{echo time} \times \frac{1}{2}(\text{speed of sound})$ ), and can be processed and analysed further.

Since ultrasonic sensors work with sound waves, some inherent disadvantages or weaknesses (shown in Figure 7.18) are important, namely:

- (1) The range of the sensor, i.e. if the object is too far away the ultrasonic waves will dissipate before making contact with the surface of the object or be reflected back to the receiver unit.
- (2) The sensor should be perpendicular to the object, otherwise, the ultrasonic wave will be reflected away from the receiver unit. The waves will reflect at  $90^\circ$  to the angle of entry.

- (3) The size of the object of interest must be large enough to reflect a significant portion of the emitted waves.
- (4) If the object of interest is a soft or porous material, the ultrasonic waves will likely be absorbed and not reflected back.

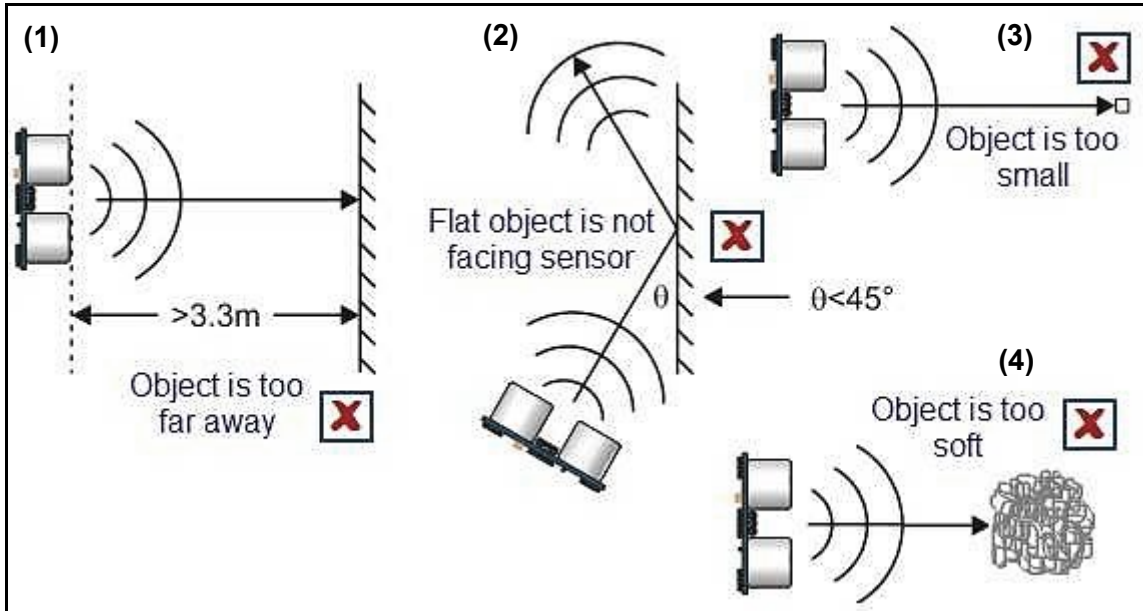


Figure 7.18: Disadvantages or weaknesses relating to ultrasonic sensors (GeeksTips.com, 2019)

Industrial applications of ultrasonic sensors include (Gillespie, 2018):

- Liquid level sensing;
- Trash level sensing;
- Production lines;
- Vehicle detection for car washes, automotive assembly, and parking garage applications;
- Anti-collision detection;
- People detection;
- Contouring or profiling; and,
- Presence detection.

#### 7.4.5. Touch sensors

Touch sensors are becoming increasingly common across various industries and used for various purposes, becoming the standard for new smartphones and tablets. Other applications for touch sensors include (Engineers Garage, 2012):

- (1) Commercial (i.e. medical devices, vending machines, fitness devices and gaming)

- (2) Appliances (i.e. ovens, washing machines, dishwashers and refrigerators)
- (3) Transportation (i.e. streamlining control for vehicle manufacturers)
- (4) Industrial Automation (i.e. Position and liquid level sensing, touch control applications)
- (5) Consumer Electronics (i.e. smartphones, computers, smartwatches and smart televisions)

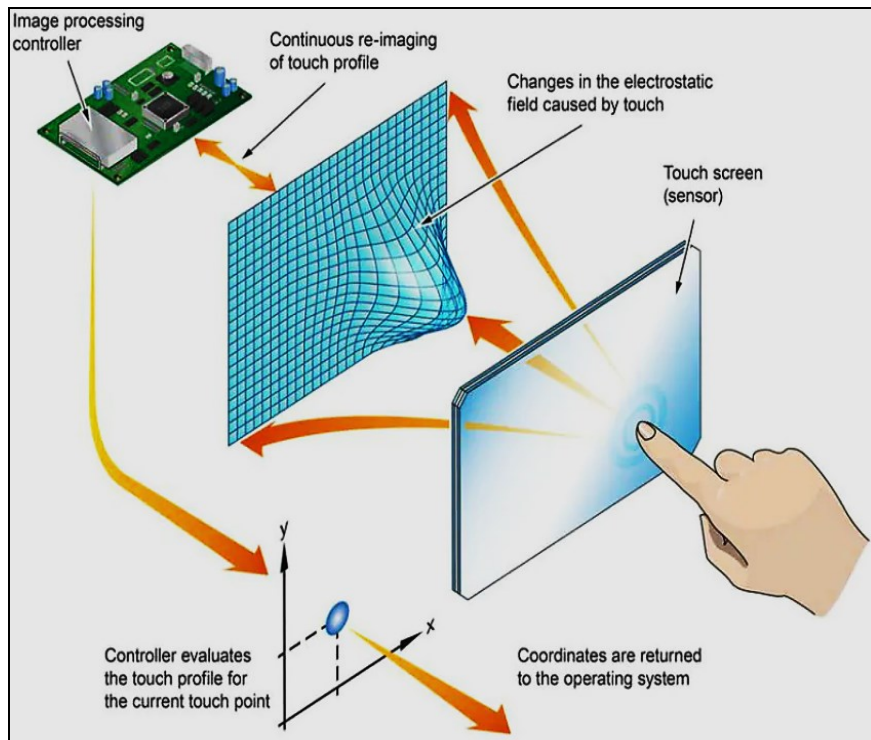
Gudino (2018) divides touch sensors into two distinct categories, based on the way they are constructed and how they function. These two types are (1) Capacity and (2) Resistive touch sensors.

### **(1) Capacitive touch sensors**

The function of these sensors is based on the principle of capacitive coupling, defined as *“the transfer of alternating electrical signals or energy from one segment of a circuit to the other using a capacitor”* (Sunpower Electronics Ltd., 2014). This technology is robust, reliable and visually transparent and is often found in gaming machines, cash dispensers, kiosk systems and industrial systems (TCI.de, 2019).

Using capacity coupling, the sensor, therefore, detects anything that is conductive or more conductive than the air surrounding the capacitors within the sensor (Gudino, 2018). Therefore, a human finger is considered the conductive material (or electric charge conductor) that allows the sensor to function, as in the case of a touch screen from a smartphone.

Staying with the same example, one’s smartphone is allowed to identify the position of one’s finger as well as the movement across the screen by sensing the change in the electrostatic field on the screen’s surface (or capacitive surface) (Gudino, 2018). This process is illustrated in Figure 7.19.



**Figure 7.19: Touch screen based on the capacitive sensor principle (TCI.de, 2019)**

Figure 7.19 illustrates the changes in the electrostatic field due to the conductor (or one's finger) touching the capacitive surface (or screen). An image processing controller is used to interpret these changes, therefore, pinpointing the location of one's finger (Gudino, 2018).

There are some advantages and disadvantages associated with capacitive touch sensors, which are summarised in Table 7.2.

**Table 7.2: Advantages and disadvantages for capacitive touch sensors (TCI.de, 2019)**

Advantages	Disadvantages
Extremely resistant	Requires bare fingers (or capacitive medium)
Very accurate and sensitive	Deep scratches can affect the function in the damaged area.
Good optical transparency	More expensive compared to resistive type
Good resolution	

## (2) Resistive touch sensors

Contradictory to the capacitive touch sensors (with only a glass layer), the resistive touch sensor consists of multiple layers of materials. The resistive sensor consists of two main layers. The front layer is a flexible plastic surface covered with a thin layer of conductive material (typically Indium Tin Oxide). The second layer is a hard plastic (or glass) layer, also covered with the same conductive material (Gudino, 2018). These two layers are separated by a non-conductive spacer (spacer dots), shown in Figure 7.20.

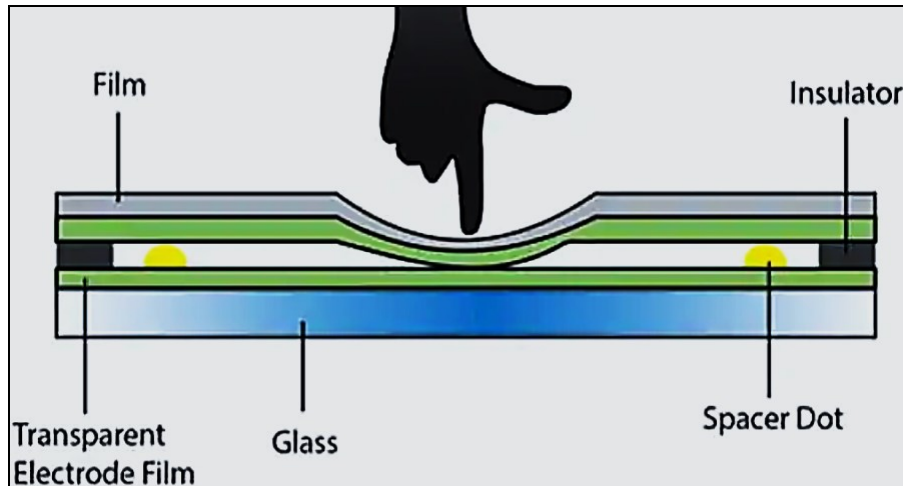


Figure 7.20: Touch screen based on the resistive sensor principle (Gudino, 2018)

Touching the screen with one's finger, by pressing onto the flexible plastic layer until the conductive material makes contact with the conductive material on the glass layer, will register a signal (or touch event) due to the resistance or voltage measured through this electrical contact of the two conductive materials (TCI.de, 2019).

There are some advantages and disadvantages associated with capacitive touch sensors, which are summarised in Table 7.3.

Table 7.3: Advantages and disadvantages for resistive touch sensors (TCI.de, 2019)

Advantages	Disadvantages
Cheaper compared to capacitive touch sensors	Reduces visual transparency
Compatible to various media	Plastic surface can be damaged
High resolution	
Low power consumption	

#### 7.4.6. Pressure Sensors

A pressure sensor is defined by HBM (n.d.) as “an instrument consisting of a pressure-sensitive element to determine the actual pressure applied to the”. The measured pressure (mechanical energy or displacement) is converted into an electrical signal that is displayed as an output.

Pressure sensors are commonly classified on its working principle, namely (Avnet Inc., 2019):

##### (1) Piezo-resistive pressure sensors

Piezo-resistive pressure sensors are one of the most common types of pressure sensors used. These sensors utilise a strain gauge that consists of a conductive material that is attached to a thin film or diaphragm, similar to touch sensors. Once pressure is applied to this conductive material, its electrical resistance changes, illustrated in Figure 7.21. This change in electrical resistance is measured and converted into an output signal.

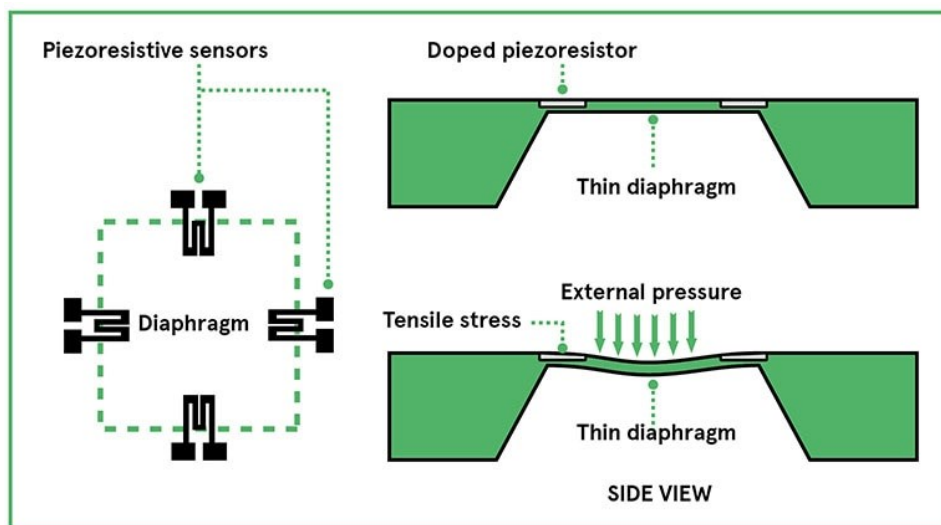


Figure 7.21: Piezo-resistive pressure sensor (Avnet Inc., 2019)

##### (2) Capacitive pressure sensors

Capacitive pressure sensors consist of one rigid plate containing a capacitor and one flexible diaphragm containing electrodes. The pressure is measured when the electrodes on the flexible diaphragm are deflected towards the capacitor, illustrated in Figure 7.22. The resulting change in capacitance is directly proportional to the pressure applied to the sensor.

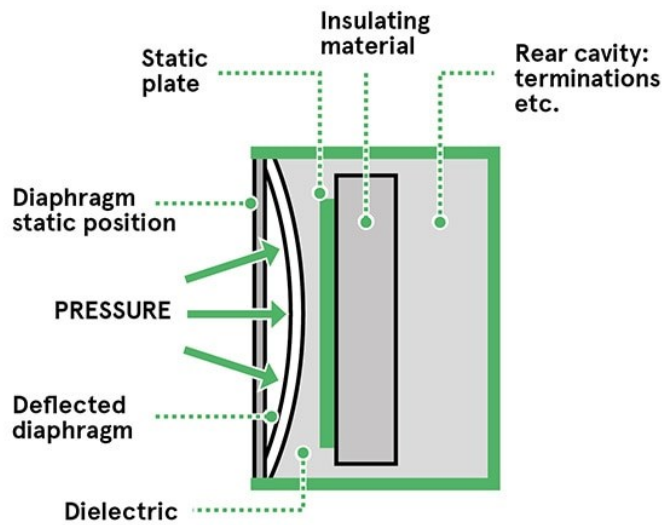


Figure 7.22: Capacitive pressure sensor (Avnet Inc., 2019)

(3) Strain-gauge pressure sensors

A strain-gauge pressure sensor is designed as a Wheatstone bridge. When pressure is applied to a diaphragm, it causes the diaphragm to deflect. The current generated due to this deflection is measured and amplified by the Wheatstone bridge in order to yield an output representative of the applied pressure. A circuit diagram of the layout of this sensor is given in Figure 7.23.

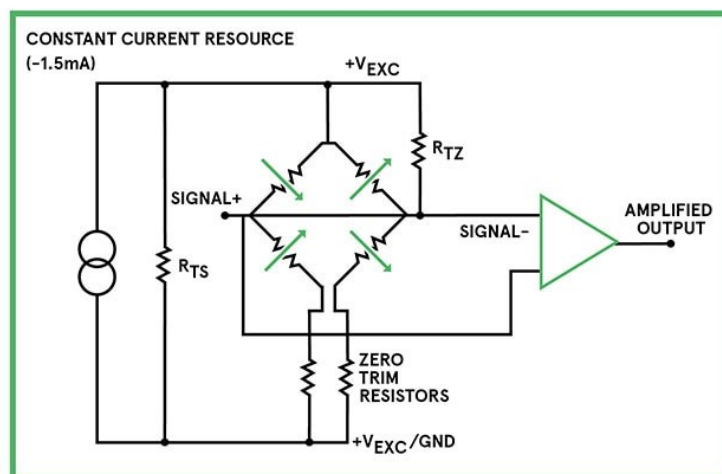


Figure 7.23: A circuit diagram of a strain-gauge pressure sensor, containing a Wheatstone bridge layout (Avnet Inc., 2019)

(4) Piezoelectric pressure sensors

A piezoelectric sensor incorporates a piezoelectric material, such as quartz, and measures the charge generated when a force (or pressure) is applied to the surface of this material, illustrated in Figure 7.24. The measured charge (voltage) is directly proportional to the pressure applied.

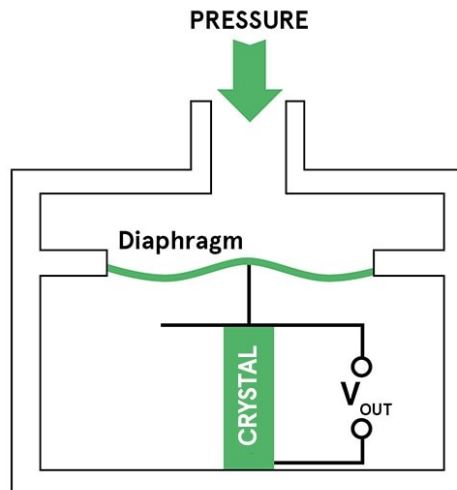


Figure 7.24: Piezoelectric pressure sensor (Avnet Inc., 2019)

(5) Optical pressure sensors

Optical pressure sensors are used to record the change in light received by the measuring diode due to the applied pressure. The applied pressure will move the diaphragm and opaque vane, blocking a larger amount of light emitted by the LED (light-emitting diode) in the sensor, illustrated in Figure 7.25. This reduction in light is measured by the measuring diode and compared to the reference diode, which is not blocked for the LED's light.



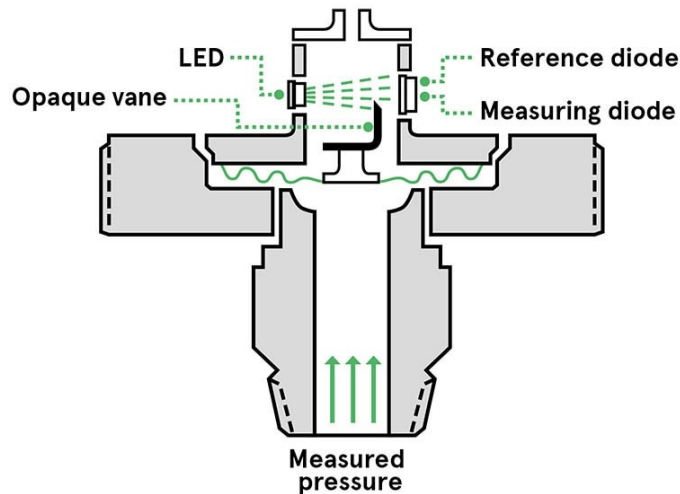


Figure 7.25: A simplified optical pressure sensor (Avnet Inc., 2019)

#### 7.4.7. Proximity sensors

A proximity sensor is defined as “a device that detects the presence or absence of a nearby object and converts it into a signal which can be read easily by a person or an electrical instrument” (Sharma, 2019).

Since proximity sensors are classified as non-contact sensors, these sensors have the advantage of long functional life and high reliability (Engineers Garage, 2012). Proximity sensors (also known as motion sensors) are most commonly used in:

- The retail industry (e.g. to correlate between the motion of the customer and the products they might be interested in, or in parking areas to indicate the availability of parking (Sharma, 2019)); and,
- The security industry (e.g. activation of security cameras and alarms when motion is detected).

A proximity sensor functions are similar to infrared sensors, in the sense of transmitting and receiving a signal. By emitting an electrostatic field or electromagnetic signal, the proximity sensor can detect changes in such a field or measure the specifications of the returned signal (Engineers Garage, 2012).

There are several types of proximity sensors available, including (Fargo Controls Inc., 2018):

##### (1) Inductive proximity sensors

These sensors are used to identify metallic objects or materials without making contact (Sharma, 2019). Using a coil and oscillator, an electromagnetic field is

created around the sensor. Once a metallic object moves into this electromagnetic field, the amplitude of the oscillator changes, indicating an object within the vicinity of the sensing device.

(2) Capacitive proximity sensors

These sensors are used to detect and identify both metallic and non-metallic objects without making contact. Using the variation in capacitance between the sensor and an object of interest, a capacitive proximity sensor can detect an object when it moves past the sensitive side of the device. This capacitance variation creates an electric circuit within the sensor, which starts to oscillate. This oscillation (rise and fall) drives the output voltage.

(3) Photoelectric proximity sensors

These sensors detect consist of a transmitter and receiver, detecting objects by emitting a light beam which is either reflection from the surface of an object or transmitted directly towards the receiver unit. There are four types of photoelectric sensors available, shown in Figure 7.26.

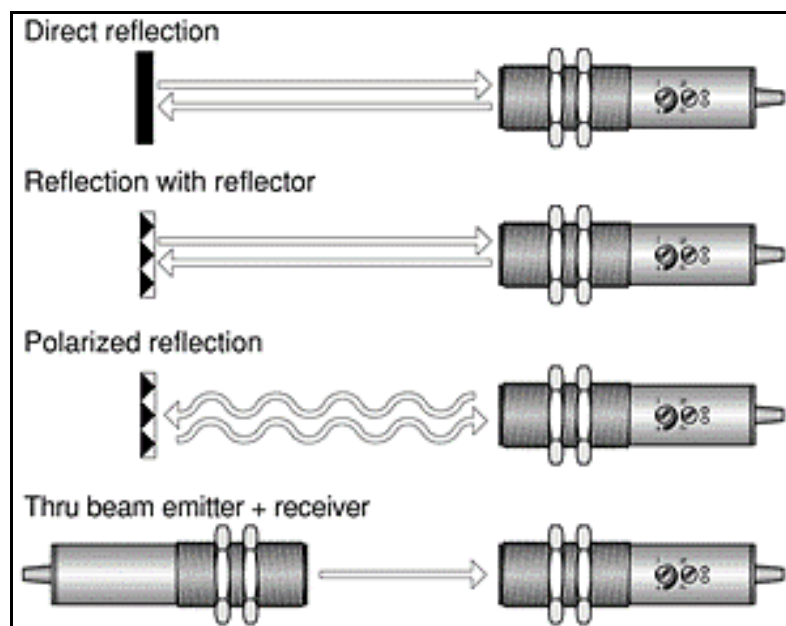
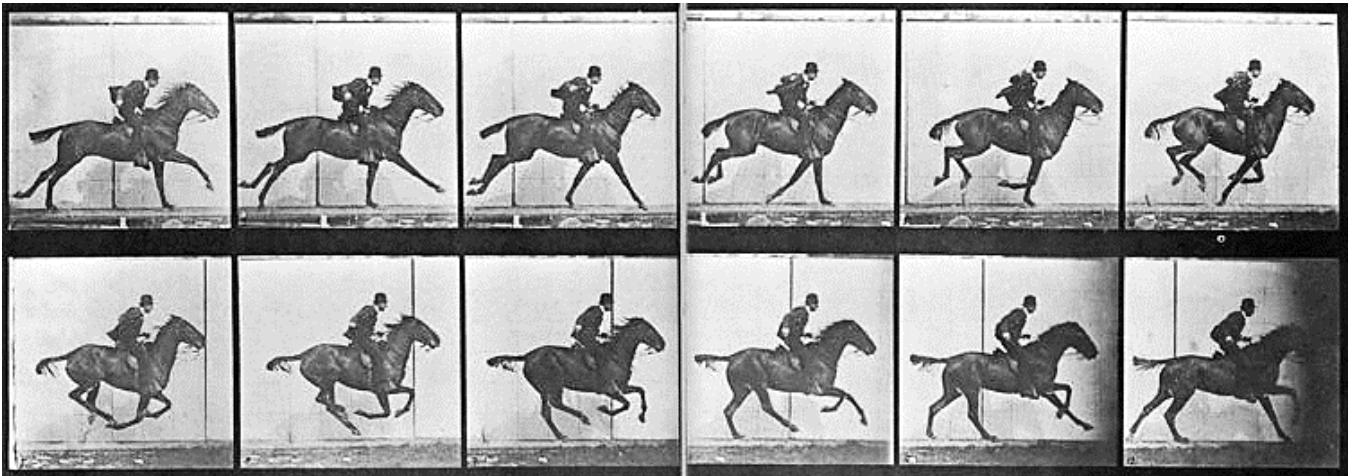


Figure 7.26: Types of photoelectric proximity sensors (Fargo Controls Inc., 2018)

## 7.5. HISTORY OF HIGH-SPEED PHOTOGRAPHY

The first significant advancement in high-speed photography was made by Eadweard Muybridge in 1878 when he was tasked to determine whether a horse lifted all four of its hooves off the ground while galloping. Muybridge used 24 cameras, linked to a shutter

release system, and positioned along the travelling path (The Atomic Heritage Foundation, 2017), capturing the images in Figure 7.27.



**Figure 7.27: The first high-speed images captured by Eadweard Muybridge in 1879 (Yigiter, 2018)**

With these images, Muybridge could prove that a horse does lift all four hooves while galloping (The Atomic Heritage Foundation, 2017).

Later, in 1886, Peter Salcher (an Austrian physicist) captured the first images of a bullet travelling at supersonic speed. These images assisted Professor Ernest Mach in his research in supersonic motion (The Atomic Heritage Foundation, 2017).

In the 1930s, Bell Telephone Laboratories developed a camera capable of capturing images at a rate of 5,000 frames per second (fps), after desiring a faster camera than what was available at that time. Later, Wollensak Optical Company improved on this design and developed a high-speed camera capable of 10,000 fps (The Atomic Heritage Foundation, 2017). Today, high-speed cameras are capable of capturing images at much higher frame rates, i.e. between 10,000 fps and 500,000 fps. Recently, the world's fastest high-speed camera was presented in an article by Doctor (2019), able to reach a shutter speed of 10 trillion fps and capable of capturing the speed of light (Doctor, 2019).

## 8.1. ANGLES OF VIEW OF SIGMA LENSES.

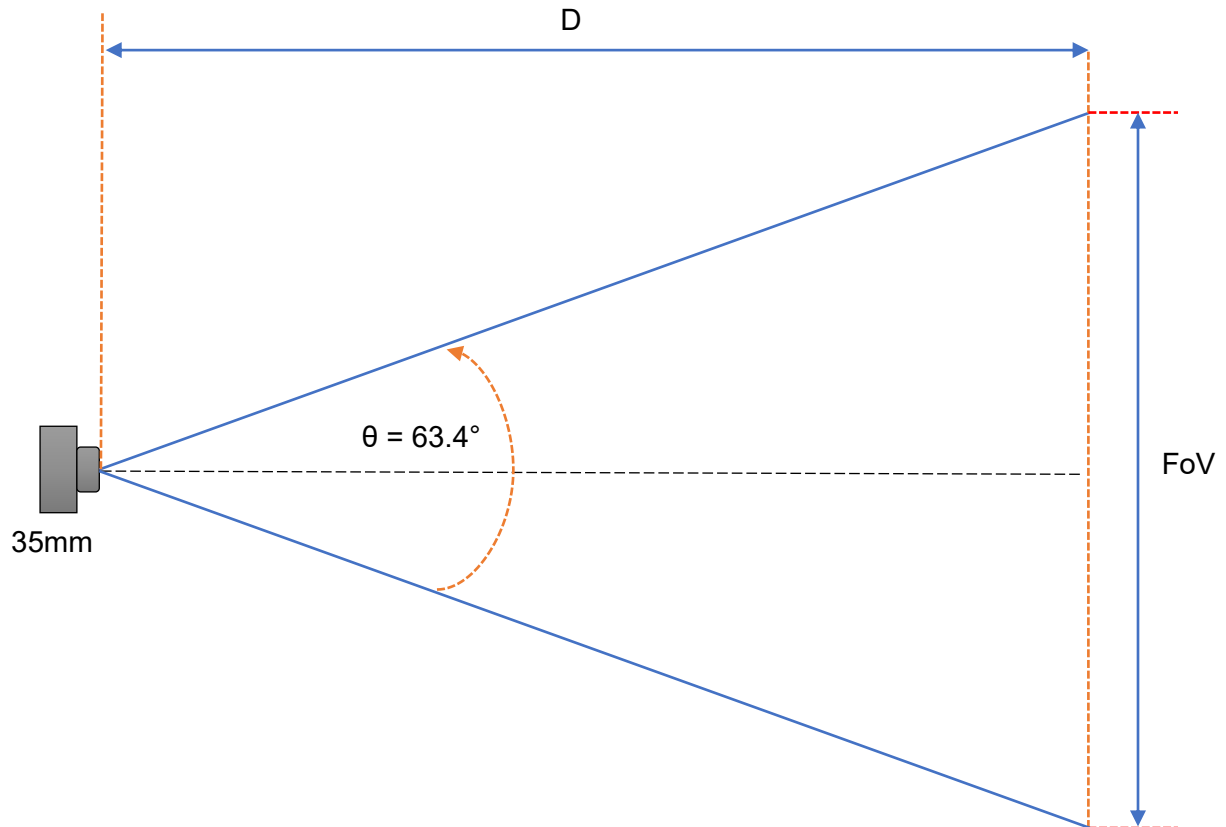


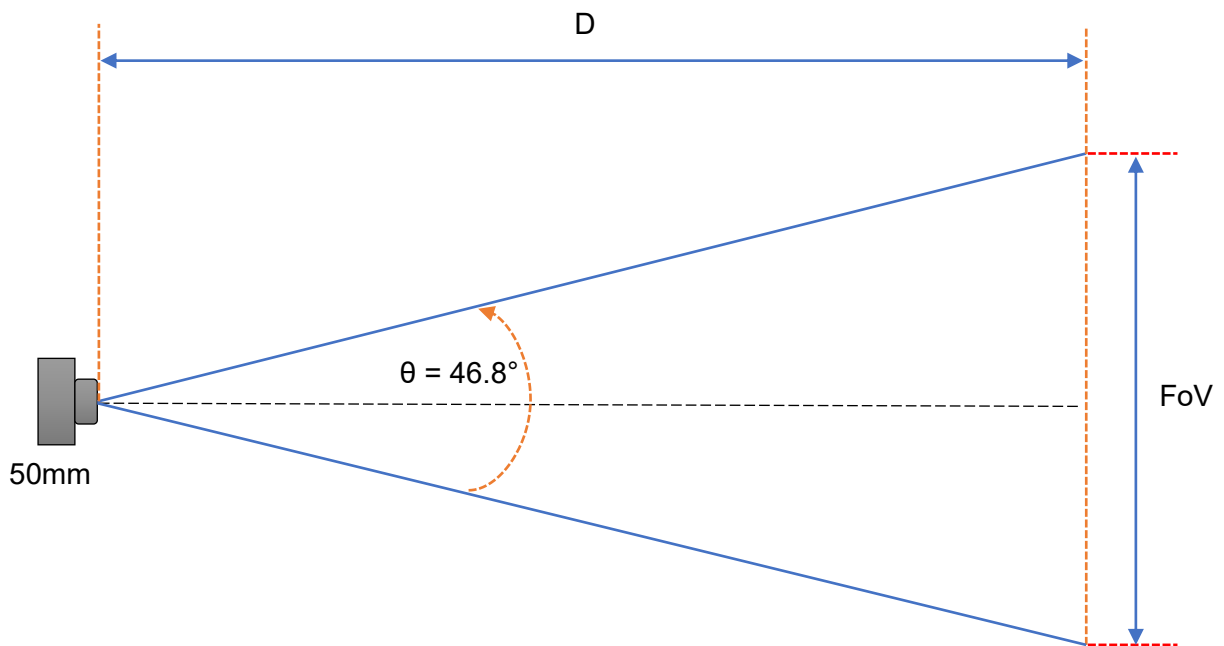
Figure 8.1: FoV schematic for a Sigma 35mm lens

The relationship between the distance to the target area ( $D$ ) and the width of the lens's field of view (FoV) for the Sigma 35mm lens can be written as:

$$FoV = 2D \tan\left(\frac{\theta}{2}\right)$$

$$FoV = 2D \tan\left(\frac{63.4^\circ}{2}\right)$$

$$\underline{FoV = D \times 1.2352}$$



**Figure 8.2: FoV schematic for a Sigma 50mm lens**

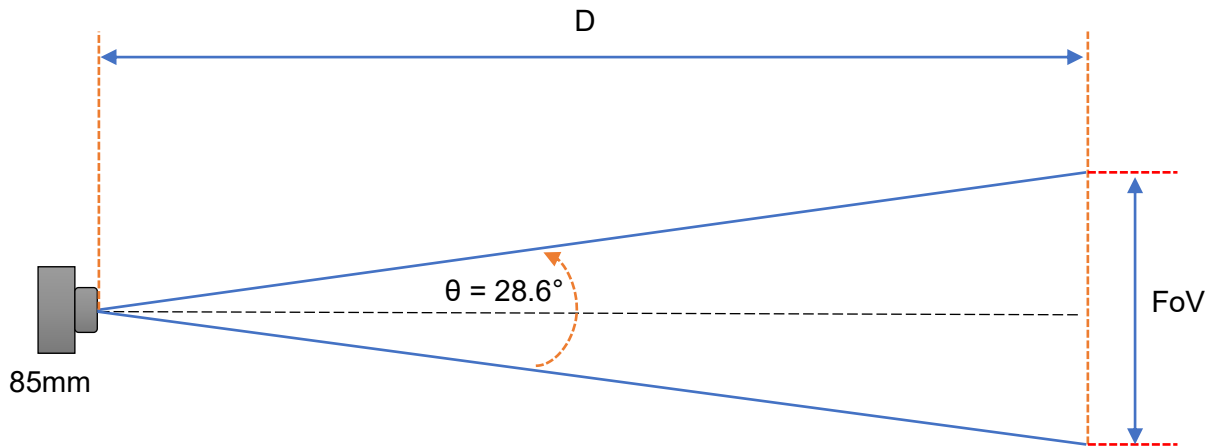
The relationship between the distance to the target area (D) and the width of the lens's field of view (FoV) for the Sigma 50mm lens can be written as:

$$FoV = 2D \tan\left(\frac{\theta}{2}\right)$$

$$FoV = 2D \tan\left(\frac{46.8^\circ}{2}\right)$$

$$FoV = D \times 0.8655$$





**Figure 8.3: FoV schematic for a Sigma 85mm lens**

The relationship between the distance to the target area (D) and the width of the lens's field of view (FoV) for the Sigma 85mm lens can be written as:

$$FoV = 2D \tan\left(\frac{\theta}{2}\right)$$

$$FoV = 2D \tan\left(\frac{28.6^\circ}{2}\right)$$

$$\underline{FoV = D \times 0.5098}$$

## 8.2. SYNCHRONIZATION TEST RESULTS TO IDENTIFY POTENTIAL DELAYS IN AN IMAGE CAPTURING BETWEEN CAMERAS

Synchronization tests result showing the time captured on the stopwatch on each camera over three rounds of trigger sequences.

**Table 8.1: Synchronization tests results**

	Round1			Round2			Round3		
	Cam1	Cam2	Cam3	Cam1	Cam2	Cam3	Cam1	Cam2	Cam3
<b>1</b>	3,41	3,41	3,41	3,32	3,32	3,32	3,52	3,52	3,52
<b>2</b>	3,58	3,58	3,58	3,48	3,48	3,49	3,68	3,68	3,69
<b>3</b>	3,755	3,76	3,755	3,65	3,65	3,65	3,855	3,86	3,86
<b>4</b>	3,93	3,93	3,93	3,83	3,83	3,83	4,03	4,03	4,03
<b>5</b>	4,1	4,1	4,1	4	4	4	4,2	4,2	4,2
<b>6</b>	4,27	4,275	4,275	4,17	4,17	4,17	4,37	4,375	4,375

7	4,435	4,45	4,45	4,35	4,35	4,35	4,545	4,55	4,55
8	4,61	4,61	4,61	4,52	4,52	4,52	4,72	4,72	4,72
9	4,78	4,785	4,78	4,67	4,685	4,685	4,88	4,88	4,89
10	4,95	4,96	4,955	4,855	4,87	4,855	5,05	5,06	5,06
11	5,125	5,13	5,13	5,03	5,03	5,03	5,23	5,23	5,23
12	5,3	5,3	5,3	5,2	5,2	5,2	5,4	5,4	5,4
13	5,47	5,475	5,475	5,36	5,37	5,37	5,57	5,575	5,58
14	5,63	5,65	5,64	5,54	5,55	5,55	5,745	5,75	5,75
15	5,805	5,81	5,81	5,72	5,72	5,72	5,91	5,92	5,92
16	5,98	5,995	5,98	5,87	5,885	5,88	6,08	6,08	6,09
17	6,15	6,16	6,155	6,04	6,07	6,055	6,25	6,26	6,26
18	6,32	6,33	6,33	6,22	6,22	6,22	6,42	6,43	6,43
19	6,495	6,5	6,5	6,39	6,39	6,39	6,6	6,6	6,6
20	6,67	6,675	6,675	6,56	6,57	6,57	6,77	6,775	6,78
21	6,83	6,85	6,84	6,73	6,75	6,75	6,94	6,95	6,95
22	7	7,01	7,01	6,9	6,9	6,91	7,11	7,12	7,12
23	7,18	7,185	7,18	7,07	7,085	7,065	7,28	7,29	7,29
24	7,35	7,36	7,355	7,24	7,27	7,255	7,45	7,46	7,46
25	7,52	7,53	7,53	7,415	7,42	7,42	7,62	7,63	7,63
26	7,69	7,7	7,7	7,59	7,6	7,59	7,795	7,8	7,8
27	7,87	7,875	7,875	7,76	7,77	7,77	7,97	7,98	7,98
28	8,03	8,05	8,03	7,93	7,95	7,95	8,14	8,15	8,15
29	8,21	8,22	8,21	8,1	8,11	8,11	8,3	8,32	8,32
30	8,385	8,395	8,36	8,27	8,285	8,27	8,475	8,49	8,49
31	8,55	8,56	8,54	8,44	8,47	8,455	8,65	8,67	8,67
32	8,72	8,73	8,72	8,61	8,62	8,62	8,82	8,83	8,83
33	8,88	8,9	8,88	8,785	8,8	8,79	8,99	9	9
34	9,06	9,075	9,06	8,96	8,96	8,95	9,16	9,175	9,175
35	9,24	9,25	9,24	9,11	9,13	9,11	9,34	9,35	9,35

### 8.3. EXPORTED DATA OR RESULTS FROM USMART MAPPING SOFTWARE

Table 8.2: An example of the .csv file exported from the uSMART Softcopy stereo mapping software

<b>GCP_PM1</b>	<b>47128,762</b>	<b>2843239,433</b>	<b>1510,694</b>			<b>1</b>	<b>0</b>	<b>0</b>	<b>0</b>	<b>0</b>	<b>0</b>	<b>0</b>	<b>0</b>	<b>0;00:00:00.0000</b>
<b>GCP_PM10</b>	47174,662	2843238,28	1510,727			1	0	0	0	0	0	0	0	0;00:00:00.0000
<b>GCP_PM11</b>	47174,612	2843231,322	1510,608			1	0	0	0	0	0	0	0	0;00:00:00.0000
<b>GCP_PM12</b>	47190,569	2843230,899	1510,945			1	0	0	0	0	0	0	0	0;00:00:00.0000
<b>GCP_PM13</b>	47194,254	2843235,869	1510,964			1	0	0	0	0	0	0	0	0;00:00:00.0000
<b>GCP_PM14</b>	47188,238	2843248,888	1511,472			1	0	0	0	0	0	0	0	0;00:00:00.0000
<b>GCP_PM15</b>	47200,793	2843243,959	1511,625			1	0	0	0	0	0	0	0	0;00:00:00.0000
<b>GCP_PM16</b>	47206,035	2843243,762	1511,765			1	0	0	0	0	0	0	0	0;00:00:00.0000
<b>GCP_PM17</b>	47202,01	2843239,157	1511,561			1	0	0	0	0	0	0	0	0;00:00:00.0000
<b>GCP_PM18</b>	47204,764	2843232,18	1511,096			1	0	0	0	0	0	0	0	0;00:00:00.0000
<b>GCP_PM2</b>	47128,412	2843253,866	1510,818			1	0	0	0	0	0	0	0	0;00:00:00.0000
<b>GCP_PM3</b>	47129,391	2843260,602	1510,874			1	0	0	0	0	0	0	0	0;00:00:00.0000
<b>GCP_PM4</b>	47134,456	2843262,94	1511,383			1	0	0	0	0	0	0	0	0;00:00:00.0000
<b>GCP_PM5</b>	47151,564	2843242,872	1510,546			1	0	0	0	0	0	0	0	0;00:00:00.0000
<b>GCP_PM6</b>	47151,37	2843229,013	1510,613			1	0	0	0	0	0	0	0	0;00:00:00.0000
<b>GCP_PM7</b>	47162,173	2843237,983	1510,551			1	0	0	0	0	0	0	0	0;00:00:00.0000
<b>GCP_PM8</b>	47165,349	2843245,425	1510,819			1	0	0	0	0	0	0	0	0;00:00:00.0000
<b>GCP_PM9</b>	47174,723	2843245,698	1511,185			1	0	0	0	0	0	0	0	0;00:00:00.0000
<b>LB1</b>	47223,909	2843226,344	1511,993			1	0	0	0	0	0	0	0	0;00:00:00.0000
<b>LB2</b>	47223,704	2843226,452	1512,103			1	0	0	0	0	0	0	0	0;00:00:00.0000
<b>Name</b>	Y	X	Z	Information1	Information2	Wt	Layer	Int.	Src.	Cl.	Us.	Rtrn#	Ang.	D;HH:MM:SS.SS
<b>P1-1111</b>	47056,919	2843279,453	1516,384			1	0	0	0	0	0	0	0	0;00:00:00.0000
<b>p1-model</b>	47056,518	2843279,555	1516,394			1	0	0	0	0	0	0	0	0;00:00:00.0000



<b>P2-1111</b>	47208,455	2843266,526	1515,416			1	0	0	0	0	0	0	0	0;00:00:00.0000
<b>P3-1111</b>	47207,66	2843253,395	1514,234			1	0	0	0	0	0	0	0	0;00:00:00.0000
<b>P4-11111</b>	47207,848	2843257,991	1514,88			1	0	0	0	0	0	0	0	0;00:00:00.0000
<b>P5-11111</b>	47208,16	2843261,339	1515,337			1	0	0	0	0	0	0	0	0;00:00:00.0000
<b>S2</b>	47158,573	2843249,409	1512,449			1	0	0	0	0	0	0	0	0;00:00:00.0000
<b>S3</b>	47165,081	2843248,586	1513,47			1	0	0	0	0	0	0	0	0;00:00:00.0000
<b>S3</b>	47165,081	2843248,586	1513,47			1	0	0	0	0	0	0	0	0;00:00:00.0000
<b>S4</b>	47170,591	2843247,229	1515,874			1	0	0	0	0	0	0	0	0;00:00:00.0000
<b>TRP1</b>	47228,857	2843222,985	1512,264			1	0	0	0	0	0	0	0	0;00:00:00.0000
<b>TRP2</b>	47231,702	2843232,568	1512,778			1	0	0	0	0	0	0	0	0;00:00:00.0000
<b>TRP3</b>	47234,432	2843240,077	1513,924			1	0	0	0	0	0	0	0	0;00:00:00.0000
<b>WV2</b>	47217,62	2843303,047	1514,97			1	0	0	0	0	0	0	0	0;00:00:00.0000
<b>WV2P</b>	47237,592	2843265,885	1514,886			1	0	0	0	0	0	0	0	0;00:00:00.0000